

***tert-Butyl hydroperoxide mediated Wacker-type oxidations; taking advantage of hexafluoro-2-propanol for challenging substrates***

**Calum Maguire<sup>a</sup>, Qun Cao<sup>a,b</sup>, Selena C.L. Gilmer<sup>c</sup>, Bill C. Hawkins<sup>c\*</sup>, Peter C. Knipe<sup>a\*</sup>, Mark J. Muldoon<sup>a\*</sup>**

<sup>a</sup> School of Chemistry and Chemical Engineering, Queen's University Belfast, David Keir Building, Stranmillis Road, Belfast, BT9 5AG, UK.

Email: [P.Knipe@qub.ac.uk](mailto:P.Knipe@qub.ac.uk) and [m.j.muldoon@qub.ac.uk](mailto:m.j.muldoon@qub.ac.uk)

<sup>b</sup> College of Chemical Engineering, State Key Laboratory of Advanced Separation Membrane Materials, Zhejiang University of Technology, Hangzhou 310014, China

<sup>c</sup> Department of Chemistry, University of Otago, Dunedin 9054, New Zealand

Email: [bhawkins@chemistry.otago.ac.nz](mailto:bhawkins@chemistry.otago.ac.nz)

**Supplementary Information (SI)**

1	Additional information and data.....	1
1.1	Initial findings and work under anhydrous conditions .....	1
1.1.1	Oxidation under anhydrous conditions .....	1
1.1.2	Oxidation under aqueous conditions and the effect of dried HFIP .....	4
1.1.3	Oxidation of allyl benzyl ether (2a) under aqueous conditions .....	8
1.1.4	Comparing activity of the <i>in-situ</i> and isolated catalyst forms .....	9
1.1.5	Influence of lower TBHP content.....	11
1.1.6	Diminished activity .....	12
1.2	Additional work under aqueous conditions .....	14
1.2.1	Oxidation of allyl phenyl ether with 0.5 mol% catalyst: the effect of temperature 14	
1.2.2	Oxidation of allyl phenyl ether: effect of HFIP with 1 mol% catalyst .....	15
1.2.3	Oxidation of allyl phenyl ether with 0.5 mol% catalyst: increased quantities of HFIP at 0.5 mol% and 1 mol% catalyst loadings .....	16
1.2.4	Oxidation of allyl phenyl ether: effect of lower initial temperature .....	17
1.2.5	Gradual addition of substrate and catalyst.....	18
1.2.6	Investigating catalyst activity and potential product inhibition .....	19
1.2.7	Additional tests with allyl benzyl ether (2a) .....	21
1.3	Additional work with APE derivatives and functional group tolerance .....	22
1.3.1	Oxidation of derivatives; initial findings at 1 and 1.5 mol% catalyst loading ....	22
1.3.2	Oxidation of derivatives; reaction profiles .....	23
1.3.3	Oxidation of allyl phenyl ether; effect of additives on catalyst activity .....	24
1.4	Additional work with complex substrates.....	25
1.4.1	Oxidation of complex substrates: initial screenings with <sup>1</sup> H-NMR .....	25
1.4.2	Oxidation of complex substrates: problematic substrates .....	27
2	General Considerations .....	28
2.1	Chemicals and equipment.....	28
2.2	GC analysis of reaction samples .....	28
2.3	Safety considerations .....	32
3	Synthetic procedures.....	33
3.1	Synthesis of 2-(5-(trifluoromethyl)pyridin-2-yl)benzo[d]oxazole (5-CF <sub>3</sub> -PBO).....	33

3.2	Synthesis of [Pd(2-(5-(trifluoromethyl)pyridin-2-yl)benzo[d]oxazole) (solvent) <sub>2</sub> ][OTf] <sub>2</sub> ([Pd(5-CF <sub>3</sub> PBO)(S) <sub>2</sub> ][OTf] <sub>2</sub> ).....	34
3.3	Synthesis of allyl phenyl ether derivatives.....	35
3.3.1	Allyl 2,6-dimethylphenyl ether (4a).....	36
3.3.2	Allyl 2,6-diisopropylphenyl ether (5a) .....	36
3.3.3	Allyl 4- <i>tert</i> -butylphenyl ether (6a).....	37
3.3.4	Allyl 4-nitrophenyl ether (7a).....	37
3.3.5	Allyl 4-trifluoromethylphenyl ether (8a) .....	38
3.3.6	Allyl 4-iodophenyl ether (10a).....	38
3.3.7	Allyl 4-methoxyphenyl ether (11a).....	39
3.3.8	<i>Tert</i> -butyl 4-(allyloxy)benzoate (12a).....	39
3.3.9	Allyl 4-cyanophenyl ether (13a) .....	40
3.3.10	Allyl 3-morpholinophenyl ether (14a).....	40
3.4	Synthesis of compounds 16a to 25a .....	41
3.4.1	Synthesis of compounds 16a, 17a, 18a, 19a, 21a, 22a, 24a and 25a .....	41
3.4.2	Synthesis of compound 20a (1-(4-oxo-2-phenyl-4H-chromen-3-yl)but-3-en-2-yl acetate) 41	
3.4.3	Synthesis of compound 23a (( <i>E</i> )-3-(buta-1,3-dien-1-yl)-2-phenyl-4H-chromen-4-one) 42	
4	Oxidation reactions .....	43
4.1	Oxidation of allylic substrates: general procedure .....	43
4.2	Oxidation of allylic substrates: cold-start conditions .....	44
4.3	Oxidation of allylic substrates: effect of additives .....	45
4.4	Oxidation and isolation of allyl phenyl ether derivatives (3a to 15a) .....	46
4.4.1	1-( <i>o</i> -tolylloxy)propan-2-one (3b) .....	47
4.4.2	1-(2,6-dimethylphenoxy)propan-2-one (4b) .....	47
4.4.3	1-(2,6-diisopropylphenoxy)propan-2-one (5b).....	48
4.4.4	1-(4-( <i>tert</i> -butyl)phenoxy)propan-2-one (6b) .....	48
4.4.5	1-(4-nitrophenoxy)propan-2-one (7b) .....	49
4.4.6	1-(4-(trifluoromethyl)phenoxy)propan-2-one (8b) .....	49
4.4.7	1-(2,4,6-tribromophenoxy)propan-2-one (9b).....	50
4.4.8	1-(4-iodophenoxy)propan-2-one (10b).....	50

4.4.9	1-(4-methoxyphenoxy)propan-2-one (11b) .....	51
4.4.10	tert-butyl 4-(2-oxopropoxy)benzoate (12b) .....	51
4.4.11	4-(2-oxopropoxy)benzotrile (13b) .....	52
4.5	Oxidation of compounds 16a to 20a .....	53
4.5.1	Oxidation of 6-vinyl-6,7-dihydro-8H-benzo[2,3]oxepino[4,5-b]chromen-8-one (16a) .....	53
4.5.2	Oxidation of ethyl 6-bromo-8-methyl-5'-vinyl-4',5'-dihydro-3'H-spiro[chromane-2,2'-furan]-3'-carboxylate (17a) .....	55
4.5.3	Oxidation of ethyl 8-bromo-6-methoxy-4-methyl-5'-vinyl-4',5'-dihydro-3'H-spiro[chromane-2,2'-furan]-3'-carboxylate (18a).....	56
4.5.4	Oxidation of 3-(2-hydroxybut-3-en-1-yl)-2-phenyl-4H-chromen-4-one (19a) ...	57
4.5.5	Oxidation of 1-(4-oxo-2-phenyl-4H-chromen-3-yl)but-3-en-2-yl acetate (20a).	58
5	NMR spectra .....	59
6	References .....	151

# 1 Additional information and data

## 1.1 Initial findings and work under anhydrous conditions

### 1.1.1 Oxidation under anhydrous conditions

Oxidation of allylic ether substrates was initially tested using the *in-situ* catalyst system, [Pd(5-CF<sub>3</sub>-PBO)Cl<sub>2</sub>]/Ag[OTf] described in previous work.<sup>1</sup> Allyl phenyl ether (APE, **1a**) was initially oxidised under anhydrous conditions at a 1 mol% catalyst loading (Figure S1), where rapid oxidation to the corresponding methyl ketone, phenoxy-2-propanone (P2P, **1b**) was observed. In the absence of HFIP, the methyl ketone yield was markedly lower. However, the reaction displayed a peak-and-decay pattern, where the product yield decreased. In both cases, early sample points indicate high mass balance, but this slowly drops in the presence and absence of HFIP. Some additional, smaller signals also appeared in the GC trace.

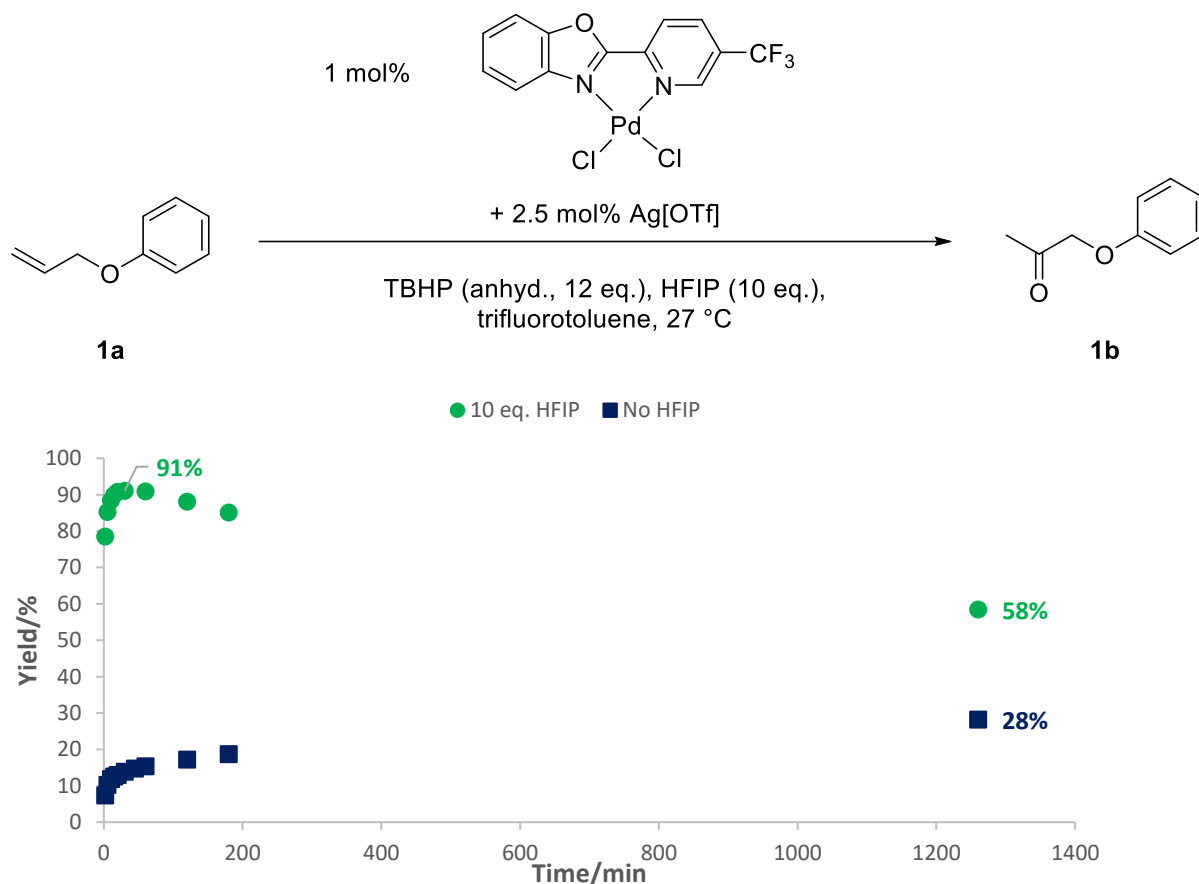


**Figure S1:** Oxidation of APE (**1a**) in the presence and absence of HFIP under anhydrous conditions. Results are an average of two reactions. Analyzed by GC-FID with an internal standard.

To check if product decomposition could be temperature dependent, Wacker oxidation of **1a** was compared at 0 °C, 27 °C and 40 °C (Figure S2). It might be reasoned that with increasing and decreasing temperature, the proposed hydrogen-bonding interaction between HFIP and the substrate/product oxygen atoms could be disrupted or enhanced respectively, possibly influencing how other components of the reaction interact with the product. Hong and co-workers noted that for their PdCl<sub>2</sub>/polyoxometalate system that increasing temperature between 30 °C and 80 °C affords little change in conversion, but slightly diminished yields of the desired methyl ketone product and increased formation of the phenol.<sup>2</sup> We found that at 40 °C, oxidation of **1a** was largely similar and product yield still dropped to similar levels as seen at 27 °C. At 0 °C, the reaction was significantly slower but remained stable for the entire reaction duration. However, these colder conditions gave a lower maximum yield compared to those at 27 °C and 40 °C.

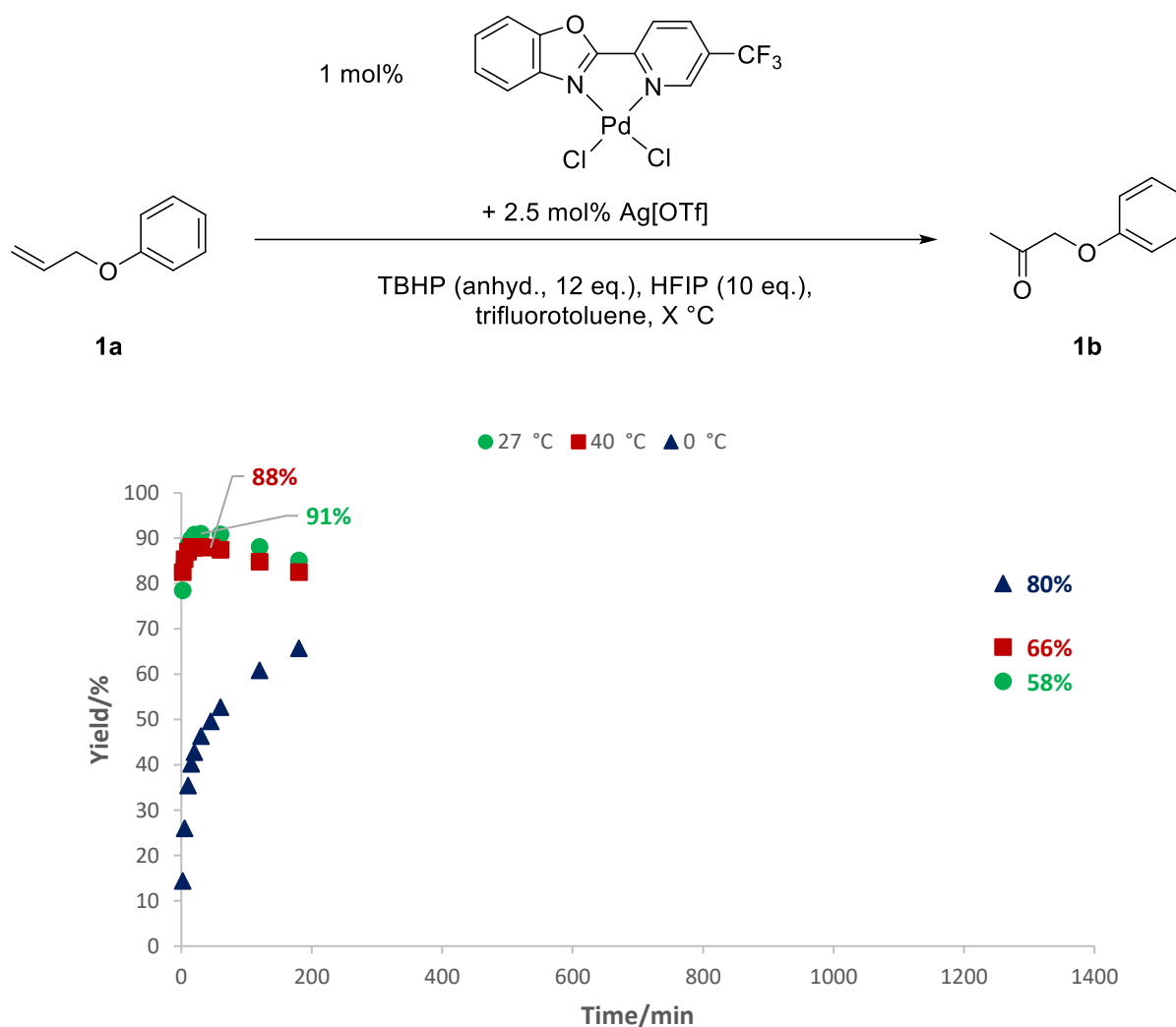


**Figure S2:** Oxidation of **1a** at 0 °C, 27 °C and 40 °C. Results are an average of two reactions. Analyzed by GC-FID with an internal standard.

## Investigating loss of phenoxy-2-propanone (P2P)

The loss of product (**1b**) and subsequent mass balance gap resulting over time from oxidation of **1a** prompted further investigation. Several control reactions were run whereby **1b** was subject to the reaction conditions with individual components removed, to see how their absence effected **1b** loss (Figure S3). Under standard conditions, **1b** content decreased to a final yield of 36%. The unassigned signals observed over the course of the reaction match closely with those seen during oxidation of **1a**. Without the catalyst present, no appreciable loss of **1b** is observed. In all other instances, when the catalyst is present, loss of **1b** results. This indicates that the process involves the catalyst.

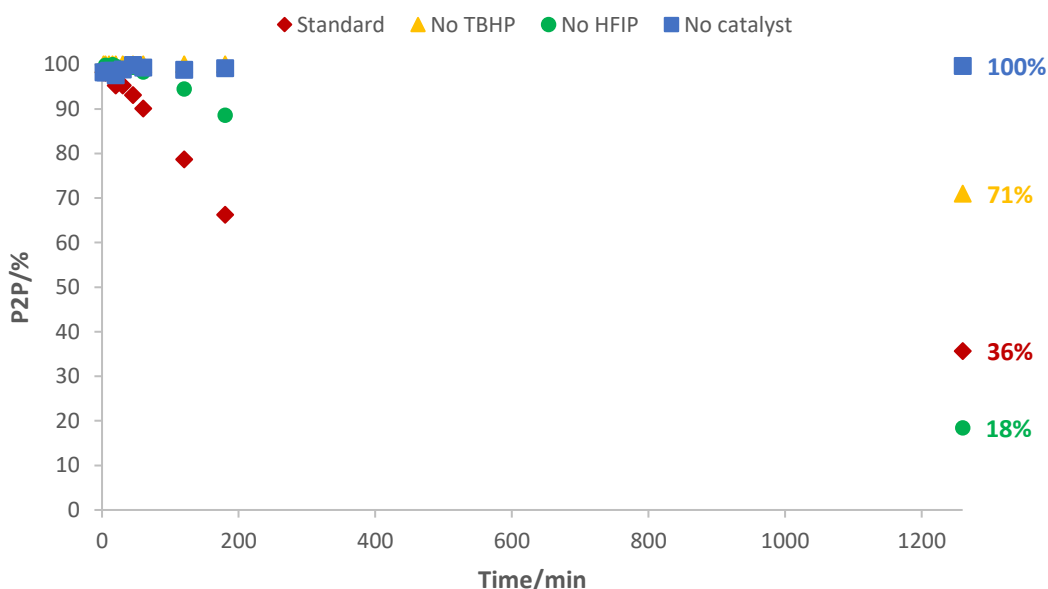
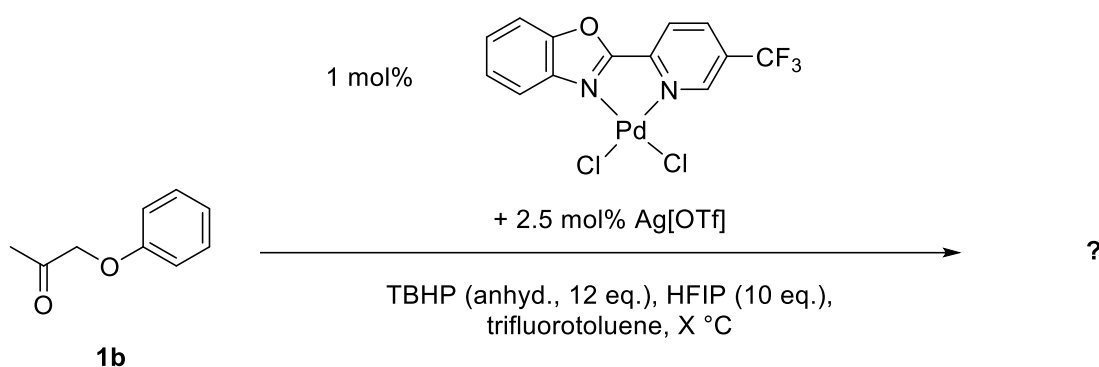


**Figure S3:** Control tests with **1b** under anhydrous reaction conditions, where reactions components have been removed. Analyzed by GC-FID with an internal standard.

Without TBHP, no appreciable loss is observed for the first three hours, but after 21 hours approx. 30% of starting **1b** was lost, suggesting that TBHP may also be contributing to the observed decay, but the presence of catalyst still allows this to occur. Without HFIP, the greatest loss of **1b** was seen, suggesting that HFIP helps prevent this process, which would make sense if HFIP and **1b** interact, possibly reducing product-catalyst interaction. All of these observations seem to point to a catalyst-promoted means for loss of **1b** and given that this occurs more readily with TBHP present, this may be oxidative in nature. The loss of **1b** was also inspected with samples from Wacker oxidation at 40 °C analyzed by gas chromatography-mass spectrometry (GC-MS). The methyl ketone product, **1b**, was confirmed. Other compounds were identified, but these were inconsistent across samples and match scores were low. Aside from **1a**, **1b** and dodecane (internal standard), two compounds that were identified consistently with high match scores were phenyl formate and benzaldehyde, but it is unclear how these species would form from **1b**. Regardless, the very low areas of these signals indicate trace quantities that would be unlikely to account for the entirety of lost material. Investigating potential reactions of **1b** in the presence of Pd(II) and/or peroxides has not suggested any clear pathways either. Further investigation of this behaviour is needed to gain a better insight, such as isolating the reaction components.

### 1.1.2 Oxidation under aqueous conditions and the effect of dried HFIP

TBHP is commonly supplied as an aqueous solution, so in order to carry out reactions under anhydrous conditions, TBHP/trifluorotoluene solutions need to be prepared. As it would be practically advantageous, the oxidation of **1a** was investigated under aqueous conditions (Figure S4). Without HFIP, the reaction was slower, which correlates with previous findings.<sup>1</sup> With HFIP, slower initial activity was seen compared to anhydrous conditions, but a similar maximum yield resulted. More notably however, the reaction under aqueous conditions does not display the previously seen product decomposition, suggesting water creates more stable conditions for **1b**.

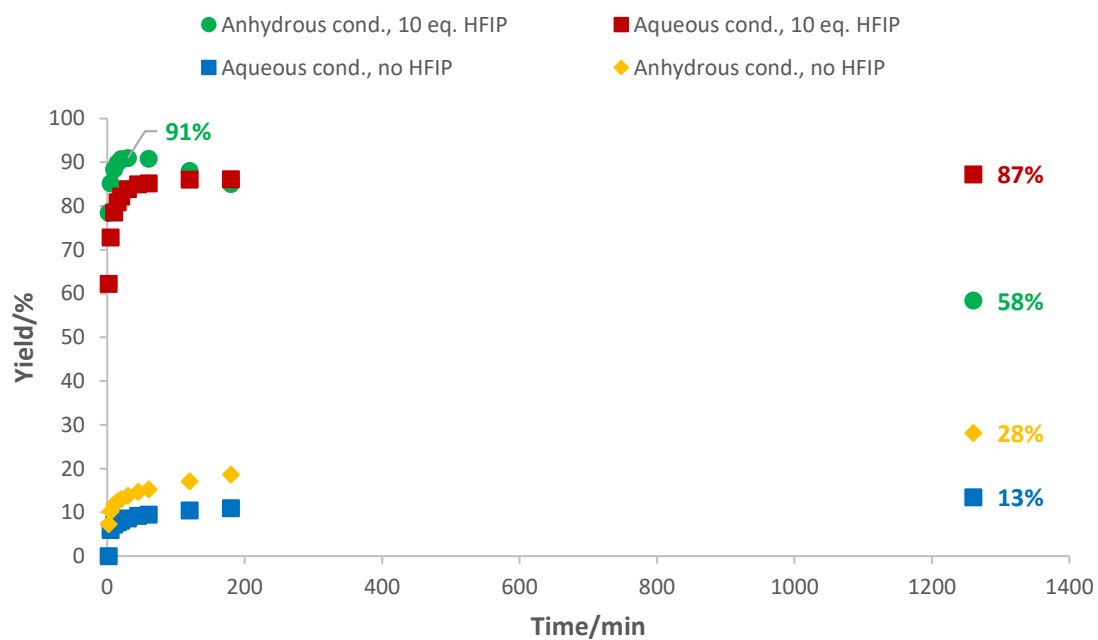
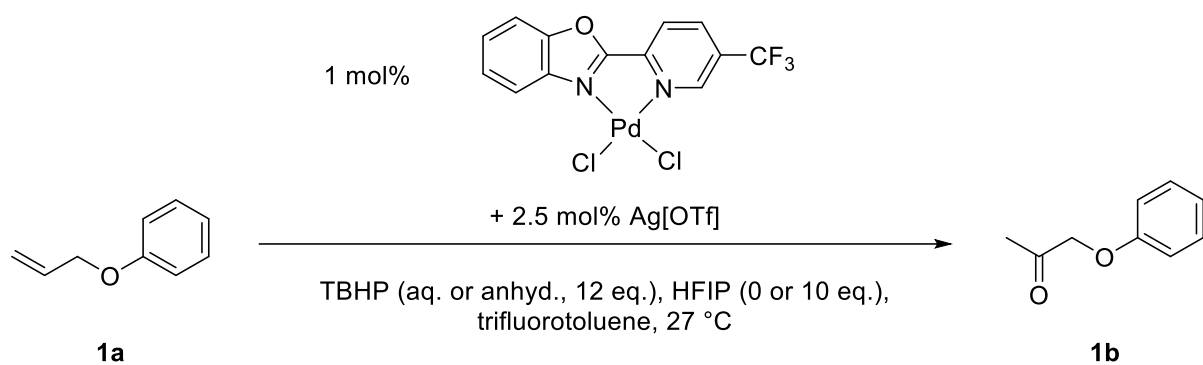


**Figure S4:** Oxidation of **1a** under aqueous and anhydrous conditions, with or without HFIP. Analyzed by GC-FID with an internal standard.

In the initial test under aqueous conditions, HFIP that was dried overnight with 3 Å molecular sieves as per the procedure for anhydrous reaction conditions was used, as it was not anticipated that this would have any effect under the conditions. However, the reaction employing this dried HFIP was found to be much less efficient compared to conditions with undried HFIP (Figure S5). This led us to consider if using molecular sieves introduces some contaminant and if there was a connection with the activity issues seen at 0.25 mol% catalyst loading.<sup>1</sup>

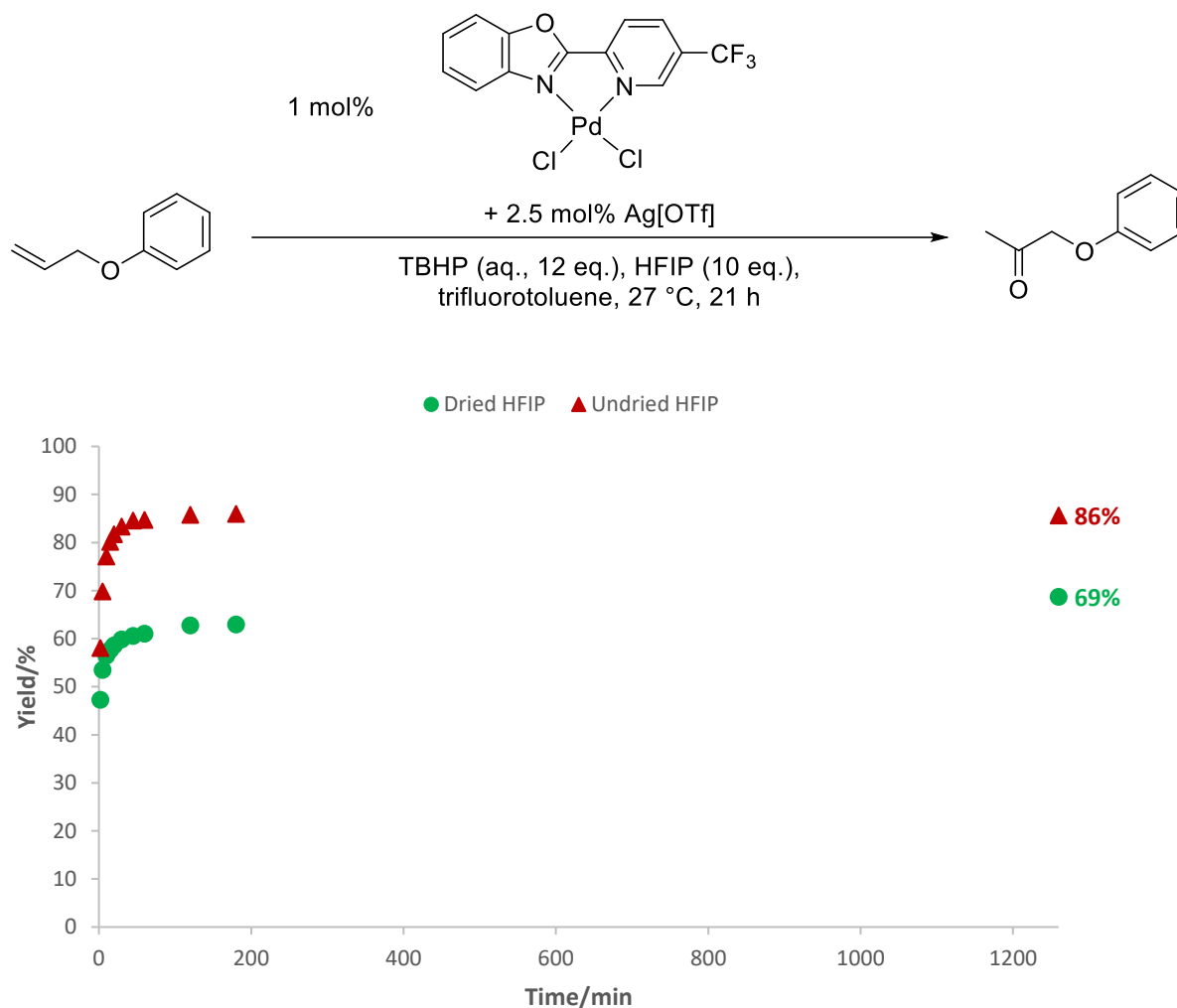


**Figure S5:** Reaction profile for the oxidation of allyl phenyl ether with *in-situ* catalyst under aqueous conditions, comparing the effect of dried and undried HFIP. Analyzed by GC-FID with an internal standard.

A control reaction whereby dried HFIP was passed through a 0.2 µm syringe filter before addition to an aqueous reaction was run; Figure S6 shows that whilst some improvement in

activity was seen, the results obtained remained inferior to those employing undried HFIP, suggesting that any potential contaminants in the dried HFIP are too small to be filtered.

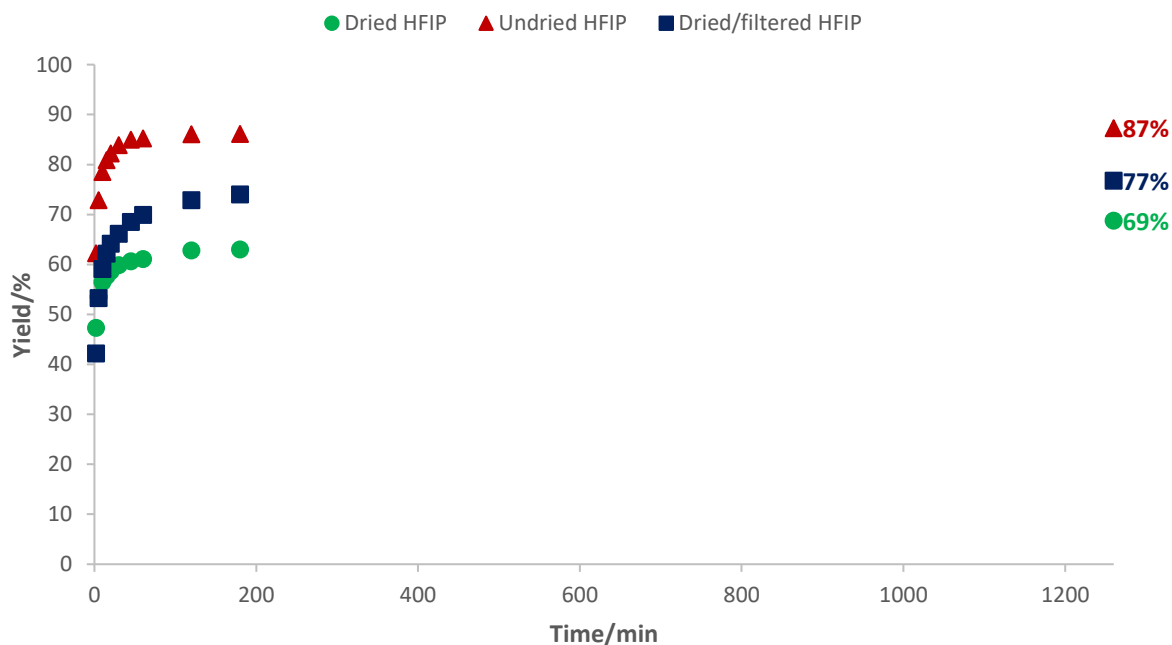
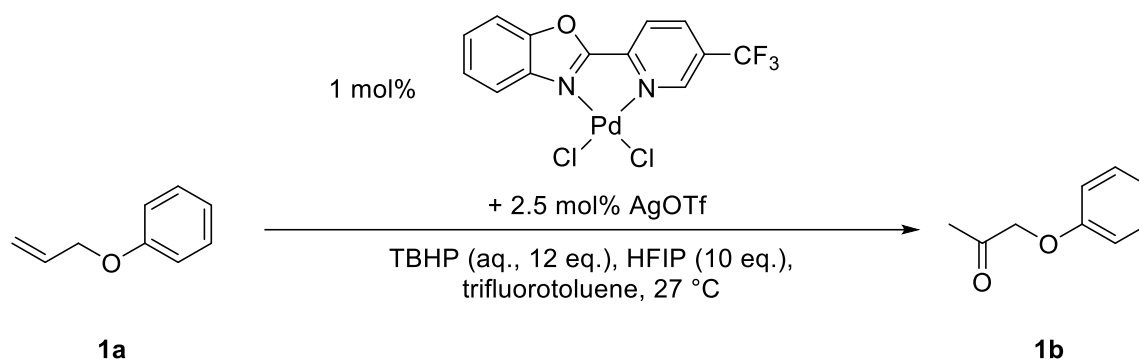


**Figure S6:** Comparison of oxidation of allyl phenyl ether under aqueous conditions with dried, undried and dried/filtered HFIP. Analyzed by GC-FID with an internal standard.

### 1.1.3 Oxidation of allyl benzyl ether (**2a**) under aqueous conditions

Another allylic ether substrate, allyl benzyl ether (ABE, **2a**) was tested under aqueous and anhydrous conditions (Figure S7). Under aqueous conditions, conversion to the methyl ketone, benzyloxyacetone (BOA, **2b**) was more rapid and affords a higher yield compared to anhydrous conditions. Under both aqueous and anhydrous conditions however, the same peak-and-decay pattern for the product is seen, although product loss was lower under aqueous conditions. Product loss appears to occur more readily for oxidation of **2a** compared to **1a**, suggesting the former is more reactive.

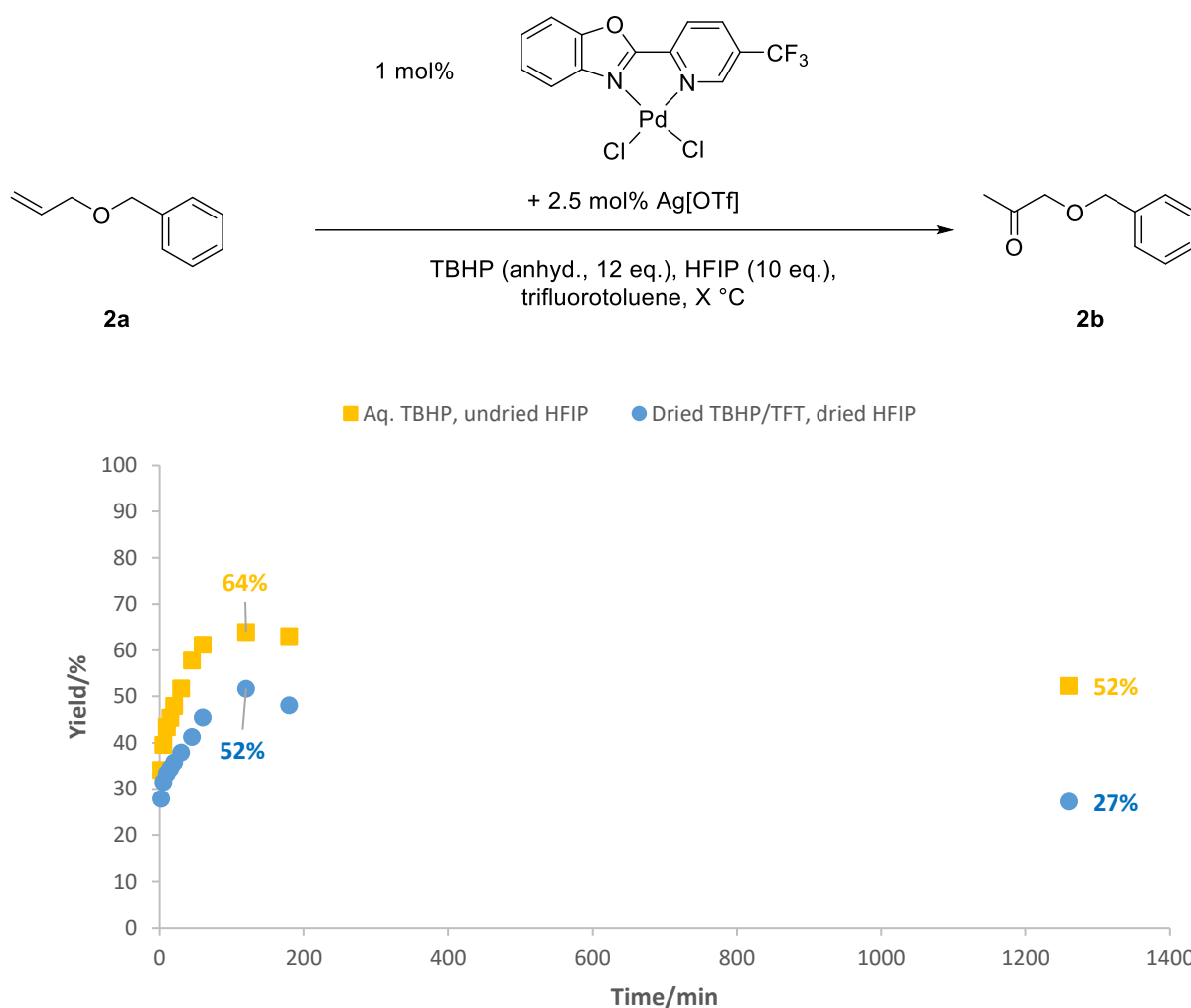


**Figure S7:** Comparisons of oxidation of **2a** in anhydrous/aqueous TBHP with dried/undried HFIP. Analyzed by GC-FID with an internal standard.

The effect of sieves was also examined when Wacker oxidation of ABE was inspected under aqueous conditions. As Figure S8 shows, better results were seen using aqueous TBHP and when dried HFIP was used, lower catalytic activity was seen.

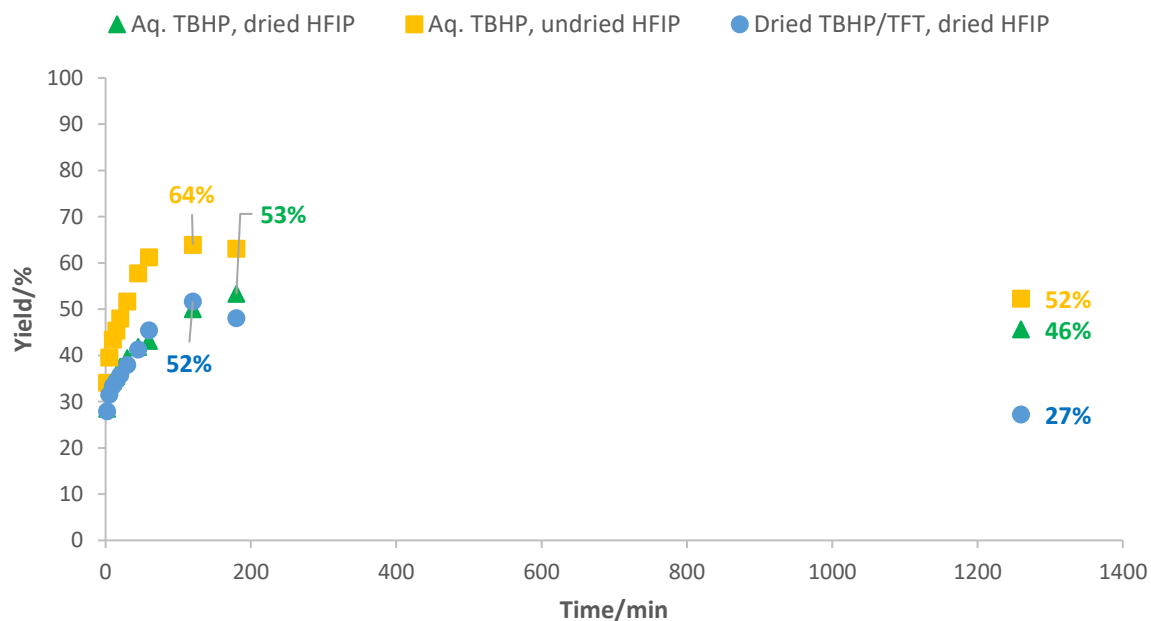
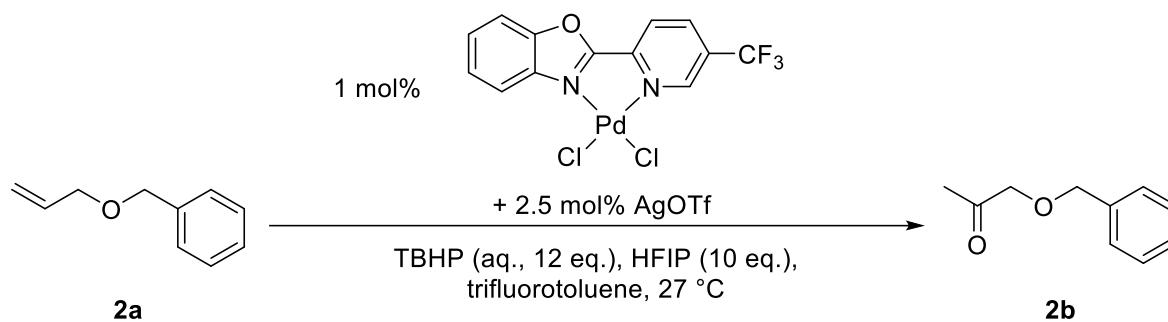


**Figure S8:** Oxidation of ABE under different conditions with dried/undried TBHP/HFIP. Analyzed by GC-FID with an internal standard.

#### 1.1.4 Comparing activity of the *in-situ* and isolated catalyst forms

A comparison between the  $[\text{Pd}(5\text{-CF}_3\text{-PBO})\text{Cl}_2]/\text{Ag}[\text{OTf}]$  and  $[\text{Pd}(5\text{-CF}_3\text{-PBO})(\text{S})_2][\text{OTf}]_2$  (where S = solvent, acetonitrile or  $\text{H}_2\text{O}$ ) complexes was carried out for oxidation of **1a**. At 27 °C, similar results were obtained between the two forms, in line with previous observations using this catalyst (Figure S9).<sup>1</sup> Running the reaction at 0 °C gives lower yields for both catalysts and 40 °C gives only slight yield improvement using the isolated catalyst. The *in-situ* catalyst form gave slightly better results, but the overall difference is small.

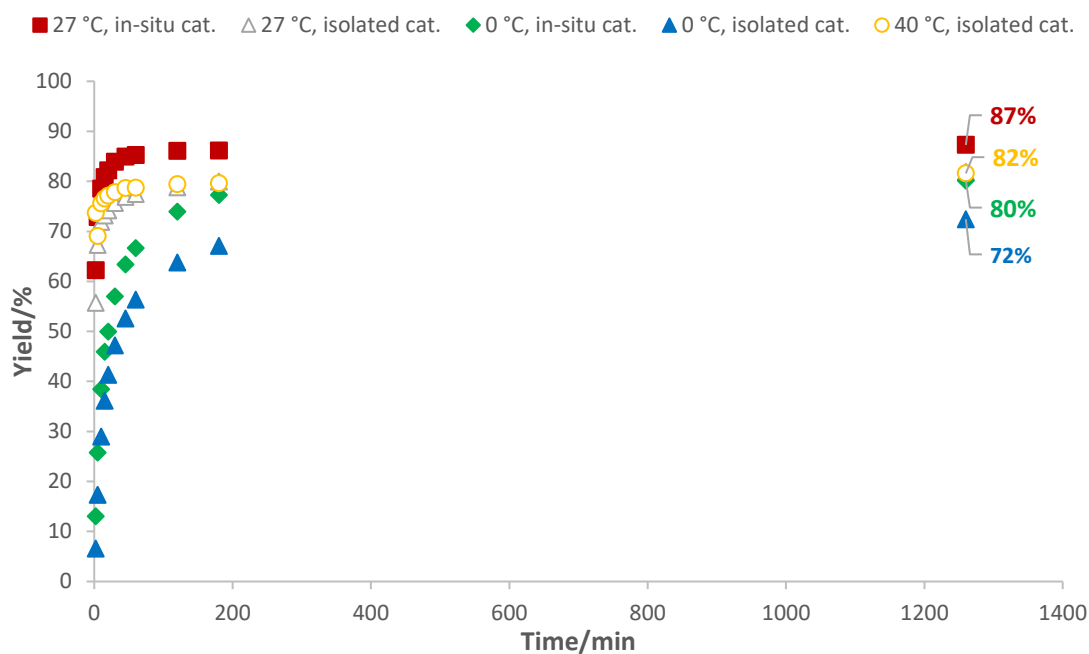
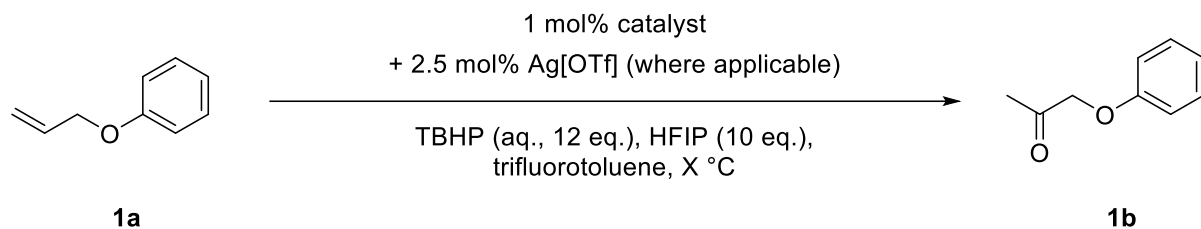


**Figure S9:** Oxidation of **1a** under aqueous conditions with *in-situ* and isolated catalysts. Analyzed by GC-FID with an internal standard.

### 1.1.5 Influence of lower TBHP content

Given that **1a** is converted rapidly to high yields of **1b**, we also considered using less TBHP. Figure S10 shows that using 6 eq. gives a lower yield compared to the normal 12 eq. TBHP. This lower yield agrees with findings in our previous work<sup>1</sup> and in work by others.<sup>3-5</sup>

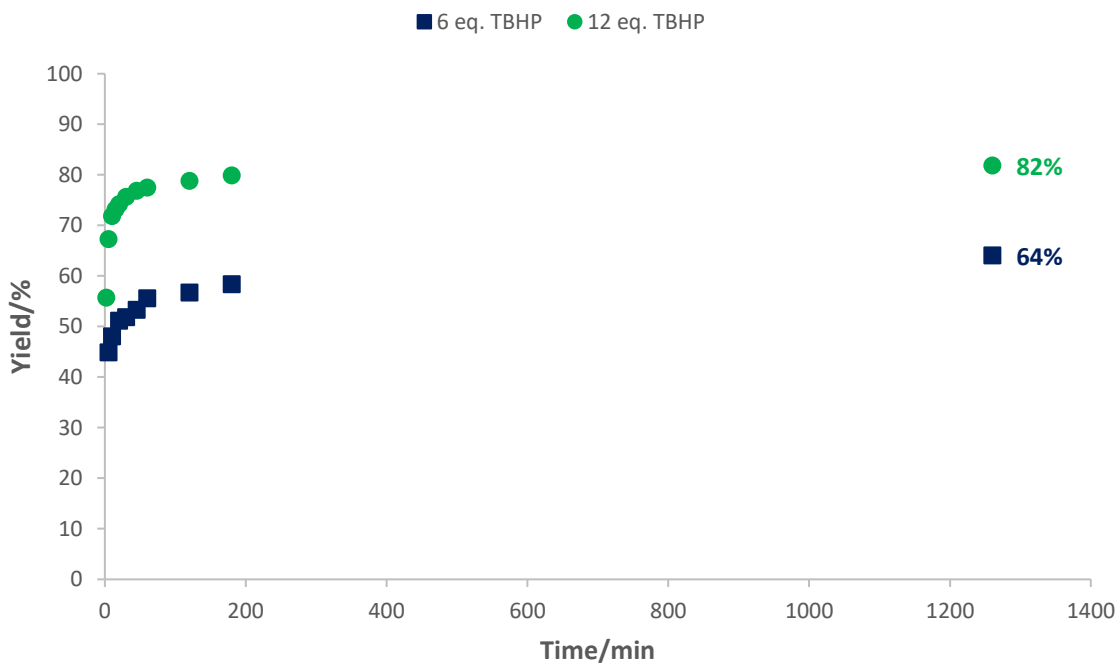
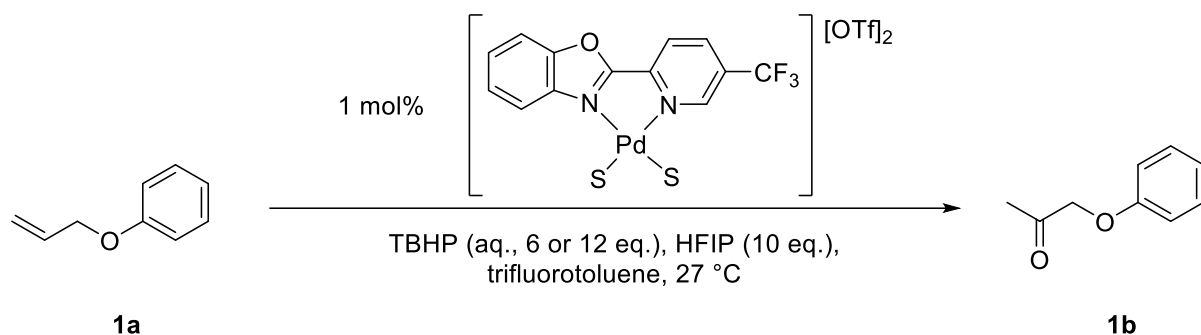


**Figure S10:** Oxidation of **1a** with 6 or 12 eq. TBHP using 1 mol%  $[\text{Pd}(5\text{-CF}_3\text{-PBO})(\text{S})_2][\text{OTf}]_2$ . Analyzed by GC-FID with an internal standard.

### 1.1.6 Diminished activity

Shortly after determining what we thought were optimal conditions, using 1 mol% catalyst, the system began to demonstrate lower yields in the oxidation of **1a**. This was seen across multiple catalyst batches and by others with different substrates within the group. In earlier studies<sup>1</sup> examining the substrate oct-1-en-3-yl acetate, we had found that when using low catalyst loadings (0.25 mol%) results had become inconsistent, due to poisoning from small impurities. For these studies with **1a** we decided to look at a number of variables. Figure S11 outlines the range of aspects inspected. The dodecane internal standard was added at the end (Figure S11, IS end) of the reaction in case it was playing a role. The slightly better performance of the *in-situ* catalyst variant gave rise to the idea that it could be some ionic component that could be causing the problem – with the inclusion of silver triflate under *in situ* conditions, it is possible that some ion-scavenging could take place. The vial was also pre-rinsed with ultra-pure deionised water (Figure S11, Rinse) and dried to try and remove any potential contaminants on the glass, as well trying a vial from a completely new tray (Figure S11, “vialtray”). New micropipettes (Figure S11, “Micropip”) and magnetic stirrers (Figure S11, “Stirbar”) were also tested. It was ultimately found that catalyst performance could be restored by increasing the HFIP content to 20 eq. (Figure S12).

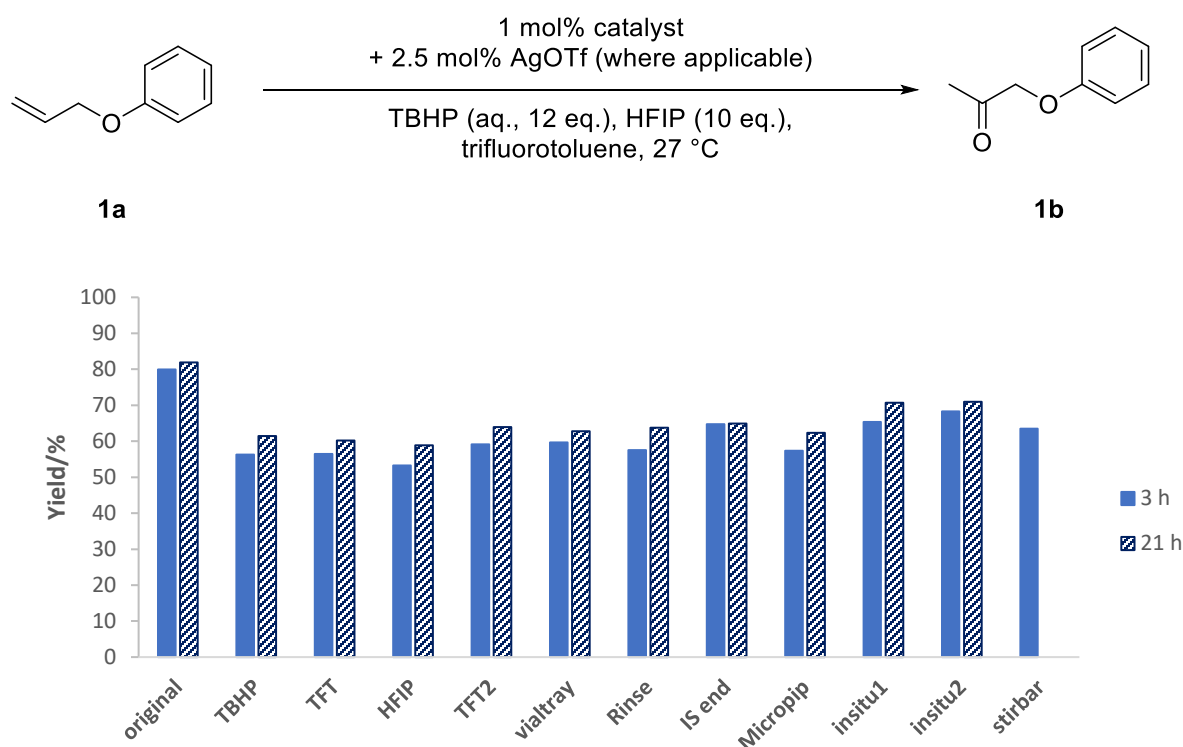


**Figure S11:** Results obtained in work investigating each reaction parameter following observation of diminished results. Unless stated (insitu1/insitu2), reactions tested the [Pd(5-CF<sub>3</sub>-PBO)(S)<sub>2</sub>][OTf]<sub>2</sub> complex. Analyzed by GC-FID with an internal standard.

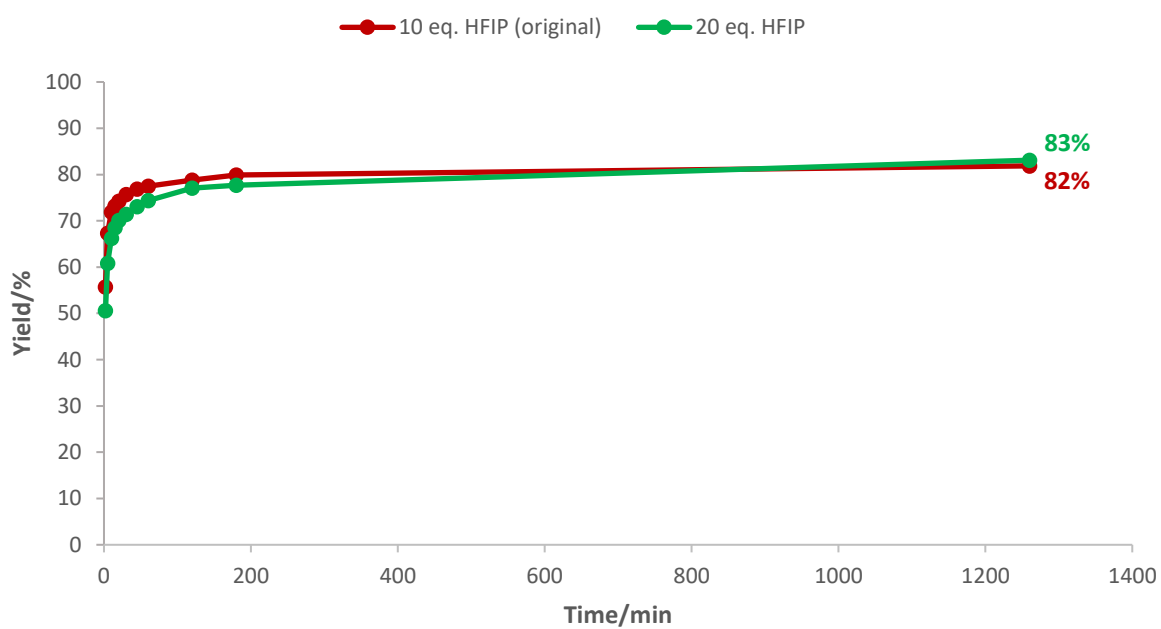
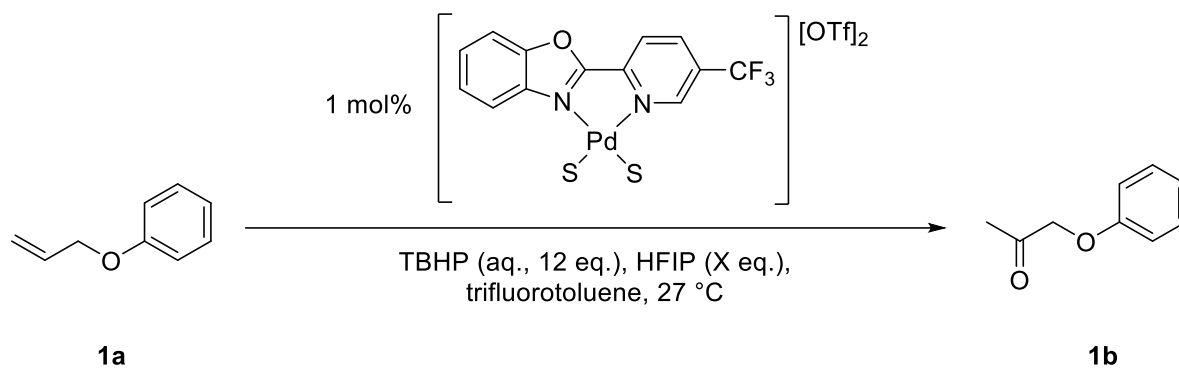


**Figure S12:** Using increased HFIP content (20 eq.) to re-establish previously seen levels of activity with 10 eq. HFIP. Analyzed by GC-FID with an internal standard.

## 1.2 Additional work under aqueous conditions

### 1.2.1 Oxidation of allyl phenyl ether with 0.5 mol% catalyst: the effect of temperature

At 0.5 mol% catalyst loading, the reaction proceeds more slowly, but also more selectively. At 27 °C, conversion reaches 48% (43% yield) and with the reaction held at 0 °C for 30 minutes before transfer to a heating block at 27 °C, conversion becomes 59% (55% yield) after 4 hours. This shows the latter approach improves performance at this lower loading as well. Additionally, the reaction profiles show catalyst activity decreases more quickly at 27 °C (Figure S13), further suggesting that initially holding the reaction at 0 °C serves to extend catalyst lifetime.

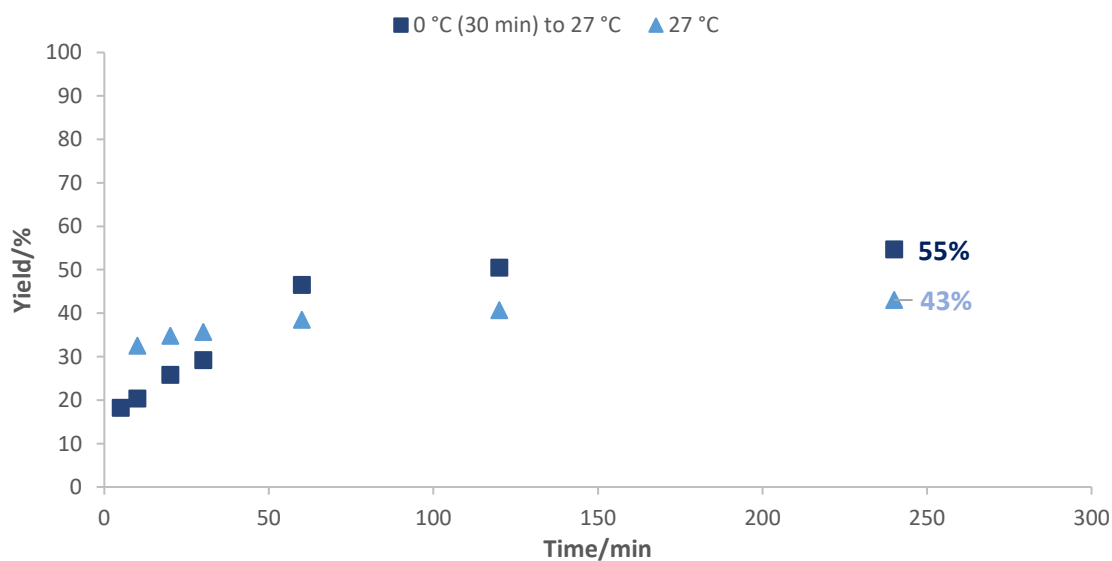
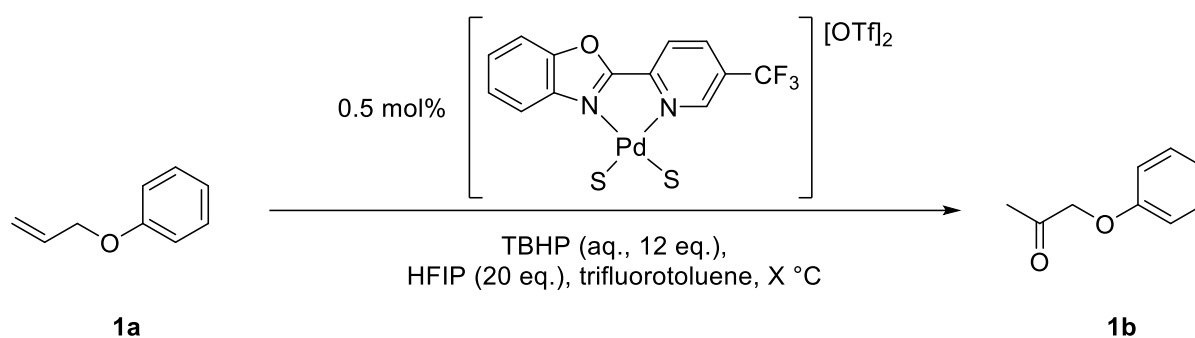


**Figure S13:** Oxidation of **1a** with 0.5 mol% catalyst at 27 °C and with 0 °C chill conditions. Analyzed by GC-FID with an internal standard.

## 1.2.2 Oxidation of allyl phenyl ether: effect of HFIP with 1 mol% catalyst

The effect of transferring reactions directly to 27 °C after initiating at 0 °C was also studied (Figure S14). In these experiments, the reaction vial was chilled at 0 °C and following stirring for 5 minutes and then addition of the substrate, the vial was immediately transferred to an aluminium block set at 27 °C. This was also done with different HFIP quantities to inspect the effect of increased HFIP content at 1 mol% catalyst loading. Little improvement was seen under these conditions and it is preferable to use less HFIP in these reactions, therefore using 20 eq. HFIP was taken as optimal moving forwards.

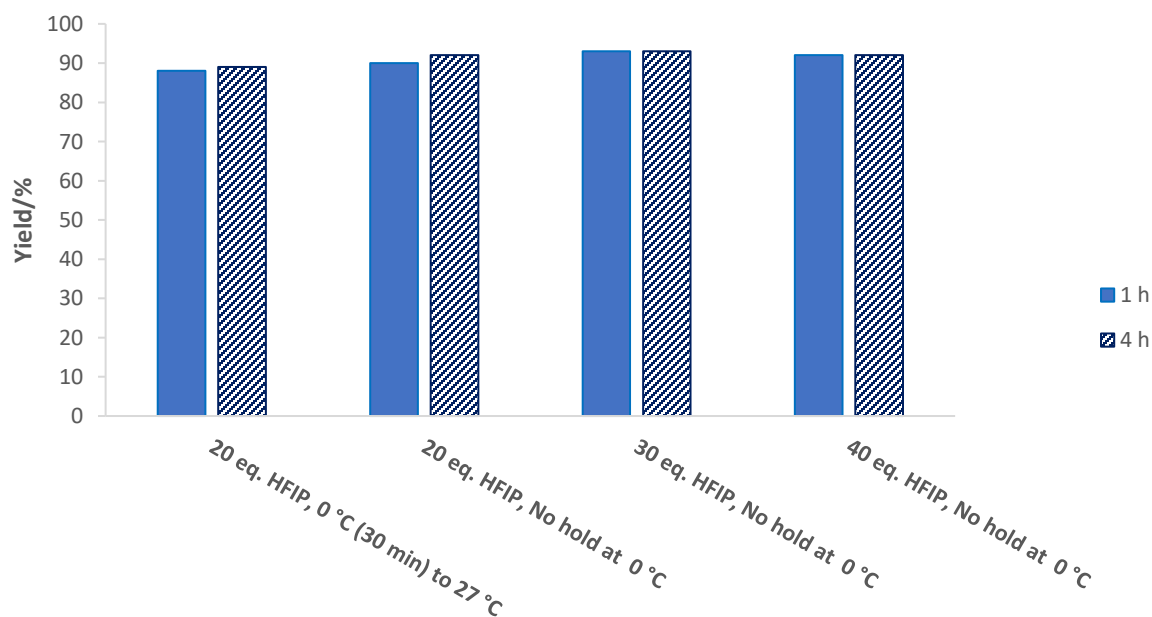
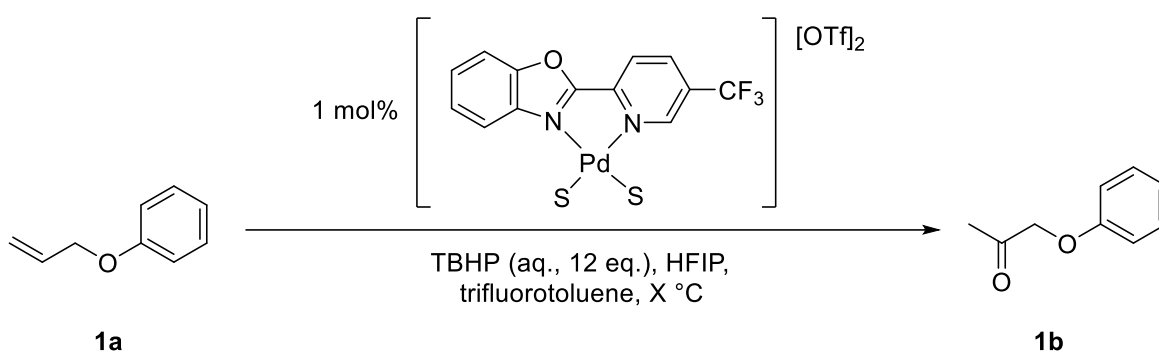


**Figure S14:** Wacker oxidation of **1a**, where reactions were transferred to 27 °C following initiation at 0 °C, with varying HFIP content. Analyzed by GC-FID with an internal standard.

### 1.2.3 Oxidation of allyl phenyl ether with 0.5 mol% catalyst: increased quantities of HFIP at 0.5 mol% and 1 mol% catalyst loadings

At 0.5 mol% catalyst loadings, increasing the HFIP content was found to be beneficial, but only to a point (Figure S15); at 50 and 60 equiv. HFIP, reduced product yield was observed. This is similar to the reduced levels of activity seen in our previous work when the  $[(5\text{-CF}_3\text{-PBO})\text{Pd}(\text{S})_2][\text{OTf}]_2$  catalyst was used to oxidize oct-1-en-3-yl acetate in pure HFIP.<sup>1</sup>

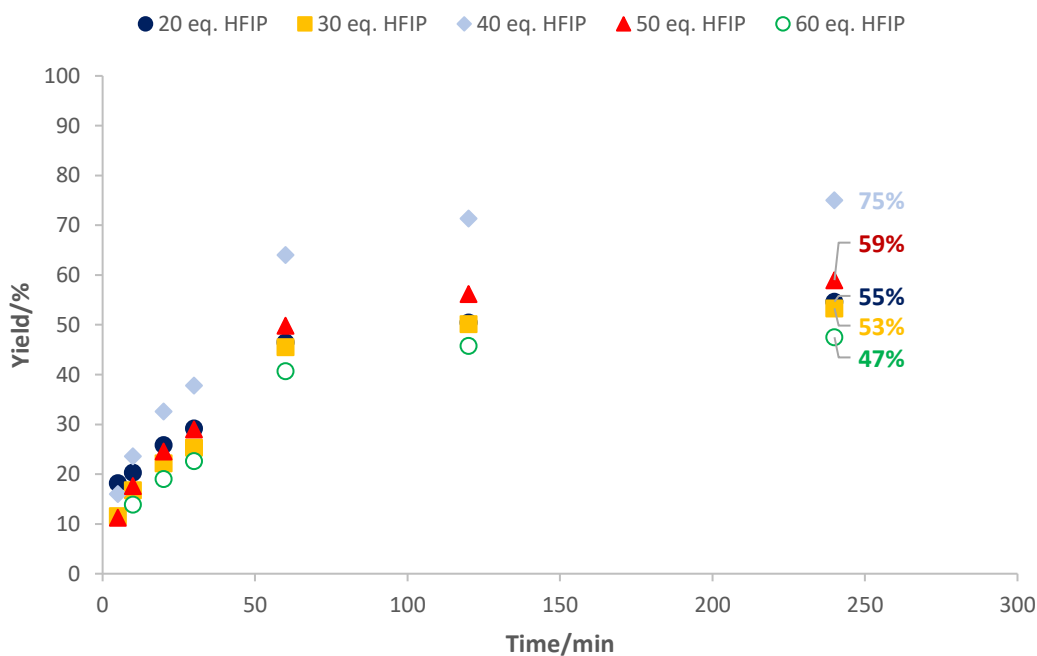
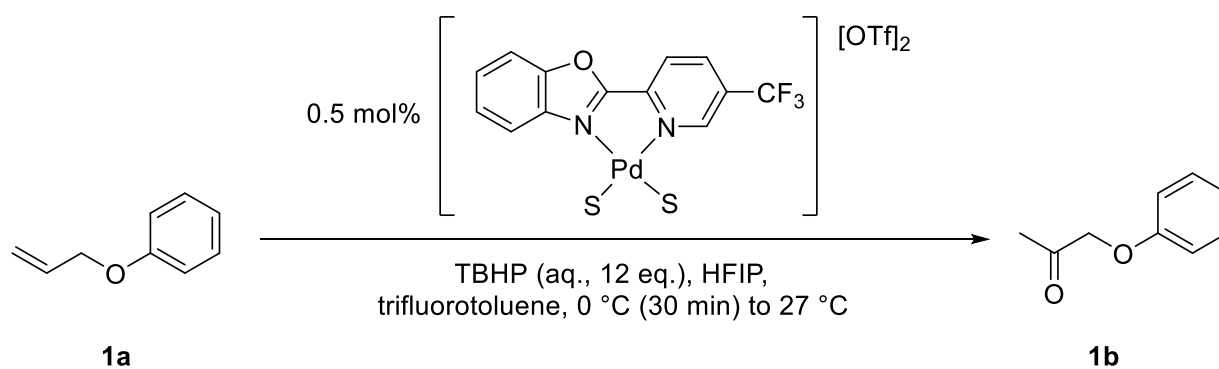


**Figure S15:** Oxidation of **1a** using 0.5 mol%  $[(5\text{-CF}_3\text{-PBO})(\text{S})_2][\text{OTf}]_2$  with different amounts of HFIP. Analyzed by GC-FID with an internal standard.

### 1.2.4 Oxidation of allyl phenyl ether: effect of lower initial temperature

For additional comparison, the reaction at 1 mol% catalyst loading was held at an even lower temperature (-10 °C) for 30 minutes prior to transfer to 27 °C (Figure S16) but this did not afford any improvement.

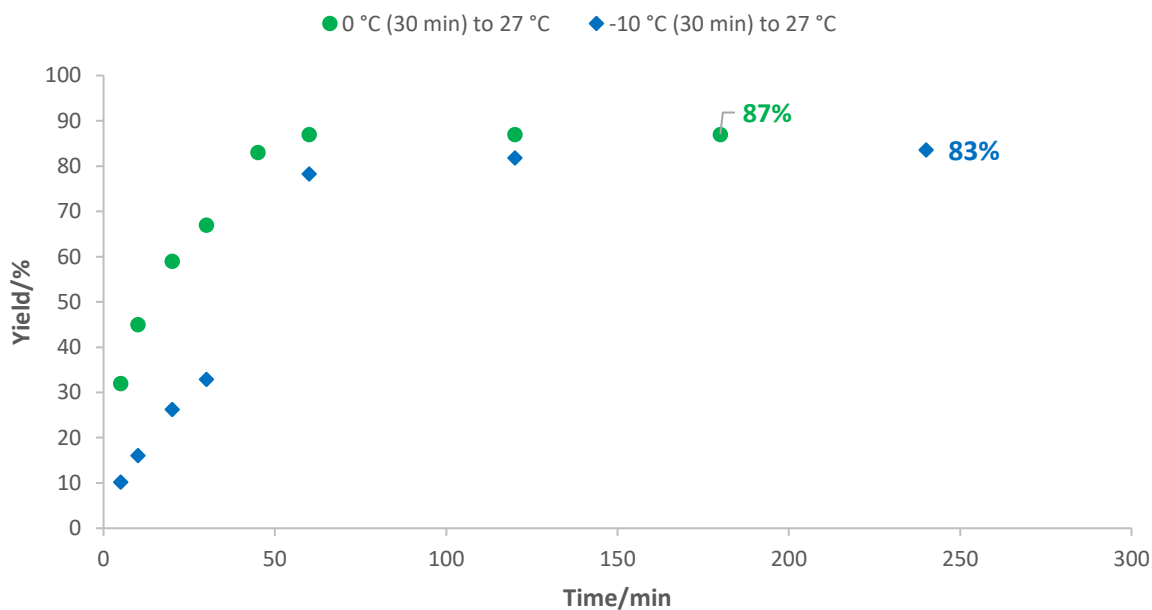
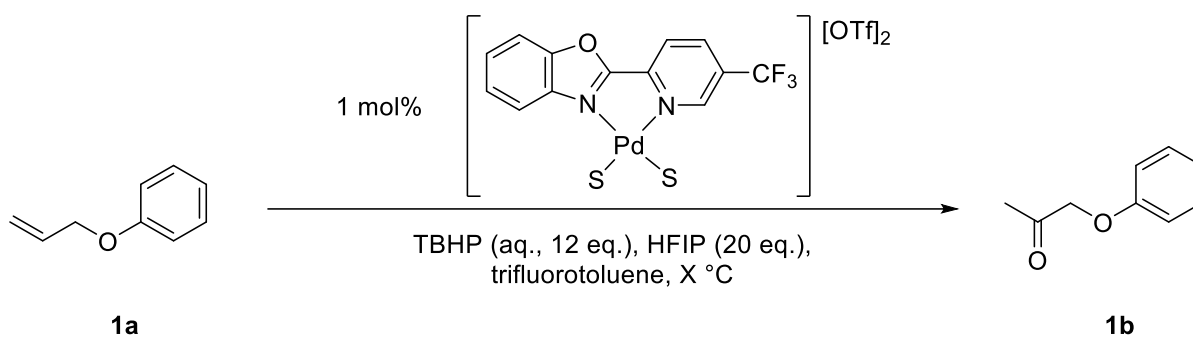


**Figure S16:** Comparison of oxidation of **1a** when held at 0 °C for 30 minutes or the entire reaction or at -10 °C for 30 minutes before transfer to 27 °C. Analyzed by GC-FID with an internal standard.

### 1.2.5 Gradual addition of substrate and catalyst

In an effort to further explore if the reaction could be improved at 0.5 mol%, control tests (Figure S17) were carried out in which the substrate was added gradually over a 1-hour period using a syringe pump. There was no benefit seen to adding the substrate gradually, with a yield of 64%, which was lower than standard conditions. We also examined adding the catalyst in two portions; with an initial 0.25 mol% portion and a second portion after 2 hours, and this approach also led to a lower yield.

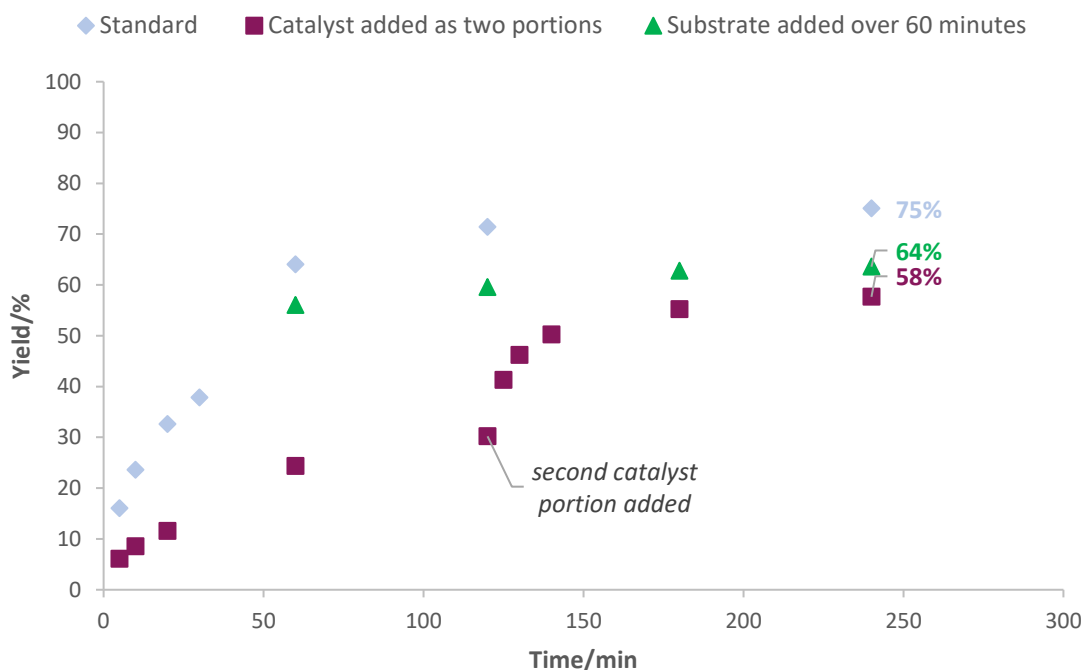
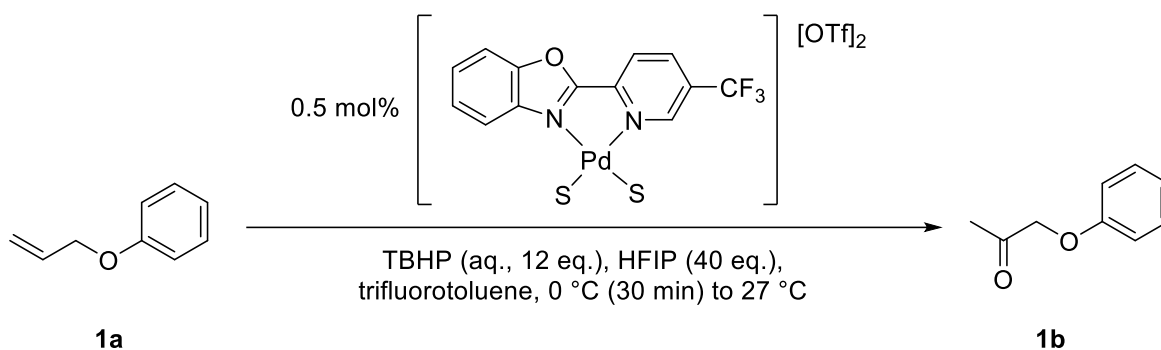


**Figure S17:** Results obtained for the oxidation of **1a** using alternative approaches for catalyst/substrate addition. Analyzed by GC-FID with an internal standard.

## 1.2.6 Investigating catalyst activity and potential product inhibition

Given that oxidation of **1a** with 0° C start conditions proceeds with complete conversion, it was considered if the catalyst remained active. A control reaction where additional **1a** (1 eq.) was added after 3.5 h was carried out to see if any further conversion to **1b** resulted. Figure S18 shows that additional product formation is minimal with catalyst activity is very low by this point.

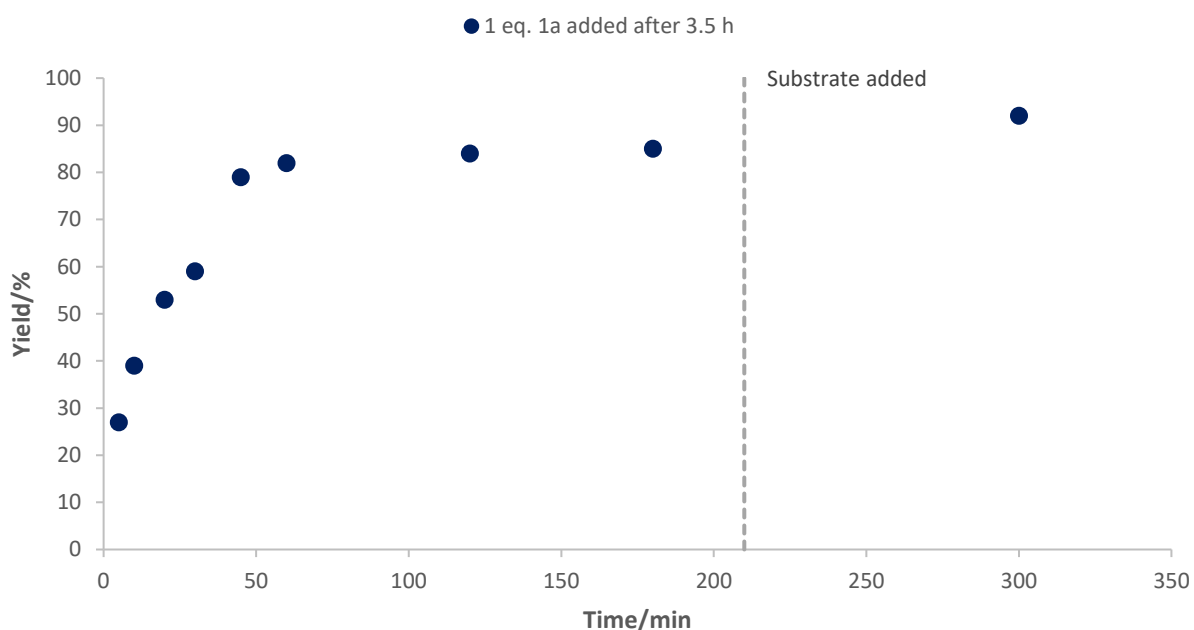
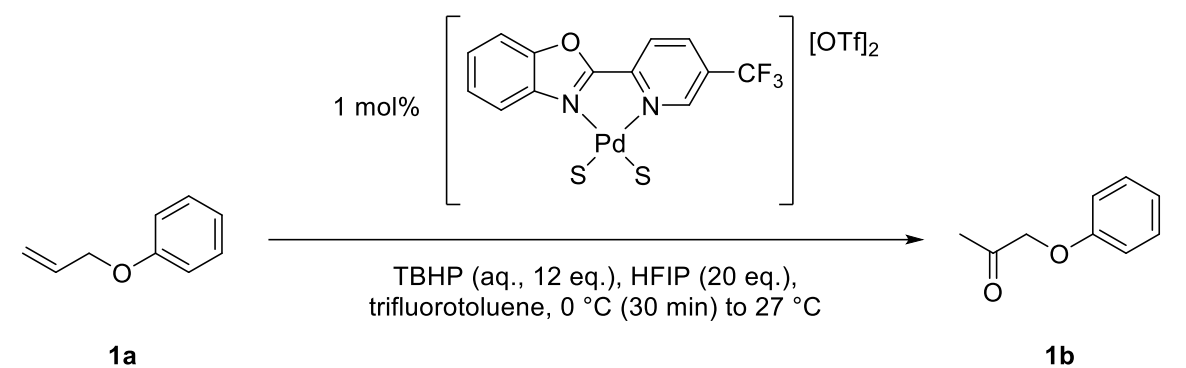


**Figure S18:** Oxidation of **1a** with 1 mol%  $[\text{Pd}(5\text{-CF}_3\text{-PBO})(\text{S})_2][\text{OTf}]_2$  with additional substrate added after 3.5 hours. Analyzed by GC-FID with an internal standard.

In previous work with this catalyst, product inhibition of the catalyst was tested using 2-octanone, which had no appreciable effect on the reaction. However, the ketone products of these allylic ethers are structurally and electronically different. To inspect potential catalyst inhibiting behavior, oxidation of **1a** was carried out with 1 eq. of **2b** added just prior to the substrate. A lower P2P yield was observed (Figure S19), indicating these methyl ketone products can impede the reaction, likely though coordinating to the Pd(II) center.

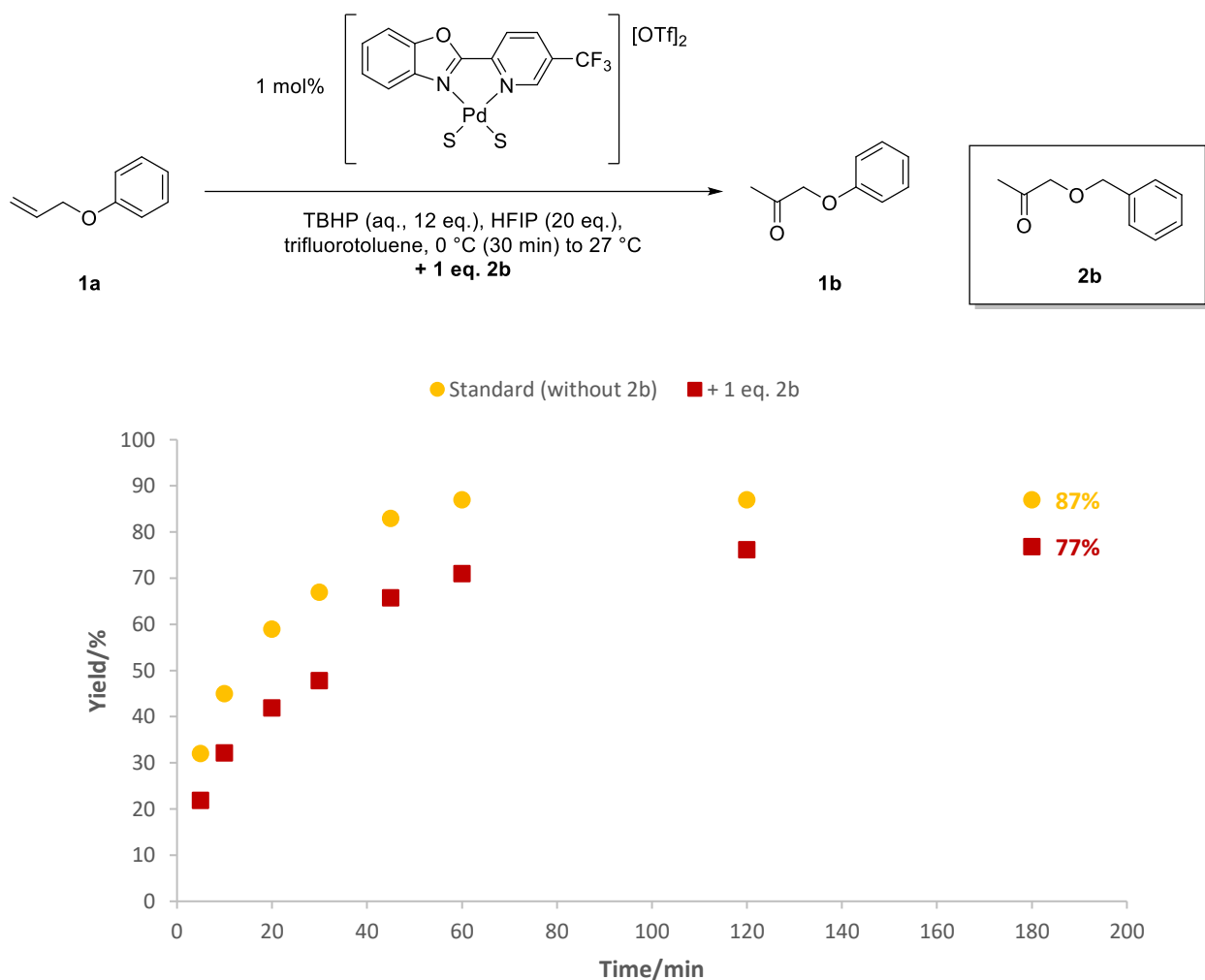


**Figure S19:** Oxidation of APE with 1 mol%  $[\text{Pd}(\text{5-CF}_3\text{-PBO})(\text{S})_2][\text{OTf}]_2$  with 1 eq. BOA added to investigate potential product inhibition of catalyst. Analyzed by GC-FID with an internal standard.

### 1.2.7 Additional tests with allyl benzyl ether (**2a**)

Given the improvement seen for substrate **1a** oxidation of **2a** was also carried out using 20 eq. HFIP under different temperature conditions. The results in Figure S20 show however, that unlike **1a**, no real benefit was observed when the reaction was held at 0 °C for 30 minutes before transfer to 27 °C, compared to maintaining the reaction at 27 °C. Holding the reaction at 0 °C for longer (1 hour) gave a significantly reduced yield, as did holding the reaction at 0 °C for its entire duration. After extended reaction times (21 or 23 h), product yield was noted to decrease slightly. This behavior was noted to occur for both **1a** and **2a** under anhydrous conditions. Some additional GC signals were noted in these reactions, but their identities were not confirmed.

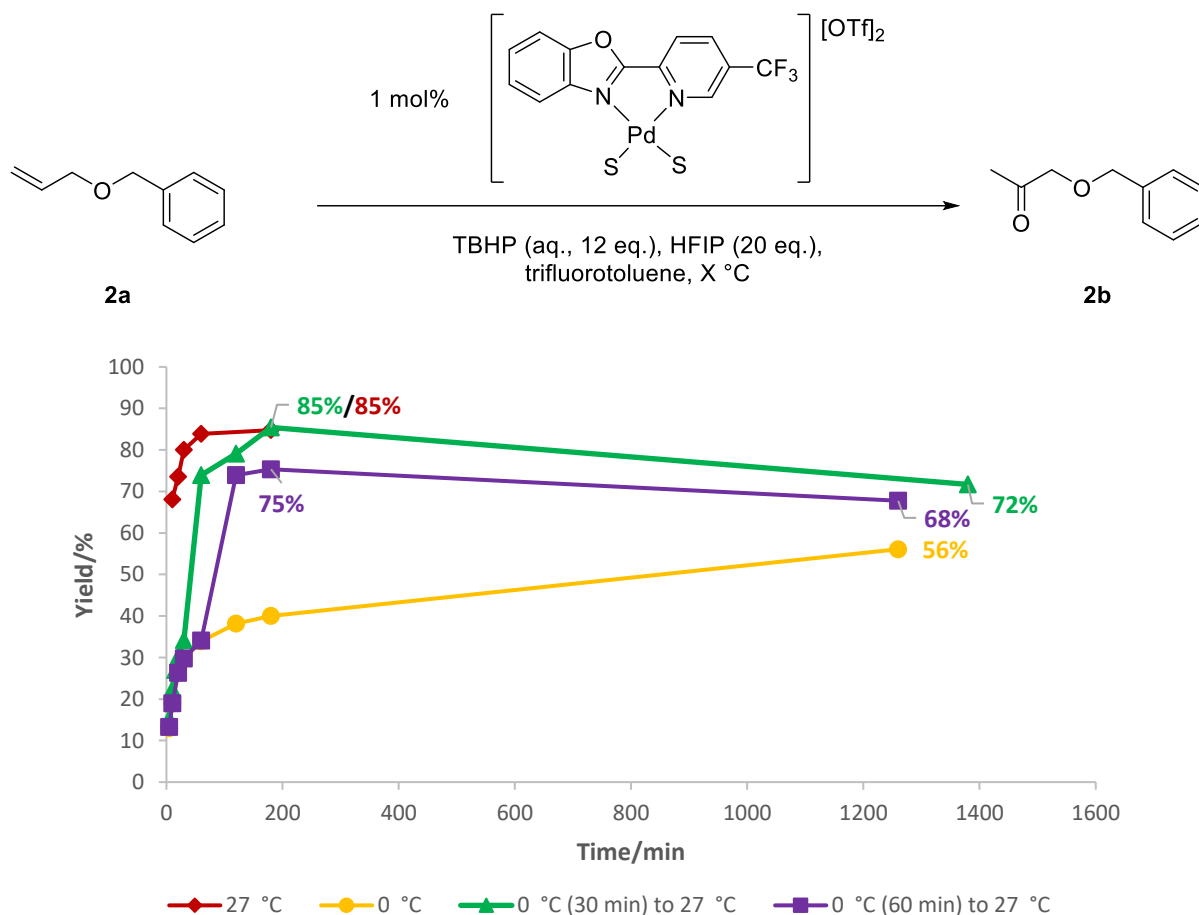
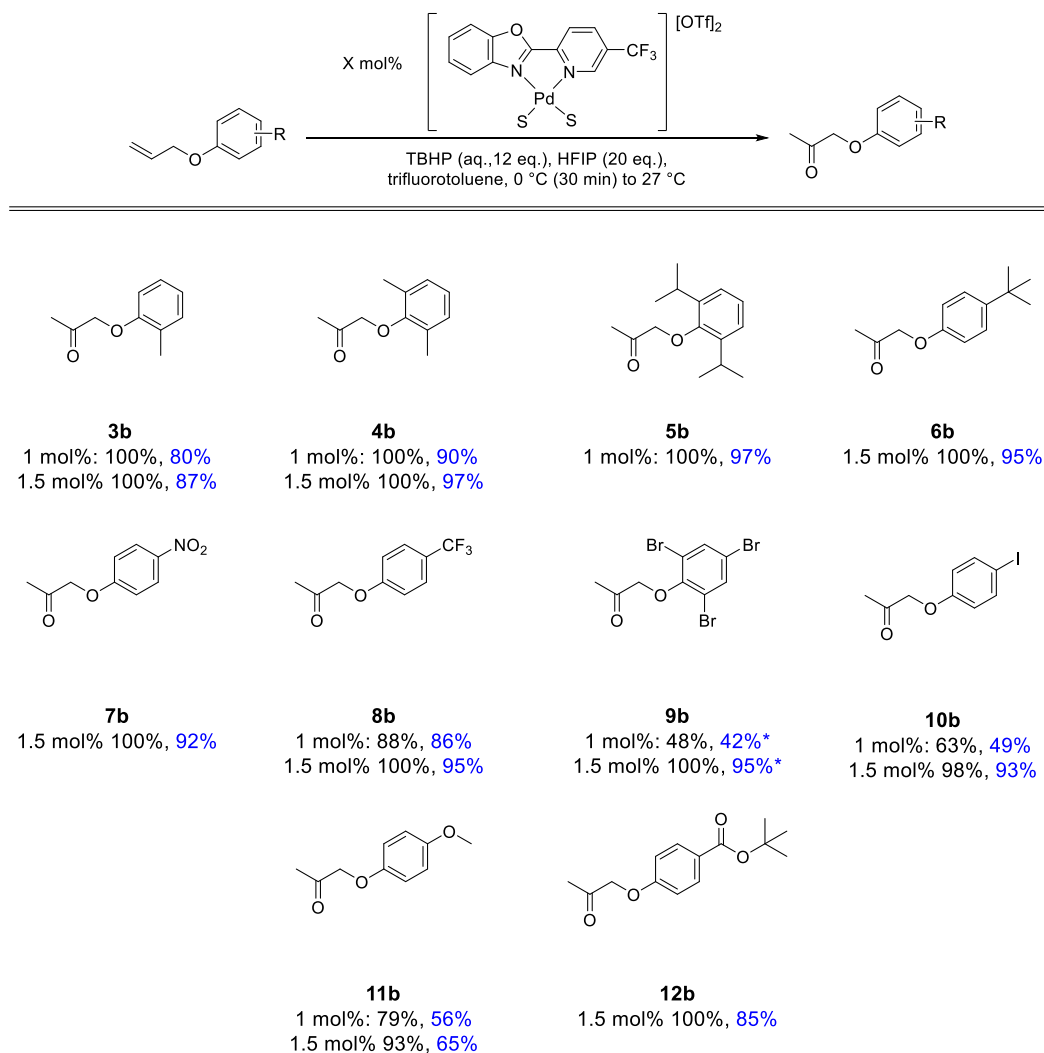


**Figure S20:** Oxidation of **1a** with  $[Pd(5-CF_3-PBO)(S)_2][OTf]_2$ : influence of temperature. Analyzed by GC-FID with an internal standard.

### 1.3 Additional work with APE derivatives and functional group tolerance

#### 1.3.1 Oxidation of derivatives; initial findings at 1 and 1.5 mol% catalyst loading

In preliminary work with **1a** derivatives, reactions were carried out 1 mol% catalyst loading (later (Fig 4) for isolated yields, 1.5 mol% was used) and the yields determined using GC analysis (Figure S21). In this optimization study, the values of relative response factors (RFs) for the methyl ketone products were estimated. See section 2.2 for more details on GC analysis.



catalyst loading: %conversion, %yield

\*Substrate too heavy for GC, conversion/yield determined using <sup>1</sup>H-NMR with anisole as internal standard

**Figure S21:** Initial screening results for Wacker oxidation of **1a** derivatives at 1 mol% or 1.5 mol% catalyst loadings. Conversions quantified using GC-FID with internal standard and yields estimated using a calculated response factor.

### 1.3.2 Oxidation of derivatives; reaction profiles

To investigate the progress of oxidation of several allyl phenyl ether derivatives, multiple samples points were taken for the oxidation of several substrates (Figure S22).

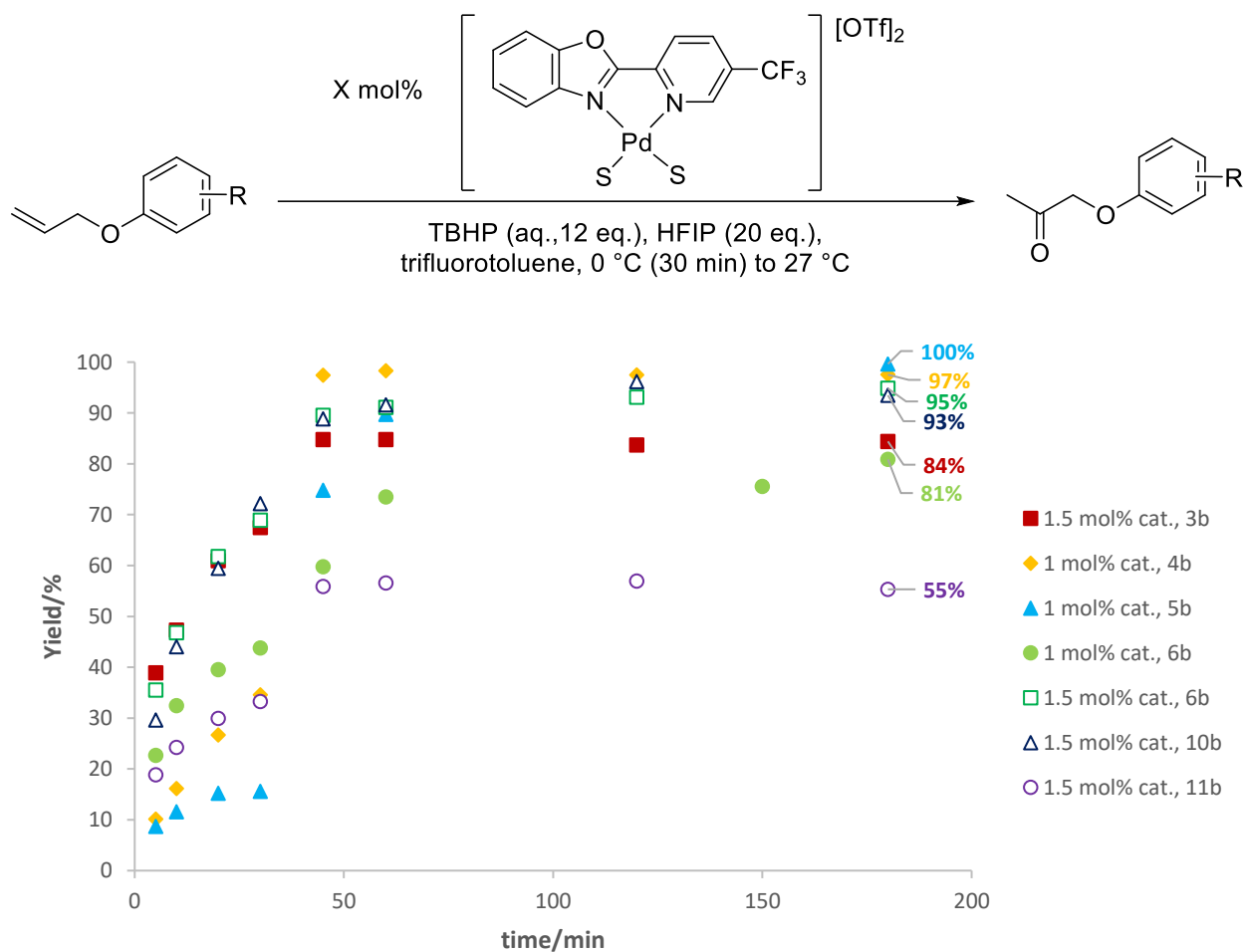


**Figure S22:** Reaction profiles for several **1a** derivatives with 1 mol% or 1.5 mol%  $[\text{Pd}(5\text{-CF}_3\text{-PBO})(\text{S})_2][\text{OTf}]_2$ . Analyzed by GC-FID with an internal standard.

### 1.3.3 Oxidation of allyl phenyl ether; effect of additives on catalyst activity

As an extension of the range of **1a** derivatives synthesized and screened, the oxidation of **1a** was carried out with the inclusion of several 'additives' at 1 eq., to inspect the effect of various functional groups on yield of **1b** by simply being present in the conditions rather than their direct effect on the substrates (Figure S23).

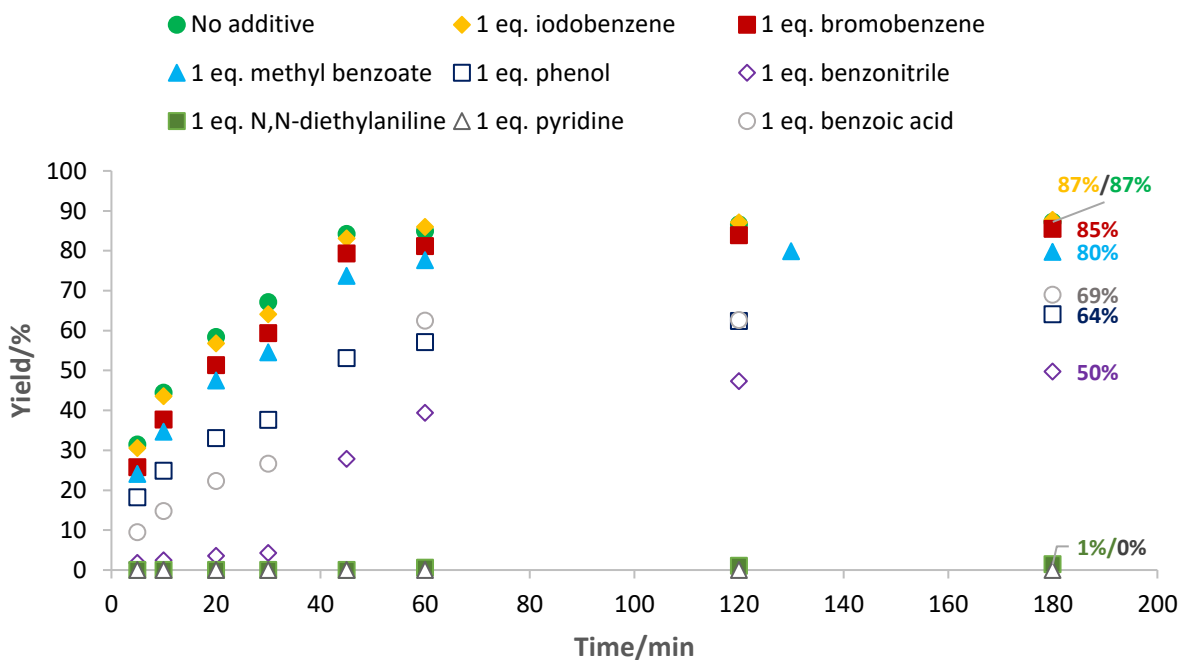
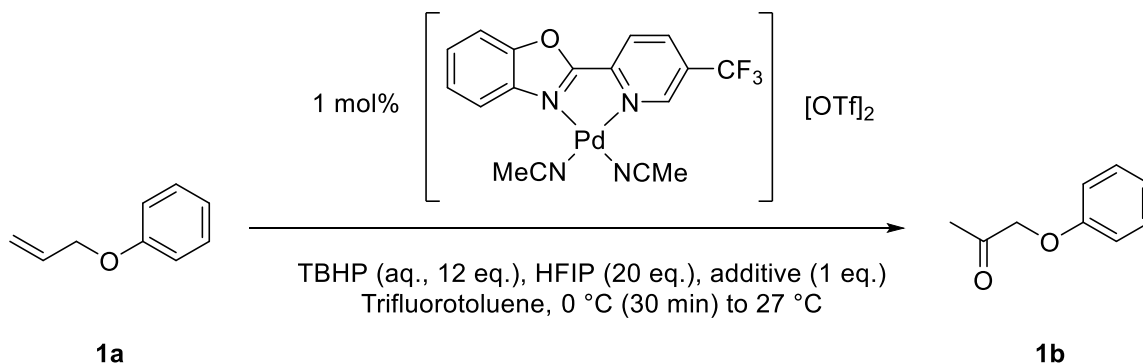


**Figure S23:** Oxidation of **1a** in the presence of different additives (1 eq.). Analyzed by GC-FID with an internal standard.

## 1.4 Additional work with complex substrates

### 1.4.1 Oxidation of complex substrates: initial screenings with <sup>1</sup>H-NMR

To investigate the system's applicability to organic synthesis, a number of complex substrates bearing alkene moieties were tested. Previous studies in the Hawkins Group investigated the use of TBHP-mediated Wacker oxidations with ligated Pd(II) complexes as part of the I synthesis of oxyisocyclointegrin.<sup>6</sup> Employing Sigman's [Pd(Quinox)Cl<sub>2</sub>] catalyst system, a yield of 76% of the corresponding methyl ketone intermediate was obtained. However, a catalyst loading of 20 mol% was required to do so.

Oxidation of the substrate was carried out using the preparative procedure described in section 4.5.1 with nitromethane used as internal standard (added when sample taken, weight recorded) and the reaction sampled for <sup>1</sup>H-NMR analysis. Initial testing with substrate **16a** with 3 mol% catalyst indicated a yield of approximately 63% according to <sup>1</sup>H-NMR analysis. However, following revision of the reaction conditions (temperature and HFIP content), an improved **16b** yield of 78% was observed by <sup>1</sup>H NMR. (Figure S24)

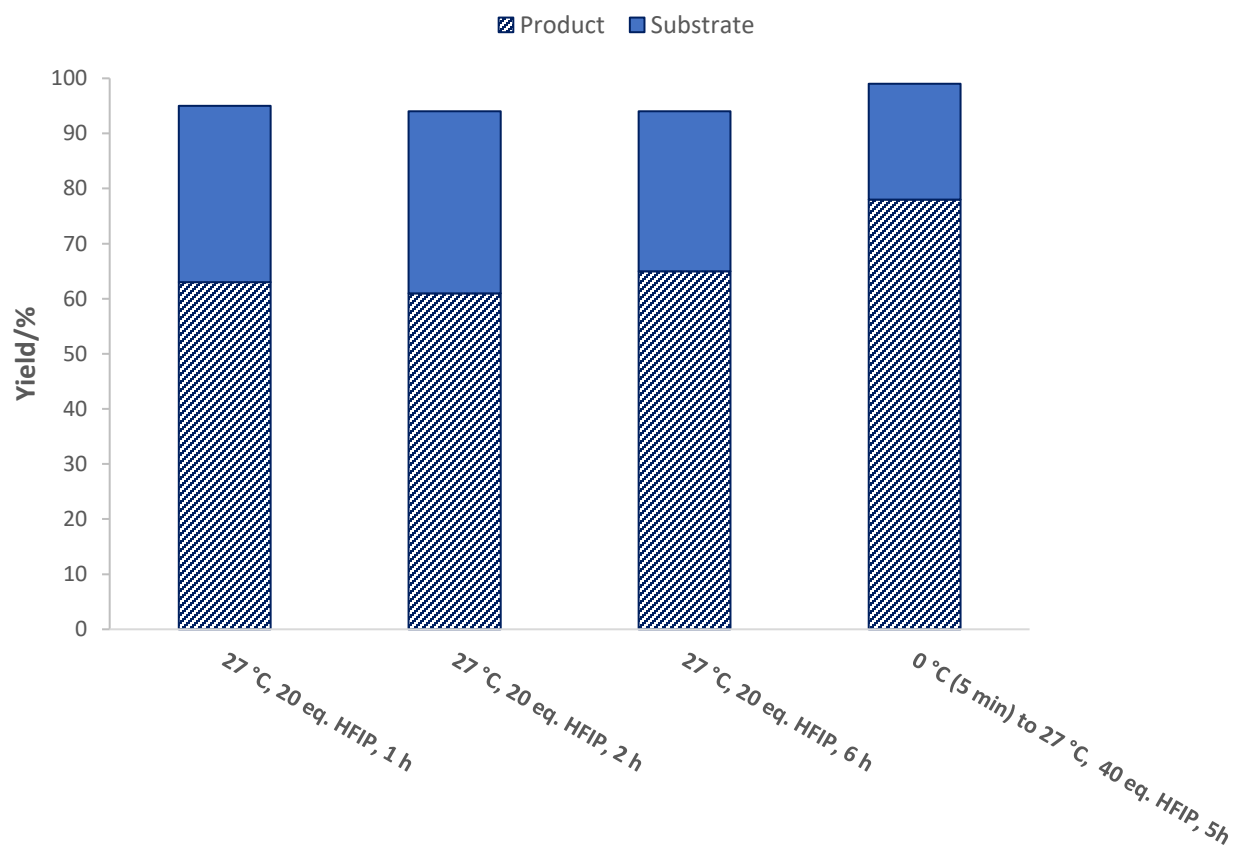
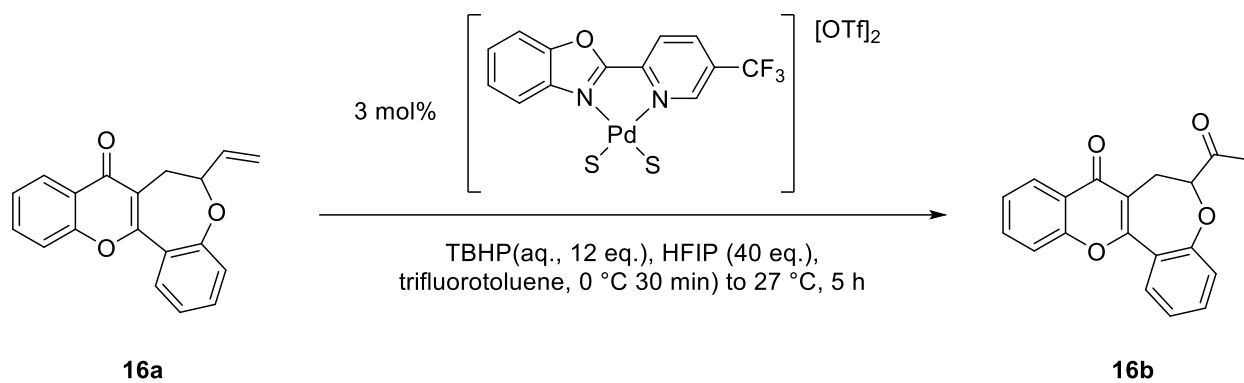


**Figure S24:** Oxidation of **16a** to **16b** under standard and modified solvent and temperature conditions. Analyzed by <sup>1</sup>H NMR with an internal standard.

### 1.4.2 Oxidation of complex substrates: problematic substrates

A number of substrates did not perform well when reacted under the conditions outlined in Figure 5. Below in Figure S25 the structures of these substrates can be seen. In these cases we were unable to obtain the desired methyl ketone product. For these substrates there was often limited conversion, and determining the exact nature of the products was challenging due to difficulty in separating and isolating the products.

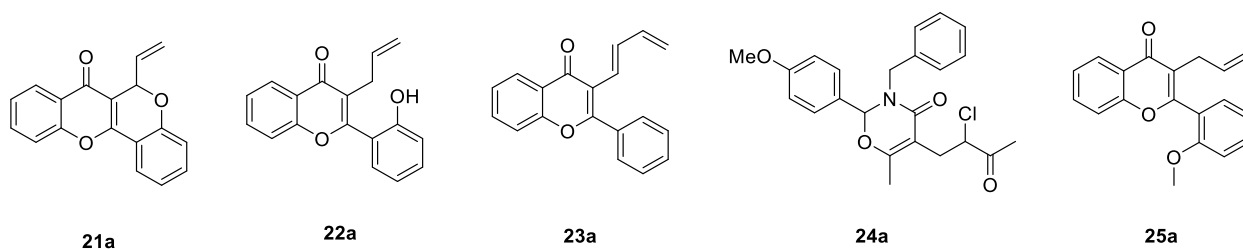


**Figure S25:** Problematic substrates

## 2 General Considerations

### 2.1 Chemicals and equipment

$^1\text{H}$ ,  $^{13}\text{C}\{\text{H}\}$  and  $^{19}\text{F}\{\text{H}\}$  NMR data was obtained using a Bruker 400 MHz or 600 MHz spectrometer. Mass spectra (ESI) data were analyzed using Waters LCT Premier TOF. IR data was obtained using an Agilent Cary 630 FTIR spectrometer. Elemental Analysis data was obtained using a Perkin Elmer PE2400 CHNS Elemental Analyzer. Reactions were stirred using an Asynt ADS-HP-NT hotplate/stirrer with an Asynt ADS-TC-NT temperature probe to control temperature. Reactions carried out at temperatures below 27 °C were cooled using a DrySyn SnowStorm reactor with a Julabo FL300 recirculating chiller. Aluminium blocks used to control the temperature of reactions were designed to house the 14 mL reaction vials that were used. A KD Scientific® KDS 200P Legacy Programmable Dual Syringe Infusion Pump was used for slow substrate addition.

For compounds **20a** and **23a** infrared spectrum was recorded on a Bruker Optics Alpha ATR FT-IR spectrometer. High resolution mass-spectrum (HRMS) was recorded on a Shimadzu LCMS-9030 TOFQ mass spectrometer using an electrospray ionisation (ESI) source in positive mode.  $^1\text{H}$  NMR and  $^{13}\text{C}$  NMR spectra were recorded at 400 MHz and 100 MHz, respectively, on a Varian 400-MR NMR system. All spectra were recorded on samples in  $\text{CDCl}_3$  at 25 °C. Chemical shifts are reported in parts per million (ppm) and referenced to the chloroform residual solvent peak.

Unless otherwise stated, all reagents were purchased from commercial suppliers and used without further purification. The aqueous TBHP used was Luperox™ TBH70X ((a 70 wt.% aqueous solution) and palladium acetate:  $\geq 99.9\%$ , trace metal basis were purchased from Sigma Aldrich (Merck). The phenols used to prepare the substrates tested were purchased from Sigma Aldrich (Merck) and Fluorochem. Three substrates, *o*-allyloxytoluene (**2a**, Fluorochem), allyl 2,4,6-tribromophenyl ether (**9a**, Merck) and *N*-allylaniline (**15a**, Alfa Aesar) were purchased. It was found that **2a** required purification by column chromatography before use (1:5 EtOAc/hexane), as some 2-methylphenol was detected when analyzed by  $^1\text{H}$  NMR. Thin layer chromatography (TLC) was carried out using Merck TLC silica gel 60 sheets and visualized with ultraviolet light. Flash column chromatography (FCC) was performed with Fluorochem silica gel 60 Å as the stationary phase and solvents employed were analytical grade.

### 2.2 GC analysis of reaction samples

Reaction samples were analysed by gas chromatography (GC) with an Agilent 7820A series gas chromatograph or an Agilent 6890N network gas chromatograph. Samples of reactions for **1a** and **2a** were separated over a Zebron ZB-1 column (30.0 m Å ~ 320  $\mu\text{m}$  Å ~ 0.5  $\mu\text{m}$  nominal). The effluent was combusted in an  $\text{H}_2/\text{Air}$  flame and detected using FID (flame ionization detector). Samples were injected at an initial 40 °C, the oven temperature then increased to 200 °C at a ramp of 30 °C/min, with a 1-minute hold time at 200 °C. For **1a**

derivatives (substrates **3a** to **14a**), a slightly different method was used; samples were injected at an initial 40 °C, the oven temperature then increased to 260 °C at a ramp of 40 °C/min, with a 1-minute hold time at 260 °C.

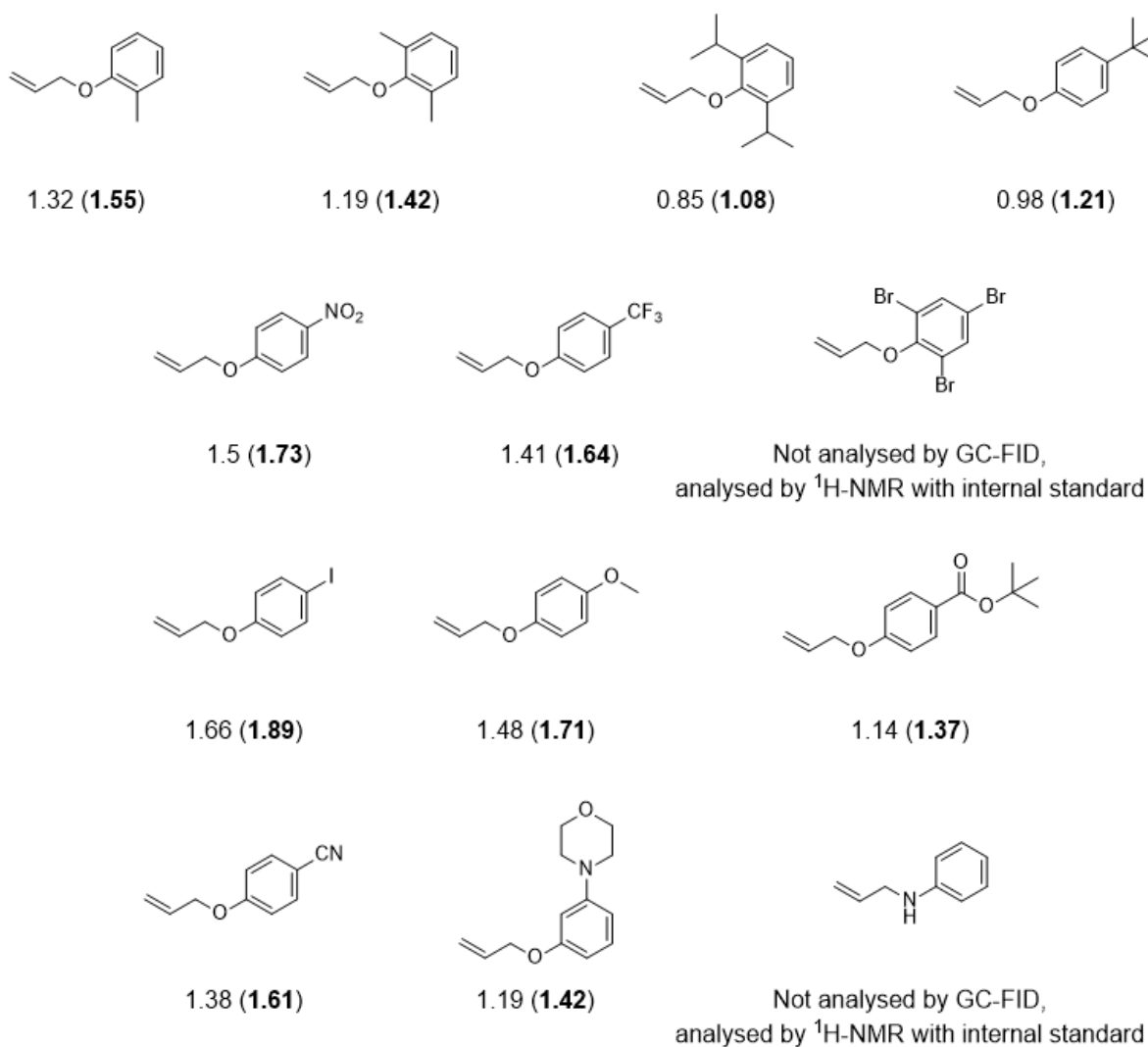
To ensure reliable operation of the GC, a relative response factor (RF) check was carried out. Before samples were analyzed, a “blank” was analyzed, and then a model mixture was analyzed. The model solution was prepared from a solution of biphenyl (standard) and acetophenone (analyte) of known quantities. Previous calibrations had found that the response factor for acetophenone is 1.7, and we checked that the GC consistently gave this result. Substrate and product RF values were determined by analyzing solutions containing known amounts of standard (dodecane) and analyte (3 different concentrations, simulating 25%, 50% and 75% analyte conversion or yield, relative to reaction concentration) for the analyte using the following calculation:

$$RF = \frac{(Area_{internal\ standard} \times Moles_{analyte})}{(Area_{analyte} \times Moles_{internal\ standard})}$$

RFs obtained were calculated with values within +/- 0.1 of each other and an average value taken. When determining substrate conversion and product yields, the above equation was re-arranged to give the following;

$$Moles_{Analyte} = \frac{(RF_{analyte} \times Area_{analyte} \times moles_{internal\ standard})}{Area_{internal\ standard}}$$

For allyl phenyl ether derivatives, the products were not commercially available. In the optimization studies which were monitored by GC, we obtained an RF for the substrate enabling accurate determination of the conversion. In the case of product yields we used a predicted product RF. In the case of **1a** the product (**1b**) was commercially available and an RF could be obtained (**1a** = 1.48, **1b** = 1.71) The RF of **1b** was found to be +0.23 compared to the RF of **1a** therefore we used this as a correction factor when estimating the RF for products that we did not have samples for (Figure S26). Note that this approach was used for optimization and isolated yields were obtained for the products reported (Figure 4).



Substrate RF (**estimated product RF**),  
with respect to dodecane as internal standard

**Figure S26:** Relative response factors (RF) values obtained for substrates and the estimated RF values for the corresponding methyl ketone products.

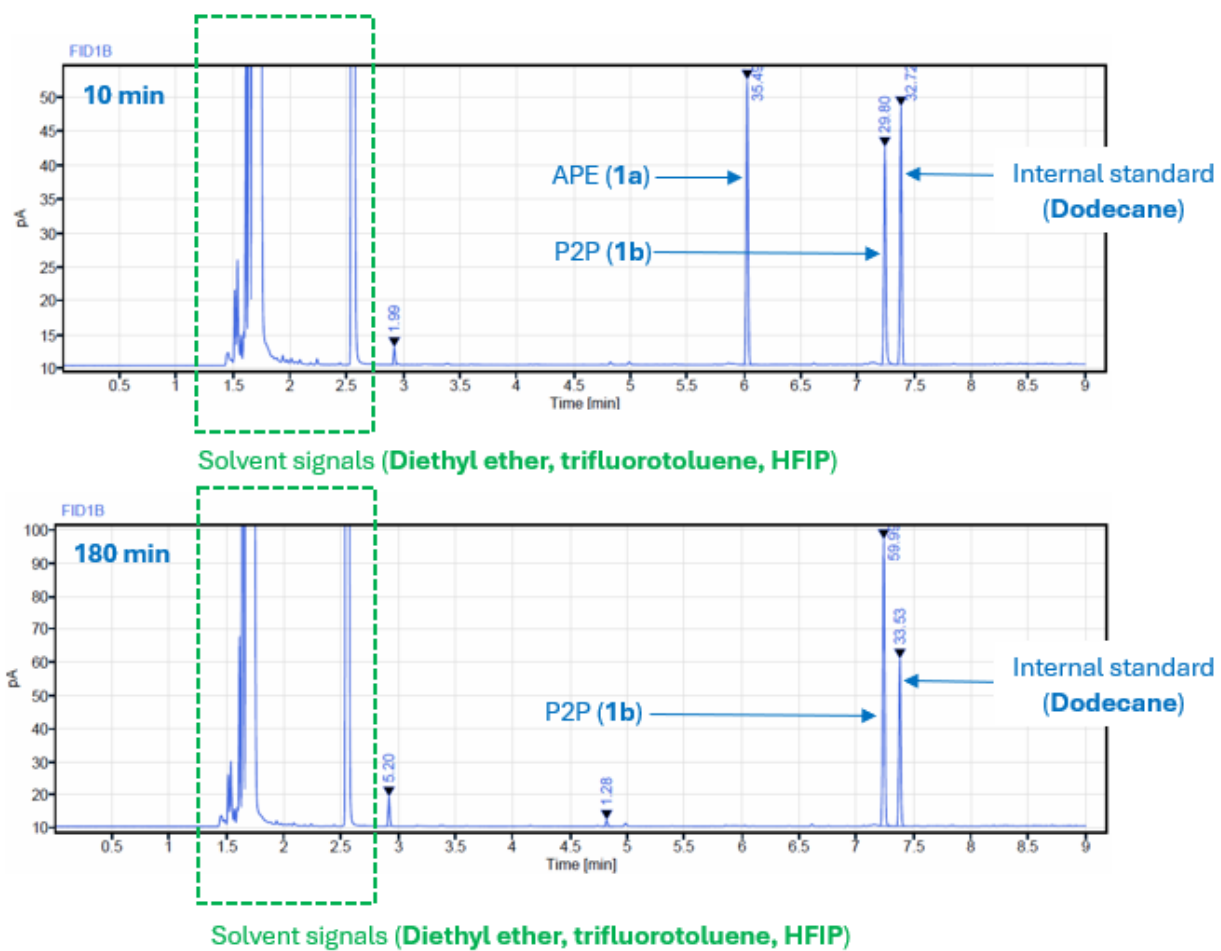
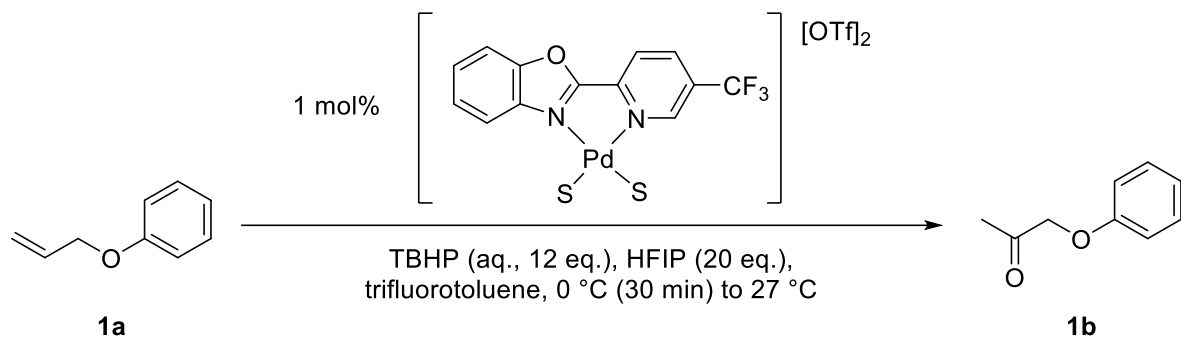


Figure S27: Example GC traces for the oxidation of 1a to 1b

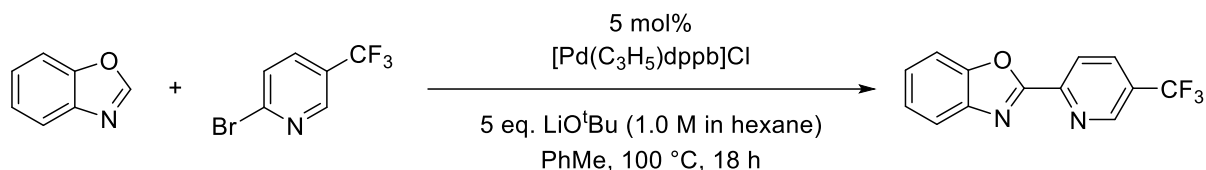
## 2.3 Safety considerations

Oxidation chemistry with peroxides requires careful consideration of safety issues. Before carrying out reactions, a full risk assessment should be carried out. Peroxides such as TBHP can become unstable/decompose with increasing temperature and various additives such as metal ions or acids and bases.<sup>7-10</sup> Therefore caution should be taken when designing experiments. It is advisable to carry out reactions on a small scale initially and to bear in mind that for certain substrates which are very reactive, there will be an exotherm. For those interested in larger scale studies, suitable temperature control should be utilized to ensure the exotherm can be controlled and calorimetric studies would be advisable. When using glassware such as in these studies, it is advisable not to properly stopper the vessels. For example, when using small glass vials, if lids are being used, ensure there is a hole in the lid to allow release of any pressure build up.

All reactions should be quenched at the end of the reaction to reduce the remaining TBHP. This also applies to solutions of TBHP that are to be disposed of. There are a range of potential reductants but we have used sodium thiosulfate or sodium metabisulfite, reductants that have been used by others for quenching TBHP.<sup>11, 12</sup> When carrying out the quench, the TBHP solution is cooled to 0 °C and a saturated solution of the aforementioned reductant added slowly. An excess of the reductant should be employed and it is advisable to check that all the TBHP has been removed. This can be done via various means (including iodide titrations<sup>13</sup> and peroxide test strips). It must be noted that for the oxidation of substrates **10a** to **13a** and **16a** to **25a**, quenching was not carried out – the reaction mixture was transferred directly to the chromatography column or preparative TLC plate, as a precaution against potential loss of material during workup. Test strips were used to check collected chromatography fractions and preparative TLC extractions before concentrating under reduced pressure.

### 3 Synthetic procedures

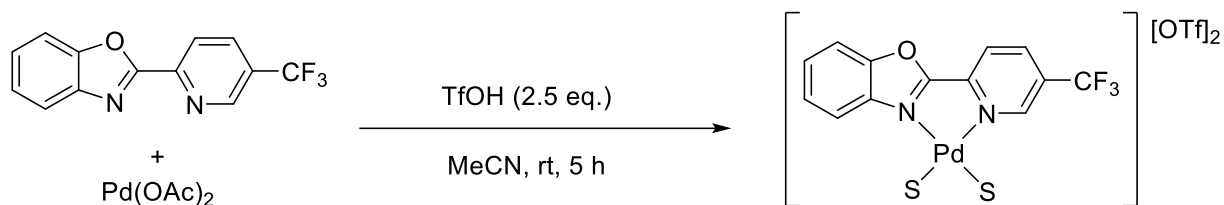
#### 3.1 Synthesis of 2-(5-(trifluoromethyl)pyridin-2-yl)benzo[d]oxazole (5-CF<sub>3</sub>-PBO)



To a two-necked 50 mL round bottom flask, benzo[d]oxazole (0.2762 g, 2.32 mmol), [PdCl(C<sub>3</sub>H<sub>5</sub>)dppb] (0.061 g, 0.1 mol) and 2-bromo-5-trifluoromethyl pyridine (0.4536 g, 2.00 mmol) were transferred with a magnetic stir bar. The flask was fitted with a waterless reflux condenser and sealed, the apparatus evacuated and backfilled with N<sub>2</sub> three times, before the addition of dry, degassed toluene (10 mL) via syringe followed by the slow addition of lithium *tert*-butoxide (1.0 M, 10 mL, 10.0 mmol), the reaction then heated to reflux at 100 °C and stirred under N<sub>2</sub> for approx. 18 hours. Product formation confirmed by TLC analysis, the reaction mixture was transferred to a 100 mL separating funnel before dilution with water (25 mL) and the product then extracted with toluene (2 x 15 mL portions), the organic layer dried over magnesium sulfate and the solvent removed under reduced pressure. The crude product was purified by dry-loaded column chromatography (15:1 hexane/ethyl acetate, both HPLC grade). The product, a white crystalline solid, was further dried under reduced pressure. Product yield; 0.4173 g, 1.58 mmol (78%).

<sup>1</sup>H NMR (400 MHz, Chloroform-d) δ 9.12 – 9.01 (m, 1H), 8.51 (dd, J = 8.2, 0.6 Hz, 1H), 8.16 (m, 1H), 7.93 – 7.82 (m, 1H), 7.76 – 7.67 (m, 1H), 7.55 – 7.40 (m, 2H). <sup>13</sup>C{<sup>1</sup>H} NMR (151 MHz, CDCl<sub>3</sub>) δ 160.11, 151.19, 149.05, 147.18 (q, 3JCF = 4.0 Hz), 141.64, 134.42 (q, 3JCF = 3.4 Hz), 128.07 (q, 2JCF = 33.6 Hz), 126.77, 125.32, 123.02 (q, 1JCF = 273 Hz), 123.01, 121.03, 111.39. <sup>19</sup>F{<sup>1</sup>H} NMR (376 MHz, Chloroform-d) δ -62.57. m/z: predicted [M+H]<sup>+</sup> = 265.0589, found [M+H]<sup>+</sup> = 265.0583. Elemental analysis: Predicted: C, 59.10; H, 2.67; N, 10.60. Observed: C, 60.11; H, 2.56; N, 10.40. Analyses in agreement with literature data and previously-published work.<sup>1, 14</sup>

### 3.2 Synthesis of [Pd(2-(5-(trifluoromethyl)pyridin-2-yl)benzo[d]oxazole)(solvent)<sub>2</sub>][OTf]<sub>2</sub> ([Pd(5-CF<sub>3</sub>PBO)(S)<sub>2</sub>][OTf]<sub>2</sub>)



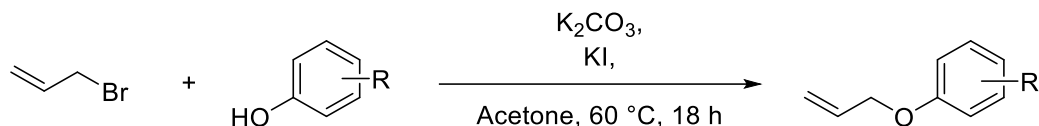
Where S = solvent (MeCN or H<sub>2</sub>O)

To a 25 mL round bottom flask fitted with a magnetic stir bar, 5-CF<sub>3</sub>(PBO) ligand (0.2638 g, 1.00 mmol) and Pd(OAc)<sub>2</sub> (0.2255 g, 1.00 mmol) were transferred and dissolved in acetonitrile (6 mL), the mixture allowed to stir for 1 hour. Following this, trifluoromethanesulfonic acid (0.3924 g, 2.614 mmol) dissolved in acetonitrile (5 mL) was added dropwise and the reaction mixture allowed to stir at room temperature for 4 hours. On addition of diethyl ether, the product precipitated out of solution. The product, a yellow solid, was filtered-off (Buchner funnel), washed with diethyl ether and dried under reduced pressure. Product yield = 0.5269 g, 0.70 mmol (70%).

<sup>1</sup>H NMR (600 MHz, Acetonitrile-*d*<sub>3</sub>) δ 8.89 (d, *J* = 8.2 Hz, 1H), 8.79 (s, 1H), 8.59 (d, *J* = 8.2 Hz, 1H), 8.03 (m, 1H), 7.88 (m, 1H), 7.87 – 7.78 (m, 2H), 1.99 (s, 3H). <sup>13</sup>C{<sup>1</sup>H} NMR (151 MHz, Acetonitrile-*d*<sub>3</sub>) δ 164.50, 151.24, 149.93, 147.45, 142.81, 135.23, 131.81 (q, <sup>2</sup>*J*<sub>CF</sub> = 36.7 Hz), 131.28, 129.75, 127.22, 122.84 (q, <sup>1</sup>*J*<sub>CF</sub> = 272.4 Hz), 120.59 (q, <sup>1</sup>*J*<sub>CF</sub> = 321.91 Hz), 118.99, 113.88, 1.35. <sup>19</sup>F{<sup>1</sup>H} NMR (376 MHz, Acetonitrile-*d*<sub>3</sub>) δ -63.14 (s, 3F), -79.33 (s, 6F). Spectra in agreement with previously-published work.<sup>1</sup>

Elemental analysis: Predicted: C, 30.39; H, 1.75; N, 7.46. Observed: C, 27.62; H, 0.97; N, 7.46. It is possible that both acetonitrile and water ligands coordinate to the Pd(II) centre; to generalise this, the coordinated ligands are denoted simply as 'S'. The dicationic nature of the catalyst is verified by the 1:2 integration ratio of the signals observed for the <sup>19</sup>F-NMR, corresponding to the -CF<sub>3</sub> group of the ligand and those of the triflate anions respectively. To obtain this quantification accurately, a D1 relaxation delay of 8 seconds is applied to the <sup>19</sup>F{<sup>1</sup>H} NMR analysis. Analysis in agreement with previously-published work.<sup>1</sup>

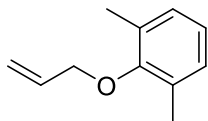
### 3.3 Synthesis of allyl phenyl ether derivatives



Substrates were synthesised following a reported procedure.<sup>[15]</sup> For most substrates, experiments with a target yield of approx. 1.00 g or 9.00 mmol were planned, with previously reported yields used to determine the quantities of components and sizes of glassware needed.

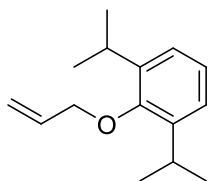
Representative example of the procedure: To a 50 mL round-bottom flask fitted with a stir bar, the desired phenol (6.00 mmol) was transferred and dissolved in acetone (13 mL). Potassium carbonate (7.5 mmol, 1.25 eq., 1.036 g) and potassium iodide (0.6 mmol, 0.1008 g) were then added, followed by allyl bromide (7.5 mmol, 648  $\mu$ L). The reaction flask was fitted with a waterless reflux condenser with a rubber septum and needle, the reaction heated to reflux at 60 °C and allowed to stir for 18 h. TLC analysis was used to confirm completion of the reaction after this time. To the flask, 1N sodium hydroxide solution (30 mL) was added and the mixture transferred to a 250 mL separating funnel. The product was extracted with ethyl acetate (3 x 20 mL) and the combined organic layers washed with brine before separation. The combined organic layers were dried over magnesium sulfate, the solvent removed under reduced pressure and the crude product purified by column chromatography (HPLC-grade ethyl acetate/hexane eluent, appropriate ratio determined by TLC tests), isolated product fractions combined and solvent removed under reduced pressure. Two substrates bearing sterically-hindering groups *tert*-butyl groups (Allyl 2,6-di(*tert*-butyl)phenyl ether and Allyl 2,4,6-tri(*tert*-butyl)phenyl ether) were not successfully formed, indicated by TLC analysis.

### 3.3.1 Allyl 2,6-dimethylphenyl ether (4a)



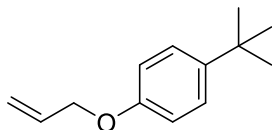
Yield = 0.889 g, 80%, yellow liquid, columned with 1:10 EtOAc/Hexane.  $^1\text{H}$  NMR (400 MHz, Chloroform-*d*)  $\delta$  7.07 – 6.97 (m, 2H), 6.97 – 6.87 (m, 1H), 6.22 – 6.02 (m, 1H), 5.50 – 5.37 (m, 1H), 5.32 – 5.21 (m, 1H), 4.36 – 4.25 (m, 2H), 2.29 (s, 6H).  $^{13}\text{C}\{\text{H}\}$  NMR (101 MHz, Chloroform-*d*)  $\delta$  155.92, 134.17, 131.01, 128.75, 123.80, 117.07, 73.04, 16.36. Spectra are in agreement with previously reported data.<sup>16</sup>

### 3.3.2 Allyl 2,6-diisopropylphenyl ether (5a)



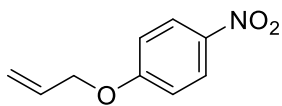
Yield = 1.734 g, 75%, clear liquid, columned with 1:20 EtOAc/Hexane.  $^1\text{H}$  NMR (400 MHz, Chloroform-*d*)  $\delta$  7.11 (s, 3H), 6.13 (m, 1H), 5.47 (m, 1H), 5.28 (m, 1H), 4.29 (m, 2H), 3.33 (m, 2H), 1.23 (d,  $J$  = 6.9 Hz, 12H).  $^{13}\text{C}\{\text{H}\}$  NMR (101 MHz, Chloroform-*d*)  $\delta$  153.35, 141.88, 134.12, 124.57, 123.97, 116.85, 75.43, 26.51, 24.08. Spectra are in agreement with previously reported data.<sup>17</sup>

### 3.3.3 Allyl 4-*tert*-butylphenyl ether (6a)



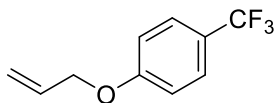
Yield = 1.661 g, 86%, clear liquid, columned with 1:5 EtOAc/Hexane.  $^1\text{H}$  NMR (400 MHz, Chloroform-*d*)  $\delta$  7.34 – 7.26 (m, 2H), 6.89 – 6.82 (m, 2H), 6.14 – 5.99 (m, 1H), 5.47 – 5.36 (m, 1H), 5.33 – 5.23 (m, 1H), 4.56 – 4.48 (m, 2H), 1.30 (s, 9H).  $^{13}\text{C}\{\text{H}\}$  NMR (101 MHz, Chloroform-*d*)  $\delta$  156.35, 143.49, 133.59, 126.19, 117.50, 114.17, 68.85, 34.07, 31.53 . Spectra are in agreement with previously reported data.<sup>18</sup>

### 3.3.4 Allyl 4-nitrophenyl ether (7a)



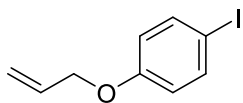
Yield = 1.830 g, 82%, yellow-orange liquid, columned with 1:5 EtOAc/Hexane.  $^1\text{H}$  NMR (400 MHz, Chloroform-*d*)  $\delta$  8.32 – 8.10 (m, 2H), 7.07 – 6.88 (m, 2H), 6.17 – 5.95 (m, 1H), 5.51 – 5.40 (m, 2H), 4.71 – 4.56 (m, 2H).  $^{13}\text{C}\{\text{H}\}$  NMR (101 MHz, Chloroform-*d*)  $\delta$  163.57, 141.59, 131.87, 125.90, 118.69, 114.70, 69.40. Spectra are in agreement with previously reported data.<sup>19</sup>

### 3.3.5 Allyl 4-trifluoromethylphenyl ether (8a)



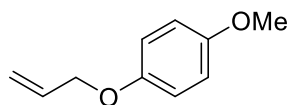
Yield = 1.1292 g, 61%, clear liquid, columned with 1:5 EtOAc/Hexane.  $^1\text{H}$  NMR (400 MHz, Chloroform-*d*)  $\delta$  7.59 – 7.48 (m, 2H), 7.04 – 6.89 (m, 2H), 6.12 – 5.96 (m, 1H), 5.49 – 5.38 (m, 1H), 5.37 – 5.26 (m, 1H), 4.66 – 4.51 (m, 2H). Spectrum in agreement with previously reported data.<sup>[20]</sup>  $^{19}\text{F}\{\text{H}\}$  NMR (376 MHz, Chloroform-*d*)  $\delta$  -61.51.  $^{13}\text{C}\{\text{H}\}$  NMR (101 MHz, Chloroform-*d*)  $\delta$  160.99, 132.52, 126.86 (q,  $J$  = 3.8 Hz), 125.77, 123.15, 123.07, 122.82, 118.16, 114.69, 68.90. C-F coupling would be expected to give a quartet in the  $^{13}\text{C}\{\text{H}\}$ -NMR spectrum, but this appears to be partially lost in baseline noise.

### 3.3.6 Allyl 4-iodophenyl ether (10a)



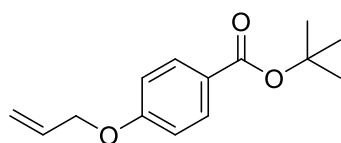
Yield = 0.9544 g, 94%, orange liquid, columned with 1:5 EtOAc/Hexane.  $^1\text{H}$  NMR (400 MHz, Chloroform-*d*)  $\delta$  7.60 – 7.49 (m, 2H), 6.75 – 6.65 (m, 2H), 6.09 – 5.96 (m, 1H), 5.44 – 5.36 (m, 1H), 5.34 – 5.25 (m, 1H), 4.54 – 4.46 (m, 2H).  $^{13}\text{C}\{\text{H}\}$  NMR (101 MHz, Chloroform-*d*)  $\delta$  158.46, 138.20, 132.83, 117.91, 117.18, 82.91, 68.86. Spectra are in agreement with previously reported data.<sup>21</sup>

### 3.3.7 Allyl 4-methoxyphenyl ether (11a)



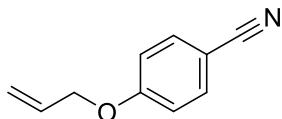
Yield = 0.8643 g, 85%, clear liquid, columned with 1:10 EtOAc/Hexane.  $^1\text{H}$  NMR (400 MHz, Chloroform-*d*)  $\delta$  6.96 – 6.69 (m, 4H), 6.16 – 5.94 (m, 1H), 5.45 – 5.35 (m, 1H), 5.31 – 5.23 (m, 1H), 4.49 (m, 2H), 3.77 (s, 3H).  $^{13}\text{C}\{\text{H}\}$  NMR (101 MHz, Chloroform-*d*)  $\delta$  153.92, 152.77, 133.63, 117.45, 115.75, 114.62, 69.55, 55.71. Spectra are in agreement with previously reported data.<sup>17, 22</sup>

### 3.3.8 *Tert*-butyl 4-(allyloxy)benzoate (12a)



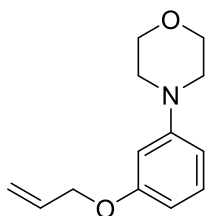
Yield = 2.771 g, 95%, clear liquid, columned with 1:10 EtOAc/Hexane.  $^1\text{H}$  NMR (400 MHz, Chloroform-*d*)  $\delta$  8.05 – 7.85 (m, 2H), 6.97 – 6.85 (m, 2H), 6.05 (m, 1H), 5.42 (m, 1H), 5.31 (m, 1H), 4.59 (m, 2H), 1.58 (s, 9H).  $^{13}\text{C}\{\text{H}\}$  NMR (101 MHz, Chloroform-*d*)  $\delta$  165.56, 161.93, 132.66, 131.34, 124.62, 118.05, 114.11, 80.52, 68.82, 28.26. *m/z*: predicted  $[\text{2M}+\text{H}]^+ = 469.2590$ , found  $[\text{2M}+\text{H}]^+ = 469.2576$ . Elemental Analysis: Predicted = C, 71.77; H, 7.74;. Obtained = C, 70.43; H, 7.99. IR (neat): 2974.4, 2926.0, 2855.1, 1707.1, 1602.8, 1509.6, 1457.4, 1420.1, 1367.9, 1289.7, 1248.7, 1155.5, 1103.3, 1013.8, 924.4, 846.1, 771.6, 693.3, 667.2, 611.3, 551.6, 514.4, 465.9  $\text{cm}^{-1}$ .

### 3.3.9 Allyl 4-cyanophenyl ether (13a)



Yield = 1.137 g, 93%, white solid, columned with 1:3 EtOAc/hexane.  $^1\text{H}$  NMR (400 MHz, Chloroform-*d*)  $\delta$  7.71 – 7.47 (m, 2H), 7.08 – 6.89 (m, 2H), 6.13 – 5.90 (m, 1H), 5.48 – 5.37 (m, 1H), 5.38 – 5.29 (m, 1H), 4.64 – 4.52 (m, 2H)  $^{13}\text{C}\{\text{H}\}$  NMR (101 MHz, Chloroform-*d*)  $\delta$  161.84, 133.95, 132.08, 119.15, 118.46, 115.46, 104.15, 69.0. Spectra are in agreement with previously reported data.<sup>23</sup>  $m/z$ : predicted  $[\text{M}+\text{H}]^+ = 160.0762$ , found  $[\text{M}+\text{H}]^+ = 160.0752$ .

### 3.3.10 Allyl 3-morpholinophenyl ether (14a)



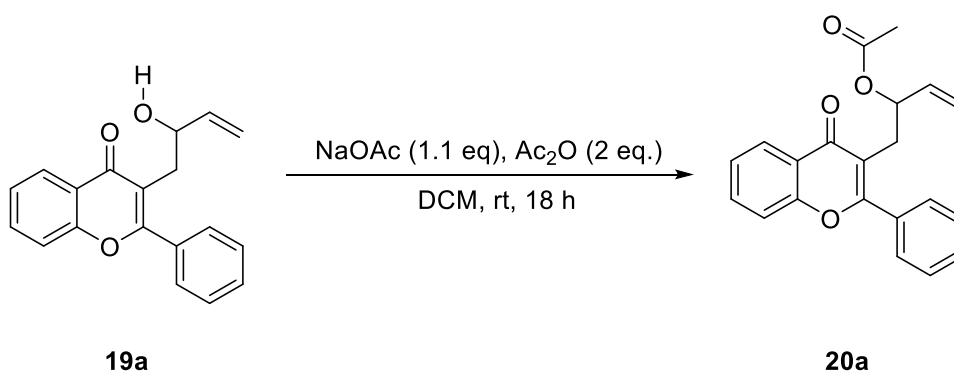
Yield = 1.0513 g, 66%, orange liquid, columned with 1:5 EtOAc/Hexane.  $^1\text{H}$  NMR (400 MHz, Chloroform-*d*)  $\delta$  7.17 (m, 1H), 6.57 – 6.40 (m, 3H), 6.13 – 5.96 (m, 1H), 5.41 (m, 1H), 5.28 (m, 1H), 4.52 (m, 2H), 3.91 – 3.78 (m, 4H), 3.23 – 3.05 (m, 4H).  $^{13}\text{C}\{\text{H}\}$  NMR (101 MHz, Chloroform-*d*)  $\delta$  159.66, 152.68, 133.43, 129.82, 117.61, 108.63, 105.50, 103.01, 68.80, 66.90, 49.27.  $m/z$ : predicted  $[\text{M}+\text{H}]^+ = 220.1338$ , found  $[\text{M}+\text{H}]^+ = 220.1338$ . Elemental Analysis: Predicted = C, 71.21; H, 7.81; N, 6.39. Obtained = C, 70.9; H, 7.58; N, 7.72. IR (neat): 2959.5, 2922.2, 2855.1, 1599.0, 1490.9, 1446.2, 1379.1, 1334.4, 1300.8, 1263.6, 1189.0, 1118.2, 1038.2, 924.4, 879.7, 834.9, 756.6, 685.8, 648.6, 570.3, 525.6  $\text{cm}^{-1}$ .

### 3.4 Synthesis of compounds 16a to 25a

#### 3.4.1 Synthesis of compounds 16a, 17a, 18a, 19a, 21a, 22a, 24a and 25a

In the case of compounds **16a**,<sup>6</sup> **17a**,<sup>24</sup> **18a**,<sup>24</sup> **19a**,<sup>25</sup> **21a**,<sup>26</sup> **22a**,<sup>26</sup> **24a**<sup>27</sup> and **25a**<sup>26</sup> these were prepared according to literature procedures and details are available in the cited papers.

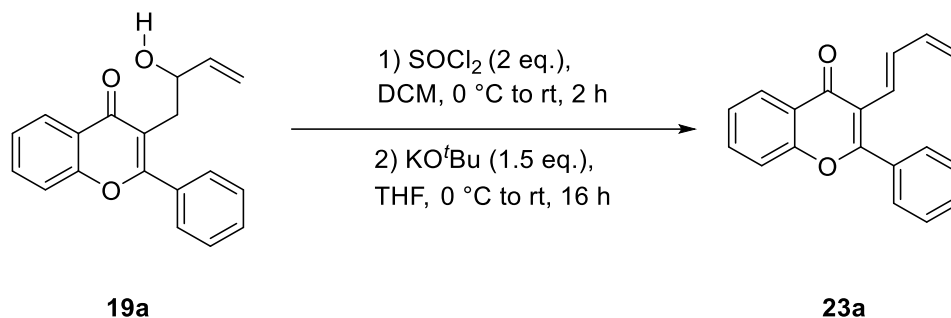
#### 3.4.2 Synthesis of compound 20a (1-(4-oxo-2-phenyl-4H-chromen-3-yl)but-3-en-2-yl acetate)



To a solution of **19a** (0.118 g, 0.407 mmol) in dichloromethane (1 mL) was added sodium acetate (0.037 g, 0.448 mmol) and acetic anhydride (0.083 g, 0.815 mmol). The reaction mixture was stirred at room temperature for 18 h before being quenched with sat. sodium bicarbonate (2 mL) and extracted with DCM (5 mL × 2). The combined organic extracts were washed with brine (5 mL), dried over Na<sub>2</sub>SO<sub>4</sub>, and reduced in vacuo. Purification by column chromatography (1:3 EtOAc/40–60 Pet. Ether) provided the title compound (0.75 g, 55%) as a yellow solid.

<sup>1</sup>H NMR (400 MHz, Chloroform-*d*), δ (ppm): 8.24 (dd, *J* = 8.0, 1.7 Hz, 1H), 7.65 (m, 3H), 7.53 (m, 3H), 7.41 (m, 2H), 5.73 (ddd, *J* = 17.2, 10.5, 6.5 Hz, 1H), 5.58 (m, 1H), 5.16 (appdt, *J* = 17.3, 1.2 Hz, 1H), 5.08 (appdt, *J* = 10.2, 1.2 Hz, 1H), 3.00 (dd, *J* = 13.8, 5.5 Hz, 1H), 2.92 (dd, *J* = 13.8, 5.5 Hz, 1H), 1.90 (s, 3H). <sup>13</sup>C NMR (100 MHz, Chloroform-*d*), δ (ppm): 178.1, 169.8, 163.3, 156.1, 136.1, 133.6, 133.3, 130.3, 128.9, 128.6, 126.0, 125.0, 122.7, 117.9, 117.4, 116.8, 73.3, 30.6, 21.1. FTIR (ATR/cm<sup>-1</sup>): 2935, 2865, 1750, 1508, 1270. HRESI-MS calculated for C<sub>21</sub>H<sub>18</sub>O<sub>4</sub>Na<sup>+</sup> [M + H]<sup>+</sup>: 335.1278; found: 335.1282.

### 3.4.3 Synthesis of compound **23a** ((E)-3-(buta-1,3-dien-1-yl)-2-phenyl-4H-chromen-4-one)

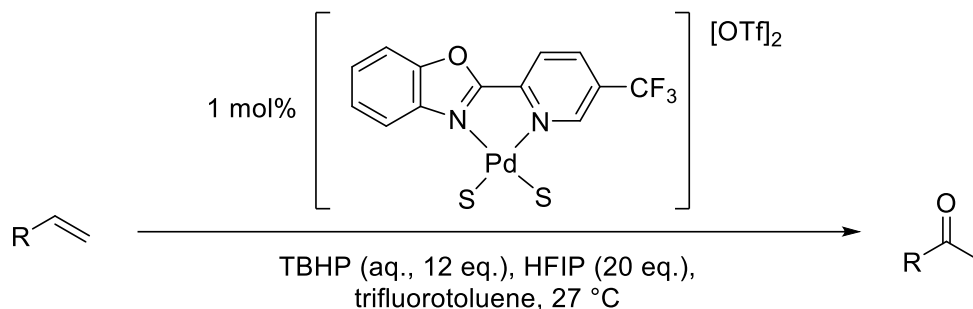


To a solution of **19a** (0.100 g, 0.342 mmol) in dichloromethane (1 mL) at 0 °C was added thionyl chloride (49  $\mu\text{L}$ , 0.684 mmol). The solution was warmed to room temperature and stirred for 2h before the solvent and volatiles were removed *in vacuo*. The crude residue was dissolved in THF (2 mL) and cooled to 0 °C before potassium *tert*-butoxide (0.057 mg, 0.513 mmol) was added before the reaction mixture was warmed to room temperature and stirred for a further 16 h before being quenched with 1M HCl (3 mL) and extracted with ethyl acetate (5 mL  $\times$  2). The combined organic extracts were washed with brine (5 mL), dried over  $\text{Na}_2\text{SO}_4$ , and reduced in vacuo. Purification by column chromatography (1:19 EtOAc/40–60 Pet. Ether) provided the title compound **23a** (0.064 g, 68%) as a pale yellow solid.

$^1\text{H}$  NMR (400 MHz, Chloroform-*d*),  $\delta$  (ppm): 8.27 (dd,  $J = 8.0, 1.5$  Hz, 1H), 7.65 (m, 4H), 7.51 (m, 3H), 7.42 (m, 2H), 6.31 (m, 2H), 5.32 (d,  $J = 17.2$ , 1H), 5.12 (d,  $J = 9.8$ , 1H)  $^{13}\text{C}$  NMR (100 MHz, Chloroform-*d*),  $\delta$  (ppm): 177.5, 163.2, 155.5, 138.5, 136.0, 133.6, 133.2, 130.8, 129.9, 128.6, 126.4, 125.2, 124.3, 123.6, 118.2, 118.0, 117.7. FTIR (ATR/ $\text{cm}^{-1}$ ): 3067, 2918, 2851, 1619, 1568, 1467, 1446. HRESI-MS calculated for  $\text{C}_{19}\text{H}_{14}\text{O}_2\text{Na}^+$   $[\text{M} + \text{H}]^+$ : 297.0886; found: 297.0882.

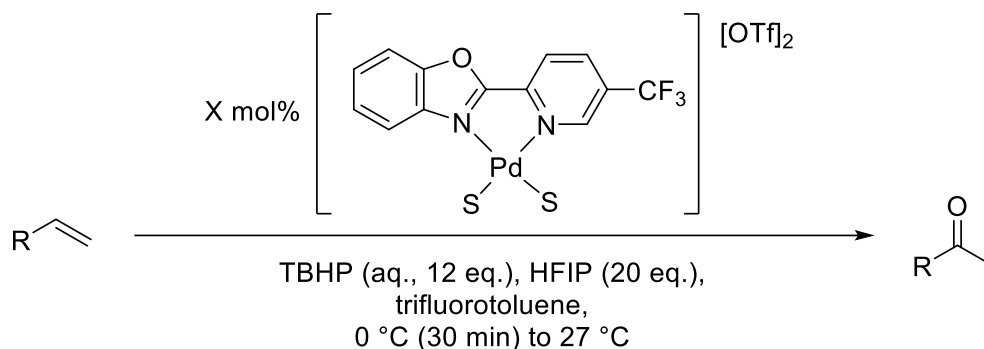
## 4 Oxidation reactions

### 4.1 Oxidation of allylic substrates: general procedure



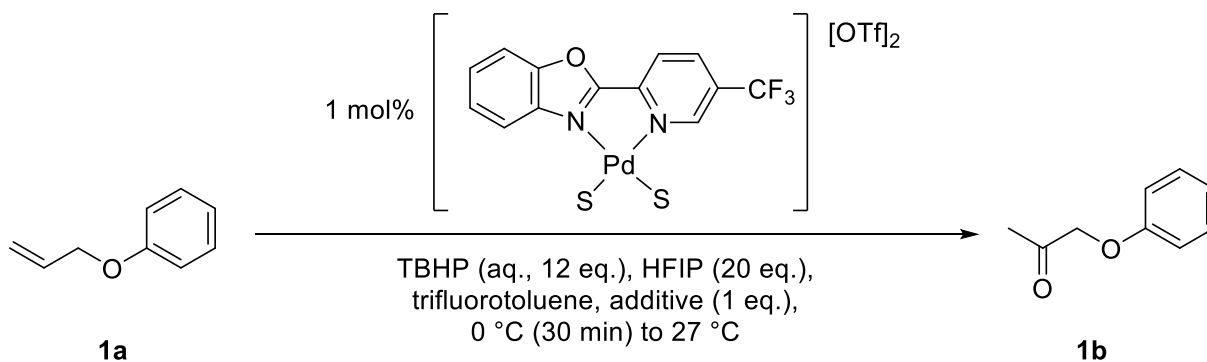
Example for oxidation of APE at 1 mol% catalyst loading, 12 eq. TBHP and 20 eq. HFIP at 27 °C; to a 14 mL glass vial, [Pd(5-CF<sub>3</sub>-PBO)(S)<sub>2</sub>][OTf]<sub>2</sub> (0.0068 g, 0.009 mmol, 1 mol%) was transferred, followed by dodecane (approx. 60 μL, weight recoded from balance). The vial was transferred to an aluminium block pre-warmed to 27 °C. Trifluorotoluene (5.6 mL), 70wt% aq. TBHP (1.5 mL, 10.8 mmol, 12 eq.) and HFIP (1.9 mL, 18 mmol, 20 eq.) were then added. Following stirring for 5 minutes at 27 °C, the substrate was added (124 μL, 0.9 mmol). Samples taken at designated intervals for GC analysis were taken as 4-5 drops filtered through a silica plug with diethyl ether. Finished reactions were transferred to an ice bath and the contents quenched with excess saturated sodium metabisulfite solution.

## 4.2 Oxidation of allylic substrates: cold-start conditions



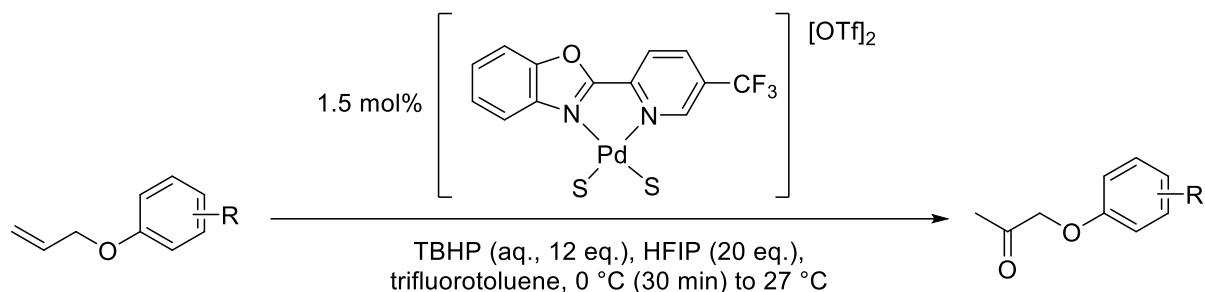
Example for oxidation of APE at 1 mol% catalyst loading, 12 eq. TBHP and 20 eq. HFIP at 0 °C for 30 minutes before transfer to 27 °C; to a 14 mL glass vial, [Pd(5-CF<sub>3</sub>-PBO)(S)<sub>2</sub>][OTf]<sub>2</sub> (0.0068 g, 0.009 mmol, 1 mol%) was transferred, followed by dodecane (approx. 60 μL, weight recorded from balance). the reaction vial was transferred to an aluminium block chilled to 0 °C. Trifluorotoluene (5.6 mL), 70wt% aq. TBHP (1.5 mL, 10.8 mmol, 12 eq.) and HFIP (1.9 mL, 18 mmol, 20 eq.) were then added. Following stirring for 5 minutes at 0 °C, the substrate was added (124 μL, 0.9 mmol). Samples taken at designated intervals for GC analysis were taken as 4-5 drops filtered through a silica plug with diethyl ether. After stirring at 0 °C for 30 minutes, the reaction vial was transferred to an aluminium block pre-warmed to 27 °C for the remainder of the reaction. Finished reactions were transferred to an ice bath and the contents quenched with excess saturated sodium metabisulfite solution.

### 4.3 Oxidation of allylic substrates: effect of additives



To a 14 mL glass vial,  $[\text{Pd}(\text{5-CF}_3\text{-PBO})(\text{S})_2][\text{OTf}]_2$  (0.0068 g, 0.009 mmol, 1 mol%) was transferred, followed by dodecane (approx. 60  $\mu\text{L}$ , weight recoded from balance). the reaction vial was transferred to an aluminium block chilled to 0 °C. Trifluorotoluene (5.6 mL), 70wt% aq. TBHP (1.5 mL, 10.8 mmol, 12 eq.) and HFIP (1.9 mL, 18 mmol, 20 eq.) were then added. Following stirring for 5 minutes at 0 °C, the desired additive (1 eq.) was added, immediately followed by the substrate (124  $\mu\text{L}$ , 0.9 mmol). Samples taken at designated intervals for GC analysis were taken as 4-5 drops filtered through a silica plug with diethyl ether. After stirring at 0 °C for 30 minutes, the reaction vial was transferred to an aluminium block pre-warmed to 27 °C for the remainder of the reaction. Finished reactions were transferred to an ice bath and the contents quenched with excess saturated sodium metabisulfite solution.

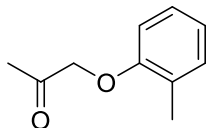
#### 4.4 Oxidation and isolation of allyl phenyl ether derivatives (3a to 15a)



To a 15 mL glass vial,  $[Pd(5-CF_3-PBO)(S)_2][OTf]_2$  (0.0102 g, 0.0136 mmol) was added before transfer to an aluminium block pre-chilled to 0 °C. To this, trifluorotoluene (5.6 mL), Luperox™ TBH70X, 70 wt% TBHP (1.5 mL, 10.8 mmol, 12 eq.) and HFIP (1.9 mL, 18 mmol, 20 eq.) were added and the reaction mixture stirred at 0 °C for 5 minutes before addition of the substrate (0.9 mmol, volume determined and tested by density prior to reaction). Following stirring at 0 °C for 30 minutes, the reaction vial was transferred to an aluminium block pre-heated to 27 °C and stirred for a further 2.5 hours. The reaction was then transferred to an ice bath and excess TBHP was quenched by stirring with saturated aqueous sodium metabisulfite solution and checked using peroxide test strips. The reaction was extracted with ethyl acetate (3 x 20 mL), dried over magnesium sulfate and filtered. The solvent was removed under reduced pressure and the crude material subject to flash column chromatography, initially with hexane to remove traces of trifluorotoluene, then with ethyl acetate/hexane (HPLC-grade, appropriate ratio determined by TLC). Product fractions were combined and solvent removed/product dried under reduced pressure. Products **3b** and **9b** were obtained from purchased substrates. Product **7b** was isolated using preparative thin layer chromatography.

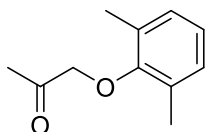
For substrates **10a**, **11a** and **12a**, initial attempts to isolate the products were problematic, giving low yields and poor purity. It is possible that the products were decomposing during reaction quenching with aqueous saturated sodium metabisulfite solution. In subsequent attempts, these substrates were isolated by direct column chromatography, without quenching. It is important to note that collected product fractions were checked with peroxide test strips prior to concentrating the collected material and drying under reduced pressure.

#### 4.4.1 1-(*o*-tolylloxy)propan-2-one (3b)



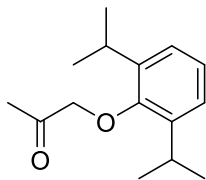
Yield = 0.1286 g, 0.78 mmol, 87%, orange oil, columned with 1:5 EtOAc/Hexane.  $^1\text{H}$  NMR (400 MHz, Chloroform-*d*)  $\delta$  7.22 – 7.08 (m, 2H), 6.92 (s, 1H), 6.66 (s, 1H), 4.52 (s, 2H), 2.31 (s, 6H).  $^{13}\text{C}\{\text{H}\}$  NMR (101 MHz, Chloroform-*d*)  $\delta$  206.53, 155.84, 131.08, 126.92, 126.88, 121.39, 110.74, 73.13, 26.74, 16.29. *m/z*: predicted  $[\text{M}+\text{Na}]^+ = 187.0730$ , found  $[\text{M}+\text{Na}]^+ = 187.0737$ . Elemental Analysis: Predicted = C, 73.15; H, 7.37; Obtained = C, 72.6; H, 7.00. IR (neat): 3027, 2918, 1722, 1591, 1495, 1431, 1357, 1305, 1230, 1185, 1126, 1062, 965, 842  $\text{cm}^{-1}$ .

#### 4.4.2 1-(2,6-dimethylphenoxy)propan-2-one (4b)



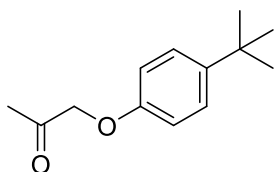
Yield = 0.1090 g, 0.61 mmol, 68%, yellow oil, columned with 1:2 EtOAc/Hexane.  $^1\text{H}$  NMR (400 MHz, Chloroform-*d*)  $\delta$  7.06 – 6.99 (m, 2H), 6.98 – 6.91 (m, 1H), 4.34 (s, 2H), 2.36 (s, 3H), 2.27 (s, 6H).  $^{13}\text{C}\{\text{H}\}$  NMR (101 MHz, Chloroform-*d*)  $\delta$  205.48, 154.94, 130.53, 129.04, 124.46, 76.57, 26.64, 16.25. Spectra in agreement with literature data.<sup>28</sup> *m/z*: predicted  $[\text{M}+\text{Na}]^+ = 201.0886$ , found  $[\text{M}+\text{Na}]^+ = 201.0891$ . Elemental Analysis: Predicted = C, 74.13; H, 7.92; Obtained = C, 72.34; H, 7.15. IR (neat): 3019, 2922, 1718, 1651, 1592, 1476, 1423, 1357, 1264, 1193, 1096, 1051, 965, 835, 768, 686  $\text{cm}^{-1}$ .

#### 4.4.3 1-(2,6-diisopropylphenoxy)propan-2-one (5b)



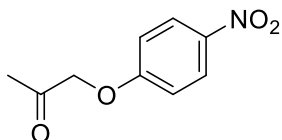
Yield = 0.1762 g, 0.75 mmol, 84%, yellow oil, Columned with 1:2 EtOAc/Hexane.  $^1\text{H}$  NMR (400 MHz, Chloroform-*d*)  $\delta$  7.12 (s, 3H), 4.34 (s, 2H), 3.32 – 3.14 (m, 2H), 2.37 (s, 3H), 1.28 – 1.18 (m, 12H).  $^{13}\text{C}\{\text{H}\}$  NMR (101 MHz, Chloroform-*d*)  $\delta$  205.46, 152.31, 141.40, 125.21, 124.23, 79.05, 77.22, 26.66, 23.98. m/z: predicted  $[\text{2M}+\text{Na}^+] = 491.3137$ , found  $[\text{2M}+\text{Na}^+] = 491.3094$ . Elemental Analysis: Predicted = C, 76.88; H, 9.46; Obtained = C, 76.28; H, 9.69. IR (neat): 3064, 2963, 2870, 1722, 1589, 1457, 1357, 1327, 1256, 1178, 1103, 1059, 999, 965, 936, 835, 790, 757, 682  $\text{cm}^{-1}$ .

#### 4.4.4 1-(4-(tert-butyl)phenoxy)propan-2-one (6b)



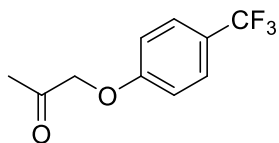
Yield = 0.1670 g, 0.81 mmol, 90%, yellow solid, columned with 1:2 EtOAc/Hexane.  $^1\text{H}$  NMR (400 MHz, Chloroform-*d*)  $\delta$  7.38 – 7.29 (m, 2H), 6.87 – 6.78 (m, 2H), 4.51 (s, 2H), 2.28 (s, 3H), 1.30 (s, 9H).  $^{13}\text{C}\{\text{H}\}$  NMR (101 MHz, Chloroform-*d*)  $\delta$  206.32, 155.48, 144.50, 126.48, 113.97, 73.22, 34.14, 31.48, 26.66. m/z: predicted  $[\text{M}+\text{Na}]^+ = 229.1199$ , found  $[\text{M}+\text{Na}]^+ = 229.1176$ . Elemental Analysis: Predicted = C, 75.69; H, 8.80; Obtained = C, 74.49; H, 8.52. IR (neat): 2959, 2870, 1722, 1610, 1513, 1465, 1435, 1364, 1297, 1234, 1185, 1118, 1066, 1014, 827  $\text{cm}^{-1}$ .

#### 4.4.5 1-(4-nitrophenoxy)propan-2-one (7b)



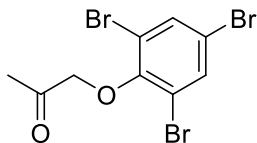
Yield = 0.1421 g, 0.73 mmol, 81%, white solid, isolated using preparative thin layer chromatography, with DCM.  $^1\text{H}$  NMR (400 MHz, Chloroform-*d*)  $\delta$  8.31 – 8.19 (m, 2H), 7.03 – 6.91 (m, 2H), 4.68 (s, 2H), 2.31 (s, 3H).  $^{13}\text{C}\{\text{H}\}$  NMR (101 MHz, Chloroform-*d*)  $\delta$  203.19, 162.47, 142.28, 126.05, 114.63, 72.98, 26.57. *m/z*: predicted  $[\text{M}+\text{NH}_4]^+$  = 213.0875, found  $[\text{M}+\text{NH}_4]^+$  = 213.0887. Elemental Analysis: Predicted = C, 55.39; H, 4.65; N, 7.18. Obtained = C, 55.49 ; H, 4.38; N, 6.96. IR (neat): 3112, 3082, 2922, 2840, 1729, 1588, 1495, 1431, 1330, 1264, 1170, 1111, 1055, 969, 842, 753, 690  $\text{cm}^{-1}$ .

#### 4.4.6 1-(4-(trifluoromethyl)phenoxy)propan-2-one (8b)



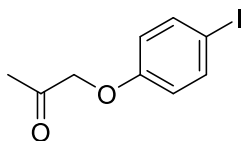
Yield = 0.1615 g, 0.74 mmol, 82%, off-white solid, columned with 1:5 EtOAc/Hexane.  $^1\text{H}$  NMR (400 MHz, Chloroform-*d*)  $\delta$  7.66 – 7.51 (m, 2H), 7.05 – 6.87 (m, 2H), 4.60 (s, 2H), 2.30 (s, 3H).  $^{13}\text{C}\{\text{H}\}$  NMR (101 MHz, Chloroform-*d*)  $\delta$  204.39, 160.06, 127.16 (q,  $J$  = 3.8 Hz), 124.17, 122.85, 114.55, 72.87, 26.59.  $^{13}\text{C}\{\text{H}\}$  NMR signals.  $^{19}\text{F}\{\text{H}\}$  NMR (376 MHz, Chloroform-*d*)  $\delta$  -61.71. *m/z*: predicted  $[\text{M}-\text{H}]^-$  = 217.0476, found  $[\text{M}-\text{H}]^-$  = 217.0445. Elemental Analysis: Predicted = C, 55.05; H, 4.16; Obtained = C, 55.10 ; H, 4.10. IR (neat): 1730, 1618, 1521, 1424, 1327, 1264, 1163, 1111, 1059, 1010, 969, 835.

#### 4.4.7 1-(2,4,6-tribromophenoxy)propan-2-one (9b)



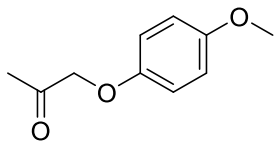
Yield = 0.3127 g, 0.81 mmol, 90%, white solid, columned with 1:5 EtOAc/Hexane.  $^1\text{H}$  NMR (400 MHz, Chloroform-*d*)  $\delta$  7.68 (s, 2H), 4.49 (s, 2H), 2.43 (s, 3H).  $^{13}\text{C}\{\text{H}\}$  NMR (101 MHz, Chloroform-*d*)  $\delta$  204.29, 151.58, 135.20, 118.63, 118.37, 76.50, 27.03. *m/z*: predicted  $[\text{M}+\text{K}]^+$  = 422.7632, found  $[\text{M}+\text{K}]^+$  = 422.7633. Elemental Analysis: Predicted = C, 27.94; H, 1.82; Obtained = C, 28.78; H, 2.00. IR (neat): 3105, 3068, 2974, 2911, 1722, 1595, 1539, 1450, 1416, 1353, 1252, 1185, 1111, 1066, 969, 857, 738, 693  $\text{cm}^{-1}$ .

#### 4.4.8 1-(4-iodophenoxy)propan-2-one (10b)



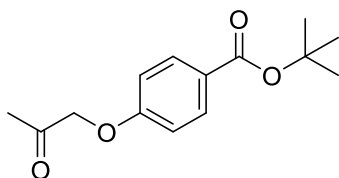
Yield = 0.1996 g, 0.72 mmol, 80%, white solid, columned with 1:3 EtOAc/Hexane.  $^1\text{H}$  NMR (400 MHz, Chloroform-*d*)  $\delta$  7.65 – 7.53 (m, 2H), 6.72 – 6.62 (m, 2H), 4.51 (s, 2H), 2.27 (s, 3H).  $^{13}\text{C}$  NMR (101 MHz, Chloroform-*d*)  $\delta$  204.97, 157.60, 138.49, 116.88, 84.04, 72.97, 26.61 *m/z*: predicted  $[\text{M}+\text{Na}]^+$  = 298.9545, found  $[\text{M}+\text{Na}]^+$  = 298.9549. Elemental Analysis: Predicted = C, 39.16; H, 3.29; Obtained = C, 39.15; H, 2.70. IR (neat): 3064, 2896, 1879, 1722, 1584, 1483, 1431, 1357, 1282, 1230, 1170, 1114, 1055, 999, 969, 820, 693  $\text{cm}^{-1}$ .

#### 4.4.9 1-(4-methoxyphenoxy)propan-2-one (11b)



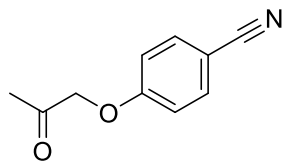
Yield = 0.1111 g, 0.62mmol, 69%, white-solid, columned with 1:3 EtOAc/hexane.  $^1\text{H}$  NMR (400 MHz, Chloroform-*d*)  $\delta$  6.94 – 6.71 (m, 4H), 4.49 (s, 2H), 3.77 (s, 3H), 2.27 (s, 3H).  $^{13}\text{C}$  NMR (101 MHz, Chloroform-*d*)  $\delta$  206.20, 154.48, 151.89, 115.53, 114.80, 73.85, 55.70, 26.61 .m/z: predicted  $[\text{M}+\text{Na}]^+$  = 203.0684, found  $[\text{M}+\text{Na}]^+$  = 203.0683. Elemental analysis: Predicted = C, 66.65; H, 6.71. Obtained = C, 66.81; H, 6.45. IR (neat): 3004, 2907, 2836, 1722, 1592, 1506, 1465, 1435, 1357, 1293, 1223, 1178, 1111, 1066, 1032, 969, 827, 716, 522.

#### 4.4.10 tert-butyl 4-(2-oxopropoxy)benzoate (12b)



Yield = 0.1865 g, 0.74 mmol, 82%, white solid, columned with 1:5 EtOAc/hexane.  $^1\text{H}$  NMR (400 MHz, Chloroform-*d*)  $\delta$  8.02 – 7.89 (m, 2H), 6.96 – 6.81 (m, 2H), 4.59 (s, 2H), 2.29 (s, 3H), 1.58 (s, 9H).  $^{13}\text{C}$  NMR (101 MHz, Chloroform-*d*)  $\delta$  204.75, 165.29, 160.90, 131.56, 125.61, 113.93, 80.78, 72.85, 28.23, 26.63. m/z: predicted  $[\text{M}+\text{Na}]^+$  = 273.1103, found  $[\text{M}+\text{Na}]^+$  = 273.1107. Elemental analysis: Predicted = C, 67.18; H, 7.25. Obtained = C, 67.02; H, 7.42. IR (neat): 2974, 2930, 1703, 1603, 1510, 1416, 1368, 1290, 1256, 1155, 1114, 1070, 1010, 969, 850, 772, 693, 656, 552, 507.

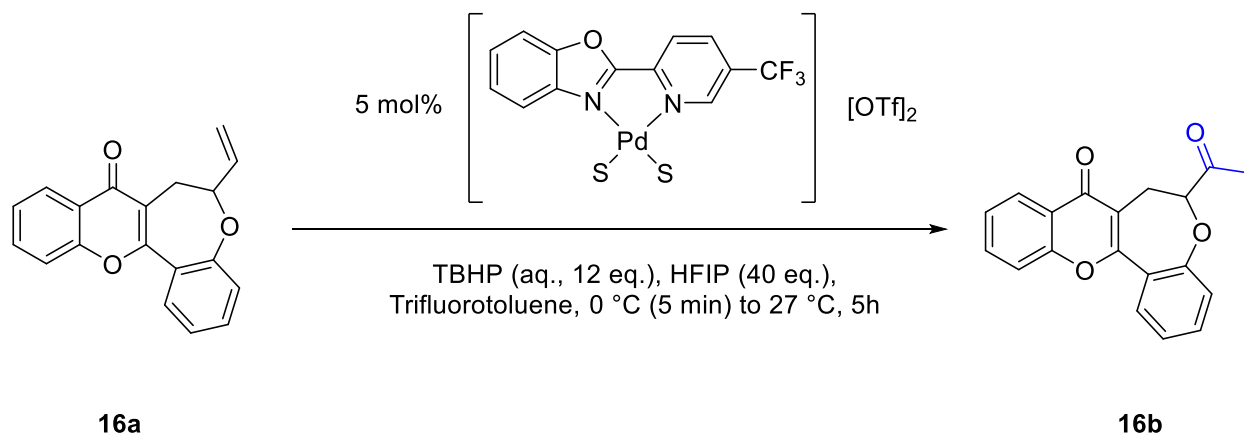
#### 4.4.11 4-(2-oxopropoxy)benzonitrile (13b)



Yield = 0.0497 g, 0.28 mmol, 31%, off-white solid, columned with 1:1 EtOAc/hexane.  $^1\text{H}$  NMR (400 MHz, Chloroform-*d*)  $\delta$  7.71 – 7.54 (m, 2H), 7.03 – 6.86 (m, 2H), 4.62 (s, 2H), 2.30 (s, 3H).  $^{13}\text{C}$  NMR (101 MHz, Chloroform-*d*)  $\delta$  203.54, 160.83, 134.20, 118.80, 115.29, 105.27, 72.74, 26.58.  $m/z$  predicted  $[\text{M}+\text{H}]^+ = 176.0712$ , found  $[\text{M}+\text{H}]^+ = 176.0711$ . Elemental analysis: predicted = C, 68.56; H, 5.18; N, 8.00. Obtained = C; 68.34; H, 5.13; N, 8.27. IR (neat): 2922.2, 2853.3, 2223.4, 1731.3, 1602.8, 1576.7, 1505.8, 1433.2, 1358.6, 1302.7, 1261.7, 1239.3, 1168.5, 1114.5, 1064.2, 967.2, 833.1, 717.5, 684.0, 657.9.

## 4.5 Oxidation of compounds 16a to 20a

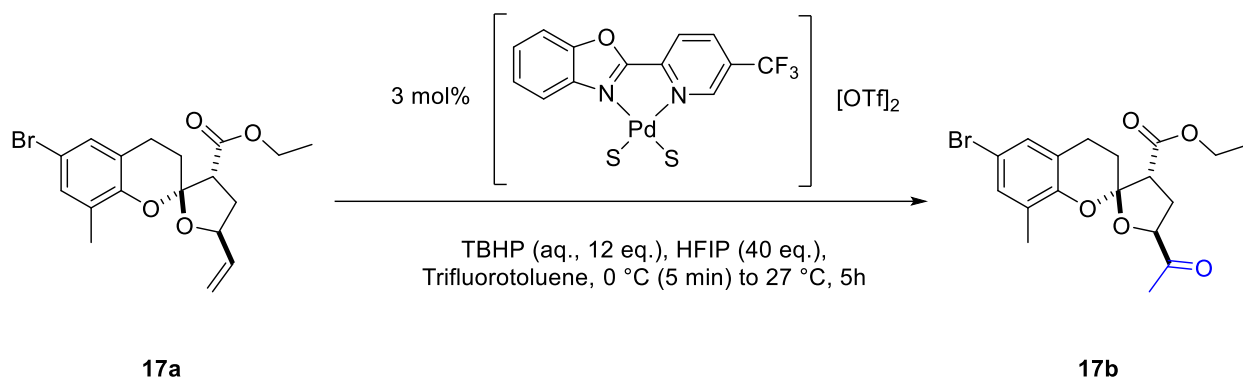
### 4.5.1 Oxidation of 6-vinyl-6,7-dihydro-8H-benzo[2,3]oxepino[4,5-b]chromen-8-one (16a)



To a clean vial, substrate (58.1 mg, 0.2 mmol) and catalyst (7.6 mg, 0.0101 mmol) were transferred and chilled to 0 °C (using an aluminium block). Trifluorotoluene (0.827 mL) and HFIP (0.84 mL, 8.00 mmol, 40 equiv.) were then added and the reaction was then initiated by the addition of 70 wt% aq. TBHP (0.333 mL, 2.40 mmol, 12 equiv.). The reaction was stirred at 0 °C for 5 minutes, before transfer to an aluminium block which was at 27 °C and left to stir for a total of 5 hours. The reaction mixture was transferred directly to a preparatory TLC plate without quenching, the reaction vial rinsed with DCM and these washings also transferred to the plate, and initially run with pet. ether to selectively elute trifluorotoluene to the front to allow separation from product. Afterwards, the TLC plate was left to dry and then run in 1:5 ethyl acetate-hexane eluent (both HPLC grade). The product band was removed and extracted with chloroform and dried overnight under reduced pressure. For 0.1 mmol scale reactions, the reaction mixture was prepared using stock solutions; a TBHP/trifluorotoluene/HFIP stock solution was prepared, a portion of which was added to a weighed amount of catalyst to form a TBHP/trifluorotoluene/HFIP/catalyst stock, a portion of which was added to the substrate to initiate the reaction. In initial experiments where <sup>1</sup>H-NMR analysis was carried out, an analogous means for preparing reactions was used on a 10 mg substrate scale. At the end of the reaction, nitromethane was added (10 μL, weight recorded), the reaction stirred for 2 minutes before a portion was taken and dissolved in CDCl<sub>3</sub> and sampled for NMR analysis. Where multiple sample points were used, an accurately measured portion of the reaction mixture, taken using a micropipette, was added to a vial containing nitromethane (10 μL, weight recorded), the contents dissolved in CDCl<sub>3</sub> and sampled for NMR analysis.

Yield = 41.5 mg, 0.135 mmol, 68%, off-white solid (0.2 mmol scale).  $^1\text{H}$  NMR (600 MHz, Chloroform-*d*)  $\delta$  8.31 – 8.21 (m, 1H), 7.95 – 7.85 (m, 1H), 7.76 – 7.66 (m, 1H), 7.55 – 7.52 (m, 1H), 7.52 – 7.48 (m, 1H), 7.45 – 7.41 (m, 1H), 7.32 – 7.27 (m, 2H), 5.08 (dd,  $J$  = 8.5, 4.3 Hz, 1H), 3.36 (dd,  $J$  = 15.6, 4.3 Hz, 1H), 3.01 (dd,  $J$  = 15.6, 8.5 Hz, 1H), 2.34 (s, 3H).  $^{13}\text{C}\{\text{H}\}$  NMR (101 MHz, Chloroform-*d*)  $\delta$  205.32, 176.38, 159.02, 156.17, 155.67, 133.76, 132.67, 128.48, 126.11, 125.16, 125.12, 123.91, 123.37, 122.63, 118.00, 117.70, 91.51, 26.59, 24.64 . m/z: predicted  $[\text{M}+\text{H}]^+$  = 307.0970, found  $[\text{M}+\text{H}]^+$  = 307.0977. Elemental analysis: predicted = C, 74.5; H = 4.61. Obtained = C, 74.2; H, 4.81. IR (neat): 1726, 1629, 1574.8, 1485, 1467, 1403, 1351, 1284, 1258, 1239, 1221, 1105, 757  $\text{cm}^{-1}$ .

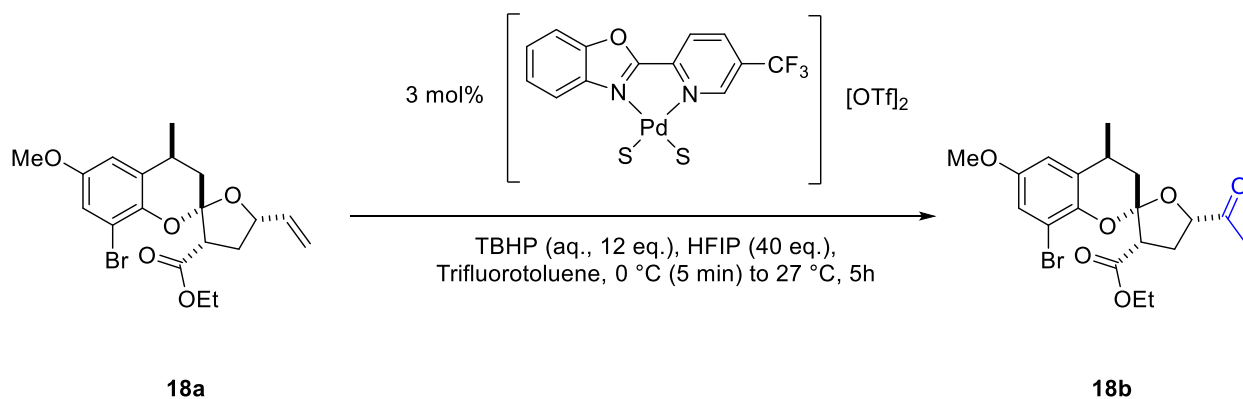
#### 4.5.2 Oxidation of ethyl 6-bromo-8-methyl-5'-vinyl-4',5'-dihydro-3'H-spiro[chromane-2,2'-furan]-3'-carboxylate (17a)



A stock solution of TBHP (0.644 mL, 4.80 mmol), HFIP (1.68 mL, 16.00 mmol) and trifluorotoluene (1.656 mL) was prepared, of which a 2 mL portion was added to the catalyst (4.6 mg, 0.00613 mmol). After stirring at 0 °C for five minutes, a 1 mL portion of this TBHP/HFIP/trifluorotoluene/catalyst stock solution was added to the substrate (38.2 mg, 0.1 mmol), the reaction stirred at 0 °C for five minutes and then transferred to a pre-warmed heating block set to 27 °C for a total stirring time of 5 h. Material isolated using prep TLC procedure in section 4.5.1. Benzannulated spiroketal substrates provided were racemic, single diastereomers.

Yield = 29.3 mg, 0.074 mmol, 74%, pale yellow solid (0.1 mmol scale).  $^1\text{H}$  NMR (400 MHz, Chloroform-*d*)  $\delta$  7.08 (s, 2H), 4.43 (t,  $J$  = 8.4 Hz, 1H), 4.24 – 4.06 (m, 2H), 3.16 – 3.04 (m, 2H), 3.03 – 2.91 (m, 1H), 2.80 – 2.66 (m, 1H), 2.62 – 2.49 (m, 1H), 2.48 – 2.37 (m, 1H), 2.13 – 2.04 (m, 1H), 2.00 (s, 3H), 1.92 (s, 3H), 1.21 (t,  $J$  = 7.1 Hz, 3H).  $^{13}\text{C}\{\text{H}\}$  NMR (101 MHz, Chloroform-*d*)  $\delta$  209.91, 168.12, 148.81, 131.26, 129.14, 128.19, 123.29, 112.71, 106.28, 82.70, 61.14, 53.44, 28.81, 28.38, 25.46, 21.93, 15.26, 14.14.  $m/z$ : predicted  $[\text{M}+\text{H}]^+$  = 397.0651, found  $[\text{M}+\text{H}]^+$  = 397.0648. Elemental analysis: predicted = C, 54.4; H, 5.33; Obtained = C, 54.6; H, 5.20. IR (neat): 1802, 1741, 1634, 1469, 1370, 1299, 1262, 1228, 1206, 1129, 1095, 1053, 1034, 1006, 993, 958, 859, 805, 762, 732  $\text{cm}^{-1}$ .

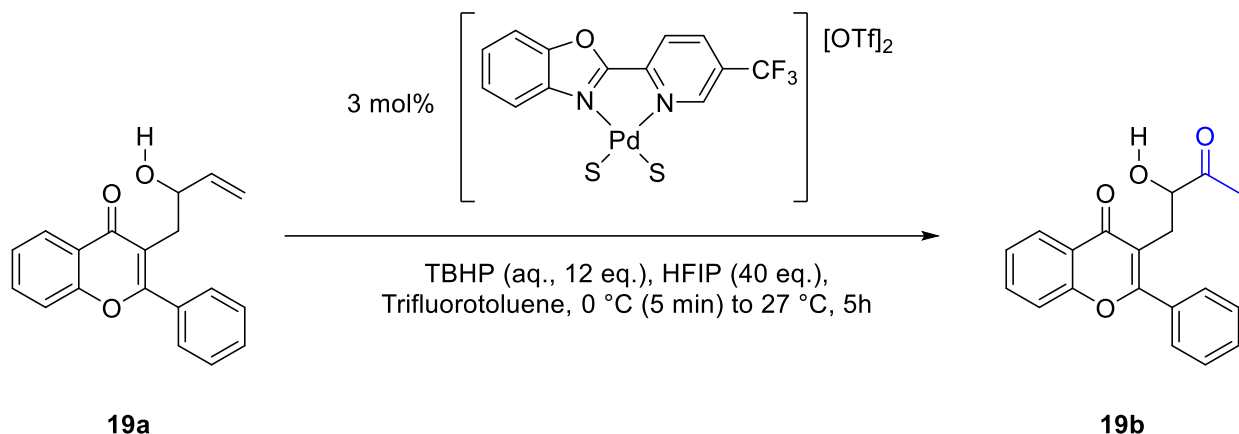
### 4.5.3 Oxidation of ethyl 8-bromo-6-methoxy-4-methyl-5'-vinyl-4',5'-dihydro-3'H-spiro[chromane-2,2'-furan]-3'-carboxylate (18a)



A stock solution of TBHP (0.644 mL, 4.80 mmol), HFIP (1.68 mL, 16.00 mmol) and trifluorotoluene (1.656 mL) was prepared, of which a 2 mL portion was added to the catalyst (4.6 mg, 0.00613 mmol). After stirring at 0 °C for five minutes, a 1 mL portion of this TBHP/HFIP/trifluorotoluene/catalyst stock solution was added to the substrate (41.2 mg, 0.1 mmol), the reaction stirred at 0 °C for five minutes and then transferred to a pre-warmed heating block set to 27 °C for a total stirring time of 5 h. Material isolated using prep TLC procedure in section 5.3. Material isolated using prep TLC procedure in section 4.5.1. Benzannulated spiroketal substrates provided were racemic, single diastereomers.

Yield = 23.5 mg, 0.055 mmol, 55%, orange solid (0.1 mmol scale). <sup>1</sup>H NMR (400 MHz, Chloroform-*d*) δ 6.97 – 6.89 (m, 1H), 6.85 – 6.73 (m, 1H), 4.47 – 4.37 (m, 1H), 4.27 – 4.15 (m, 2H), 3.75 (s, 3H), 3.31 – 3.20 (m, 1H), 3.11 – 3.02 (m, 1H), 3.00 – 2.87 (m, 1H), 2.63 – 2.51 (m, 1H), 2.25 (t, *J* = 13.2 Hz, 1H), 2.11 – 2.03 (m, 1H), 2.00 (s, 3H), 1.38 (d, *J* = 6.8 Hz, 3H), 1.24 (t, *J* = 7.1 Hz, 3H). <sup>13</sup>C{H} NMR (101 MHz, Chloroform-*d*) δ 210.50, 167.98, 153.81, 142.19, 129.21, 116.24, 112.00, 106.95, 83.05, 61.26, 55.82, 55.79, 53.35, 37.51, 29.29, 26.54, 25.18, 19.22, 14.16. *m/z*: predicted [M+Na]<sup>+</sup> = 451.0558, found [M+Na]<sup>+</sup> = 451.0555. Elemental analysis: predicted = C, 53.4; H, 5.43; Obtained = C, 53.4; H = 5.27. IR (neat): 1718, 1608, 1569, 1467, 1437, 1370, 1325, 1306, 1258, 1228, 1141, 1126, 1105, 1045, 1001, 965, 926, 885, 859, 822, 799, 758, 725 cm<sup>-1</sup>.

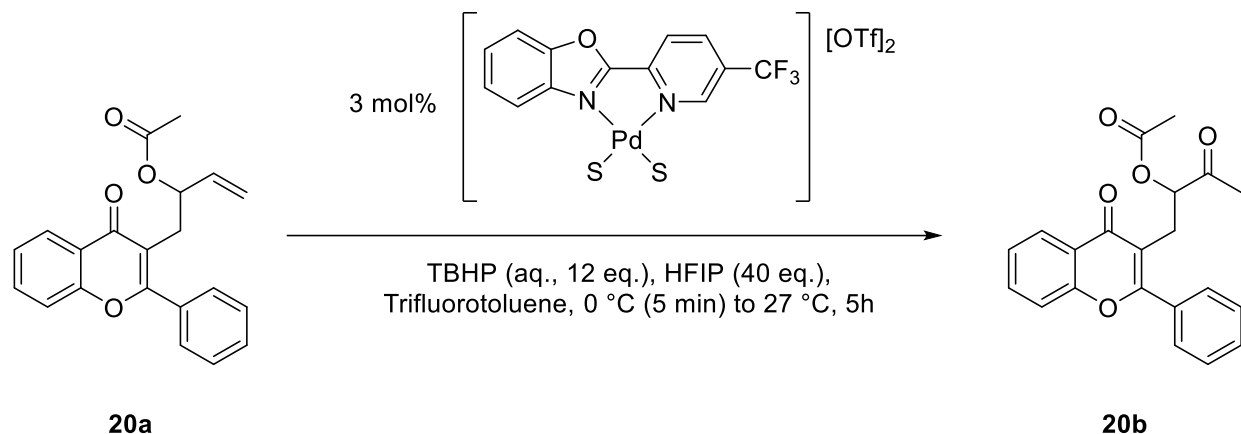
#### 4.5.4 Oxidation of 3-(2-hydroxybut-3-en-1-yl)-2-phenyl-4H-chromen-4-one (19a)



To a clean vial, substrate (50 mg, 0.0171 mmol) and catalyst (3.8 mg, 0.00513 mmol) were transferred and chilled to 0 °C (using a cooling block). Trifluorotoluene (0.707 mL) and HFIP (0.719 mL, 6.84 mmol, 40 equiv.) were then added and the reaction was then initiated by the addition of 70 wt% aq. TBHP (0.284 mL, 2.052 mmol, 12 equiv.). The reaction was stirred at 0 °C for 5 minutes, before transfer to a heating block which was pre-set to 27 °C and left to stir for a total of 5 hours. Material isolated using prep TLC procedure in section 4.5.1.

Yield = 30.0 mg, 57%, 0.0973 mmol, yellow oil (0.171 mmol scale).  $^1\text{H}$  NMR (400 MHz, Chloroform-*d*)  $\delta$  8.31 – 8.19 (m, 1H), 7.80 – 7.73 (m, 2H), 7.73 – 7.67 (m, 1H), 7.55 – 7.40 (m, 5H), 4.63 – 4.53 (m, 1H), 4.29 – 4.15 (m, 1H), 3.24 – 3.14 (m, 1H), 2.75 – 2.62 (m, 1H), 2.39 – 2.30 (m, 3H).  $^{13}\text{C}\{\text{H}\}$  NMR (101 MHz, Chloroform-*d*)  $\delta$  210.41, 179.45, 164.23, 156.26, 133.94, 132.78, 130.50, 129.28, 128.53, 125.73, 125.18, 122.64, 118.03, 117.65, 76.16, 31.01, 25.59.  $m/z$ : predicted  $[\text{M}+\text{H}]^+ = 309.1127$ , found  $[\text{M}+\text{H}]^+ = 309.1117$ . Elemental Analysis: Predicted = C, 74.01; H, 5.23. Obtained = C, 71.79; H, 5.41. IR (neat): 3304, 2942, 2830, 1448, 1420, 1114, 1021, 918, 734.

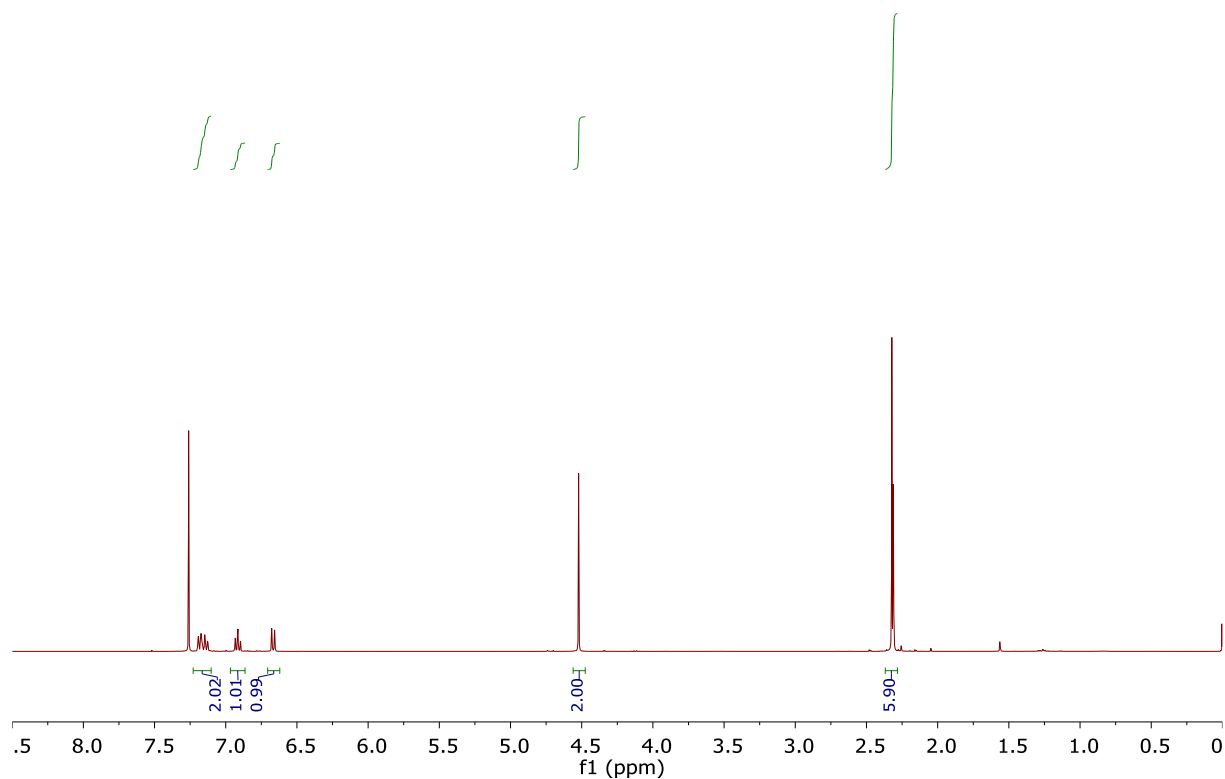
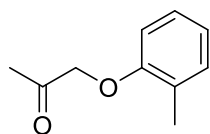
#### 4.5.5 Oxidation of 1-(4-oxo-2-phenyl-4H-chromen-3-yl)but-3-en-2-yl acetate (20a)

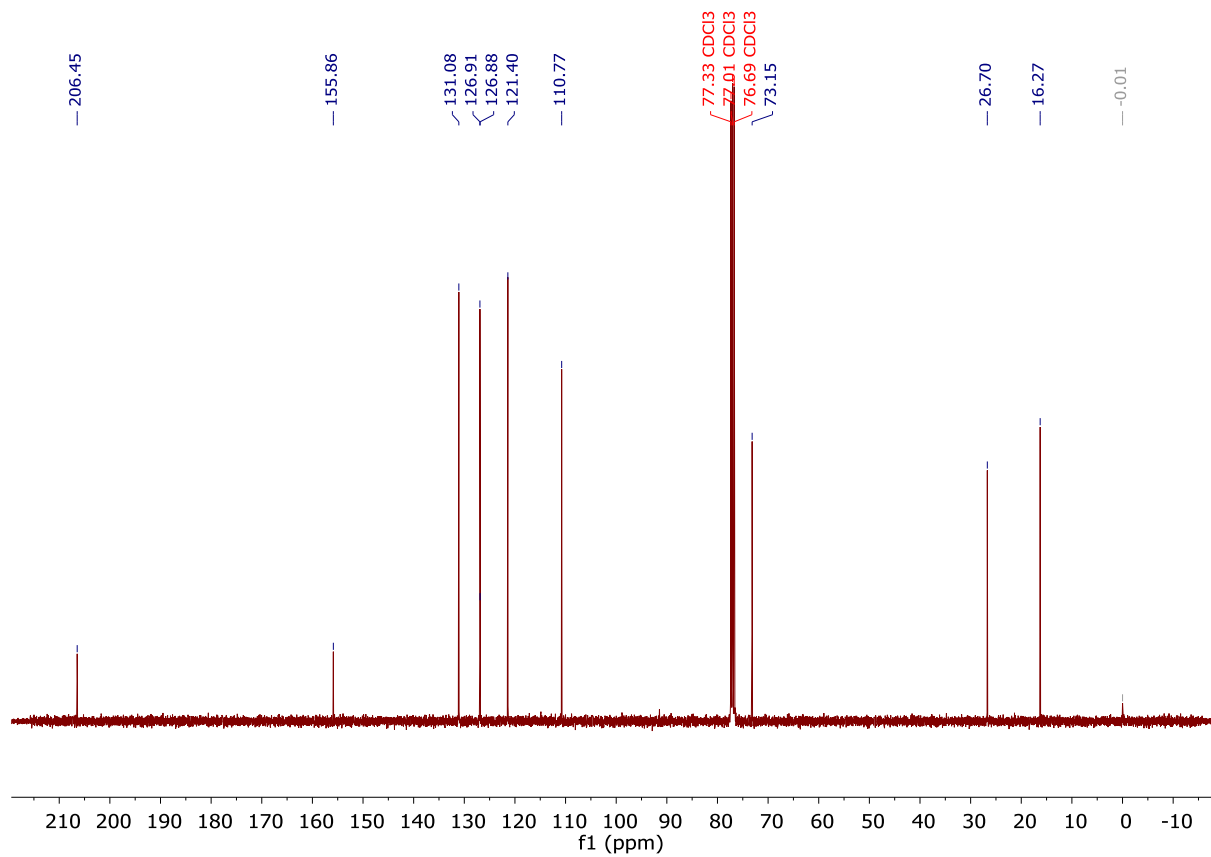


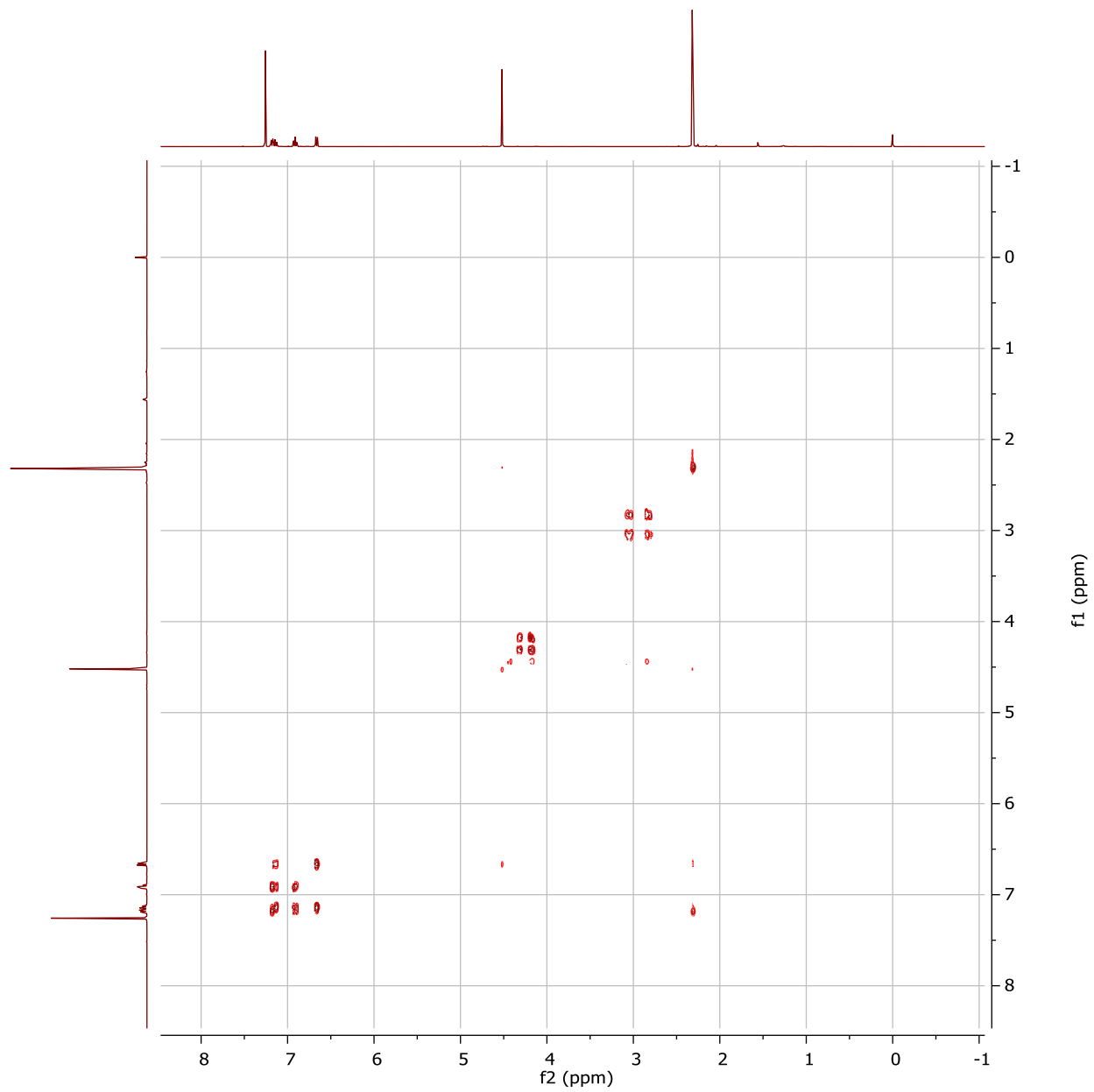
To a clean vial, substrate (50 mg, 0.149 mmol) and catalyst (3.4 mg, 0.00447 mmol) were transferred and chilled to 0 °C (using a cooling block). Trifluorotoluene (0.617 mL) and HFIP (0.626 mL, 5.96 mmol, 40 equiv.) were then added and the reaction was then initiated by the addition of 70 wt% aq. TBHP (0.247 mL, 1.788 mmol, 12 equiv.). The reaction was stirred at 0 °C for 5 minutes, before transfer to a heating block which was pre-set to 27 °C and left to stir for a total of 5 hours. Material isolated using prep TLC procedure in section 5.3. Yield = 8.8 mg, 0.0251 mmol, 17 %, yellow oil (0.149 mmol scale).  $^1\text{H}$  NMR (400 MHz, Chloroform-*d*)  $\delta$  8.33 – 8.16 (m, 1H), 7.78 – 7.65 (m, 3H), 7.60 – 7.50 (m, 3H), 7.50 – 7.41 (m, 2H), 5.45 – 5.36 (m, 1H), 3.29 – 3.19 (m, 1H), 2.94 – 2.81 (m, 1H), 2.27 (s, 3H), 2.00 (s, 3H).  $^{13}\text{C}$  NMR (151 MHz, Chloroform-*d*)  $\delta$  204.32, 178.18, 170.05, 163.92, 156.23, 133.88, 132.80, 130.55, 128.93, 128.91, 128.69, 125.82, 125.24, 122.65, 118.06, 116.50, 26.79, 26.39, 20.60 .

## 5 NMR spectra

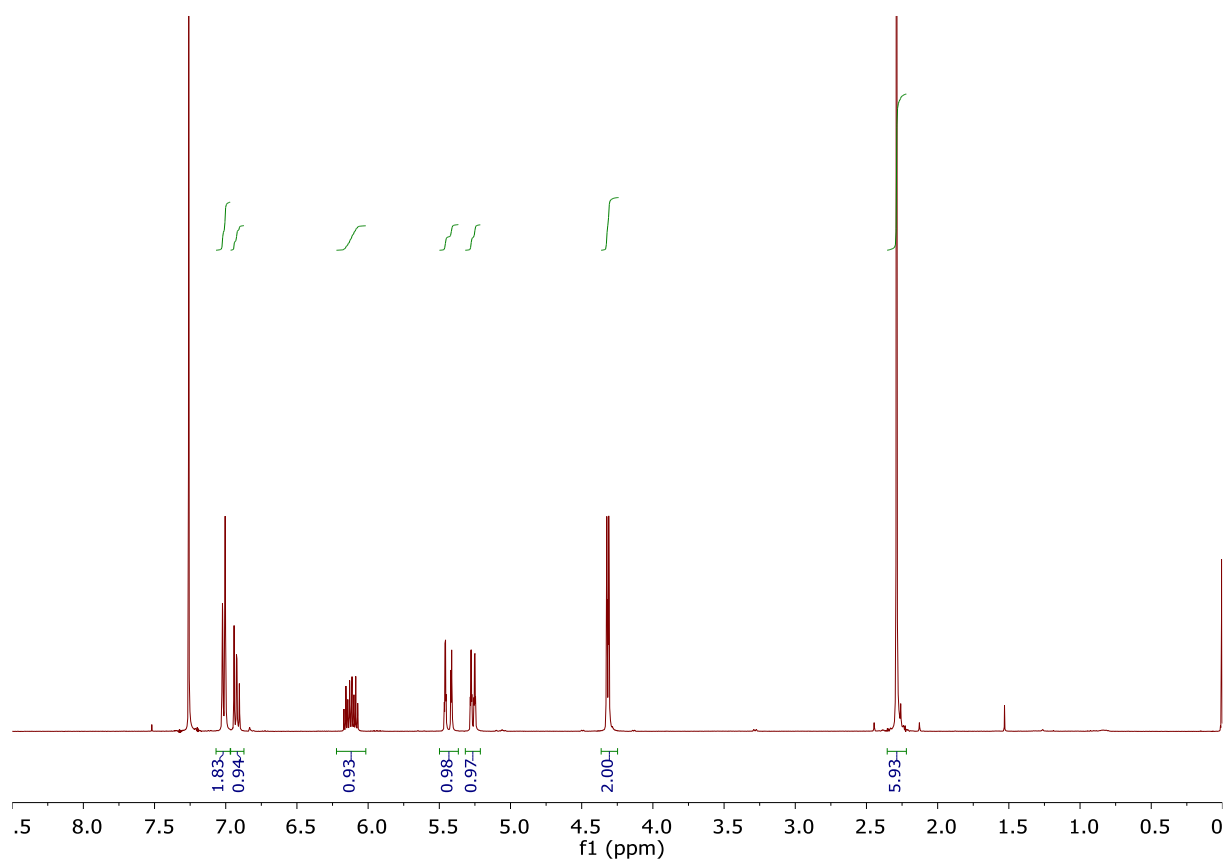
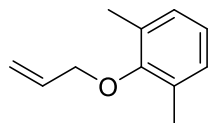
**1-(*o*-tolylloxy)propan-2-one (3b):**  $^1\text{H}$  NMR (400 MHz, Chloroform-*d*),  $^{13}\text{C}\{\text{H}\}$  NMR (101 MHz, Chloroform-*d*) and COSY.

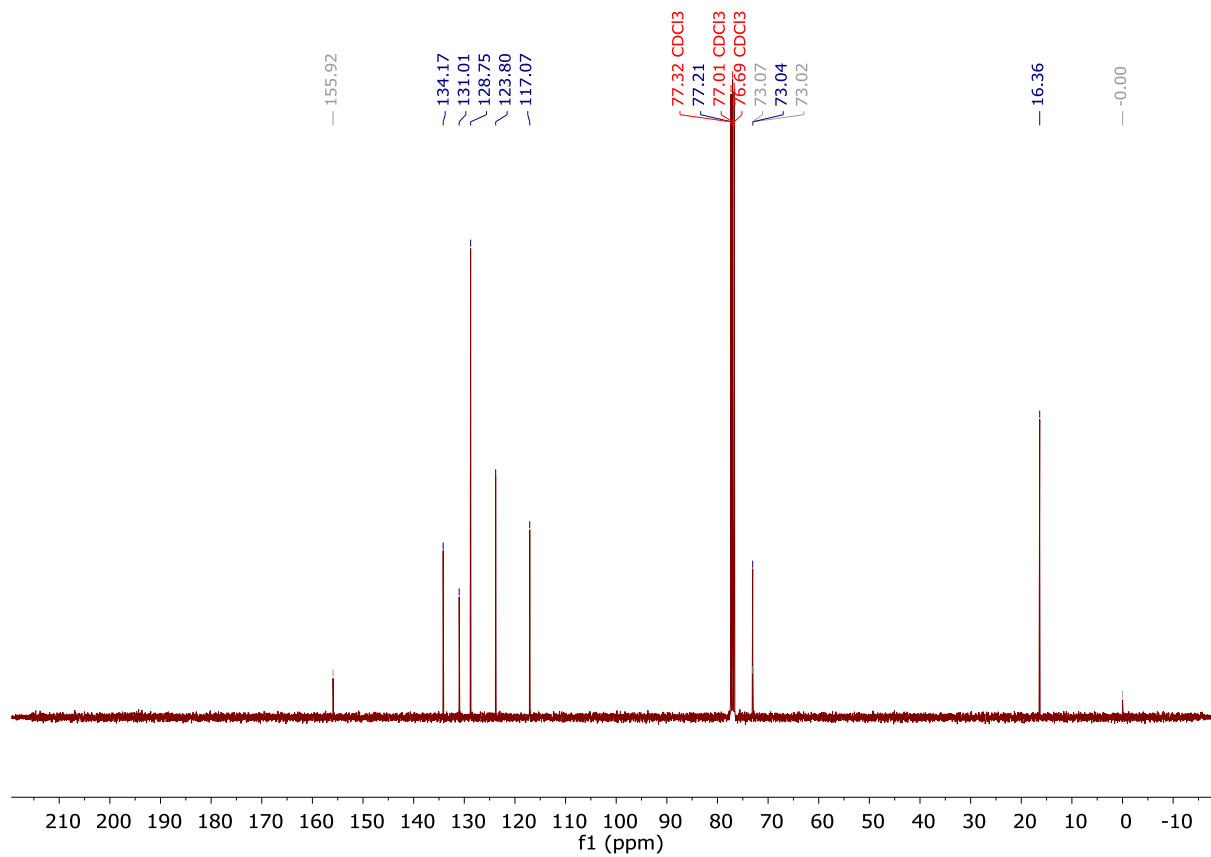




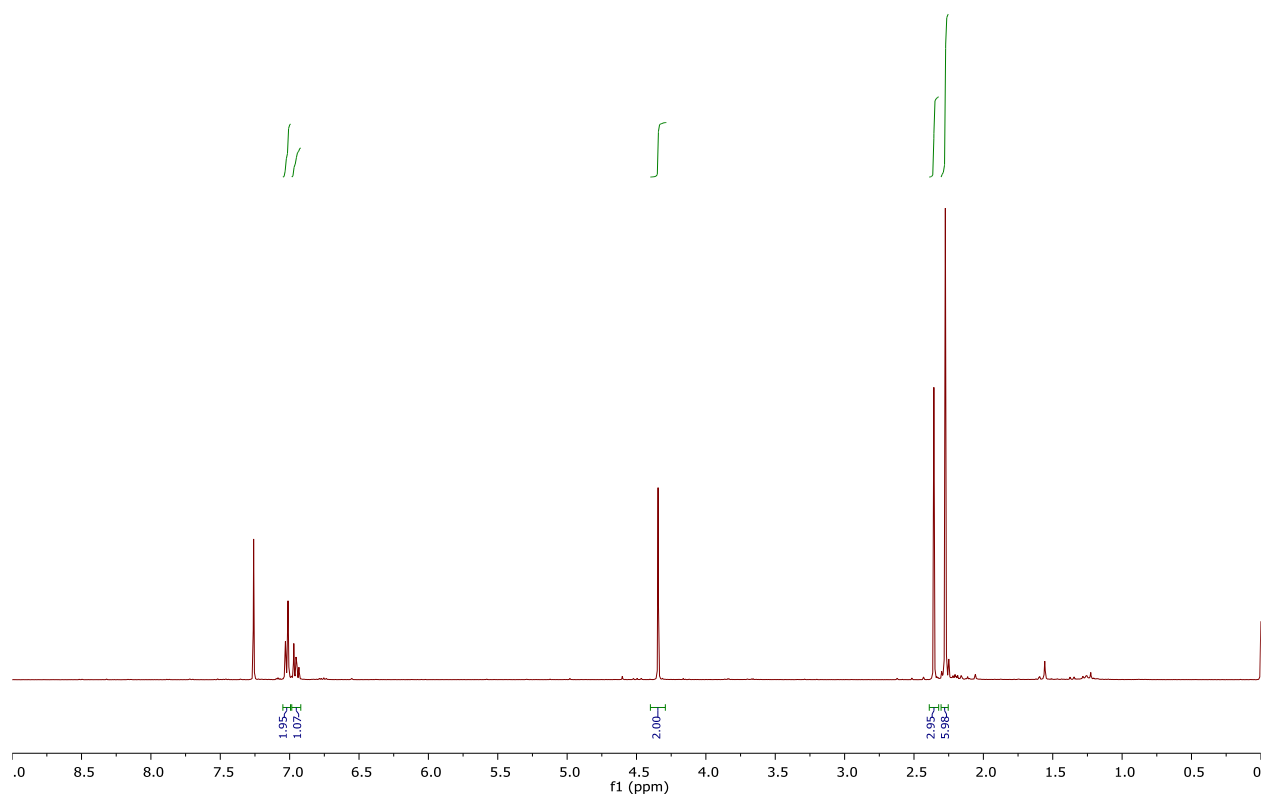
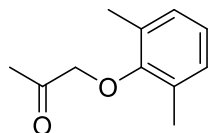


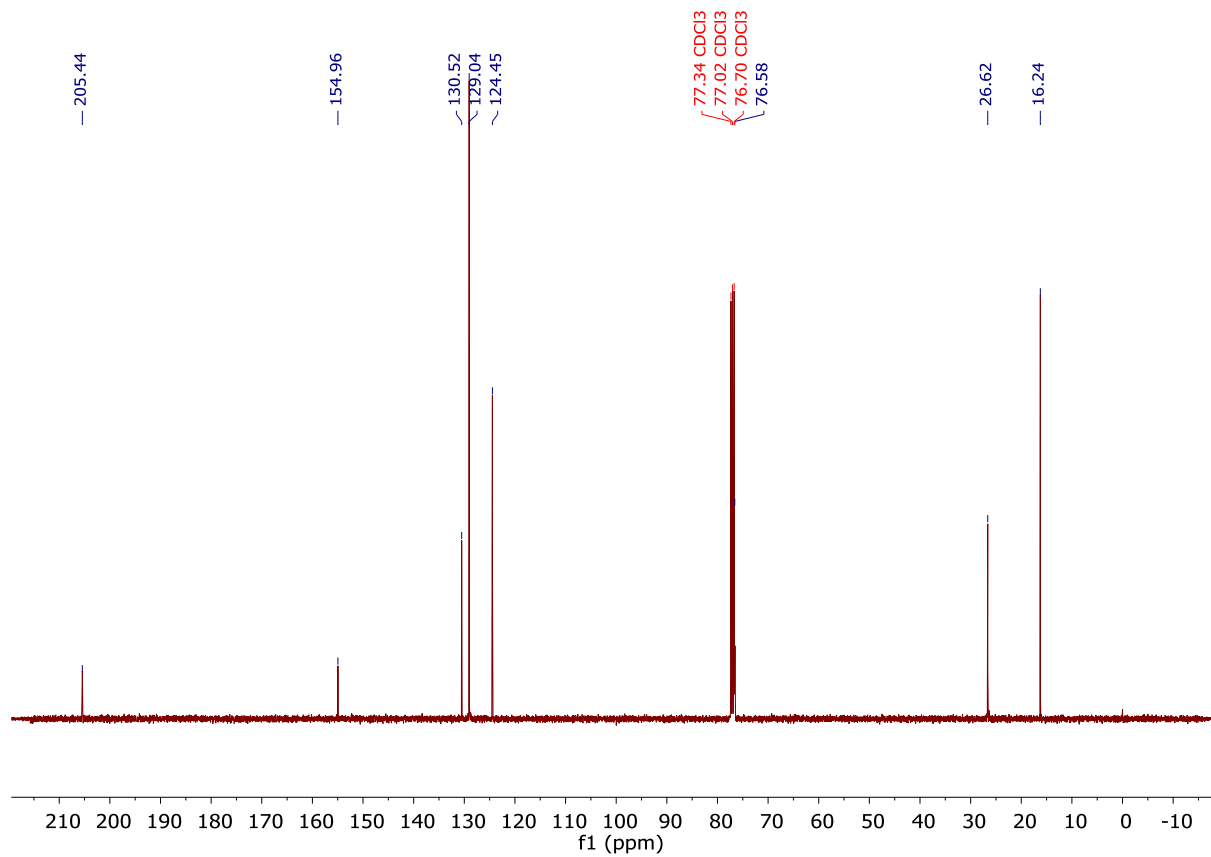
**Allyl 2,6-dimethylphenyl ether (4a):**  $^1\text{H}$  NMR (400 MHz, Chloroform-*d*),  $^{13}\text{C}\{\text{H}\}$  NMR (101 MHz, Chloroform-*d*).

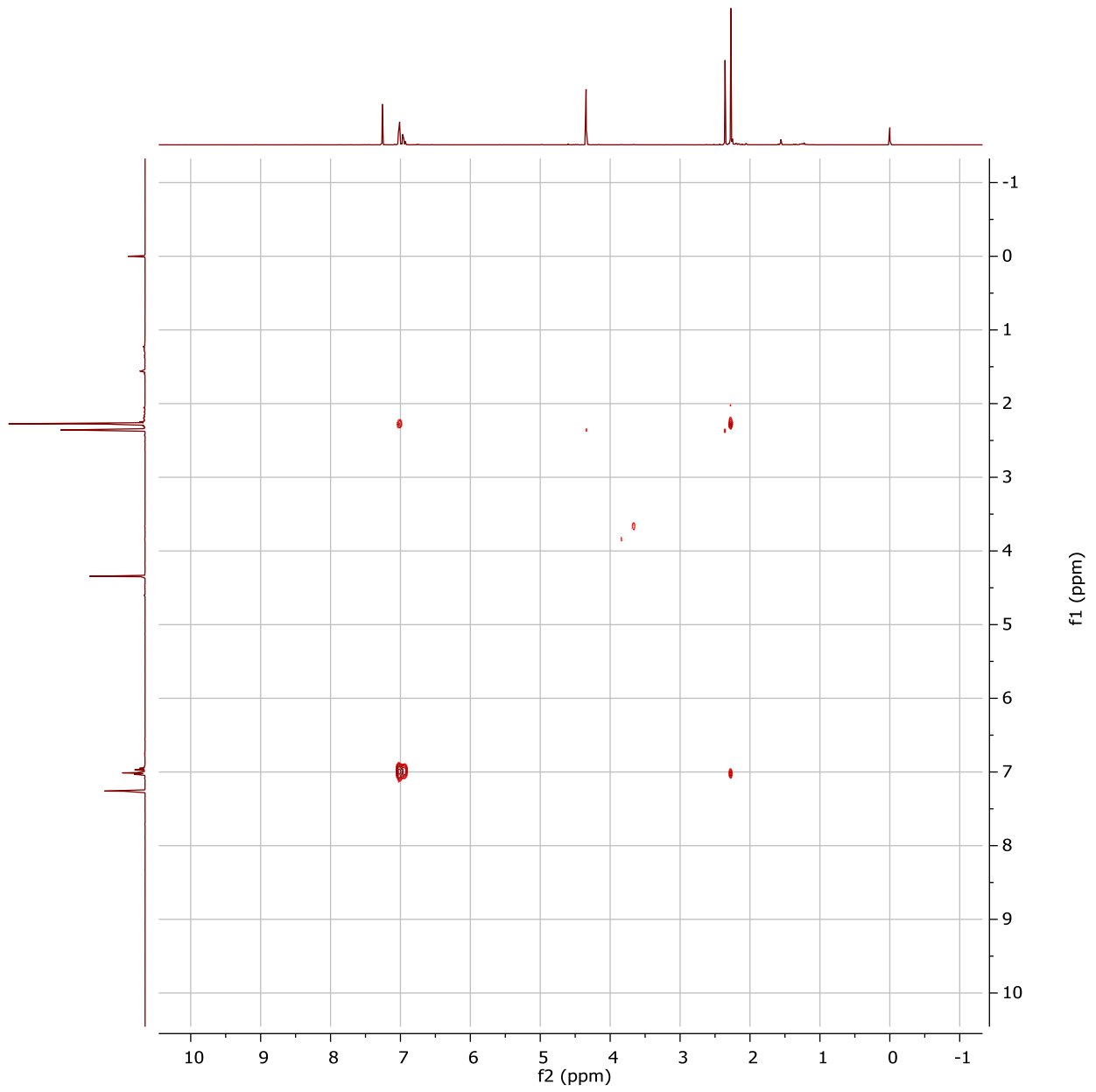




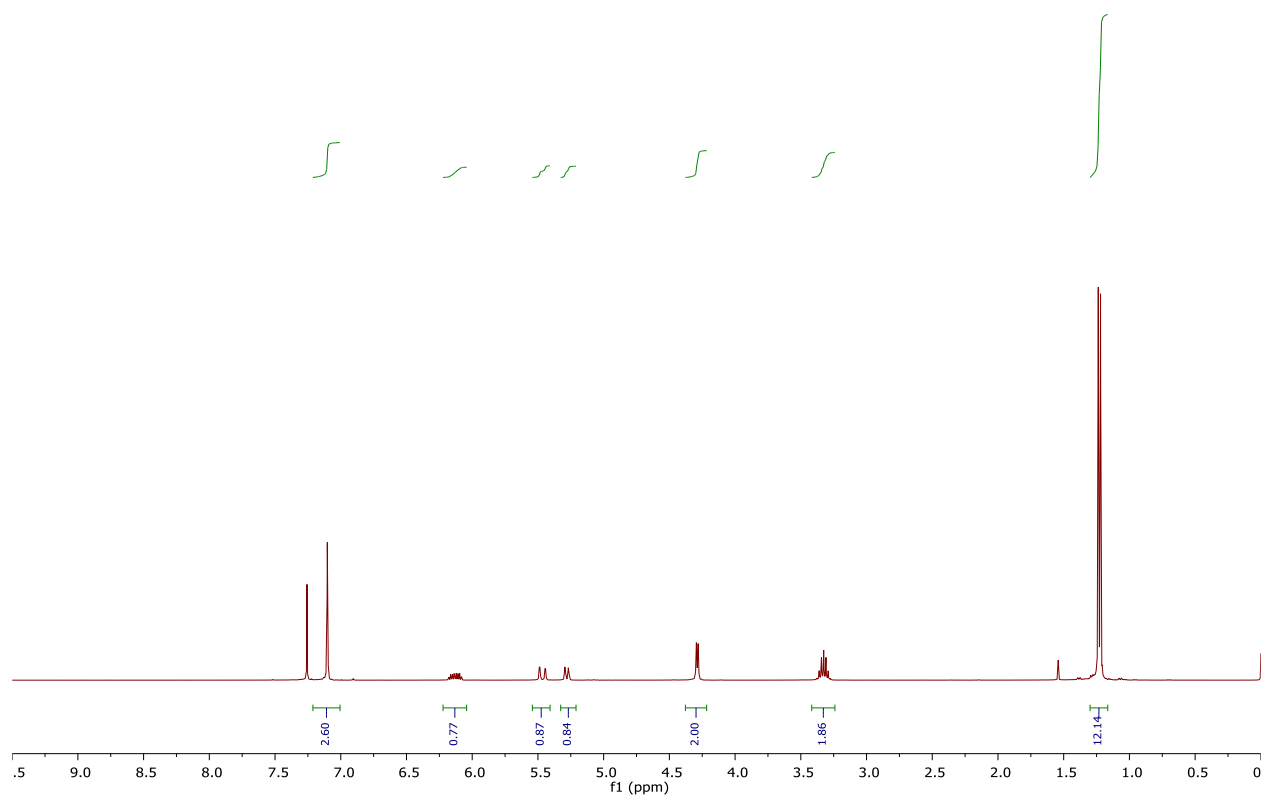
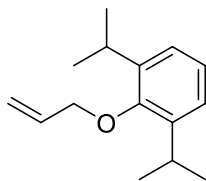
**1-(2,6-dimethylphenoxy)propan-2-one (4b):**  $^1\text{H}$  NMR (400 MHz, Chloroform-*d*),  $^{13}\text{C}\{^1\text{H}\}$  NMR (101 MHz, Chloroform-*d*) and COSY.

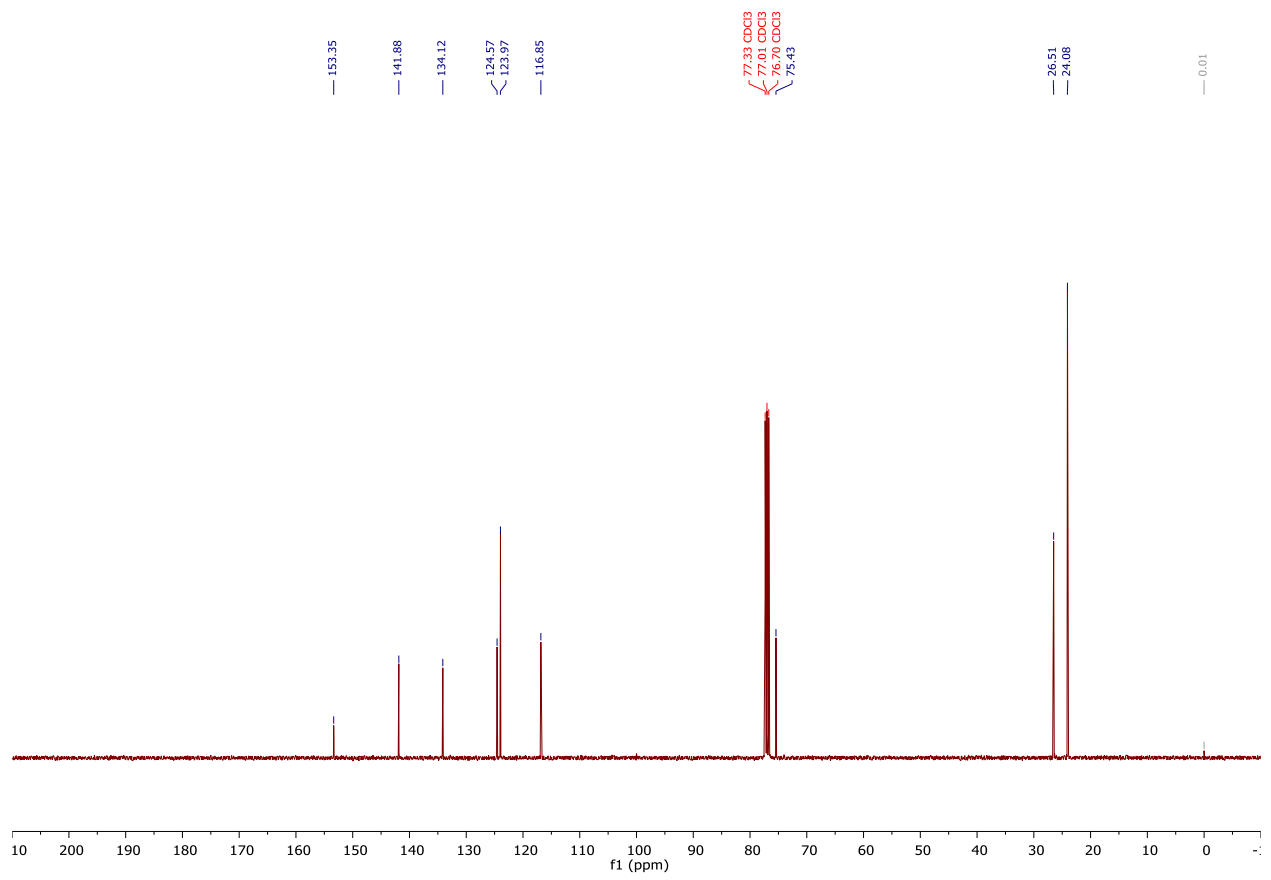




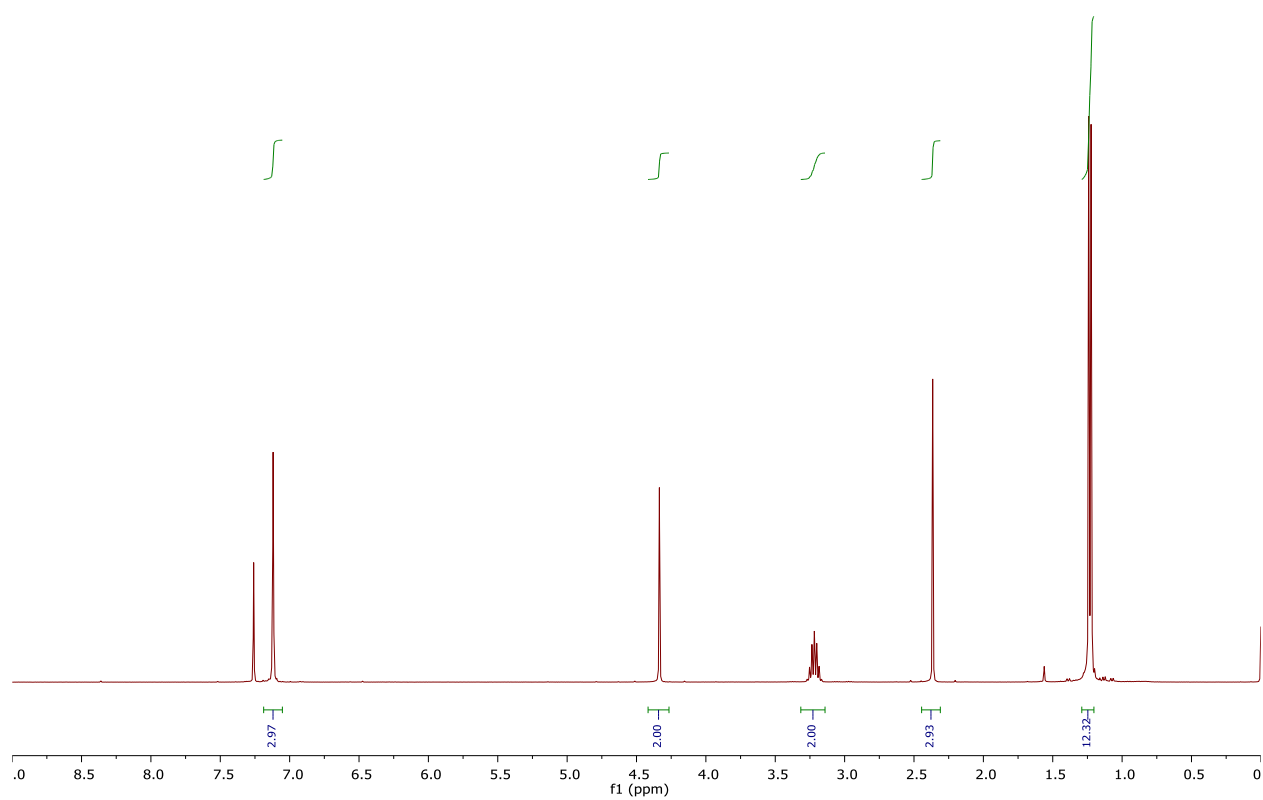
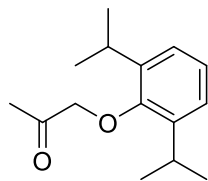


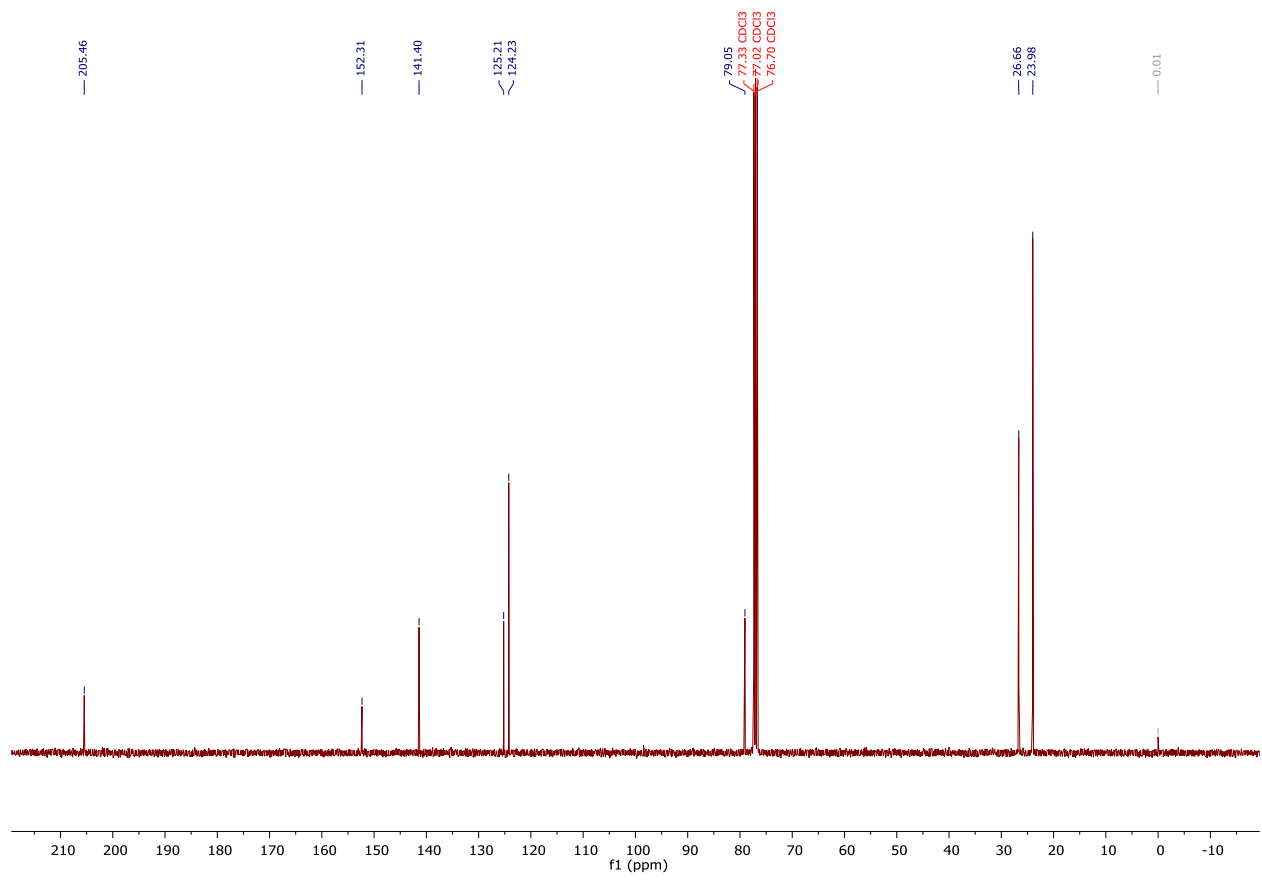
**Allyl 2,6-diisopropylphenyl ether (5a):**  $^1\text{H}$  NMR (400 MHz, Chloroform-*d*),  $^{13}\text{C}\{^1\text{H}\}$  NMR(101 MHz, Chloroform-*d*)

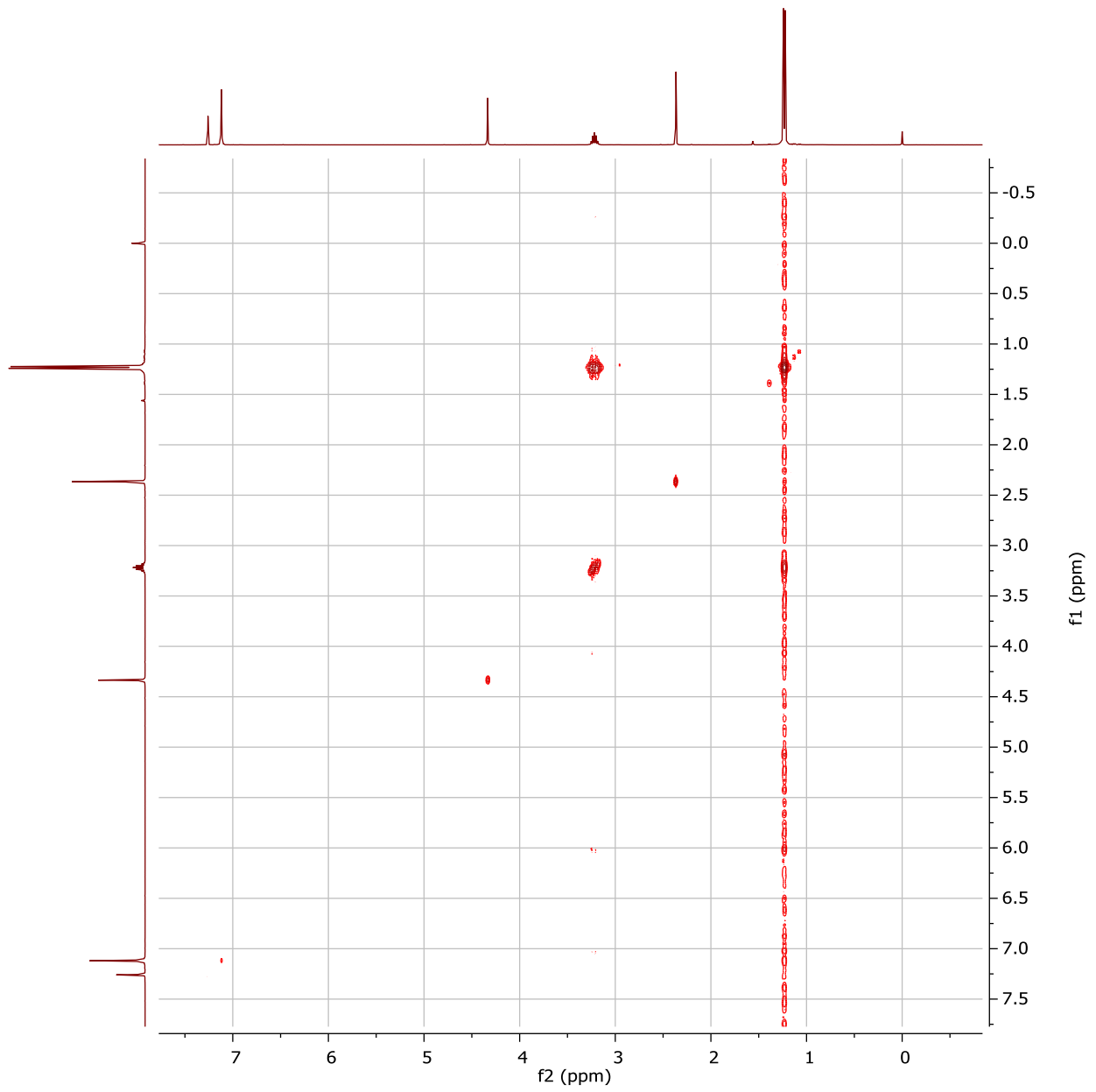




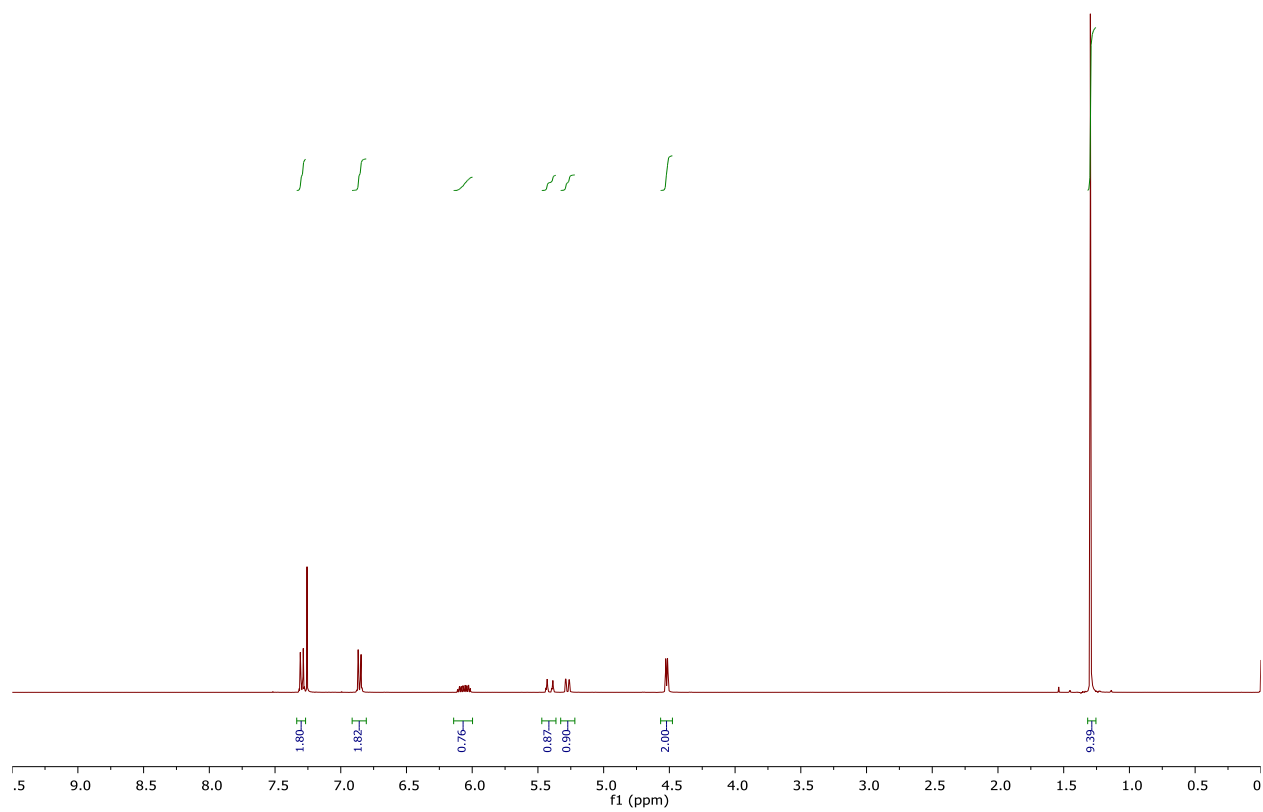
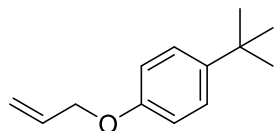
**1-(2,6-diisopropylphenoxy)propan-2-one (5b):**  $^1\text{H}$  NMR (400 MHz, Chloroform-*d*),  $^{13}\text{C}\{^1\text{H}\}$  NMR(101 MHz, Chloroform-*d*), and COSY.

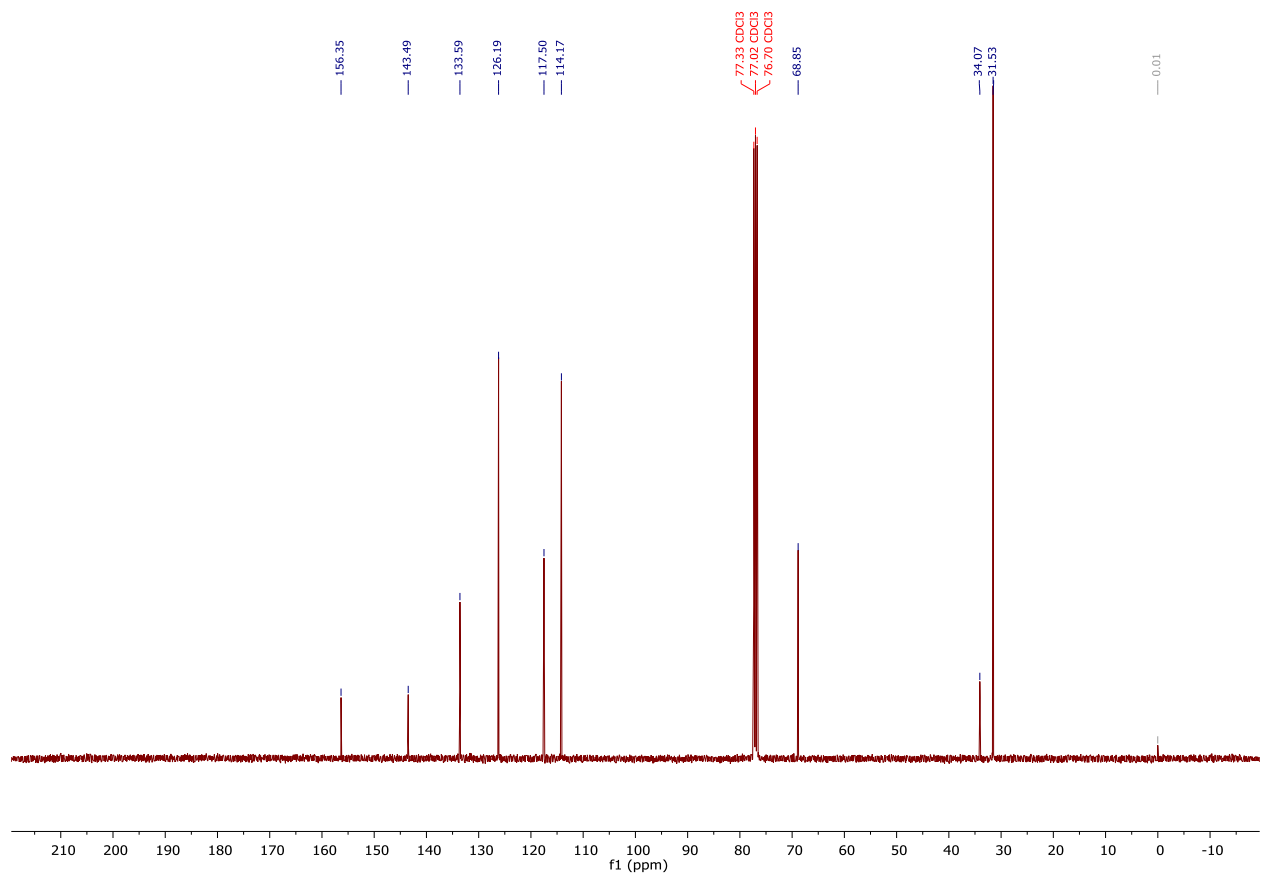




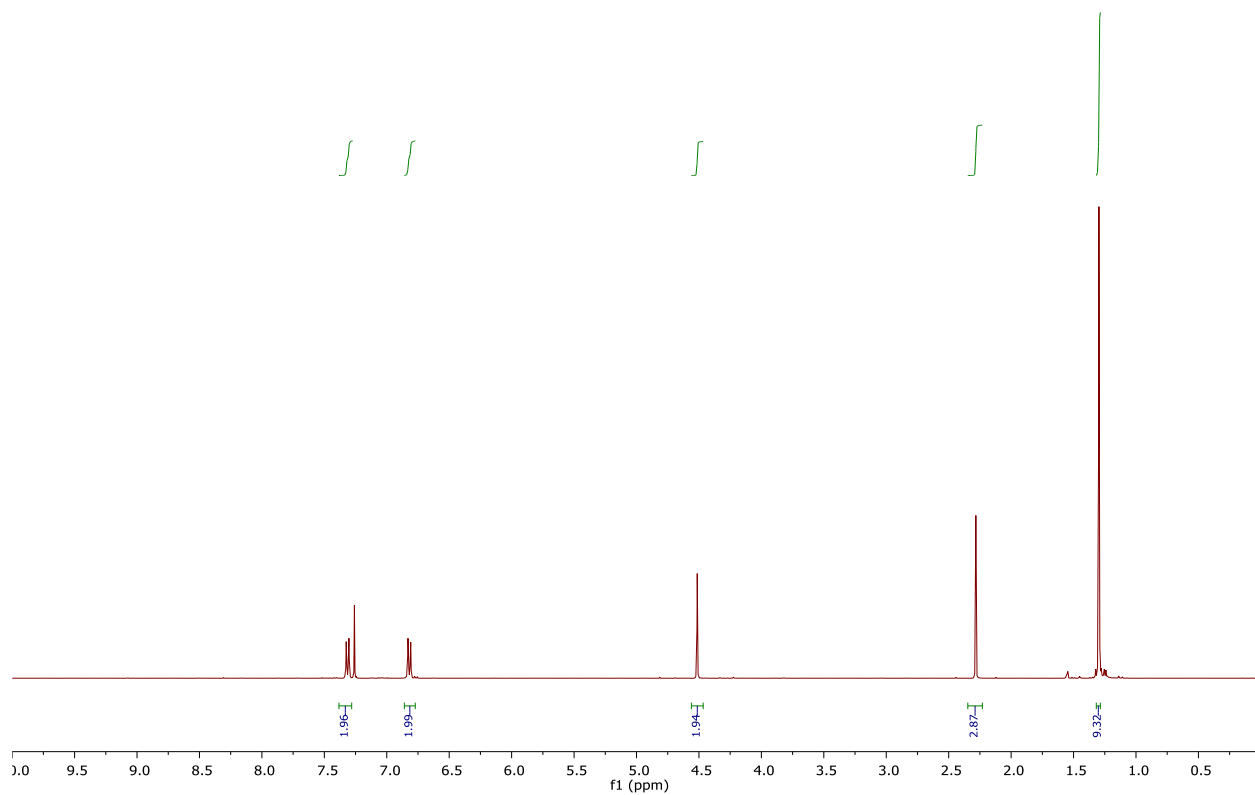
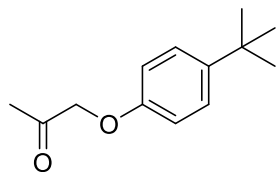


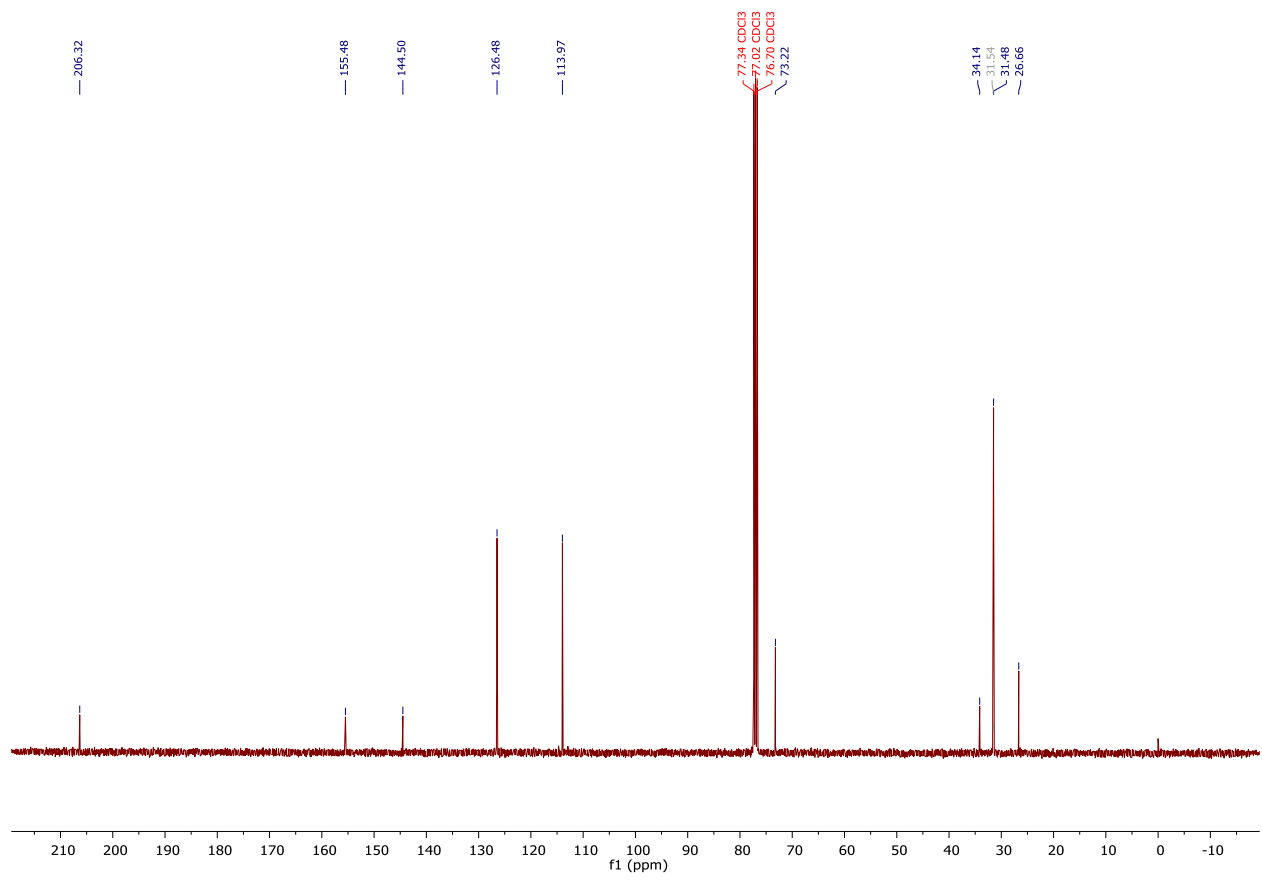
**Allyl 4-*tert*-butylphenyl ether (6a):**  $^1\text{H}$  NMR (400 MHz, Chloroform-*d*),  $^{13}\text{C}\{\text{H}\}$  NMR(101 MHz, Chloroform-*d*)

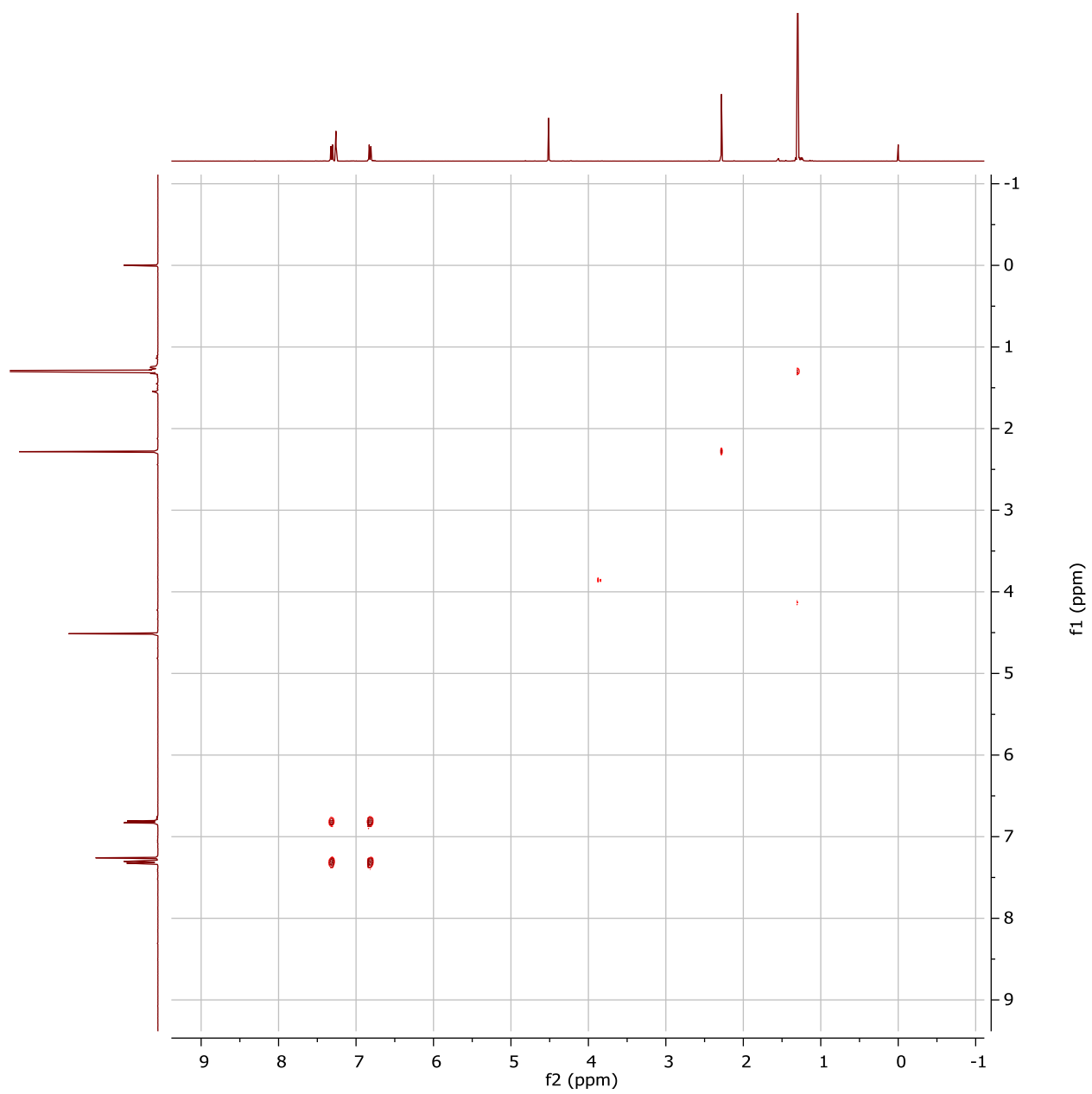




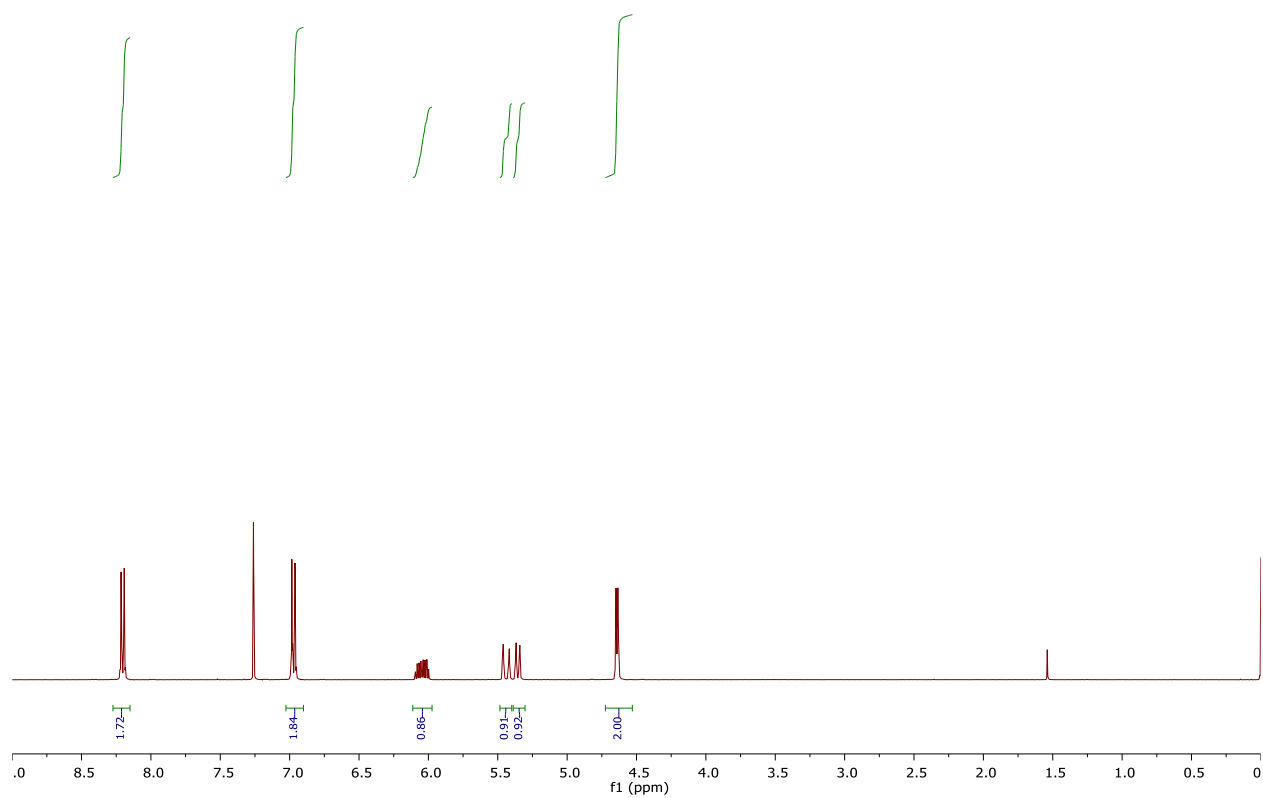
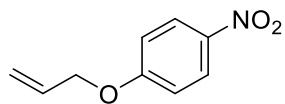
**3.2.1 1-(4-(tert-butyl)phenoxy)propan-2-one (6b):** 400 MHz, (Chloroform-*d*),  $^{13}\text{C}\{\text{H}\}$  NMR(101 MHz, Chloroform-*d*) and COSY.

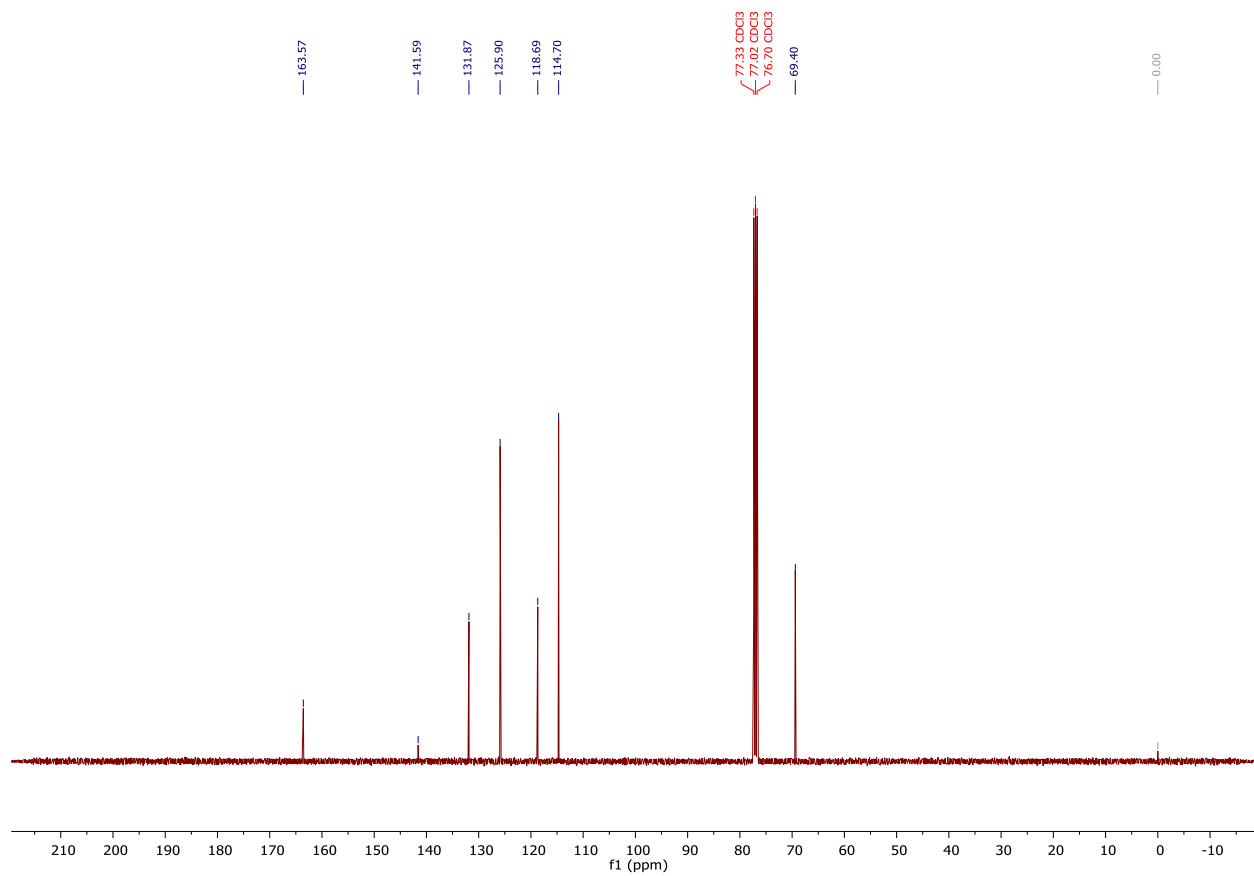




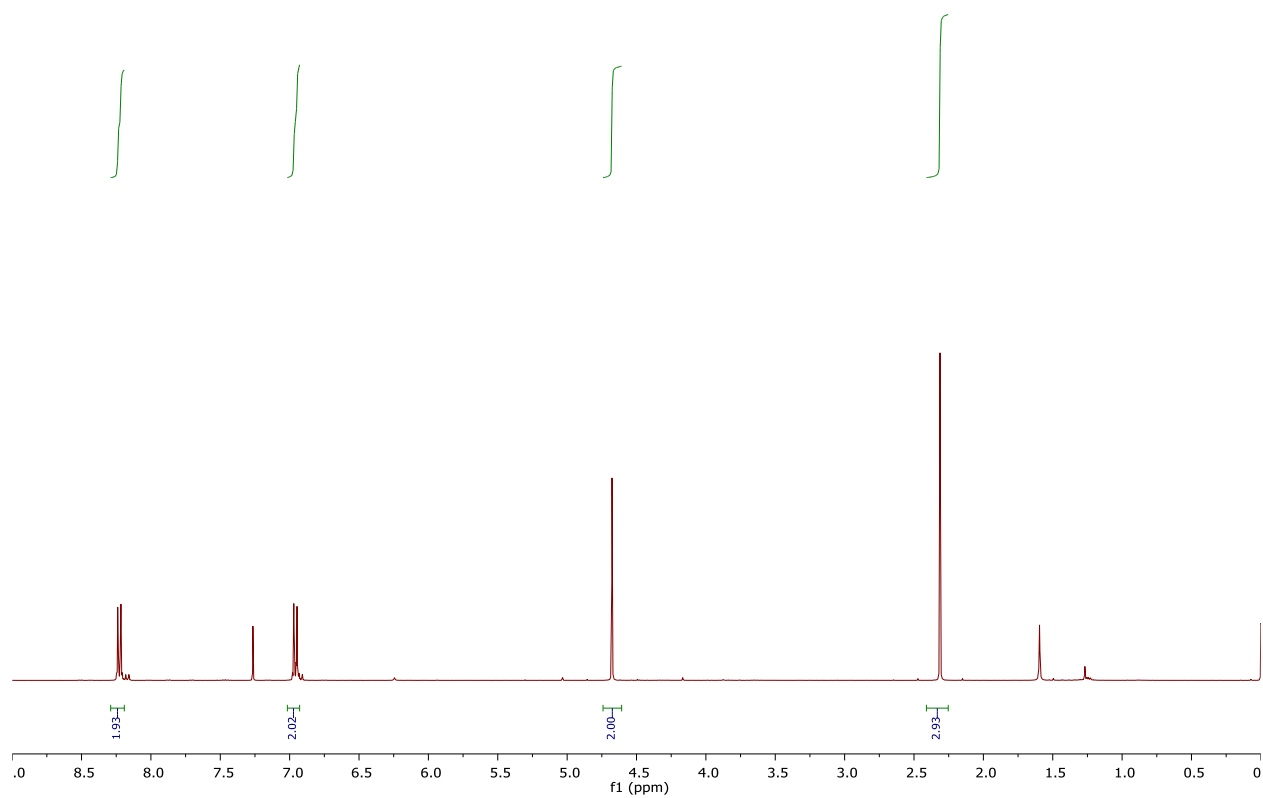
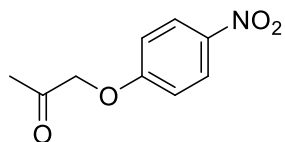


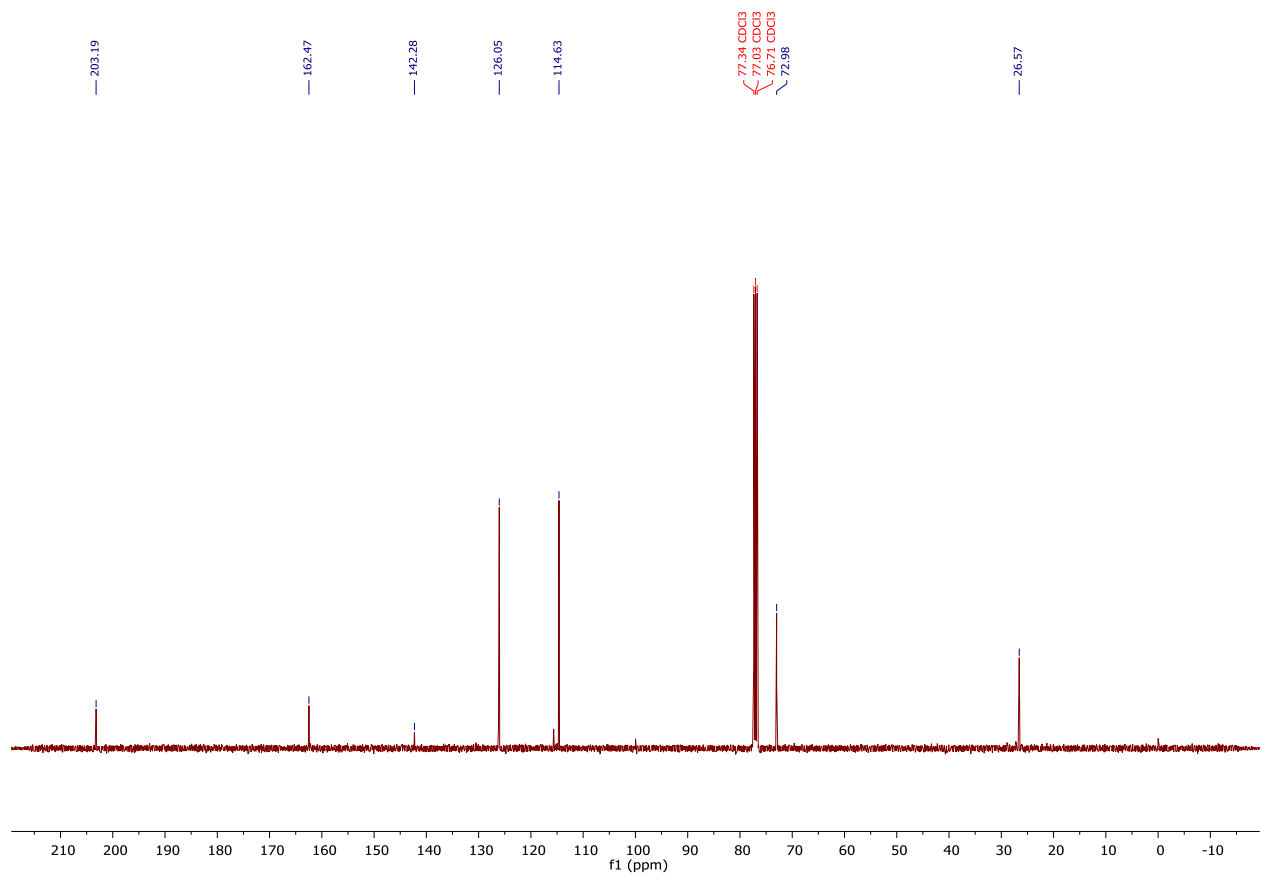
**Allyl 4-nitrophenyl ether (7a):**  $^1\text{H}$  NMR (400 MHz, Chloroform-*d*),  $^{13}\text{C}\{^1\text{H}\}$  NMR (101 MHz, Chloroform-*d*).

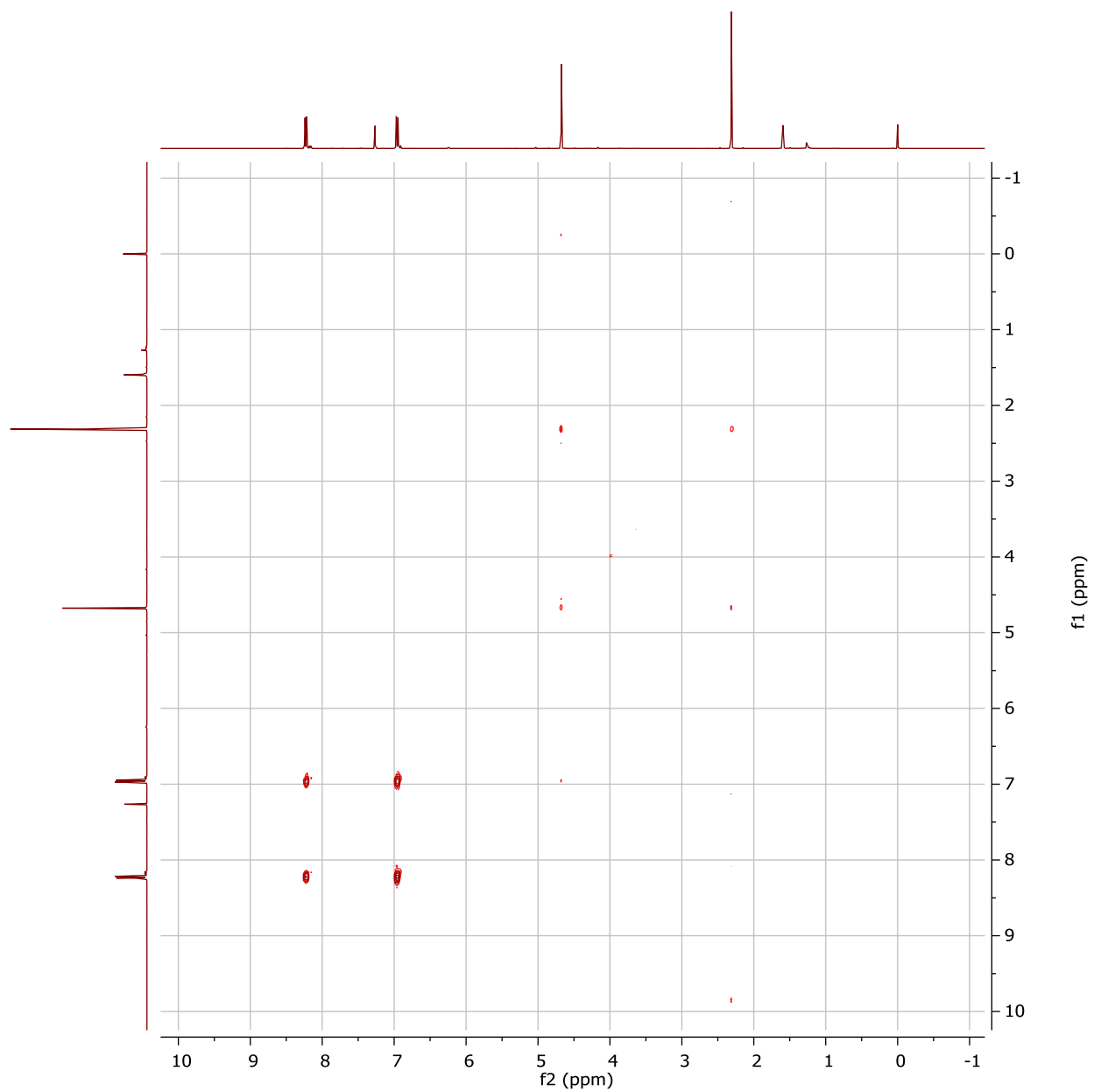




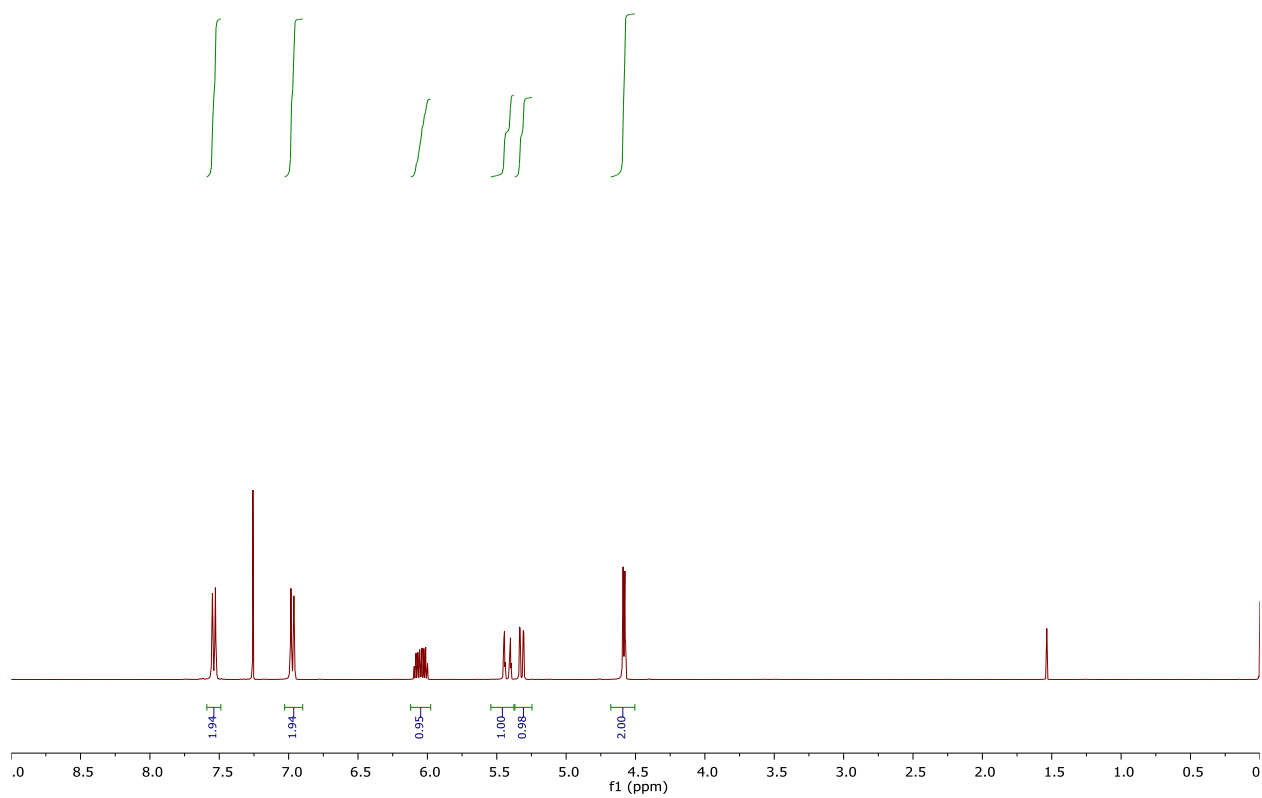
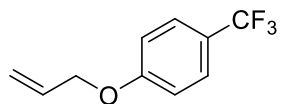
**1-(4-nitrophenoxy)propan-2-one (7b):**  $^1\text{H}$  NMR (400 MHz, Chloroform- $d$ ),  $^{13}\text{C}\{^1\text{H}\}$  NMR(101 MHz, Chloroform- $d$ ) and COSY.

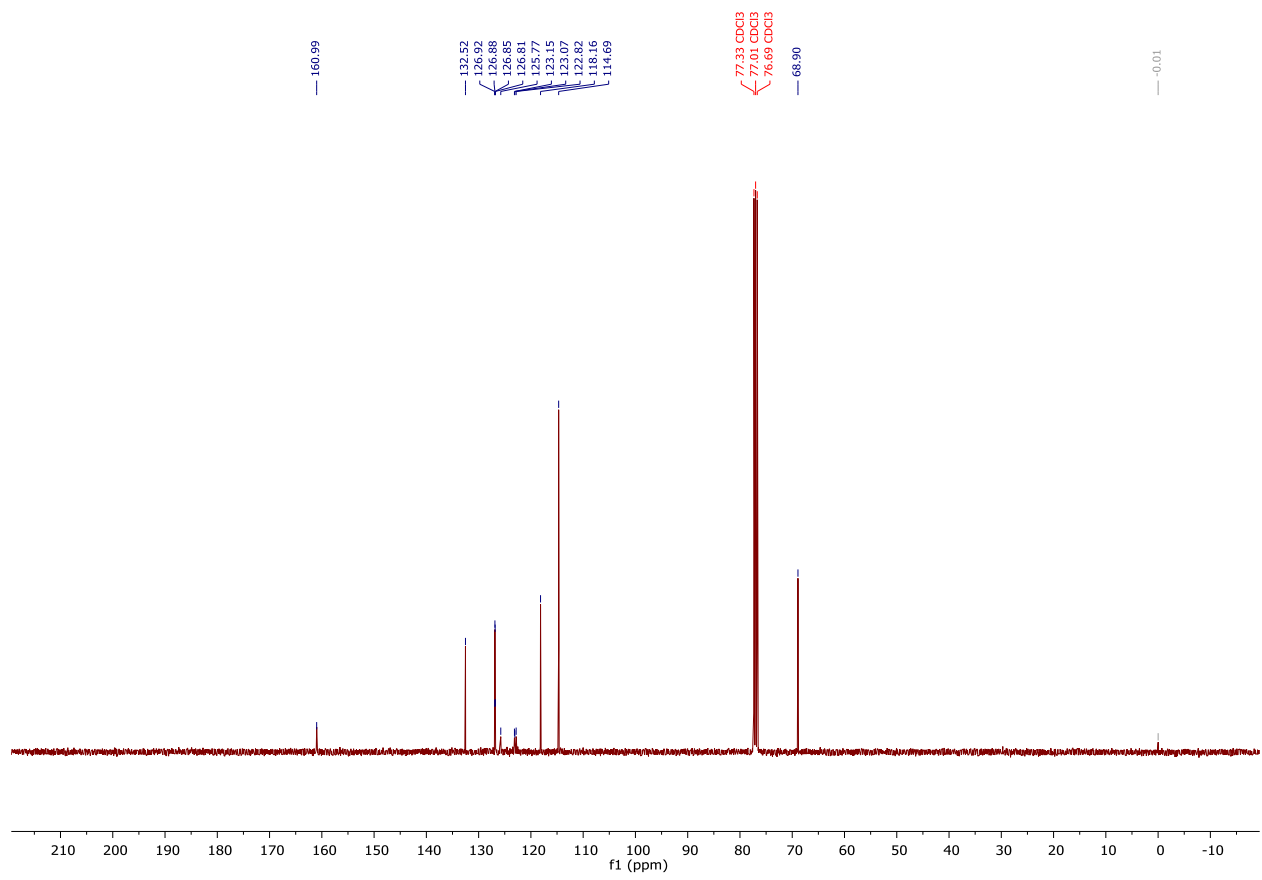


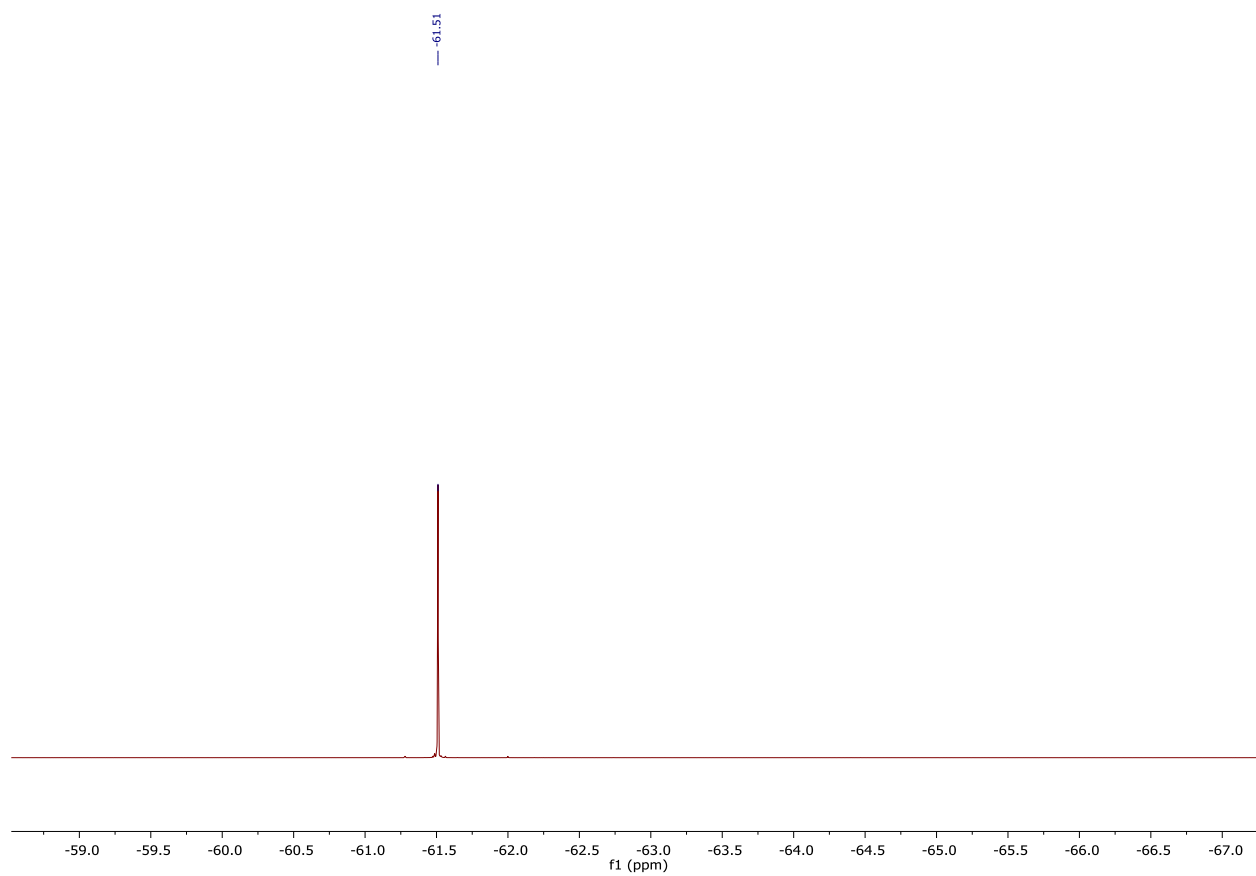




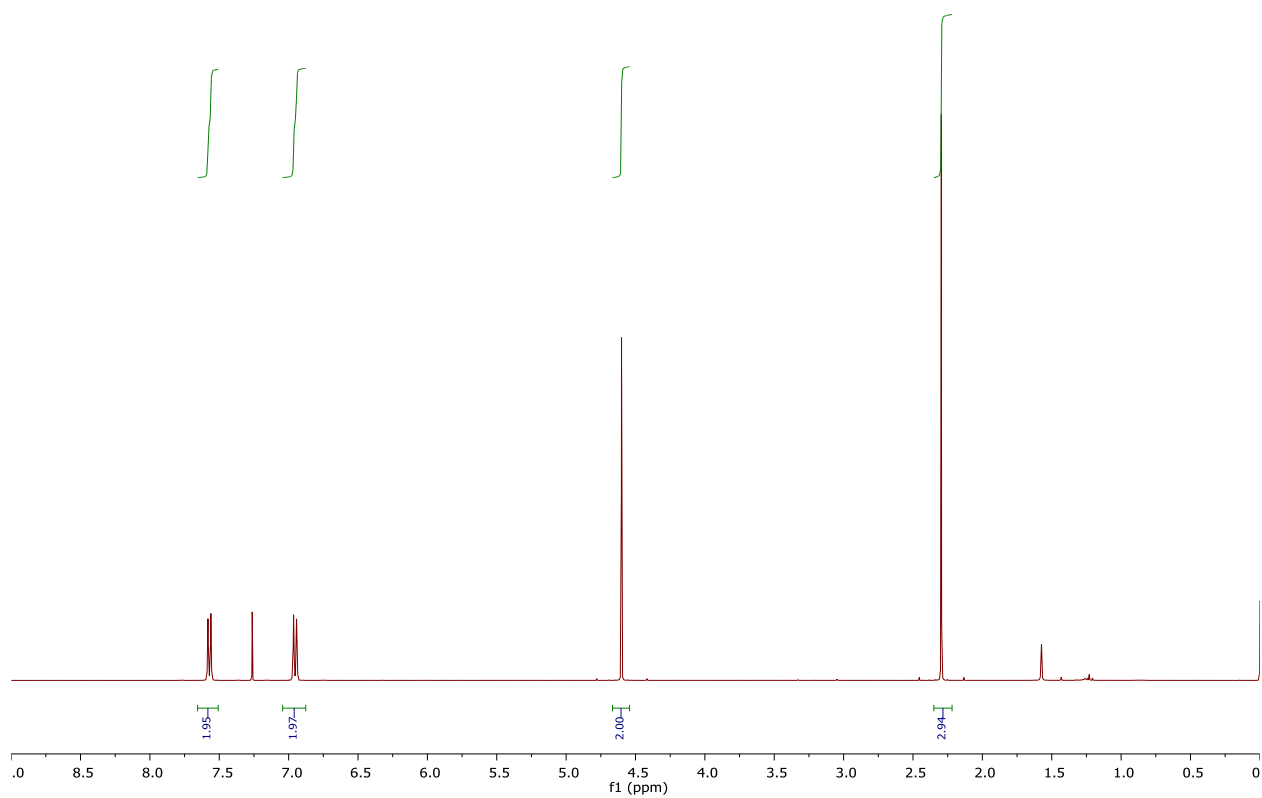
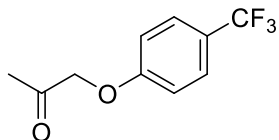
**Allyl 4-trifluoromethylphenyl ether (8a):**  $^1\text{H}$  NMR (400 MHz,  $\text{CDCl}_3$ ),  $^{13}\text{C}\{\text{H}\}$  NMR (101 MHz, Chloroform-*d*),  $^{19}\text{F}\{\text{H}\}$  NMR (376 MHz, Chloroform-*d*).

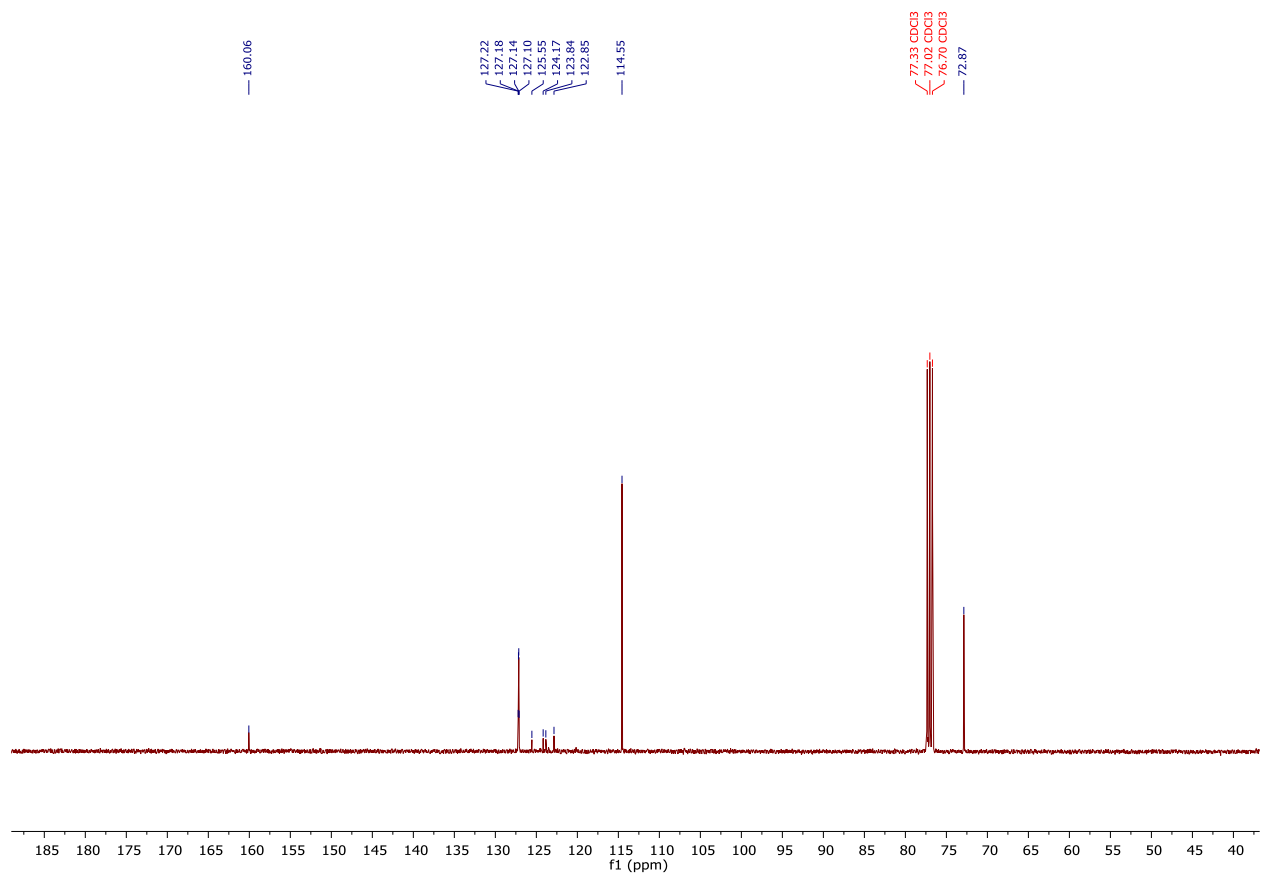


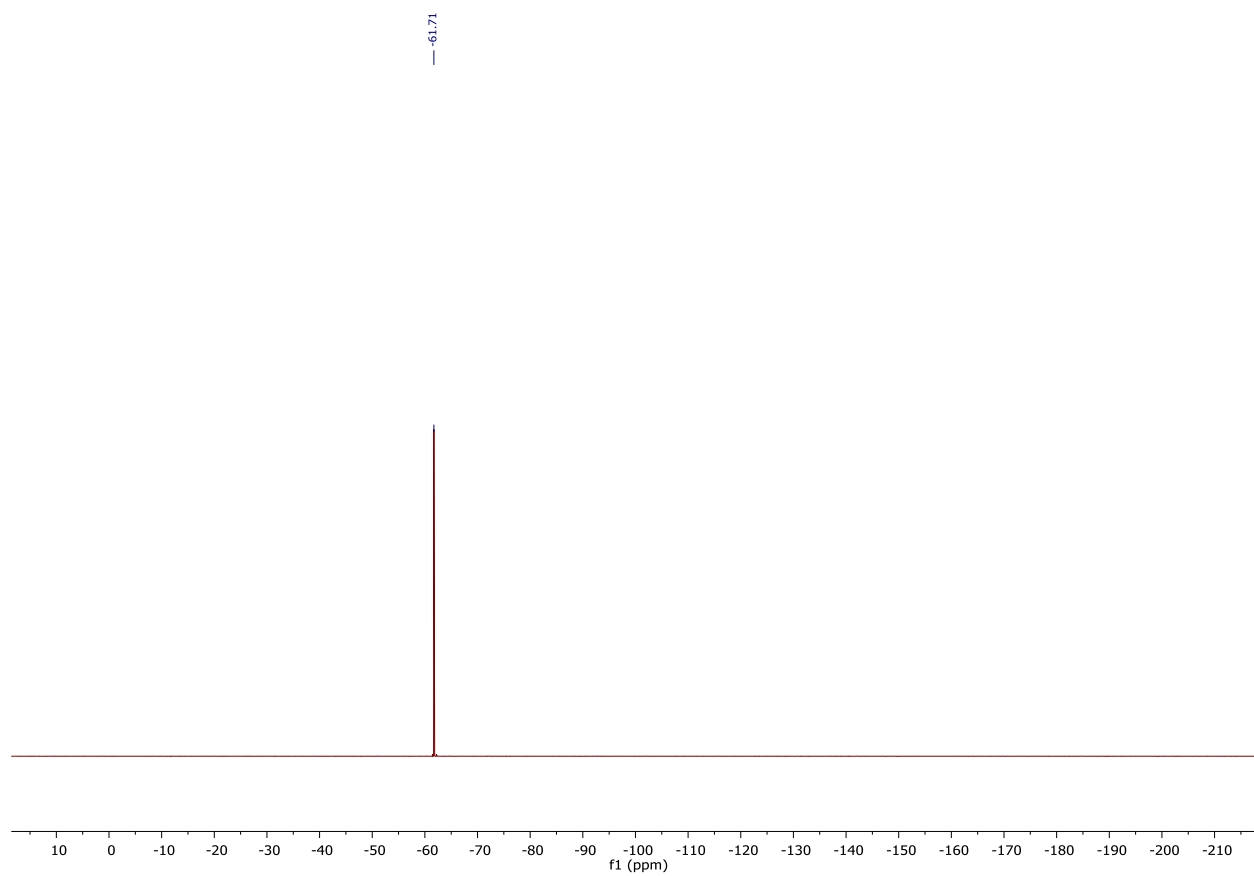


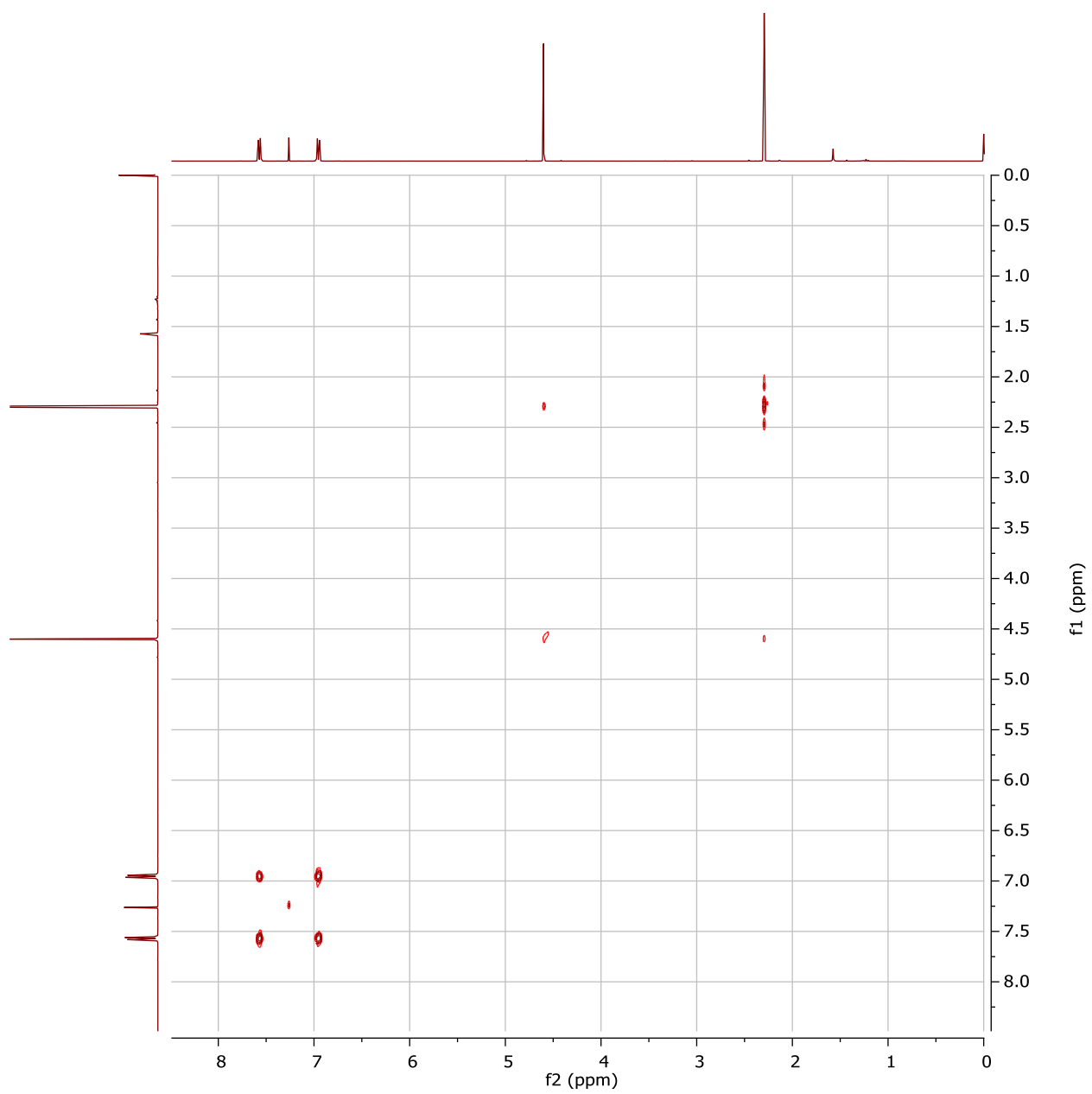


**1-(4-(trifluoromethyl)phenoxy)propan-2-one (8b):**  $^1\text{H}$  NMR (400 MHz, Chloroform-*d*),  $^{13}\text{C}\{^1\text{H}\}$  NMR (101 MHz, Chloroform-*d*),  $^{19}\text{F}\{^1\text{H}\}$  NMR (376 MHz, Chloroform-*d*) and COSY.

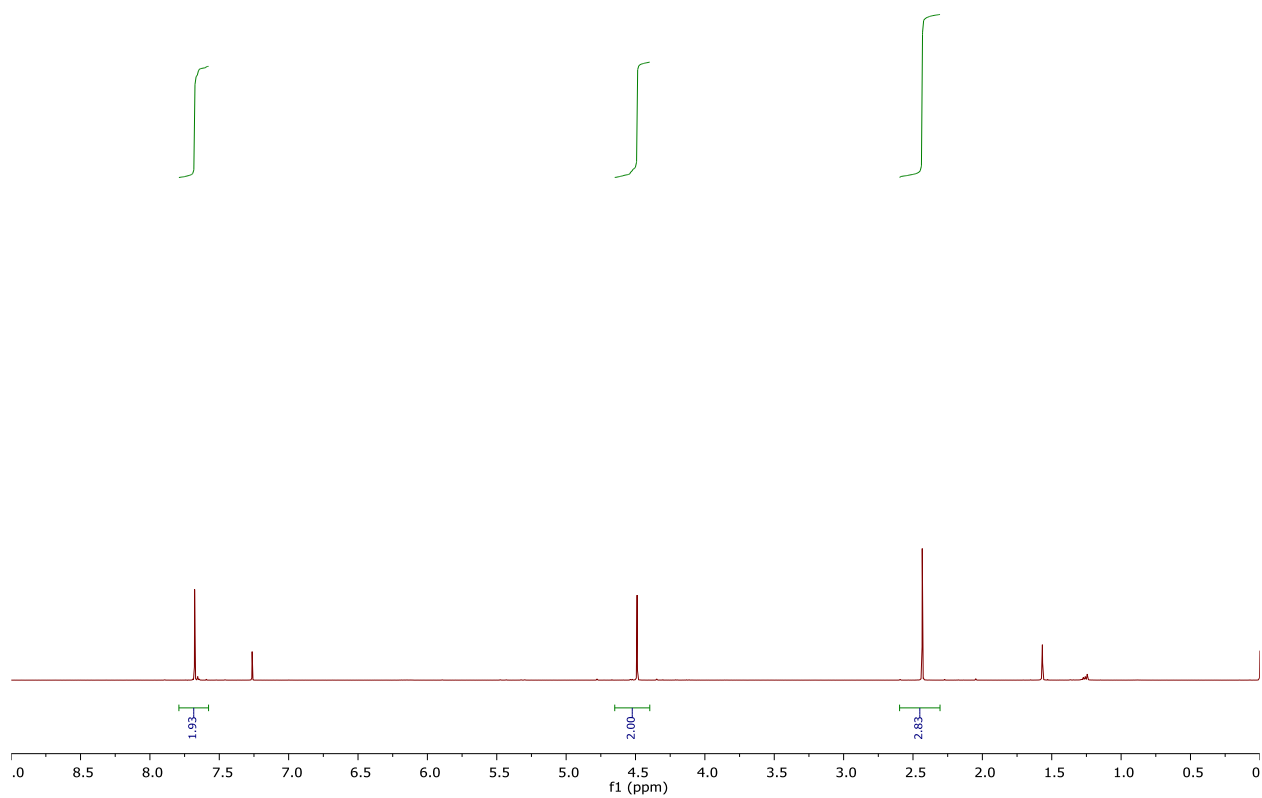
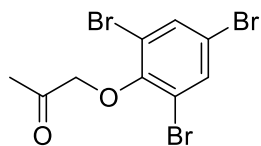


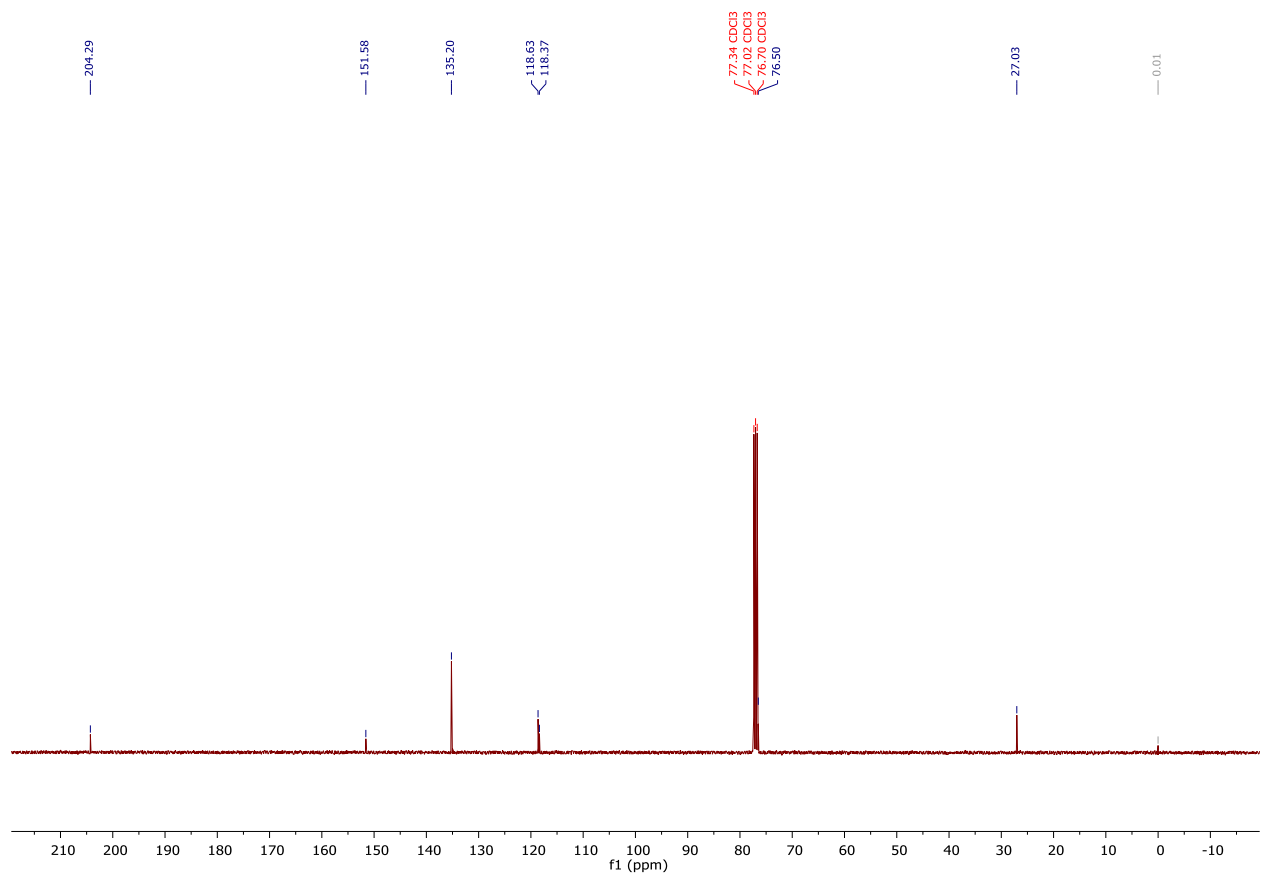


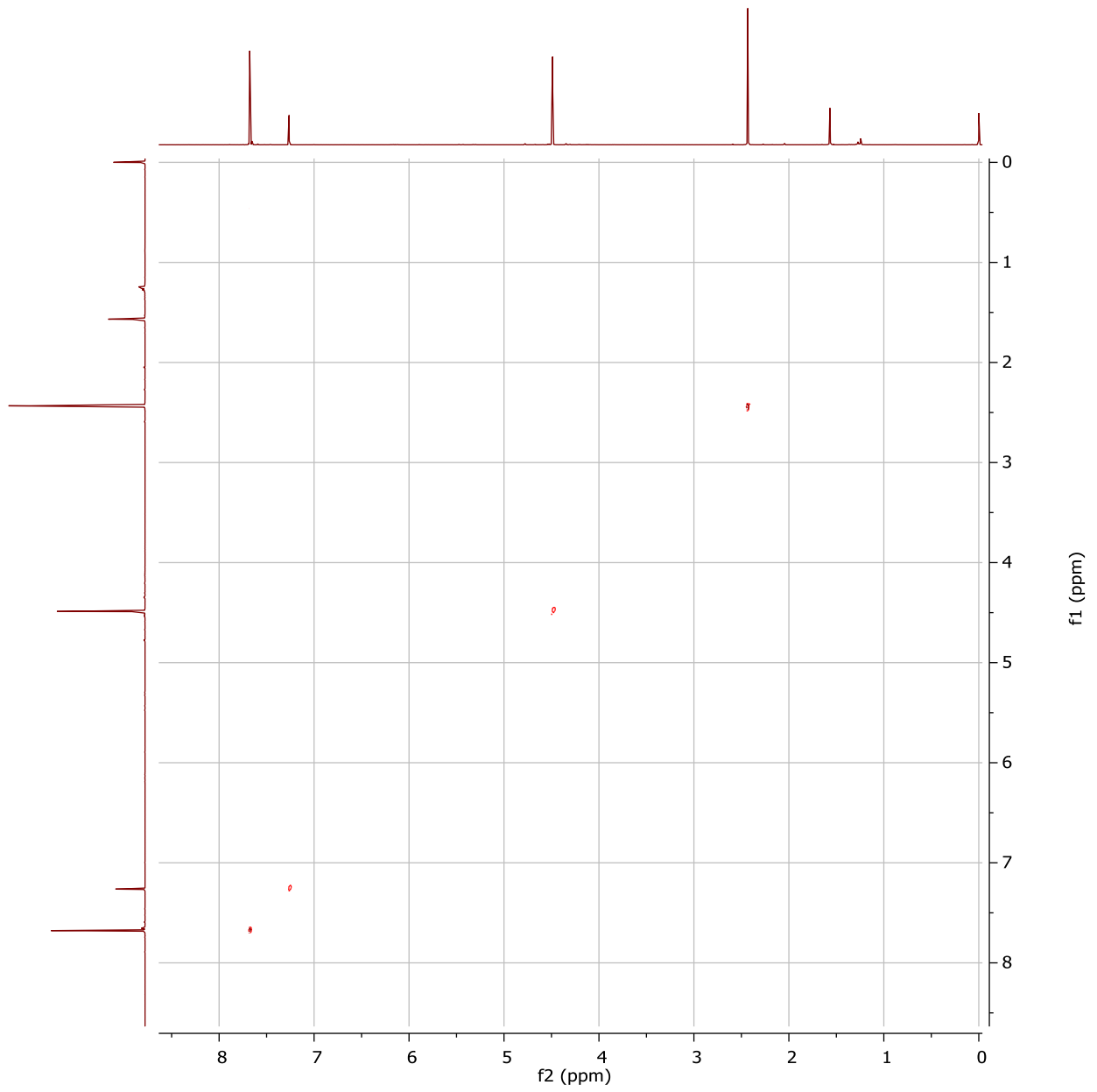




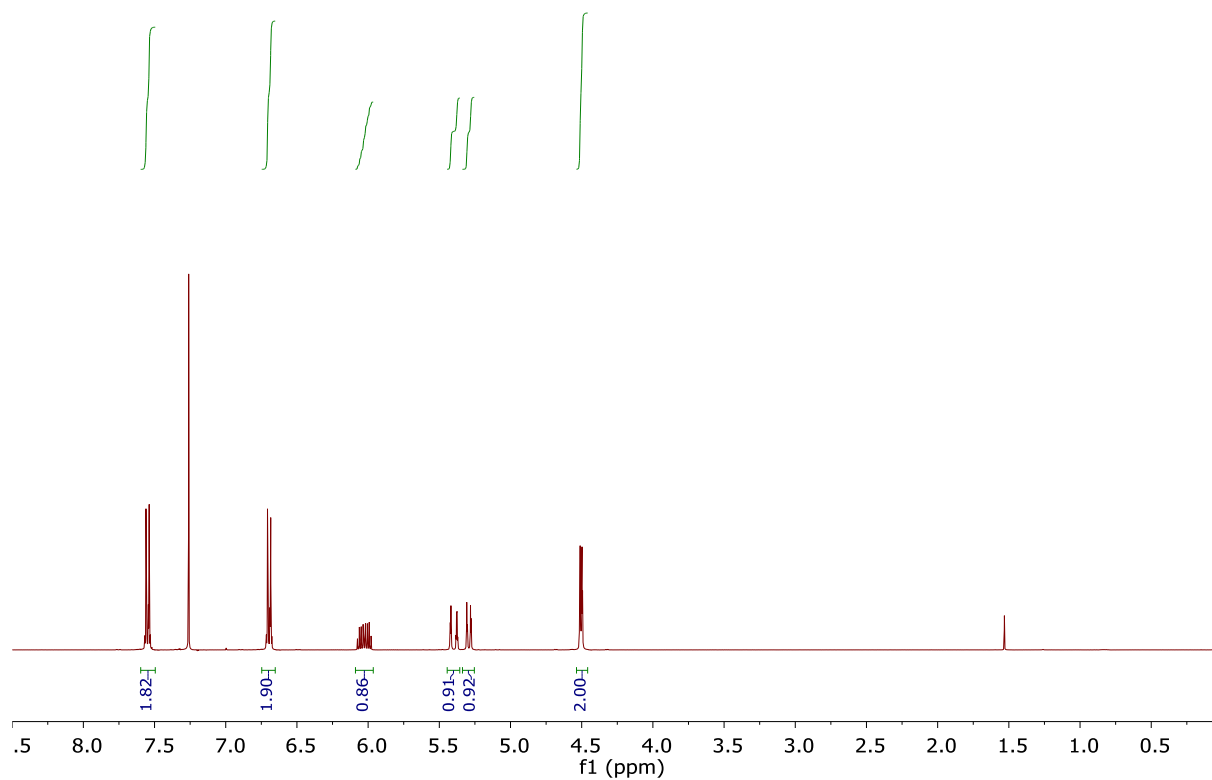
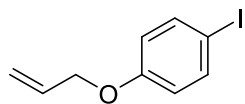
**1-(2,4,6-tribromophenoxy)propan-2-one (9b):**  $^1\text{H}$  NMR (400 MHz, Chloroform-*d*),  $^{13}\text{C}\{^1\text{H}\}$  NMR (101 MHz, Chloroform-*d*) and COSY.

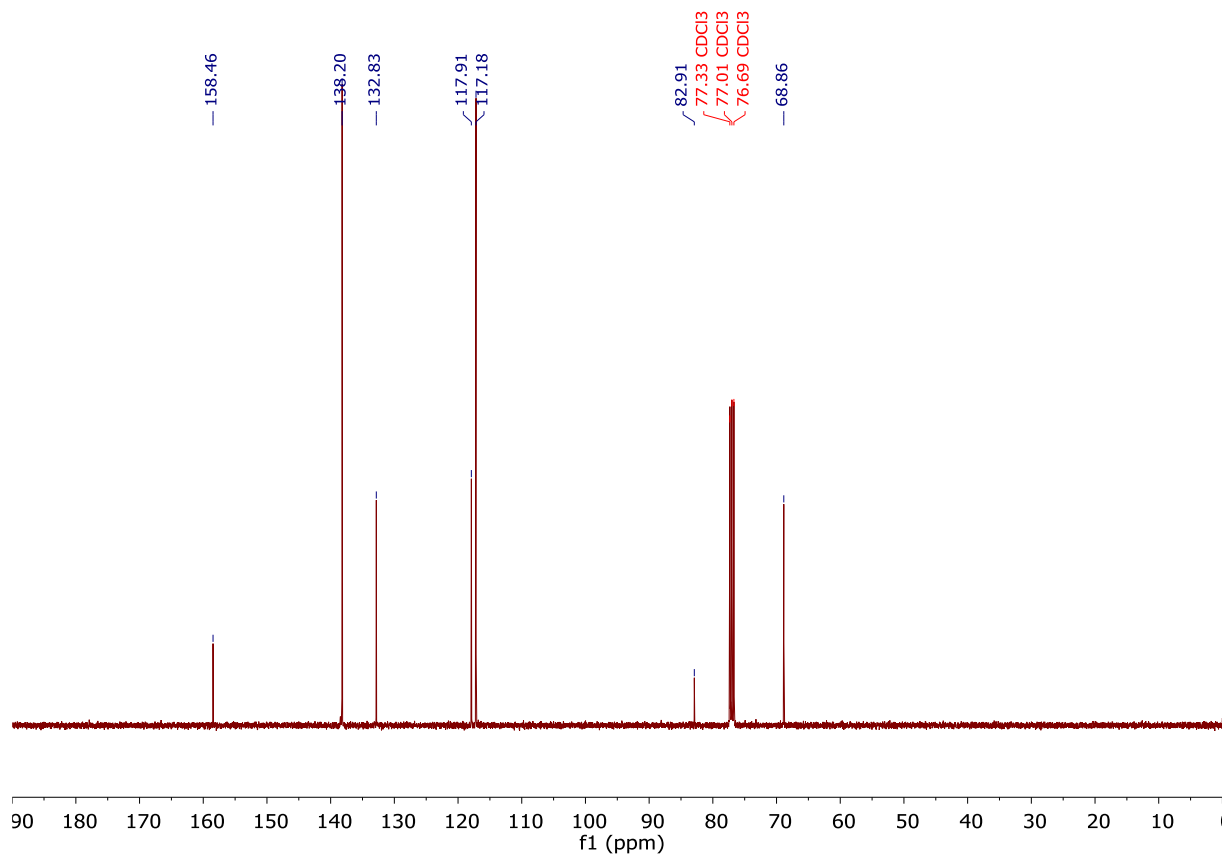




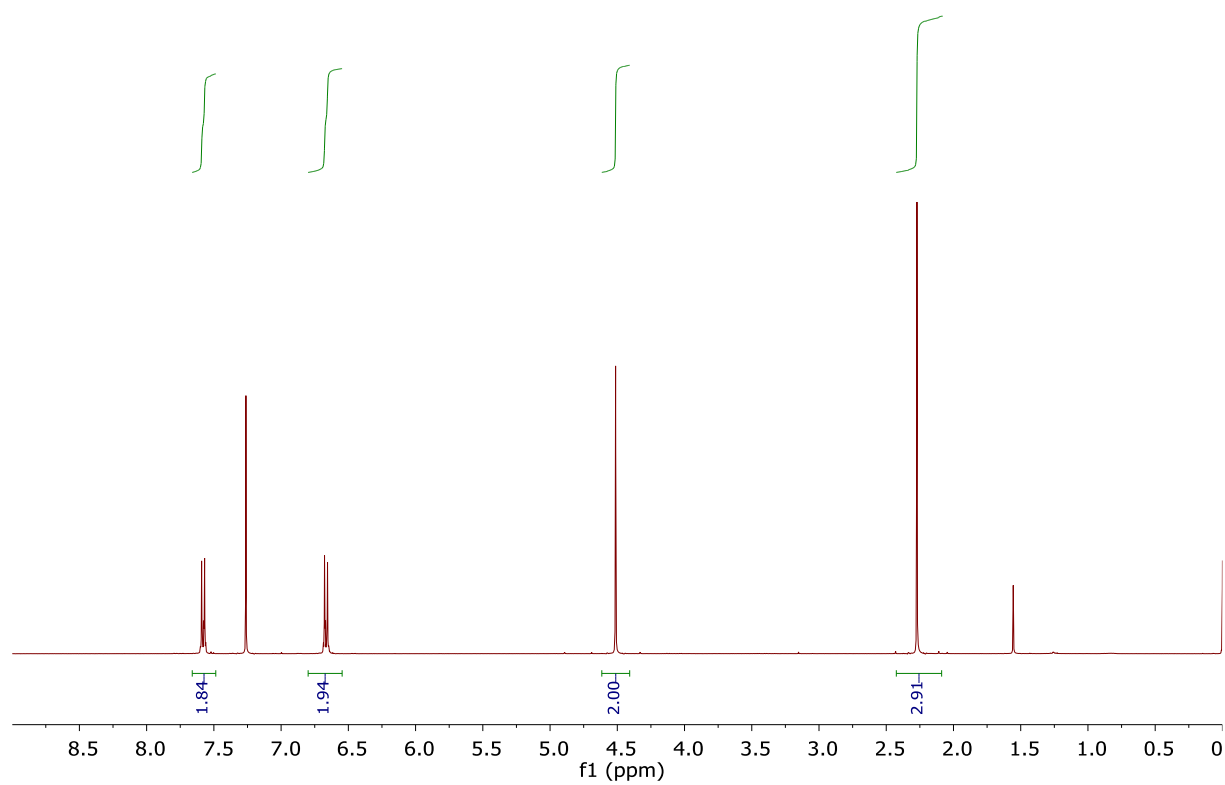
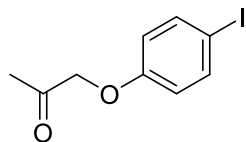


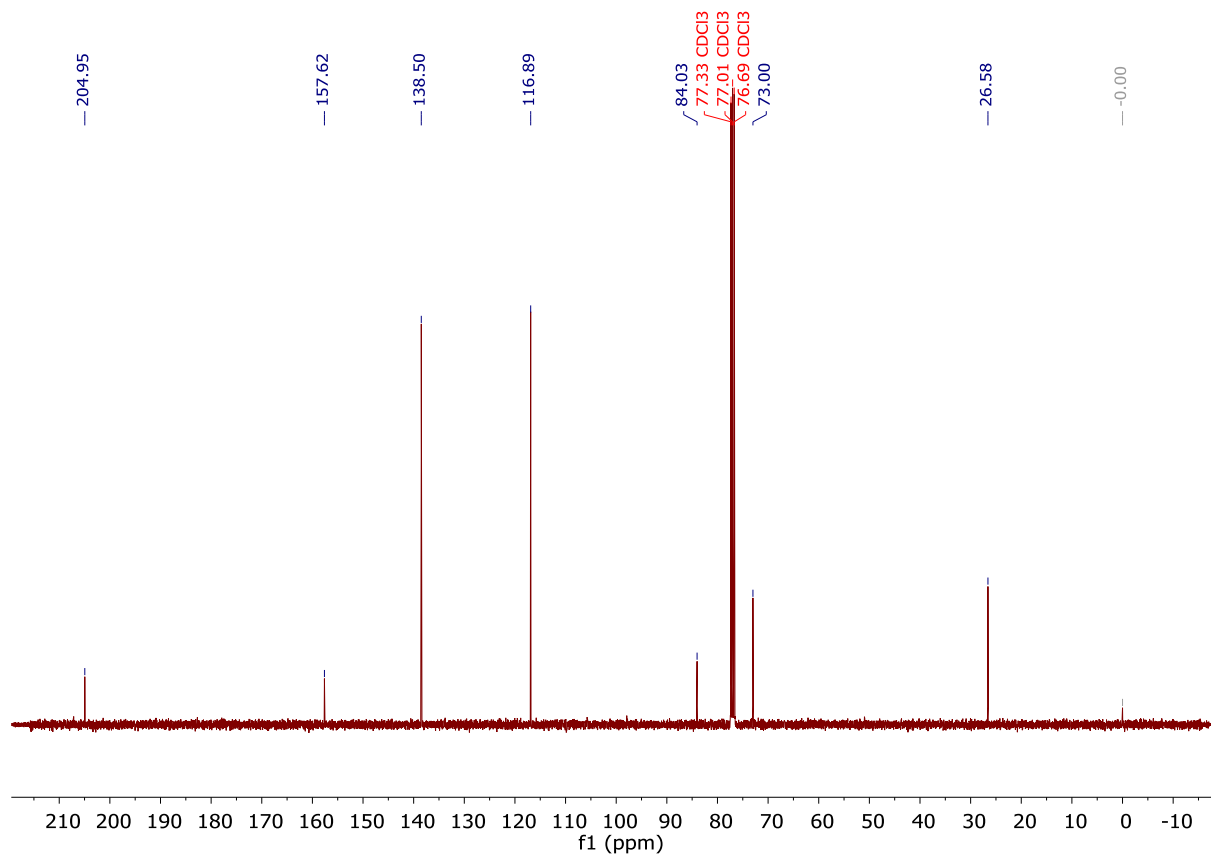
**1-(allyloxy)-4-iodobenzene (10a):**  $^1\text{H}$  NMR (400 MHz, Chloroform- $d$ )  $^{13}\text{C}\{\text{H}\}$  NMR (101 MHz, Chloroform- $d$ ).

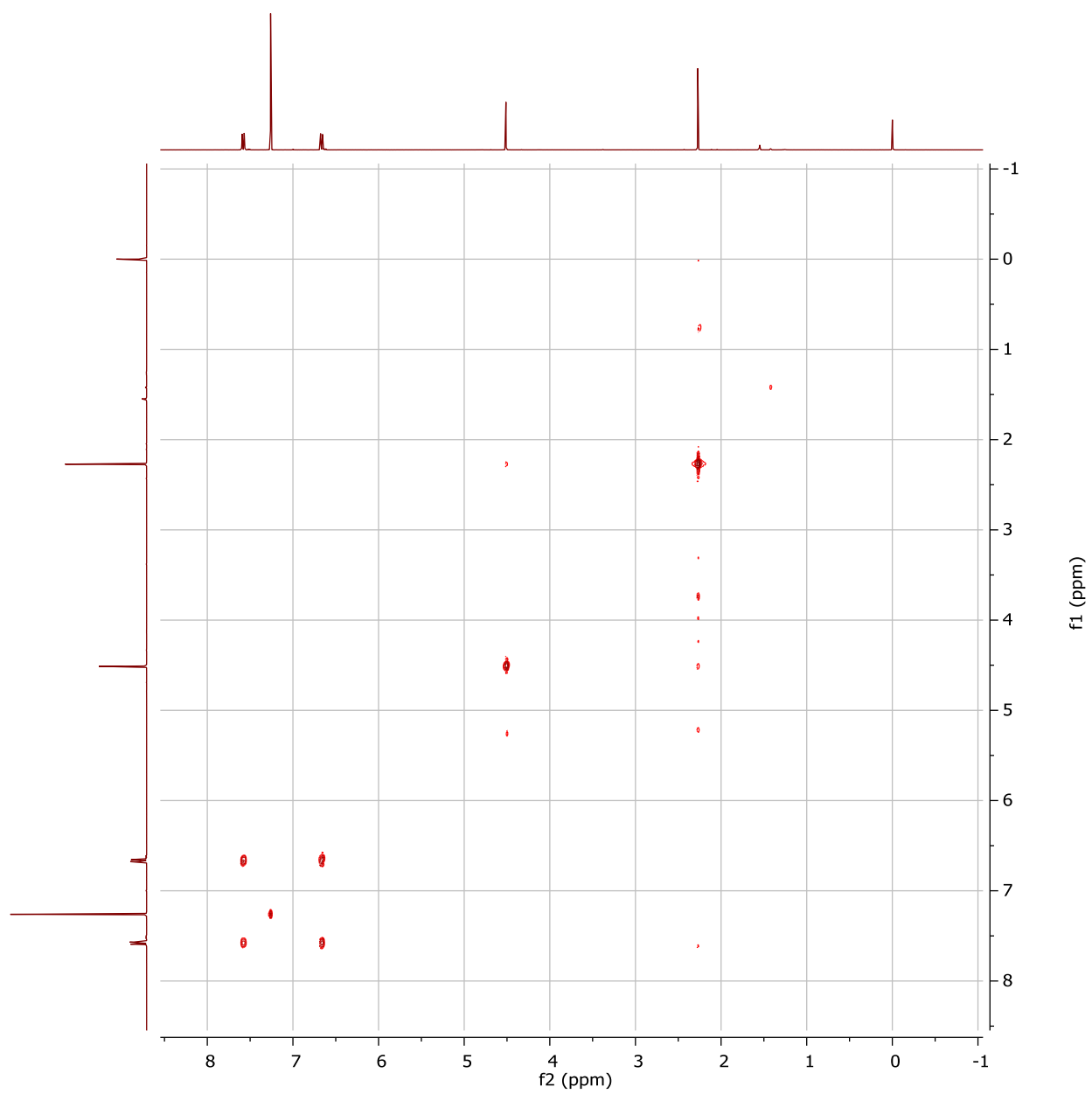




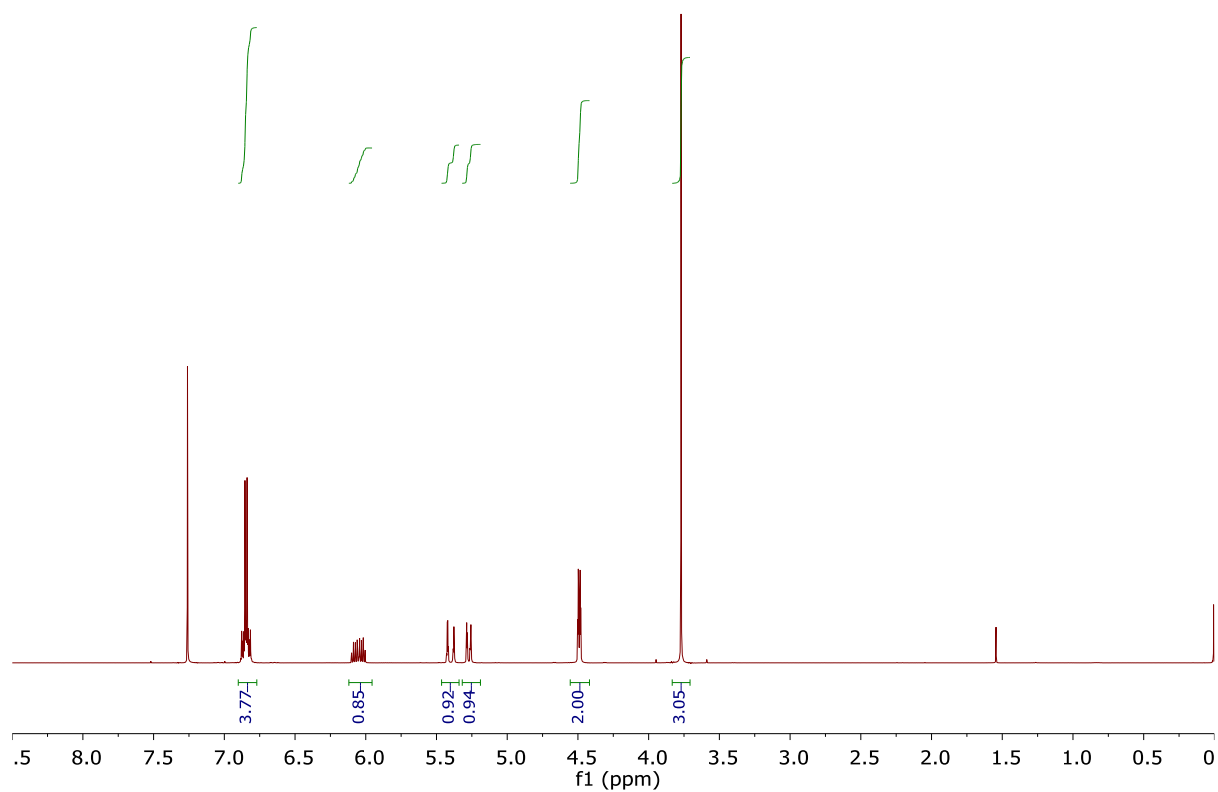
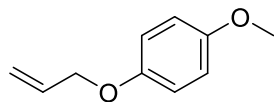
**1-(4-iodophenoxy)propan-2-one (10b):**  $^1\text{H}$  NMR (400 MHz, Chloroform-*d*),  $^{13}\text{C}\{\text{H}\}$  NMR (101 MHz, Chloroform-*d*) and COSY.

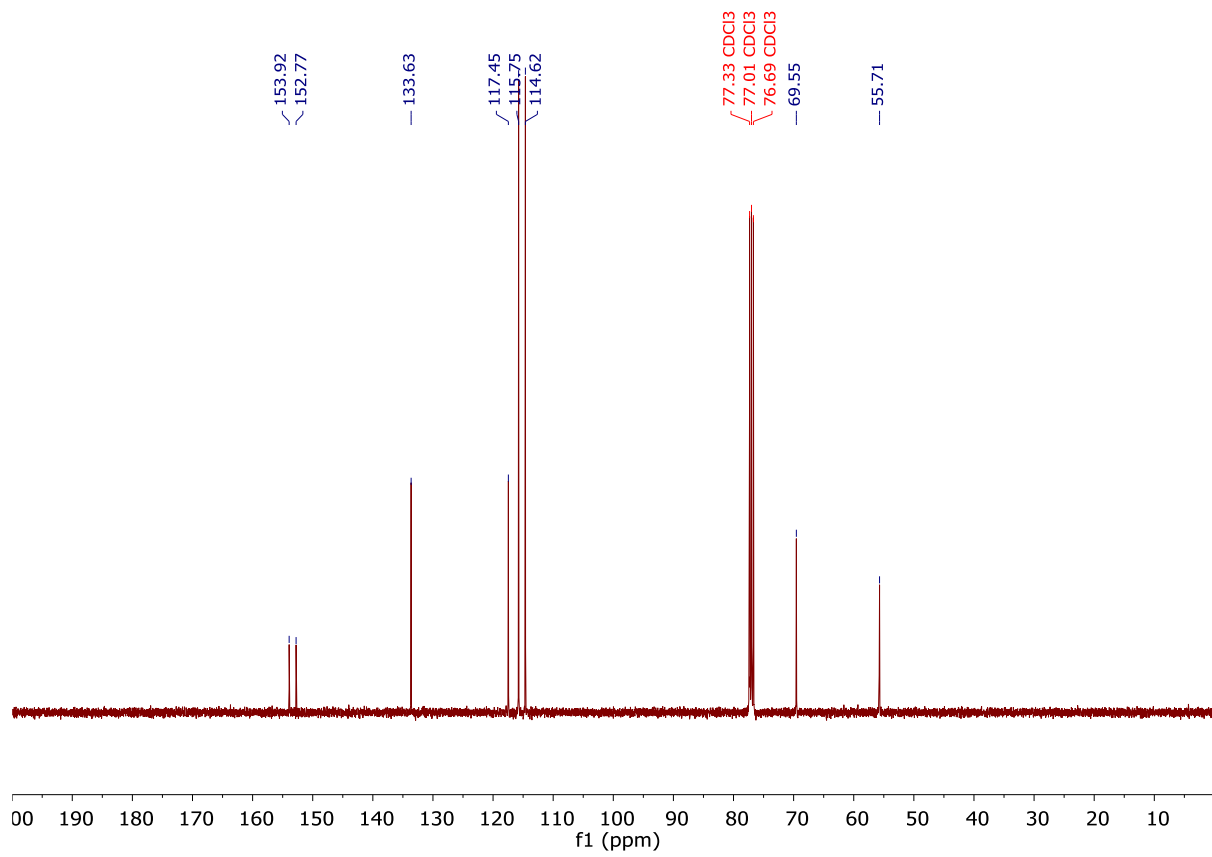




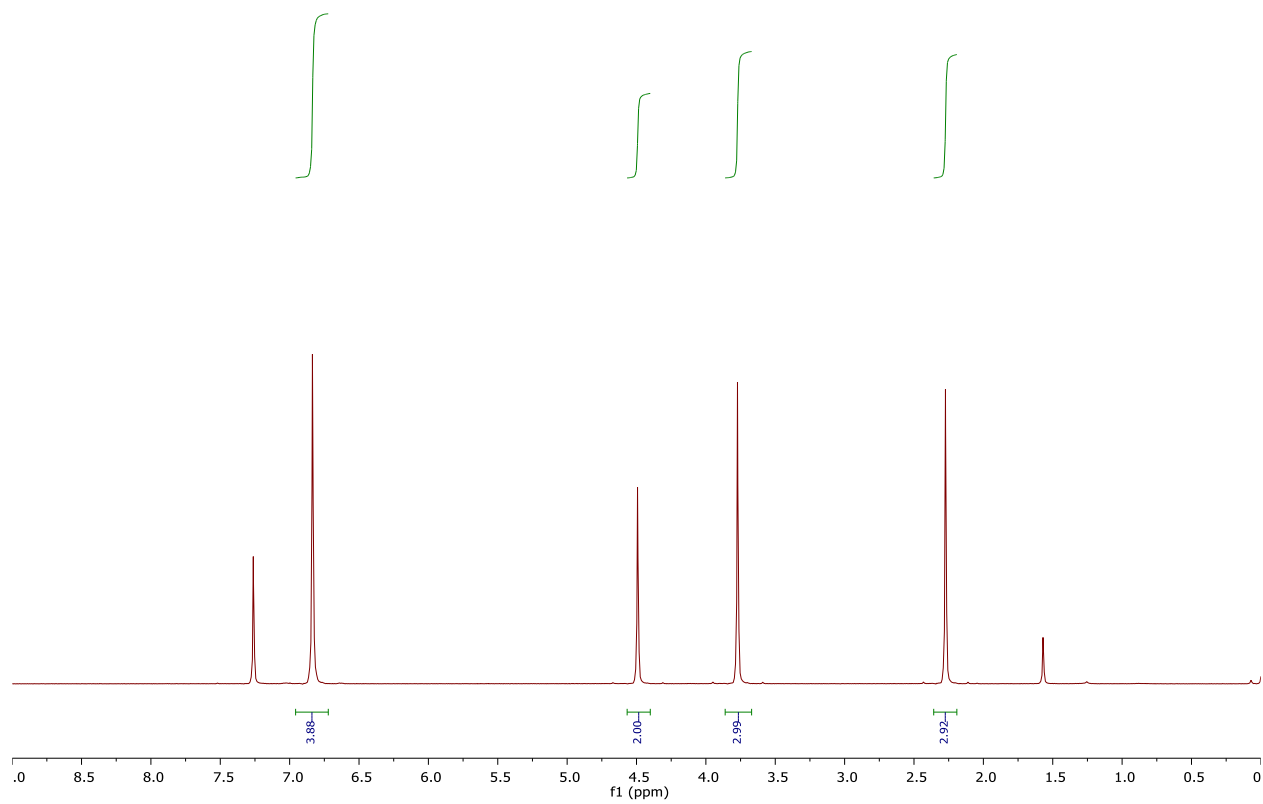
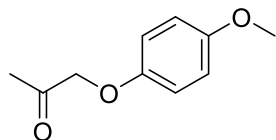


**Allyl 4-methoxyphenyl ether (11a):**  $^1\text{H}$  NMR (400 MHz, Chloroform-*d*),  $^{13}\text{C}\{^1\text{H}\}$  NMR (101 MHz, Chloroform-*d*).

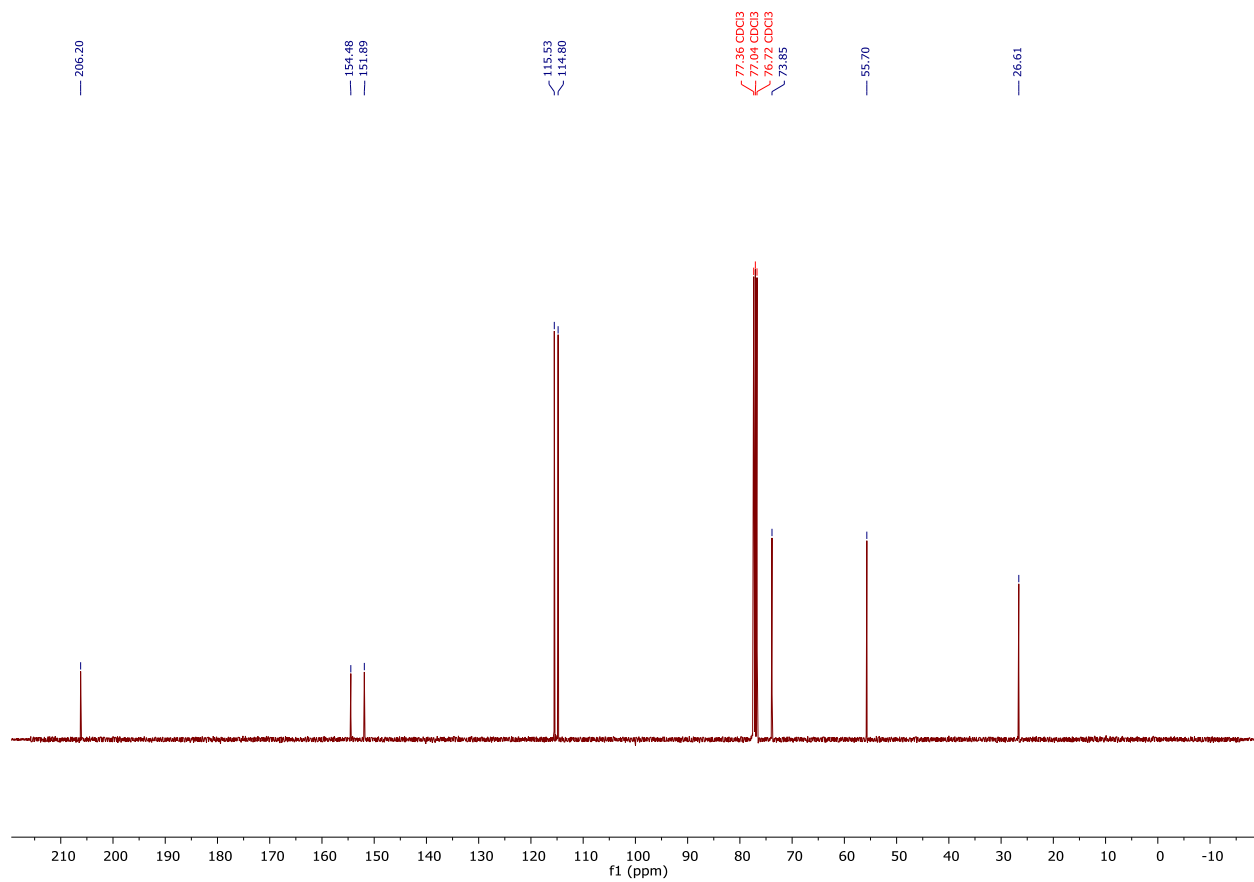


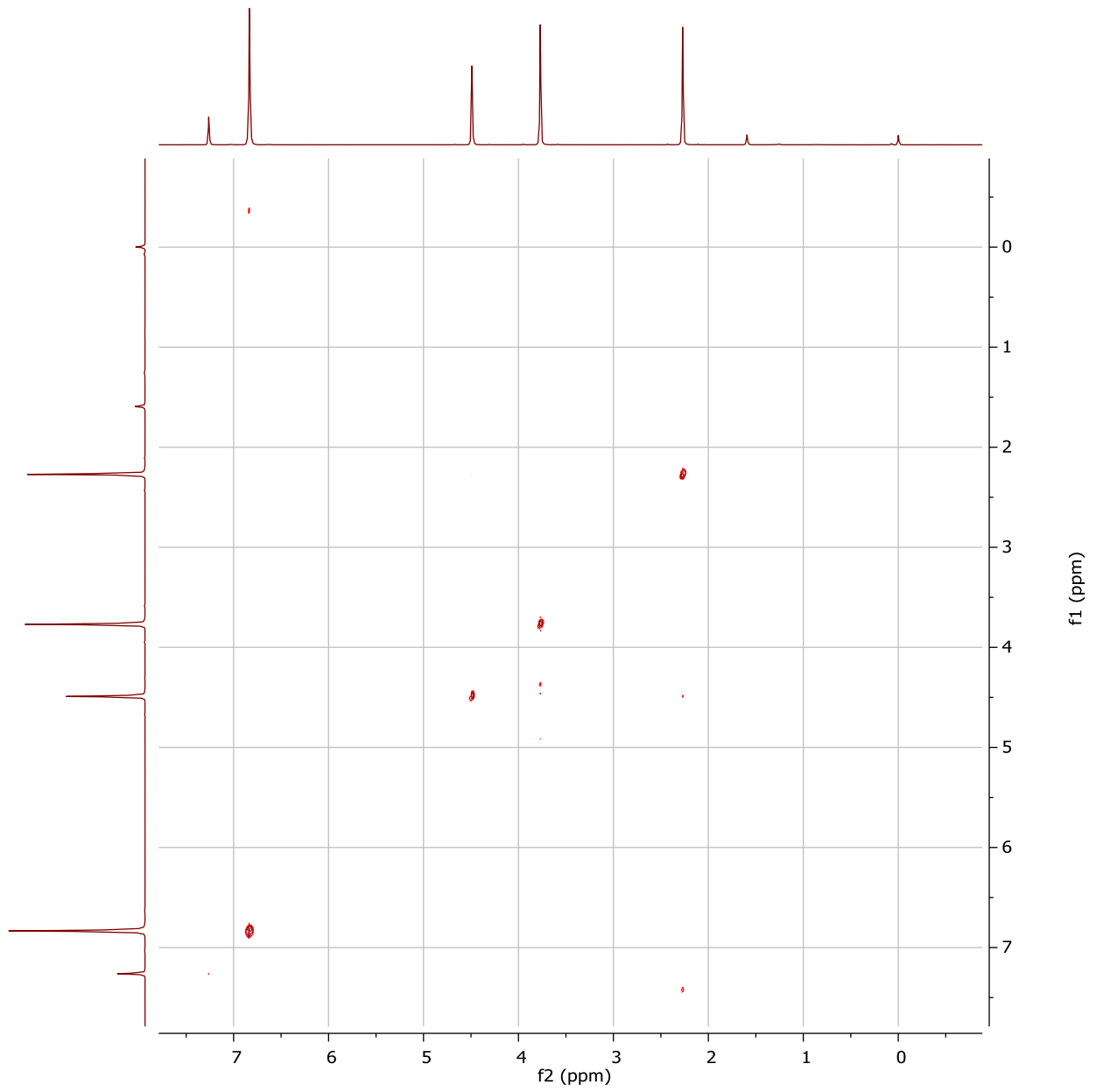


**1-(4-methoxyphenoxy)propan-2-one (11b):**  $^1\text{H}$  NMR (400 MHz, Chloroform-*d*),  $^{13}\text{C}\{^1\text{H}\}$  NMR (101 MHz, Chloroform-*d*) and COSY.

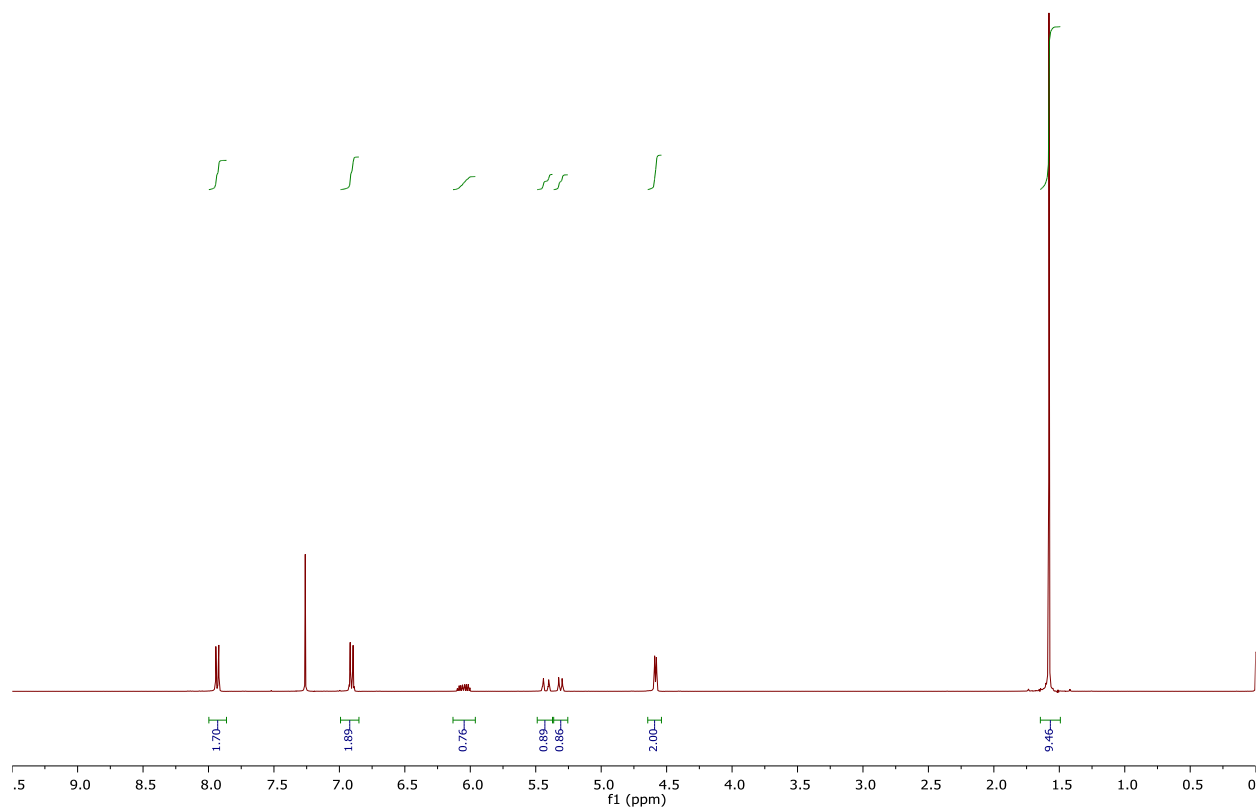
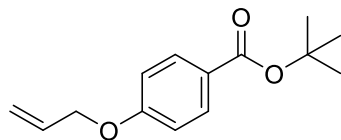


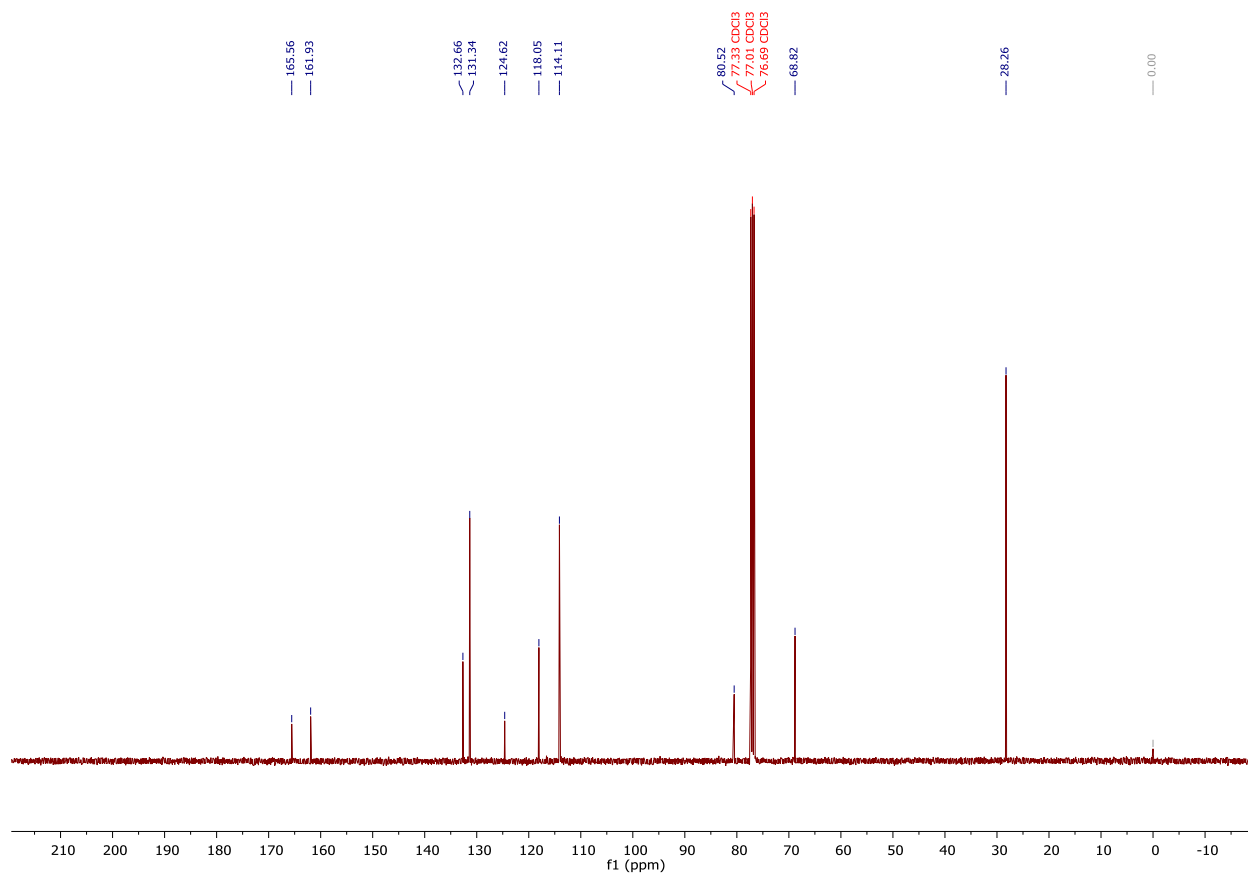
58



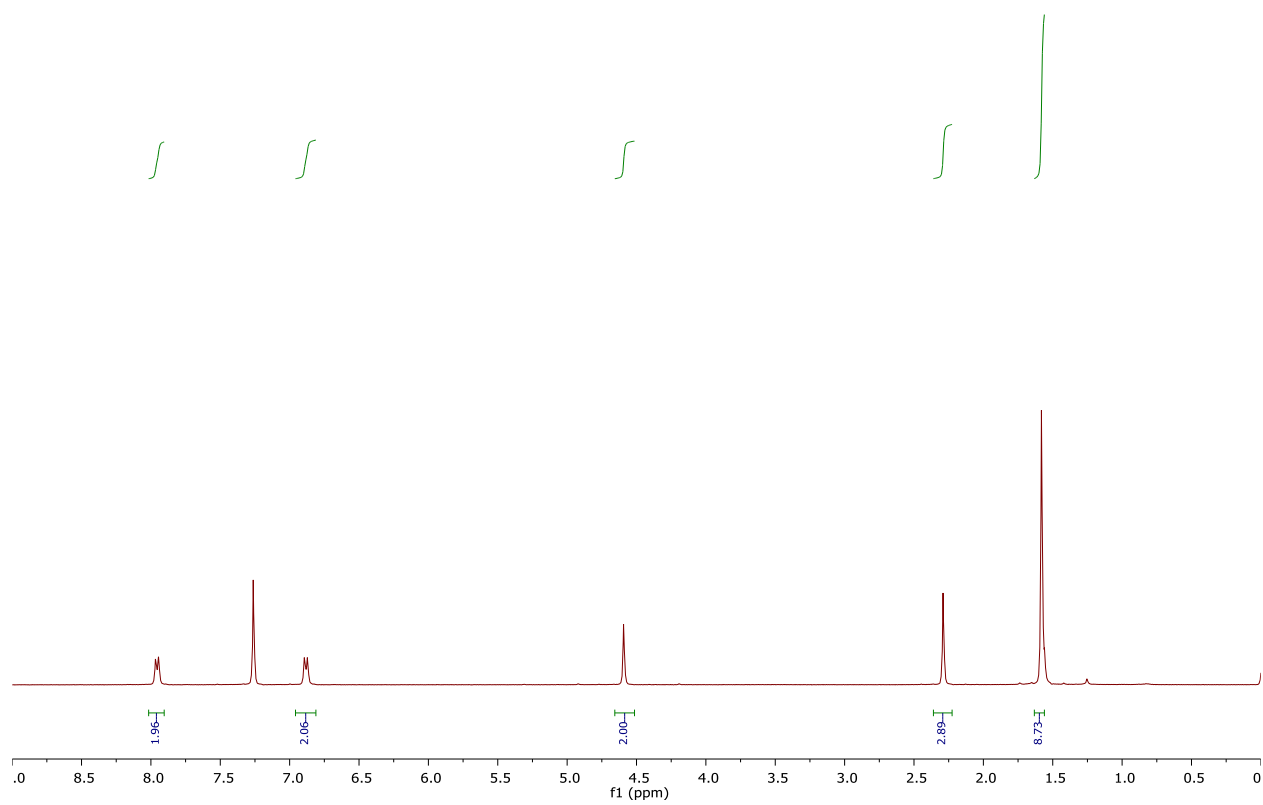
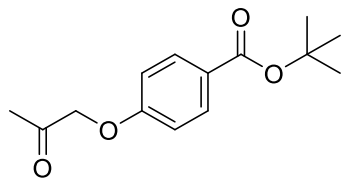


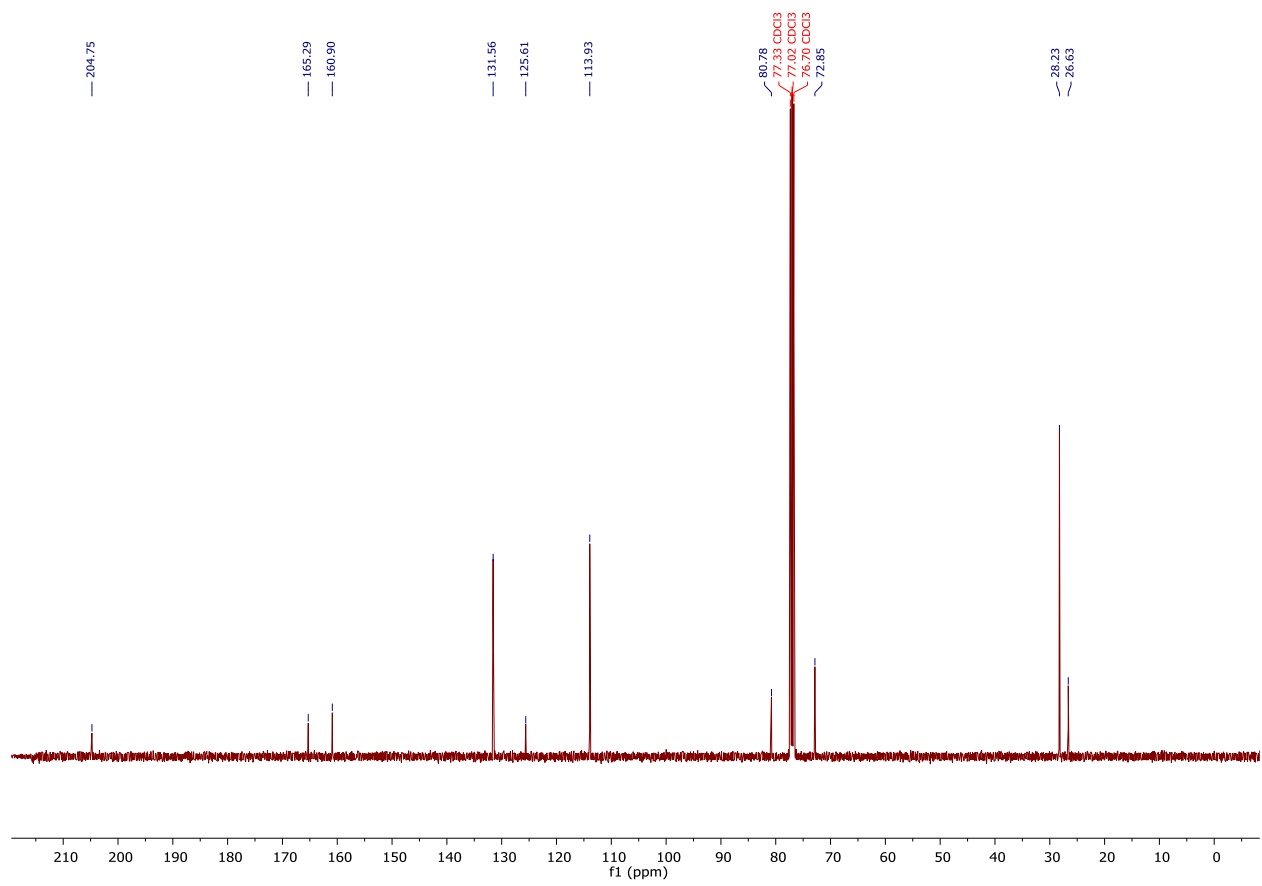
**tert-butyl 4-(allyloxy)benzoate (12a):**  $^1\text{H}$  NMR (400 MHz, Chloroform-*d*),  $^{13}\text{C}\{^1\text{H}\}$  NMR(101 MHz, Chloroform-*d*)

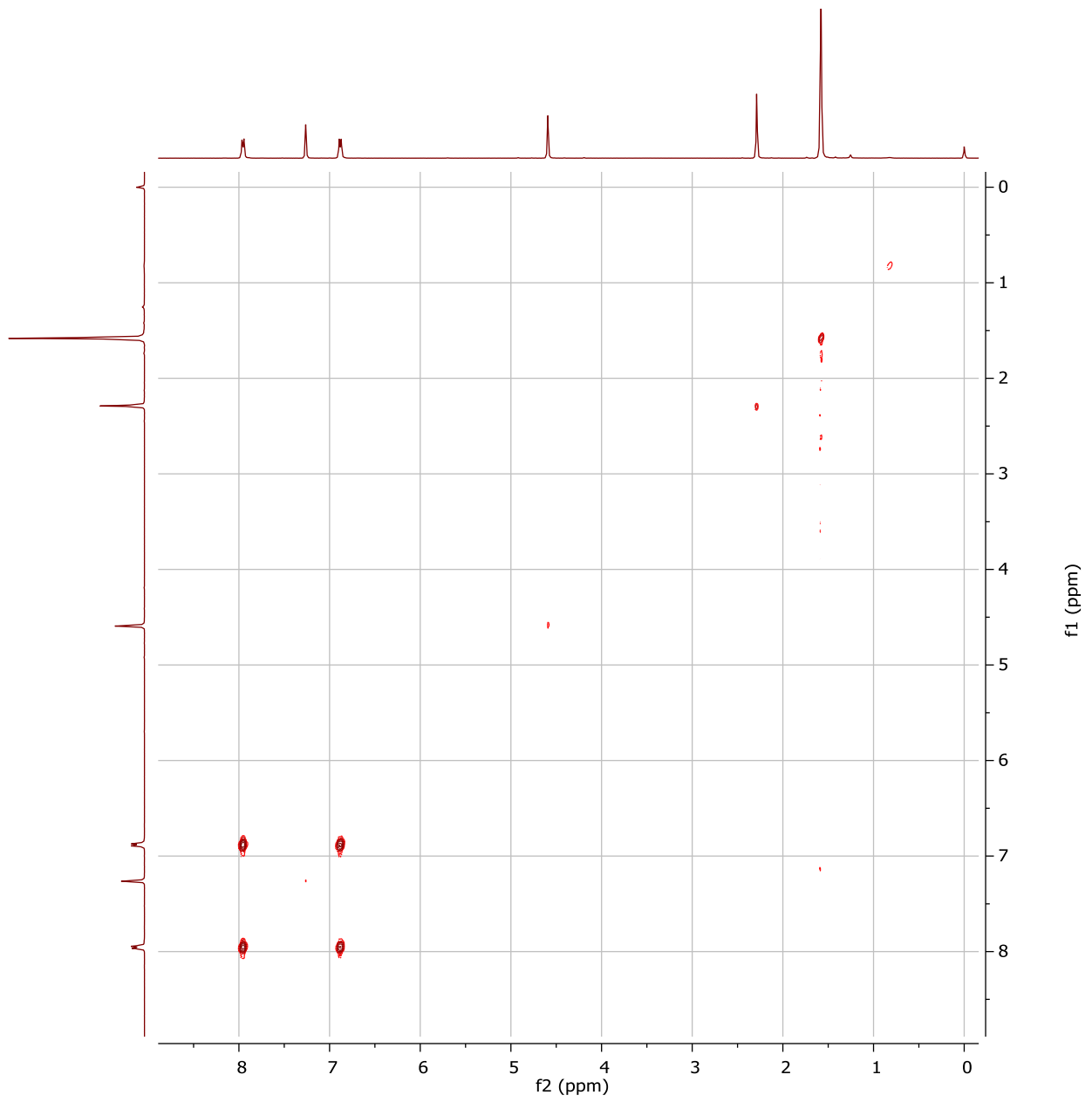




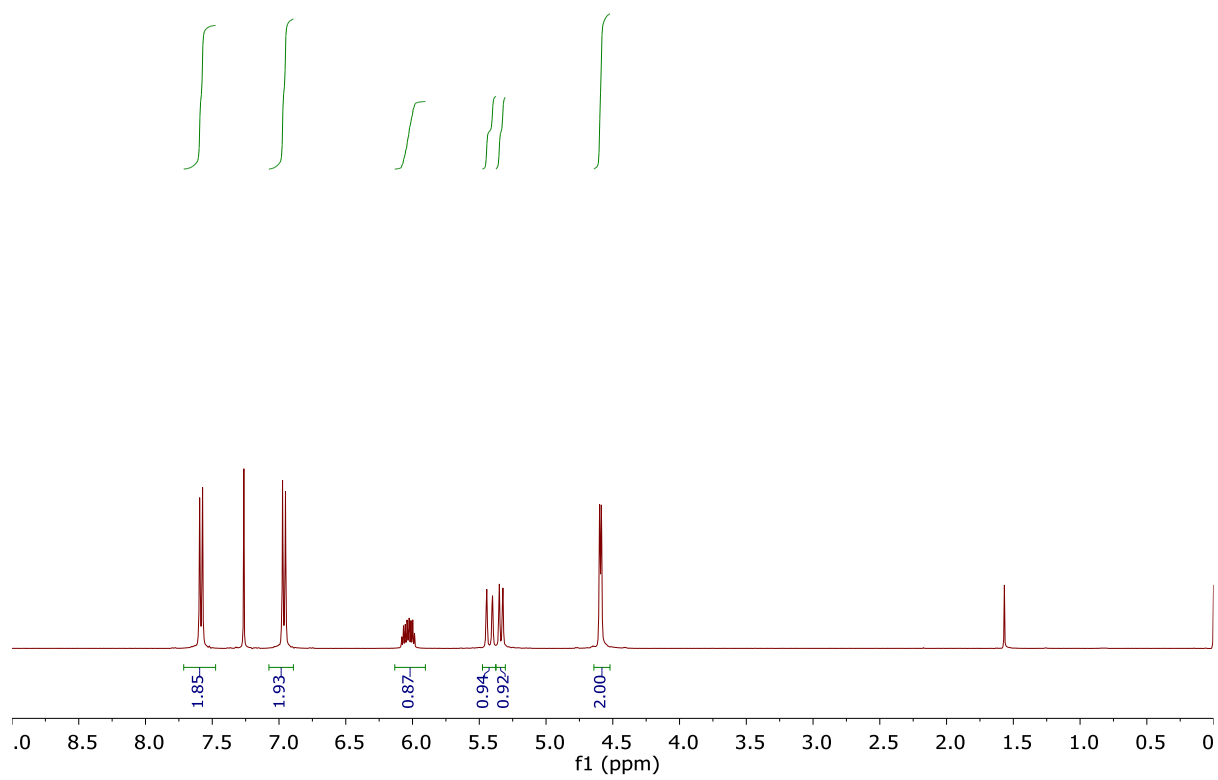
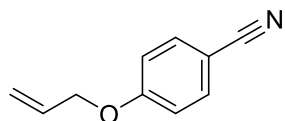
**tert-butyl 4-(2-oxopropoxy)benzoate (12b):**  $^1\text{H}$  NMR (400 MHz,  $\text{CDCl}_3$ ),  $^{13}\text{C}\{\text{H}\}$  NMR (101 MHz, Chloroform-*d*) and COSY.

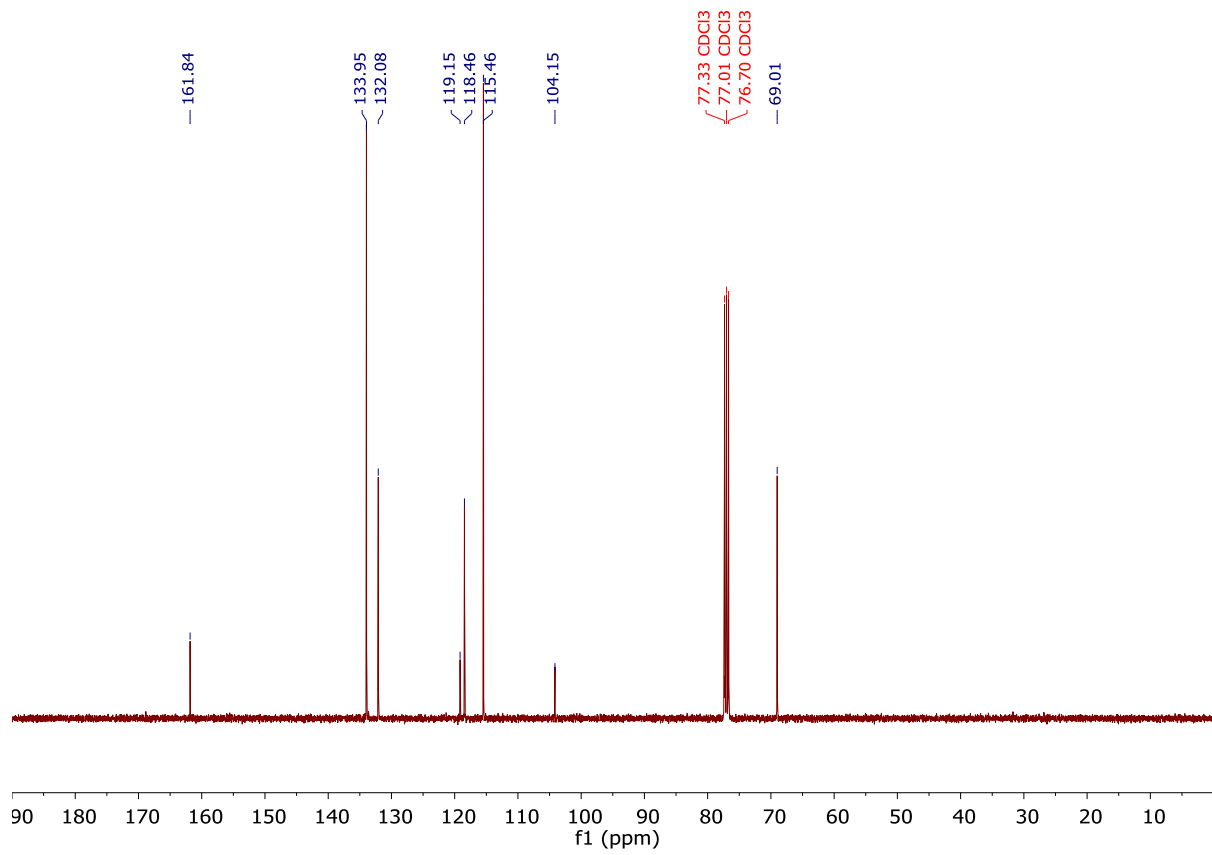




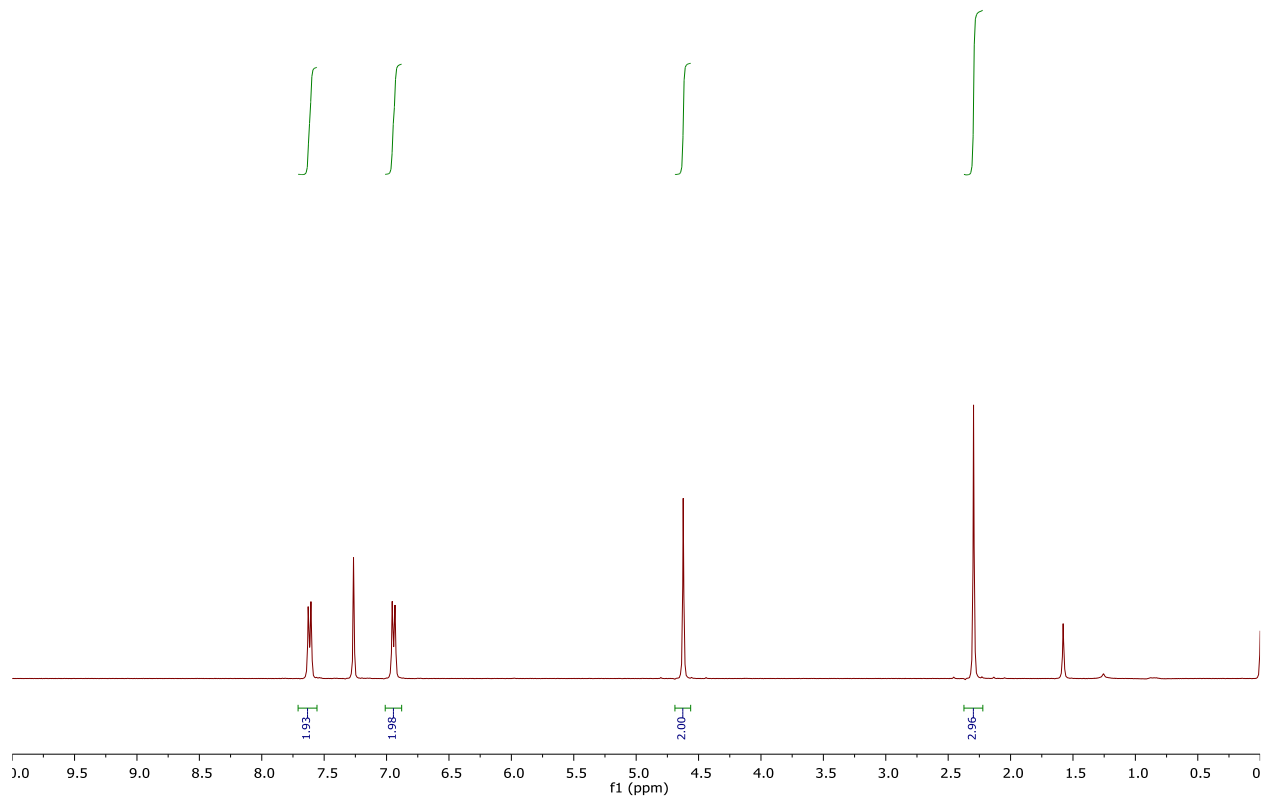
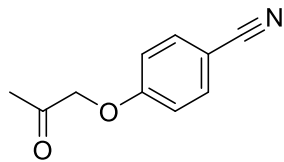


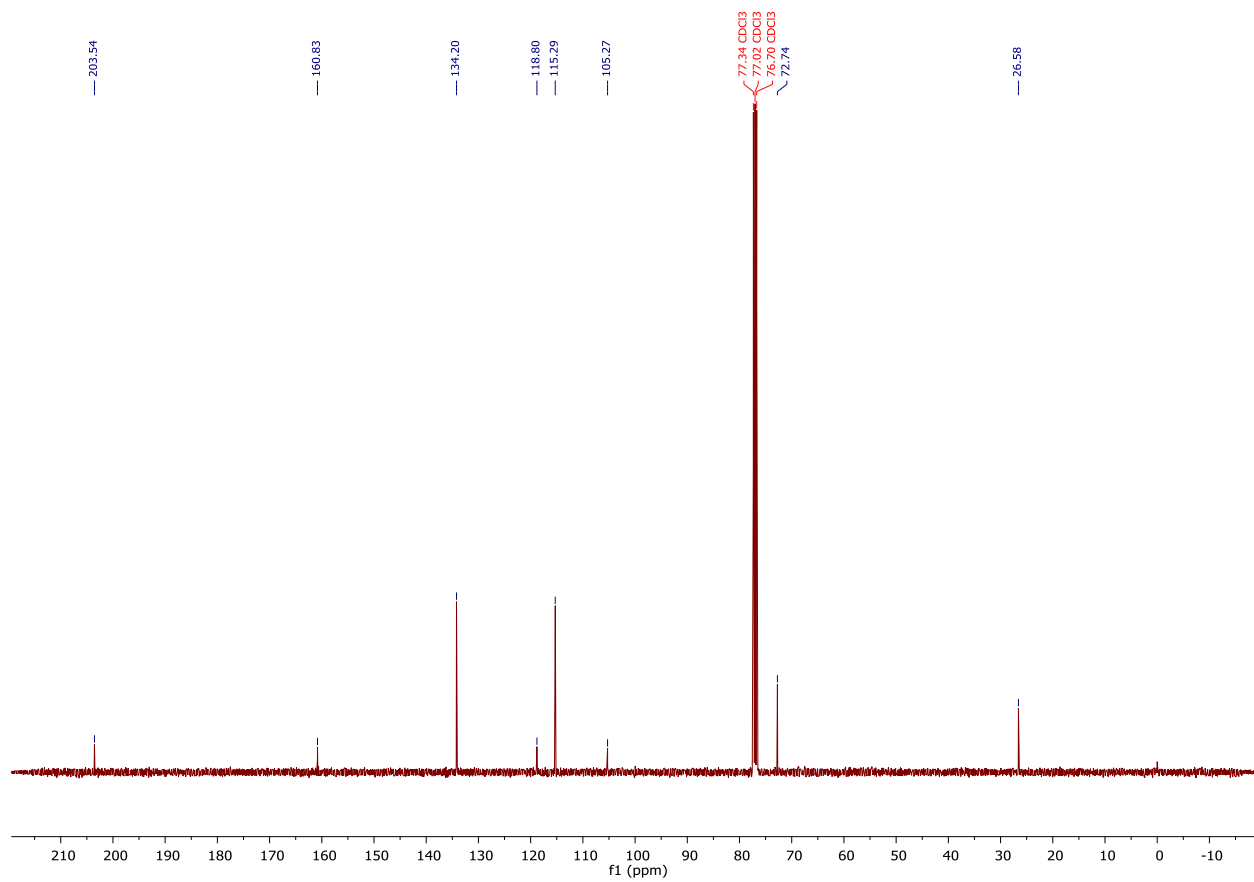
**4-(allyloxy)benzonitrile (13a):**  $^1\text{H}$  NMR (400 MHz, Chloroform-*d*),  $^{13}\text{C}\{^1\text{H}\}$  NMR (101 MHz, Chloroform-*d*).

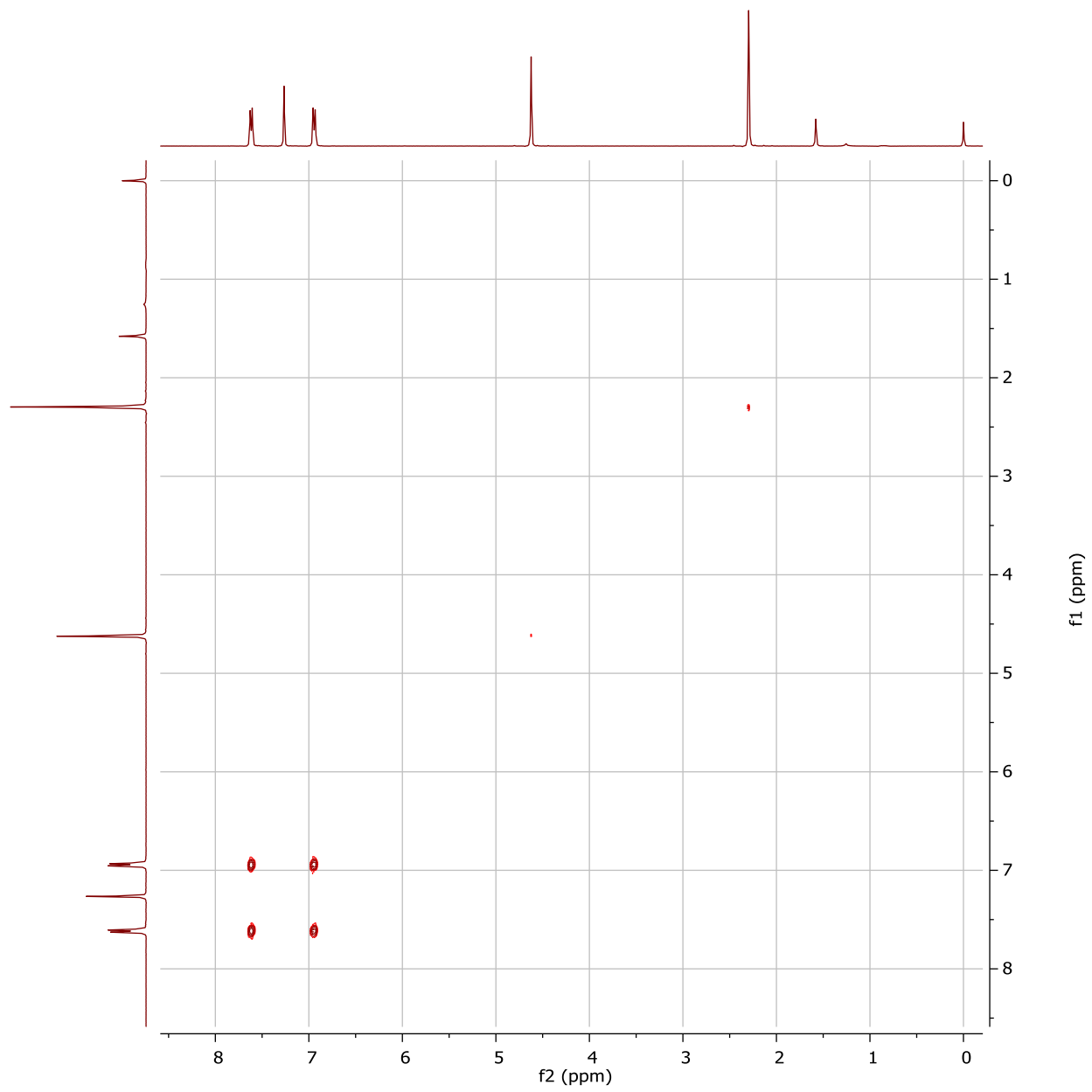




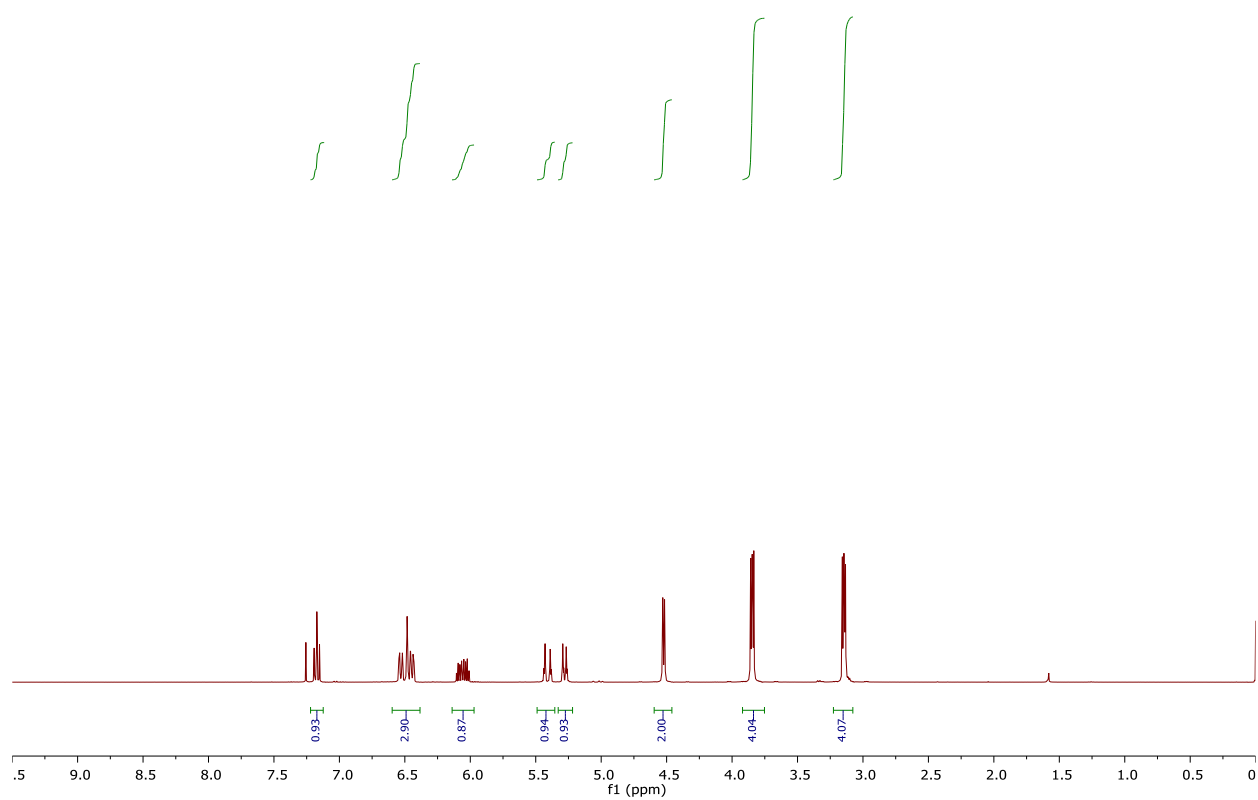
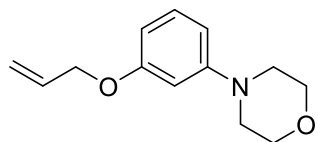
**4-(2-oxopropoxy)benzonitrile(13b):**  $^1\text{H}$  NMR (400 MHz, Chloroform-*d*),  $^{13}\text{C}\{^1\text{H}\}$  NMR (101 MHz, Chloroform-*d*) and COSY.

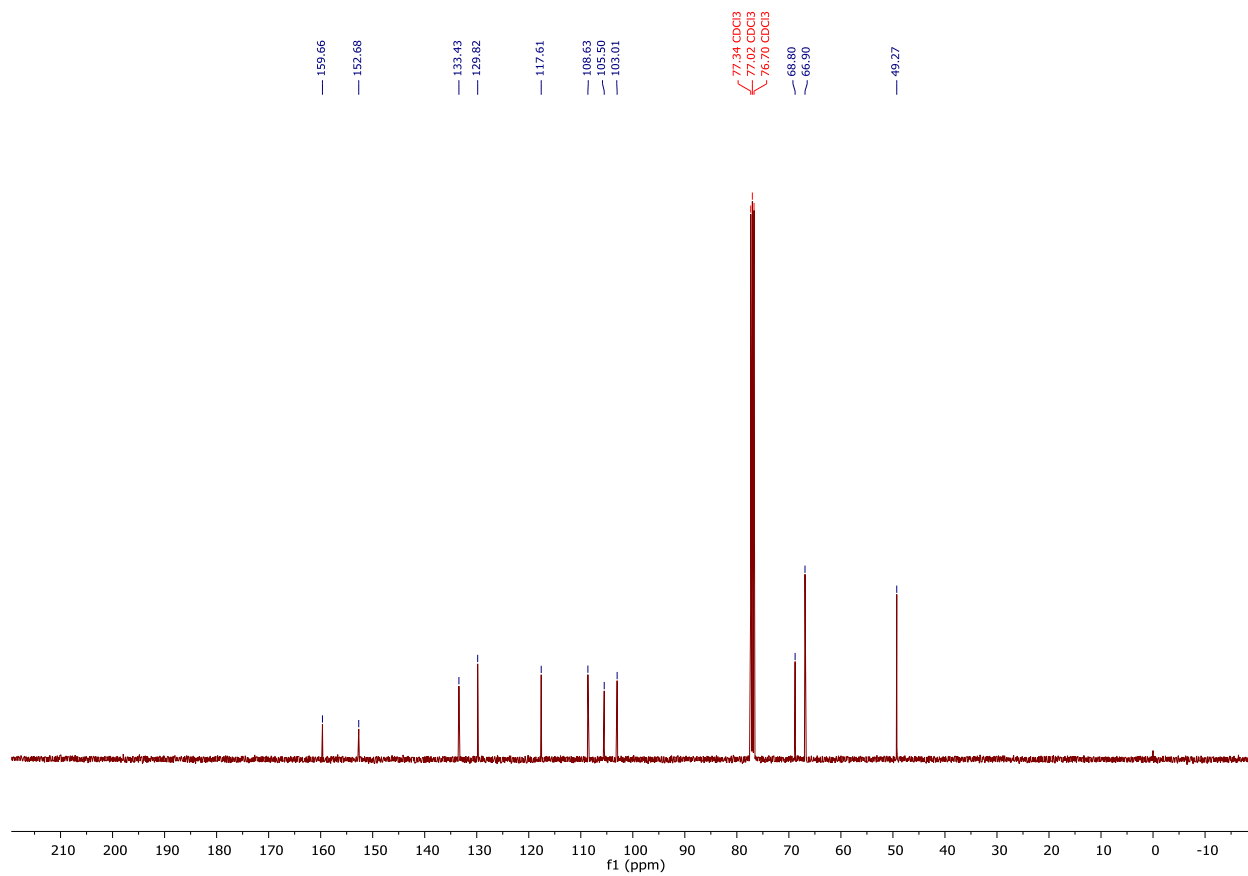




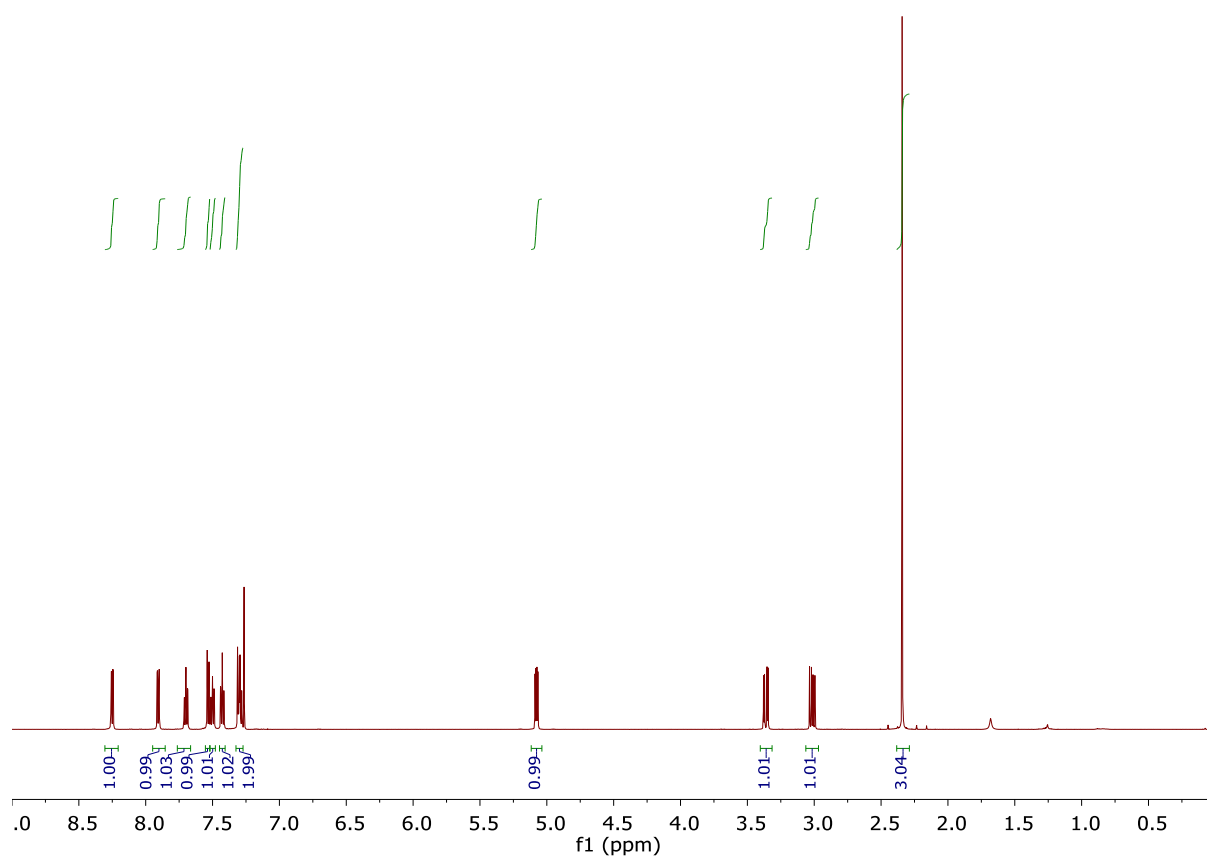
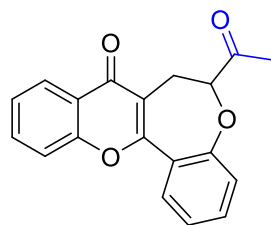


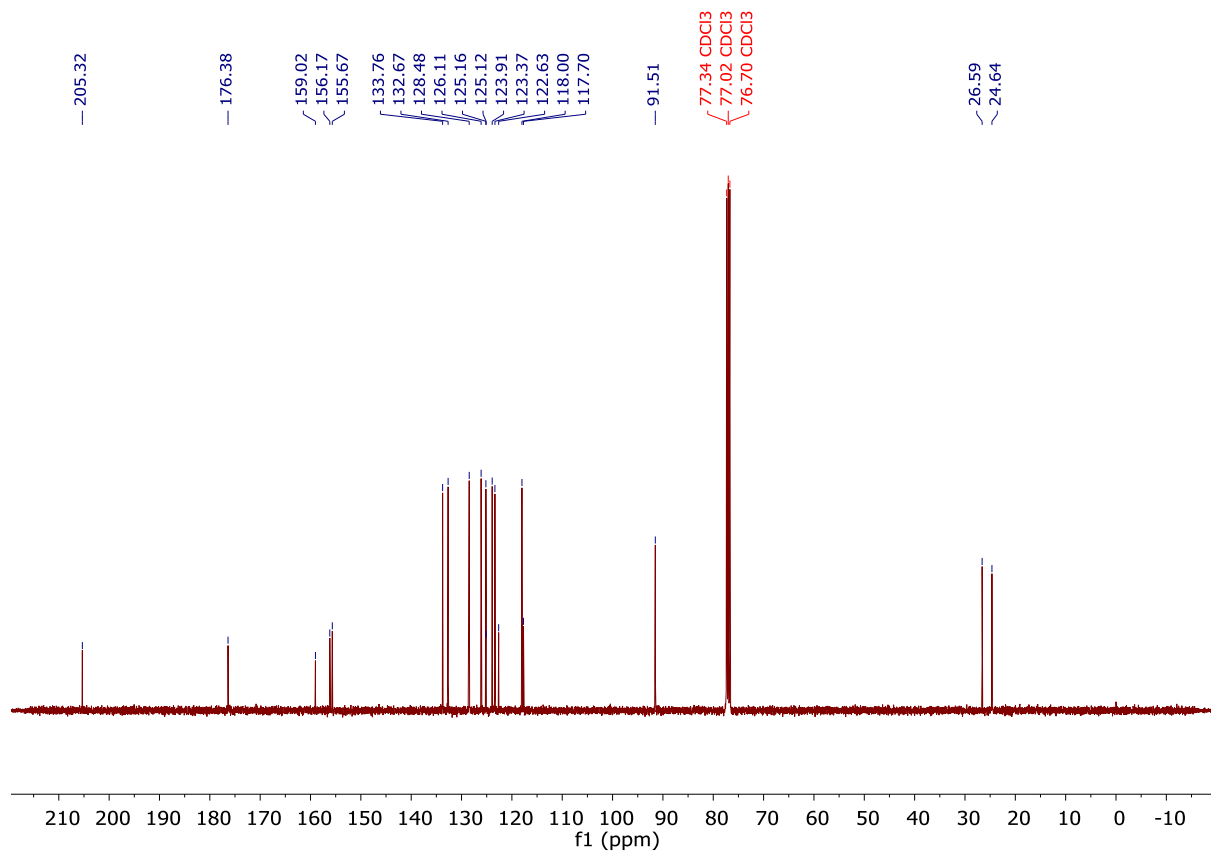
**Allyl 3-morpholinophenyl ether (14a):**  $^1\text{H}$  NMR (400 MHz, Chloroform-*d*),  $^{13}\text{C}\{\text{H}\}$  NMR(101 MHz, Chloroform-*d*).

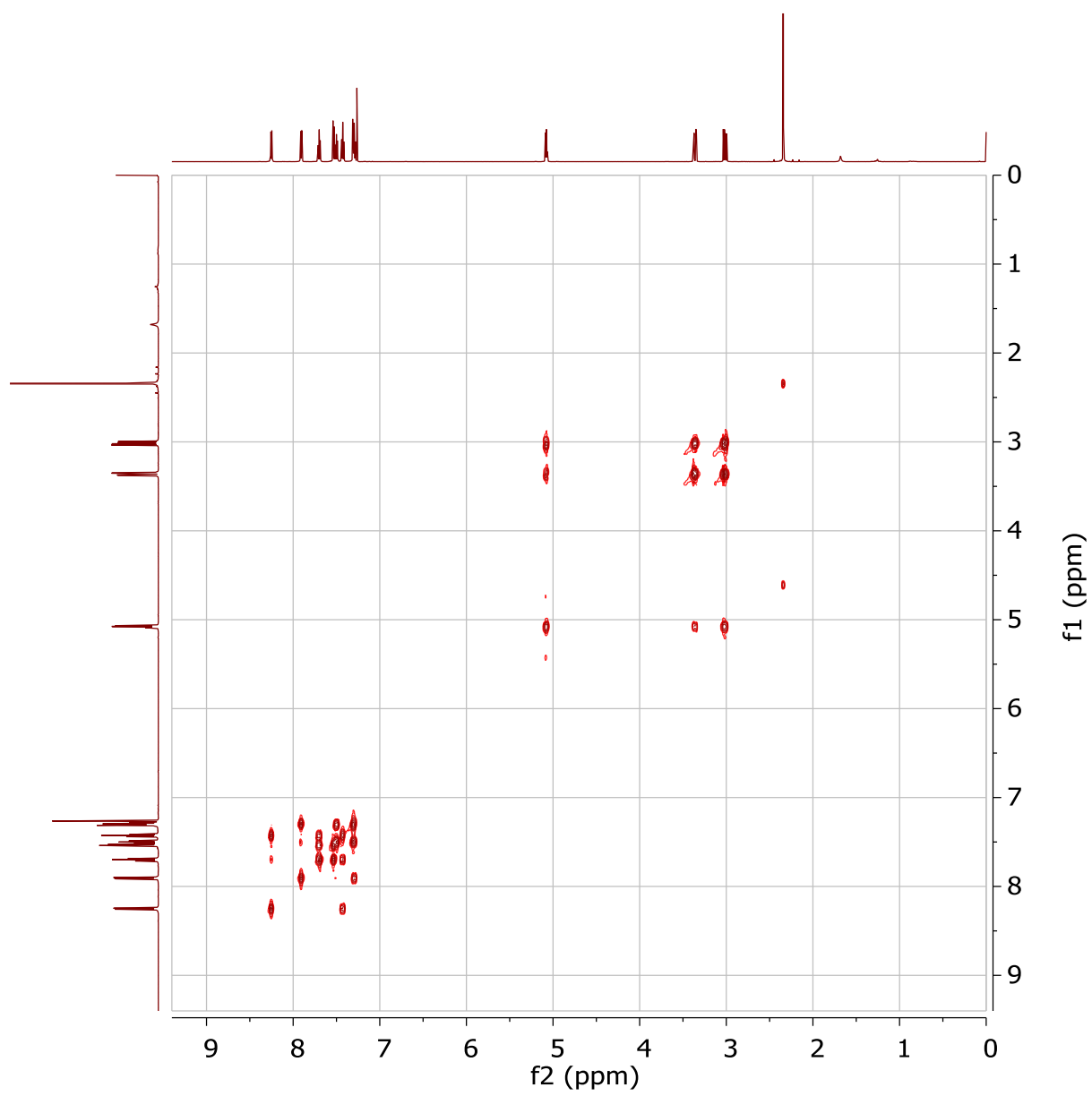


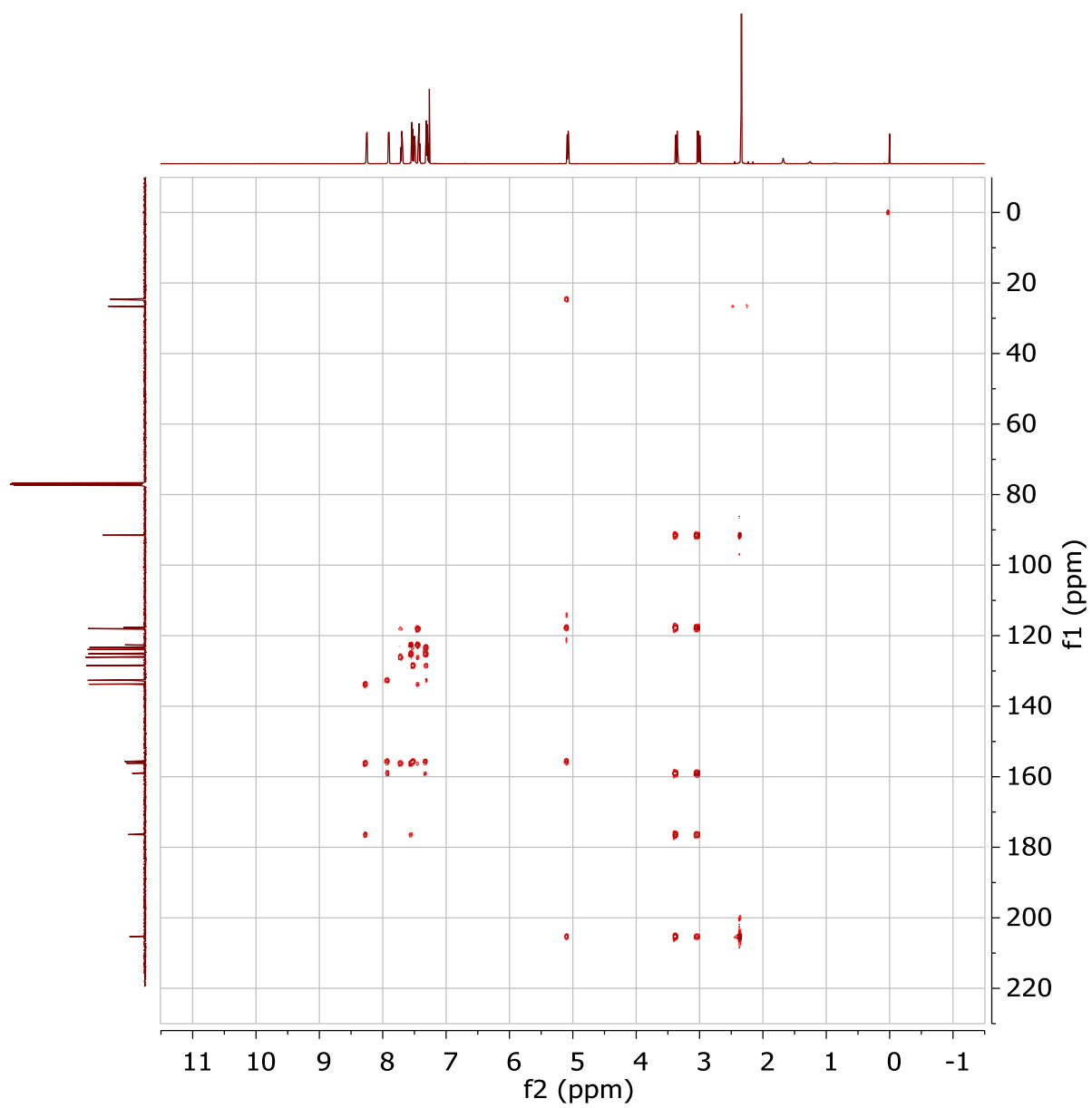


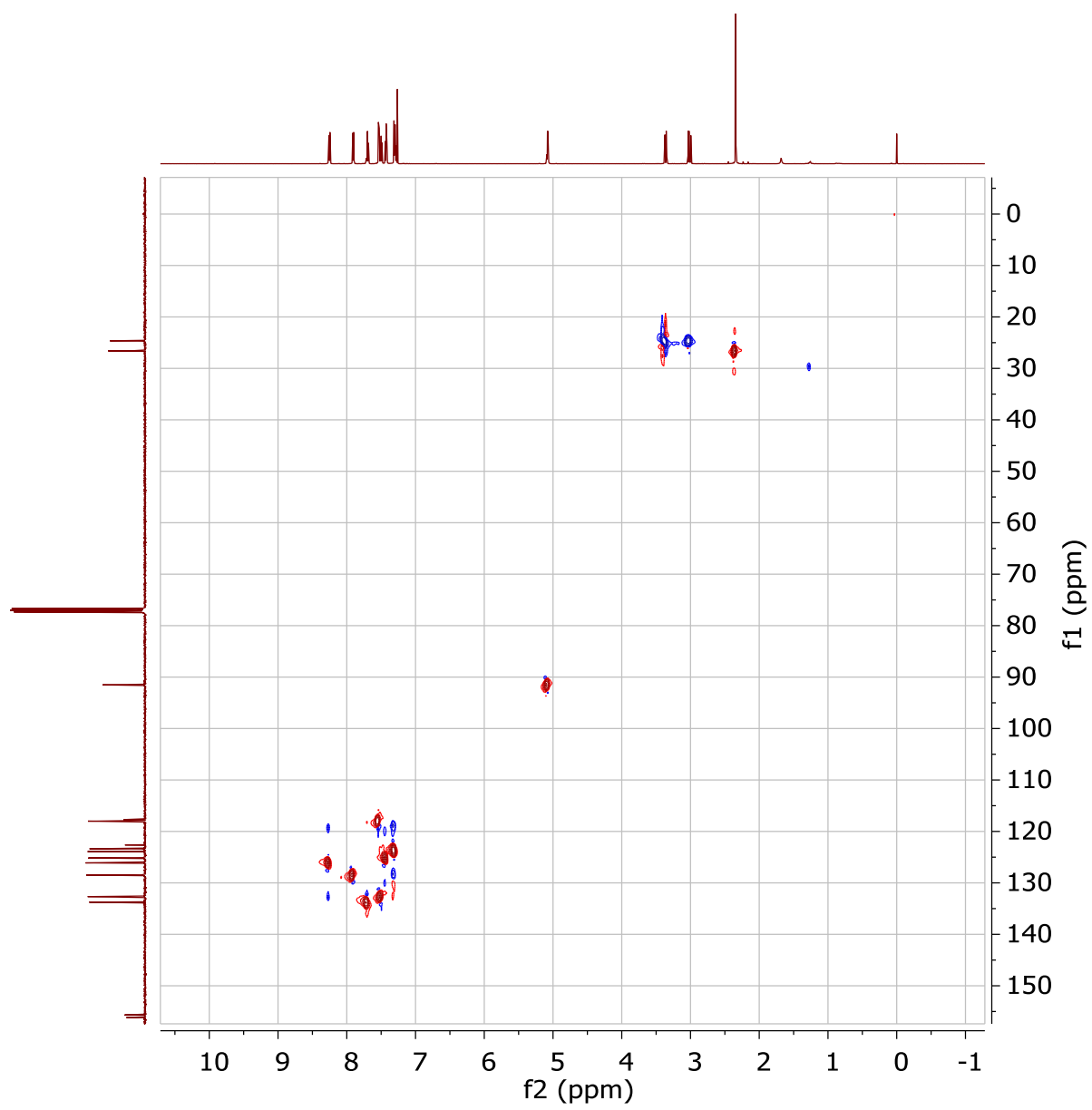
**6-acetyl-6,7-dihydro-8H-benzo[2,3]oxepino[4,5-b]chromen-8-one (16b):**  $^1\text{H}$  NMR (400 MHz, Chloroform-*d*),  $^{13}\text{C}\{^1\text{H}\}$  NMR (101 MHz, Chloroform-*d*). COSY, HMBC, HSQC.



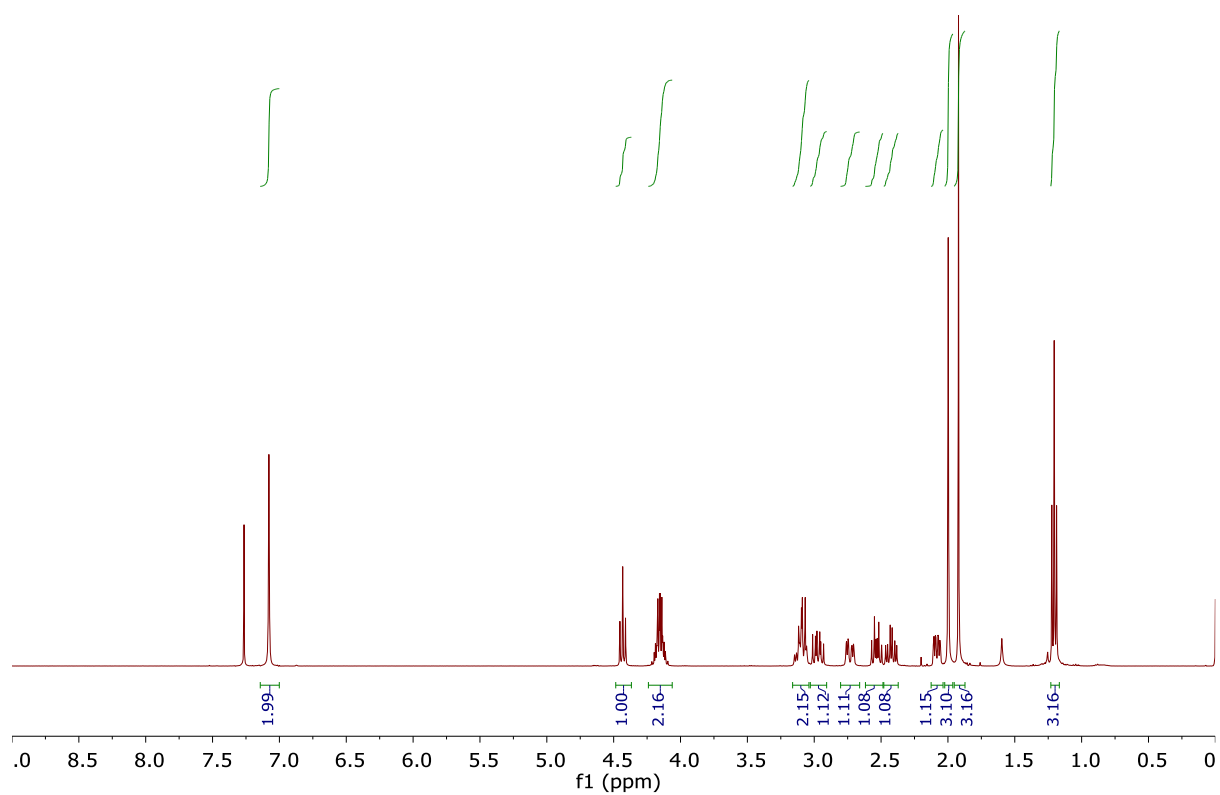
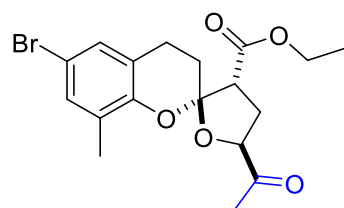


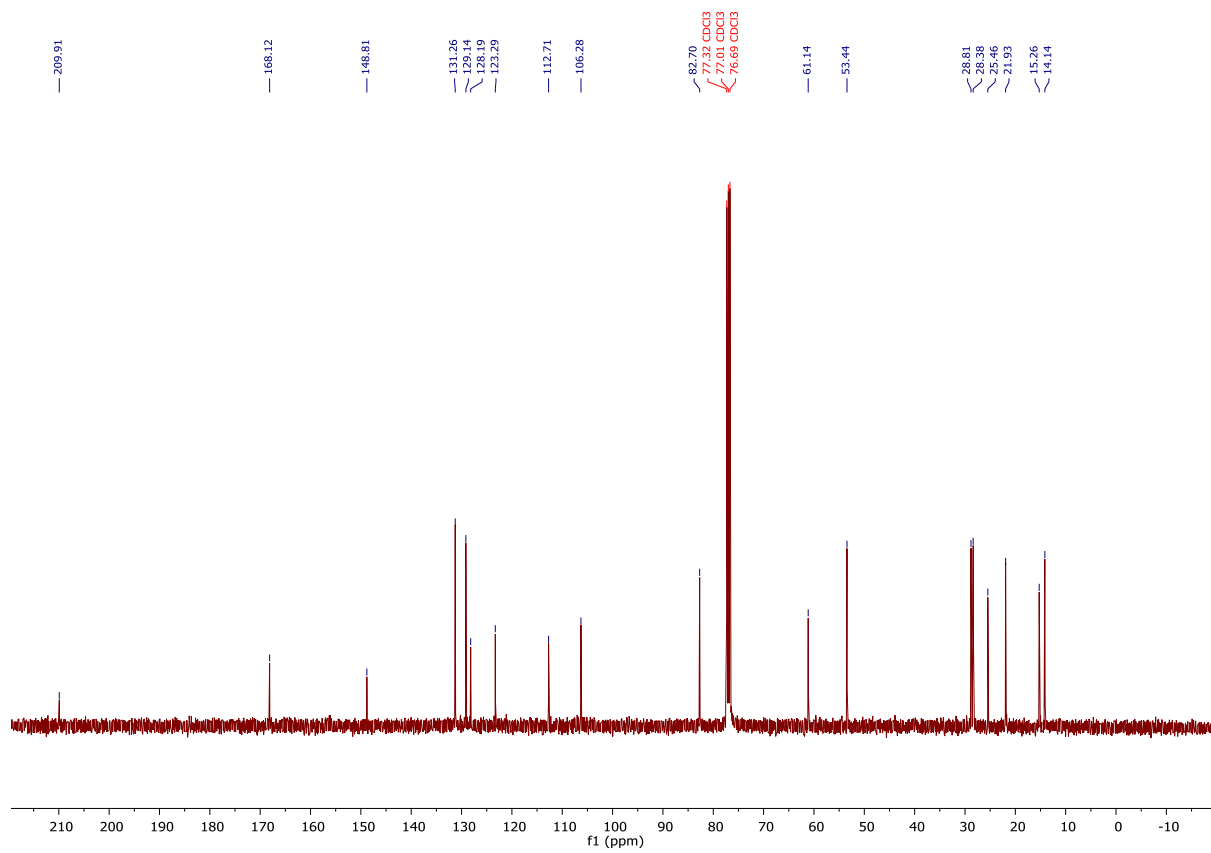


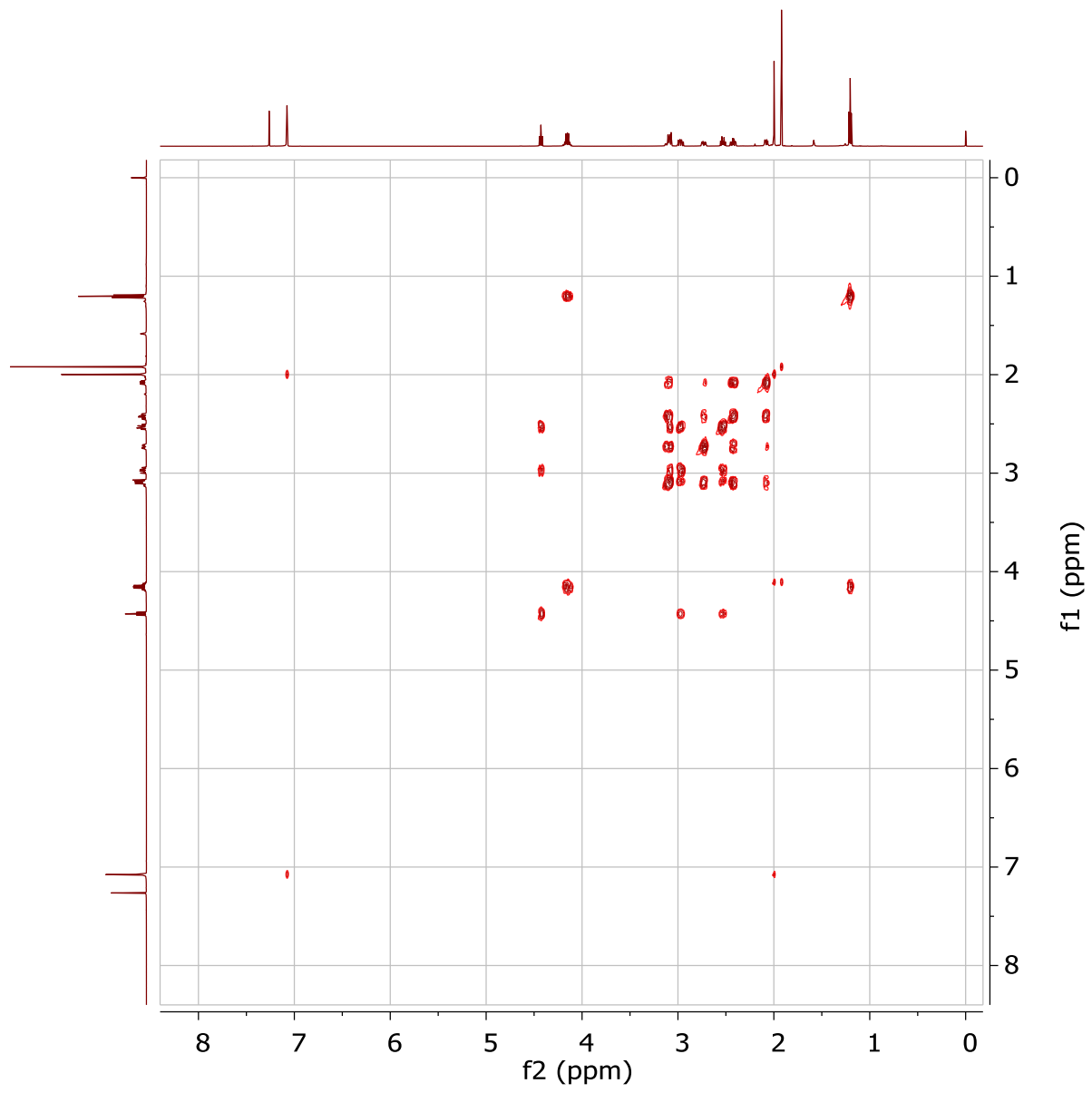


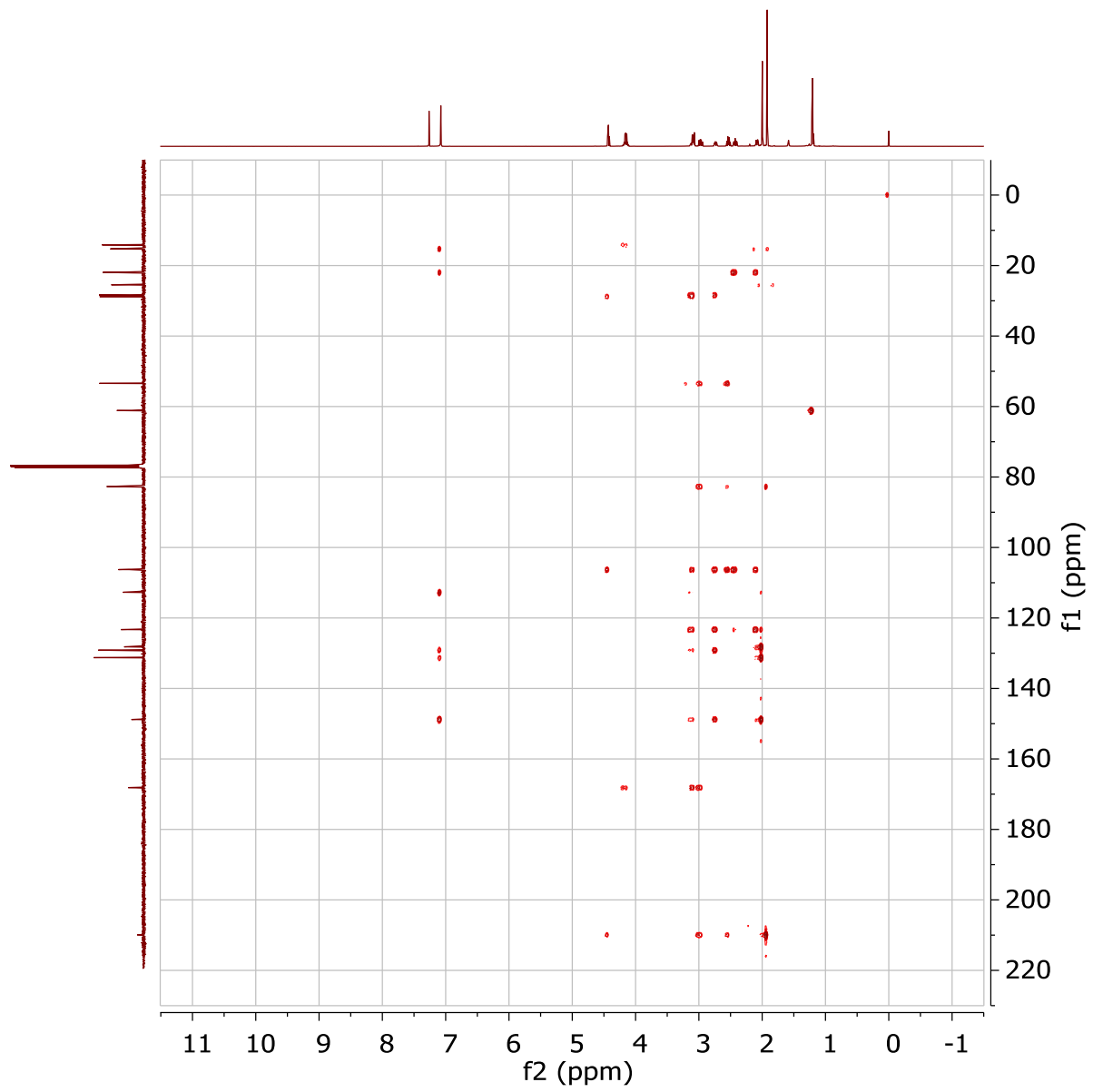


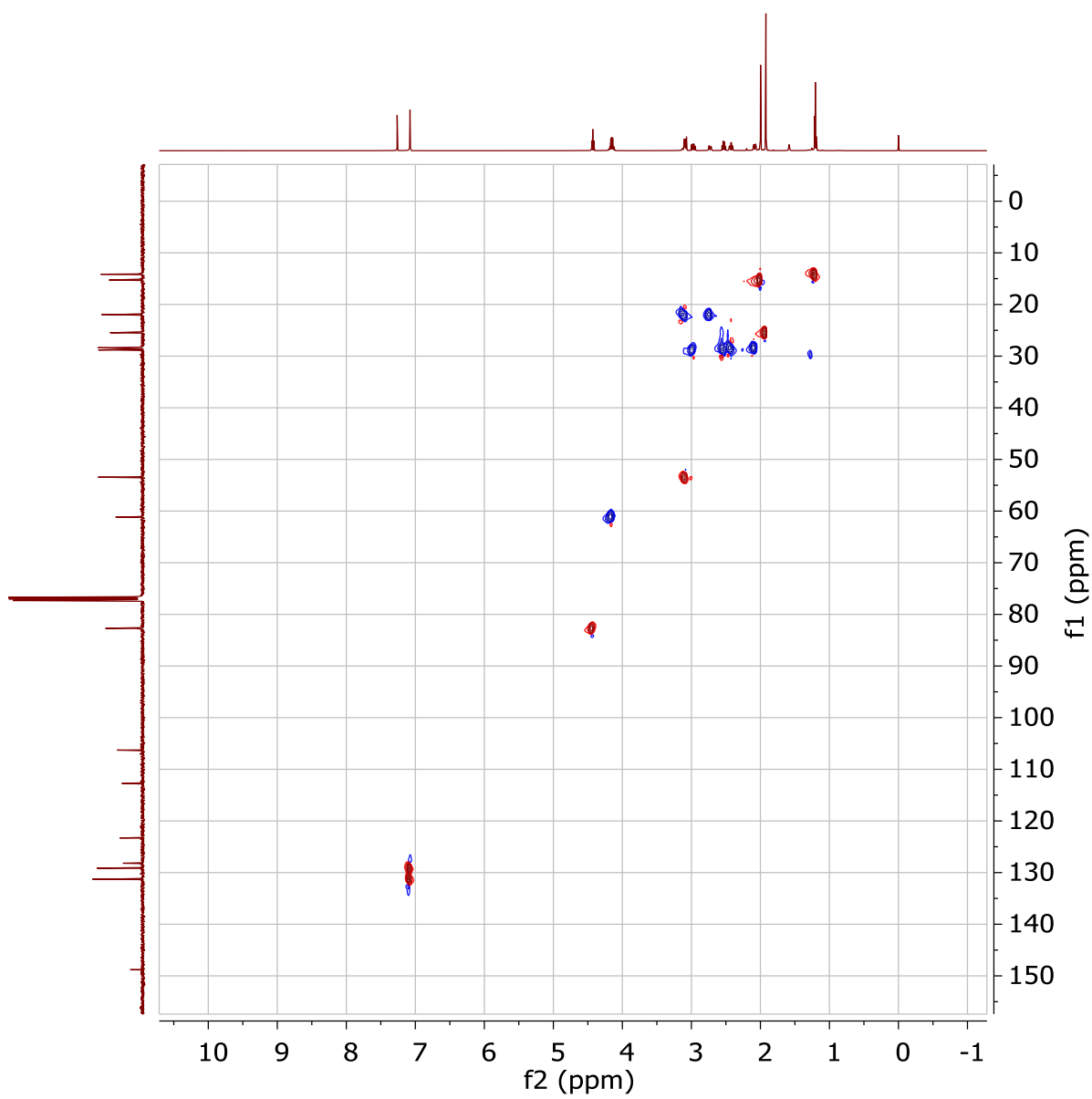
**Ethyl (2R,3'R,5'S)-5'-acetyl-6-bromo-8-methyl-4',5'-dihydro-3'H-spiro[chromane-2,2'-furan]-3'-carboxylate (17b):**  $^1\text{H}$  NMR (400 MHz, Chloroform-*d*),  $^{13}\text{C}\{\text{H}\}$  NMR (101 MHz, Chloroform-*d*). COSY, HMBC, HSQC, NOESY.

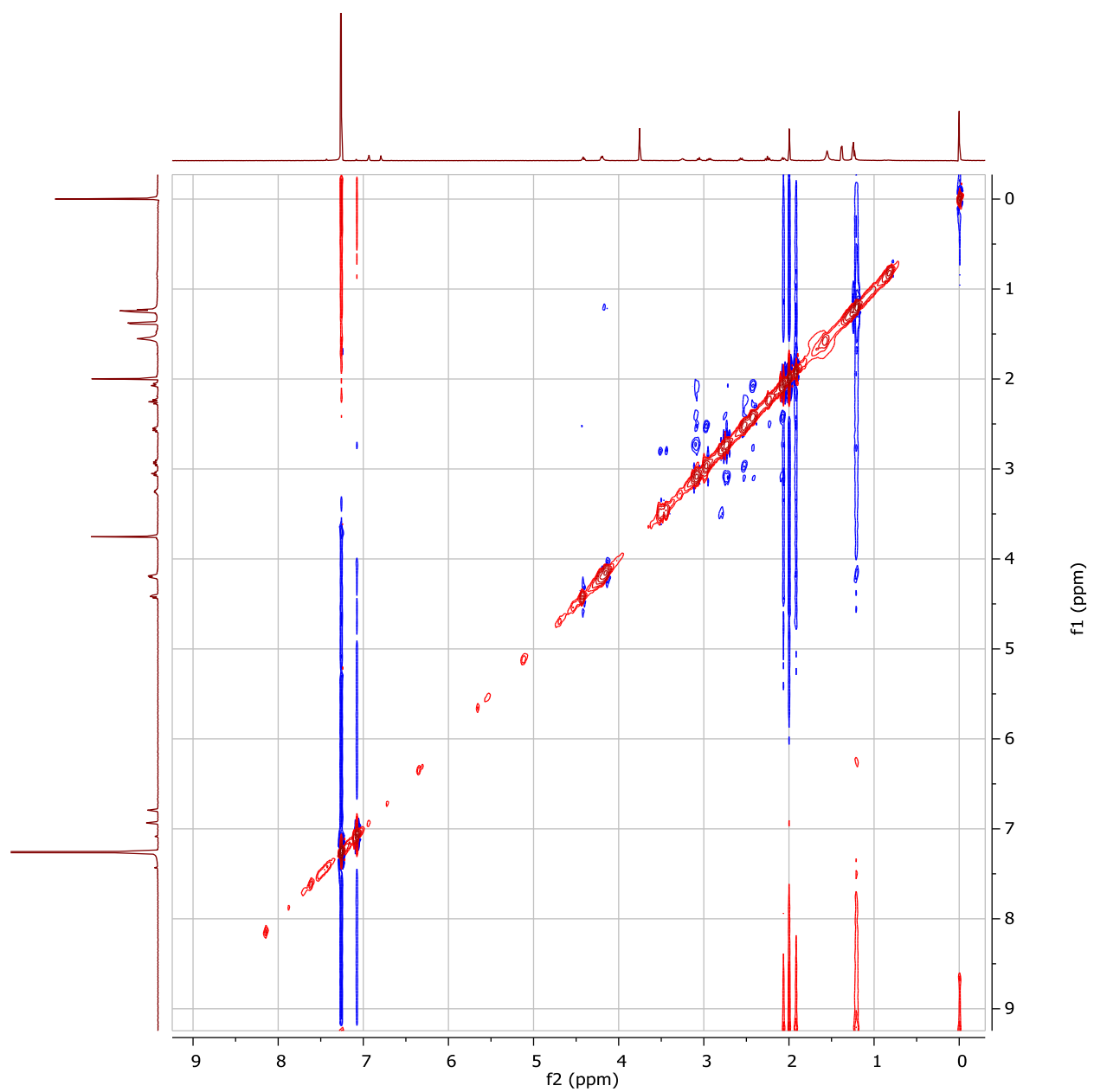




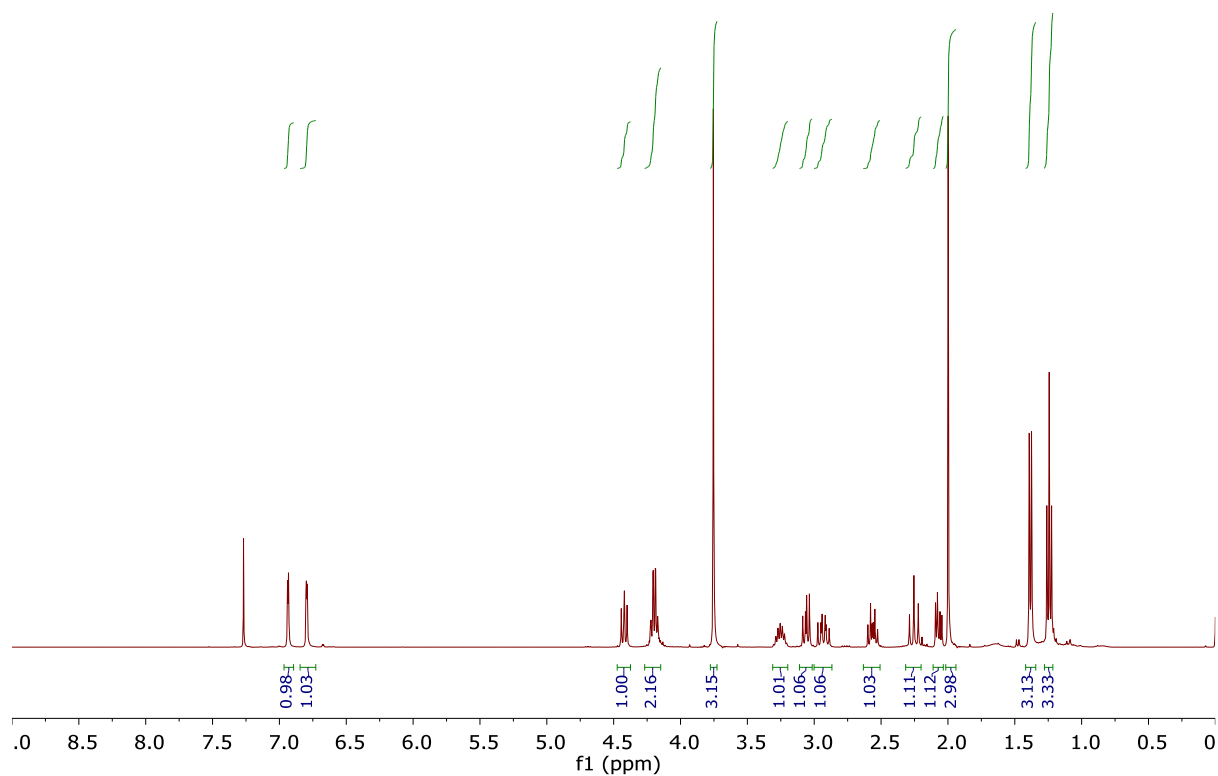
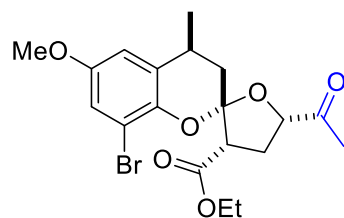


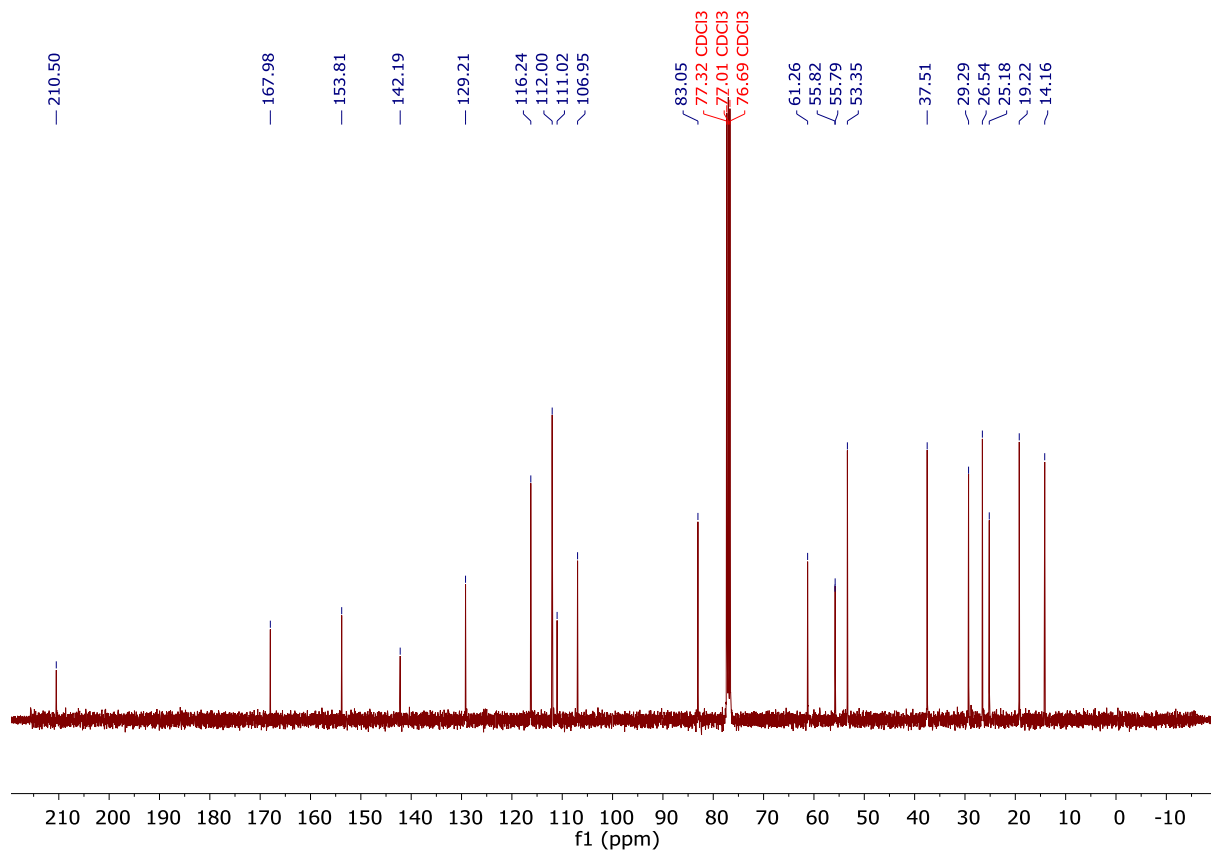


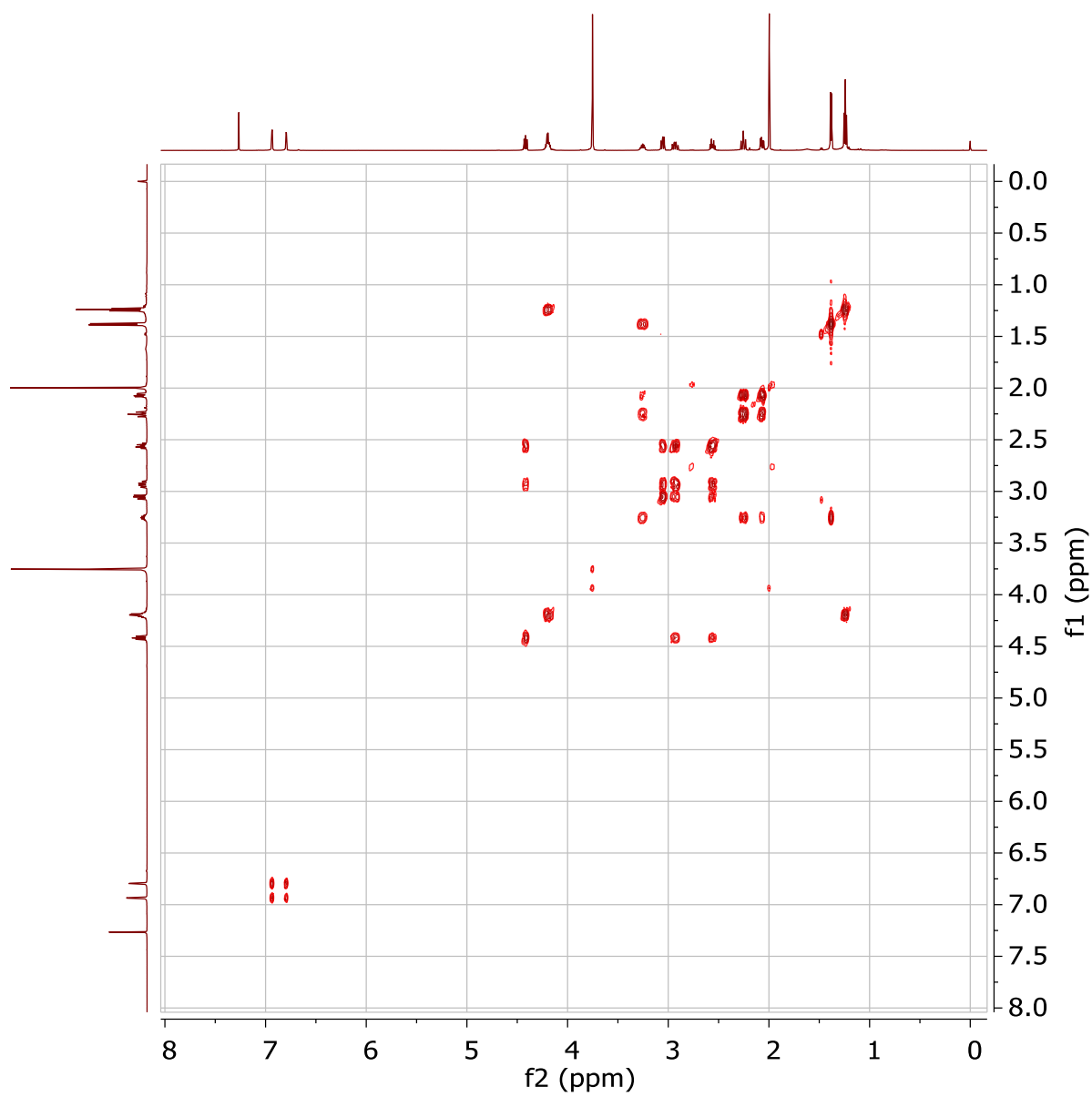


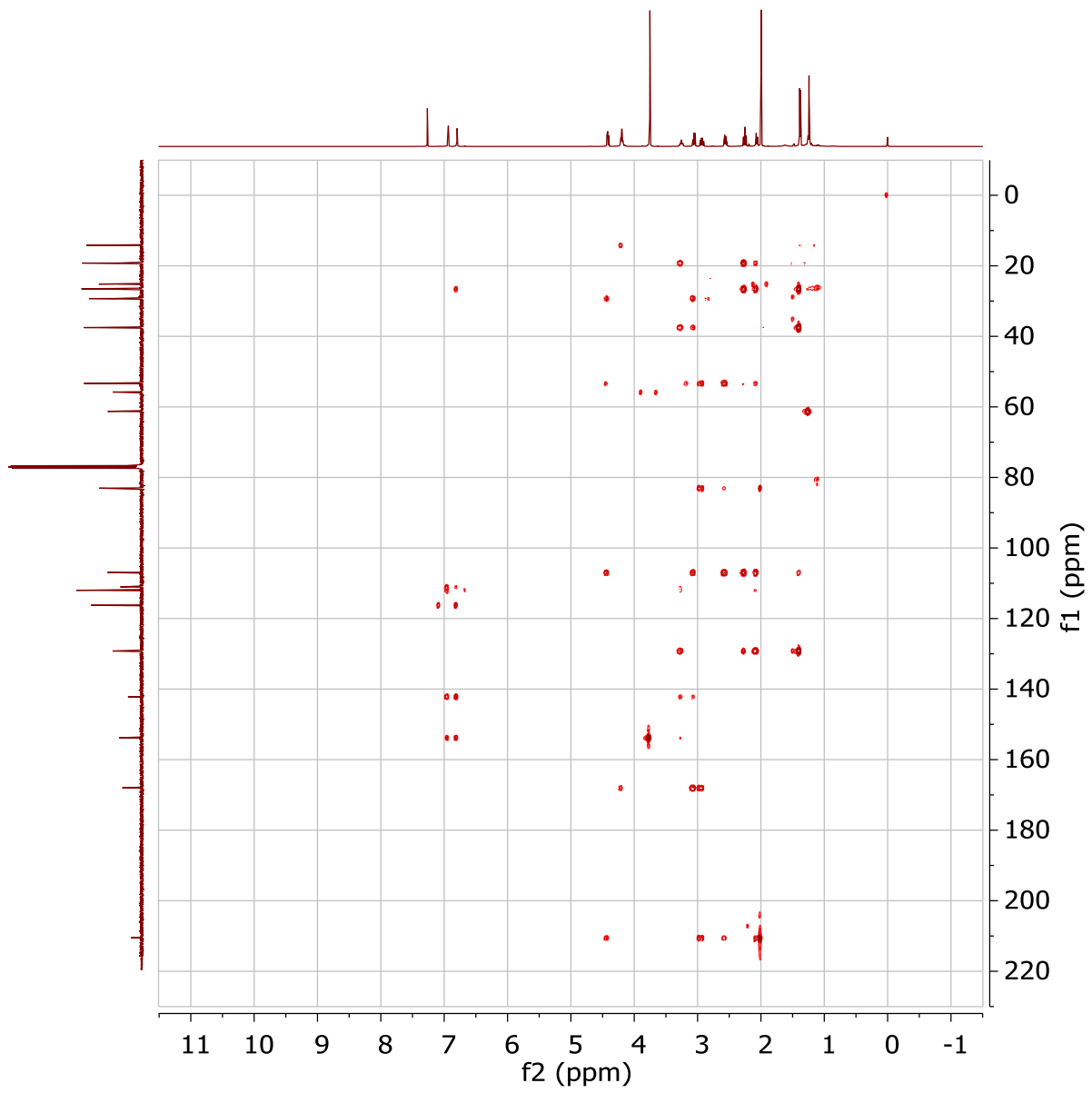


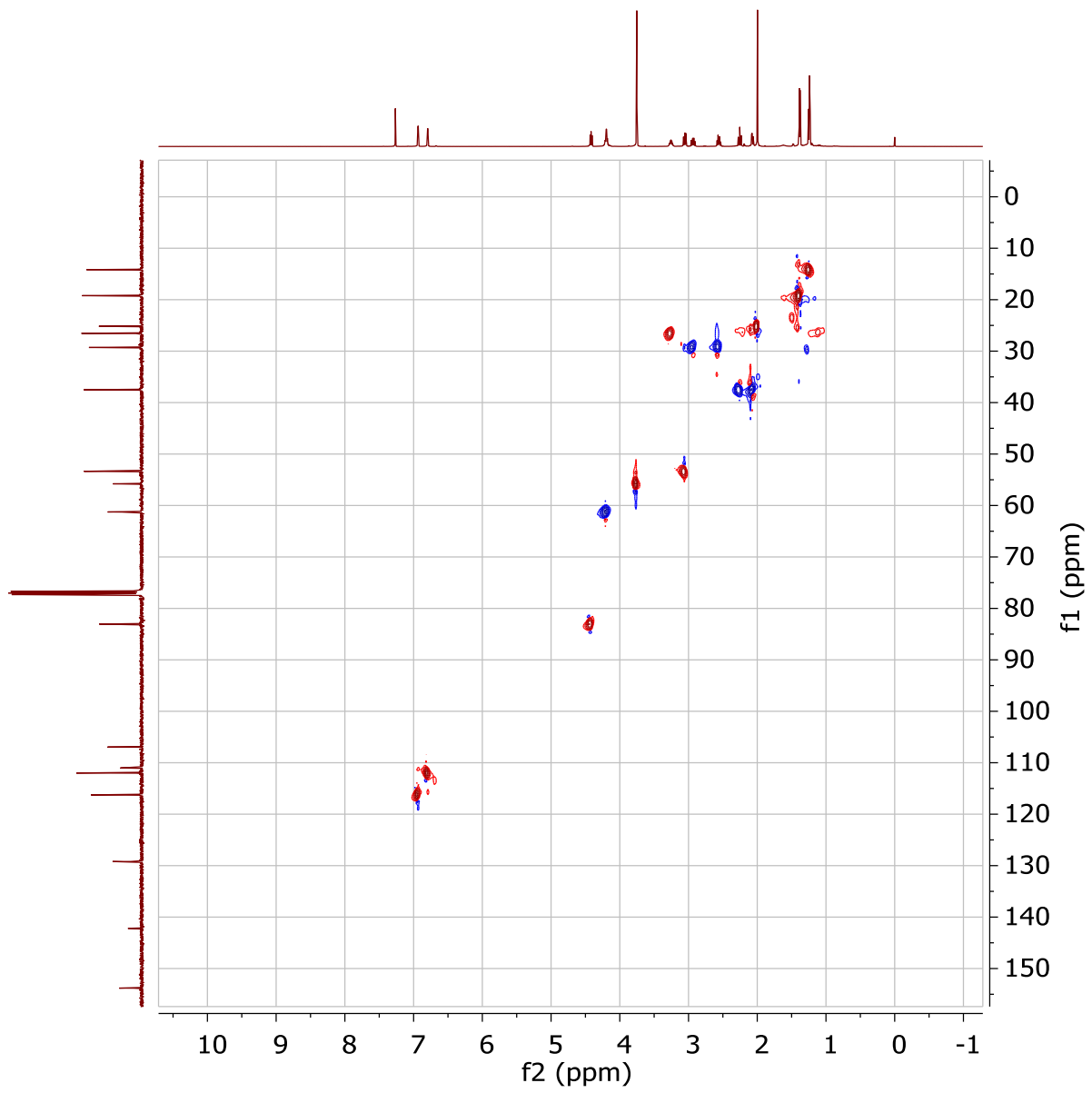
**Ethyl (2S,3'S,4S,5'S)-5'-acetyl-8-bromo-6-methoxy-4-methyl-4',5'-dihydro-3'H-spiro[chromane-2,2'-furan]-3'-carboxylate (18b):**  $^1\text{H}$  NMR (400 MHz,  $\text{CDCl}_3$ ),  $^{13}\text{C}\{^1\text{H}\}$  NMR (101 MHz, Chloroform-*d*). COSY, HMBC, HSQC, NOESY.

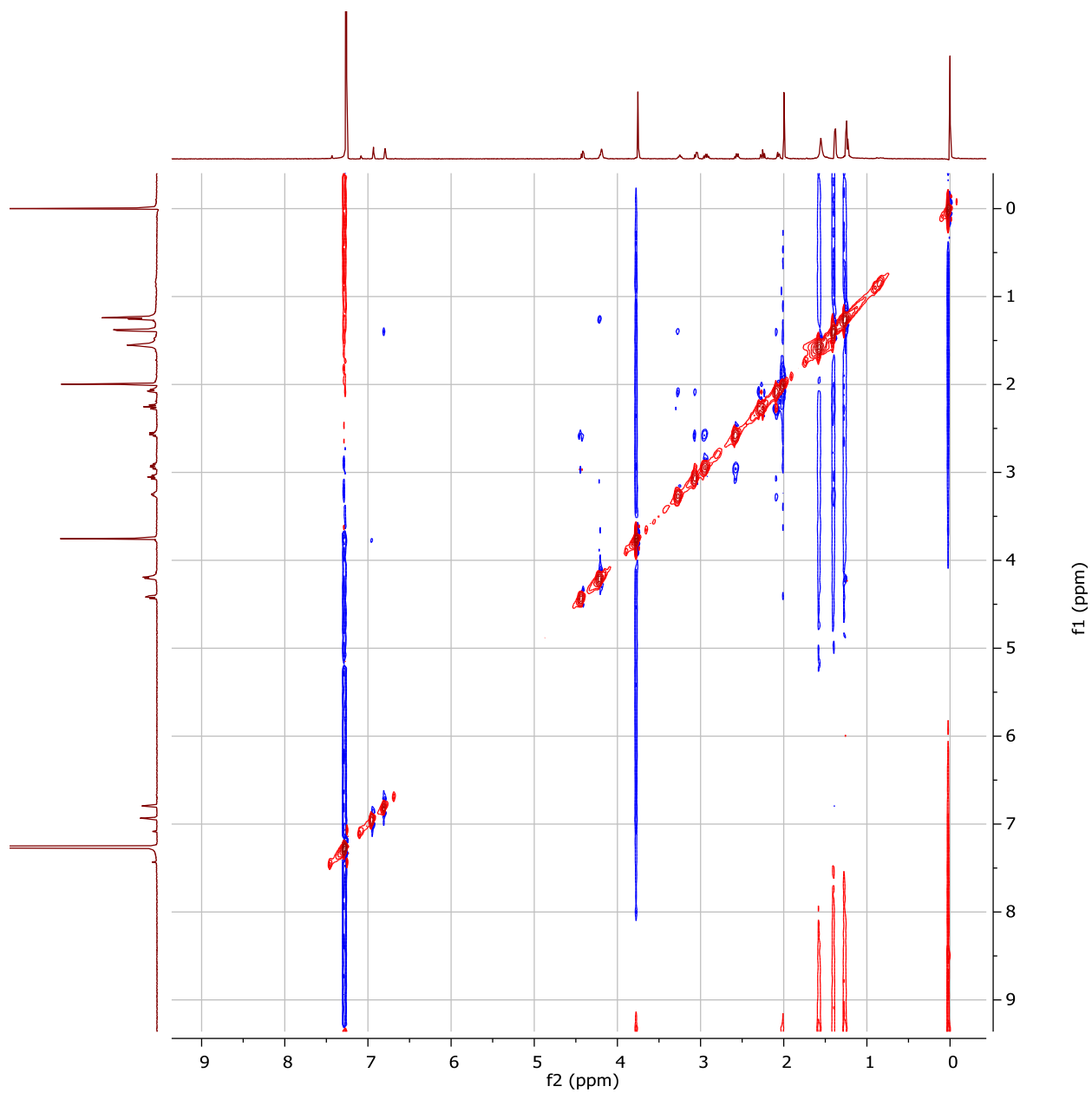




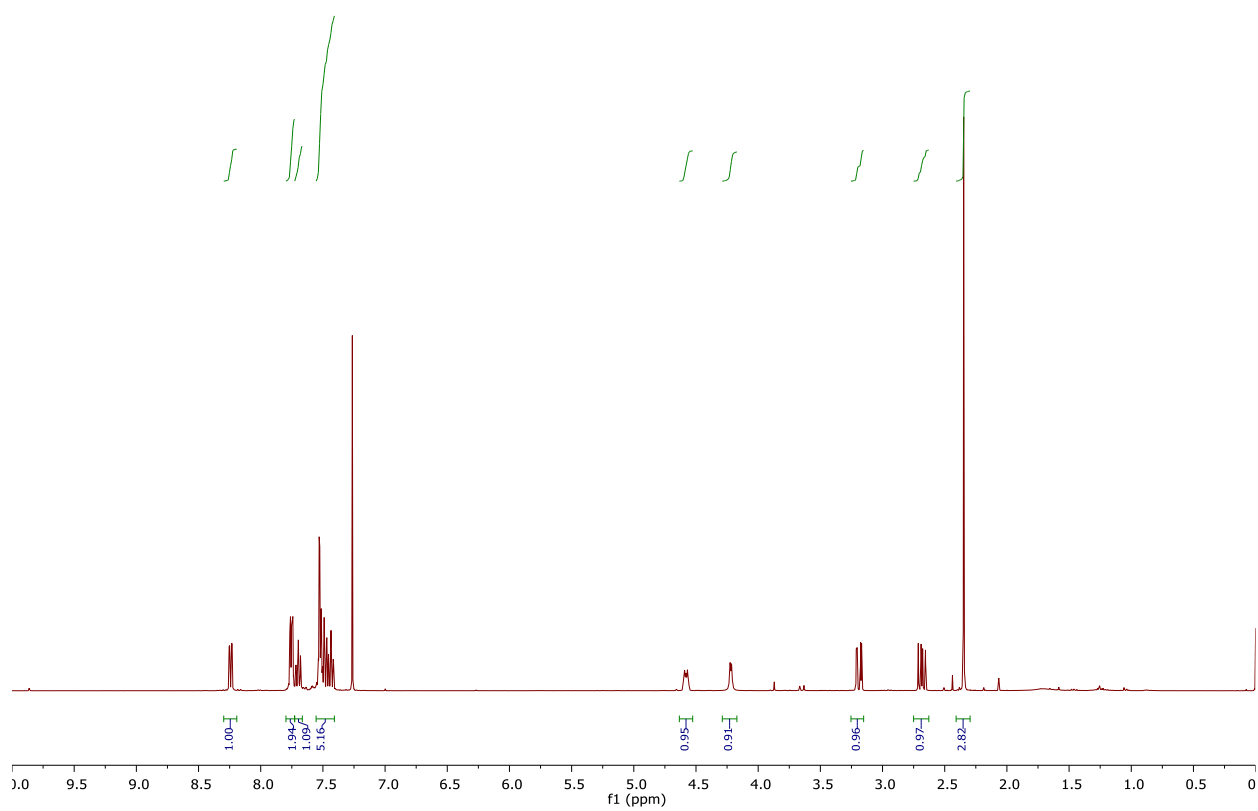
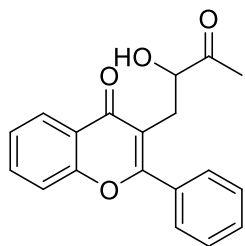


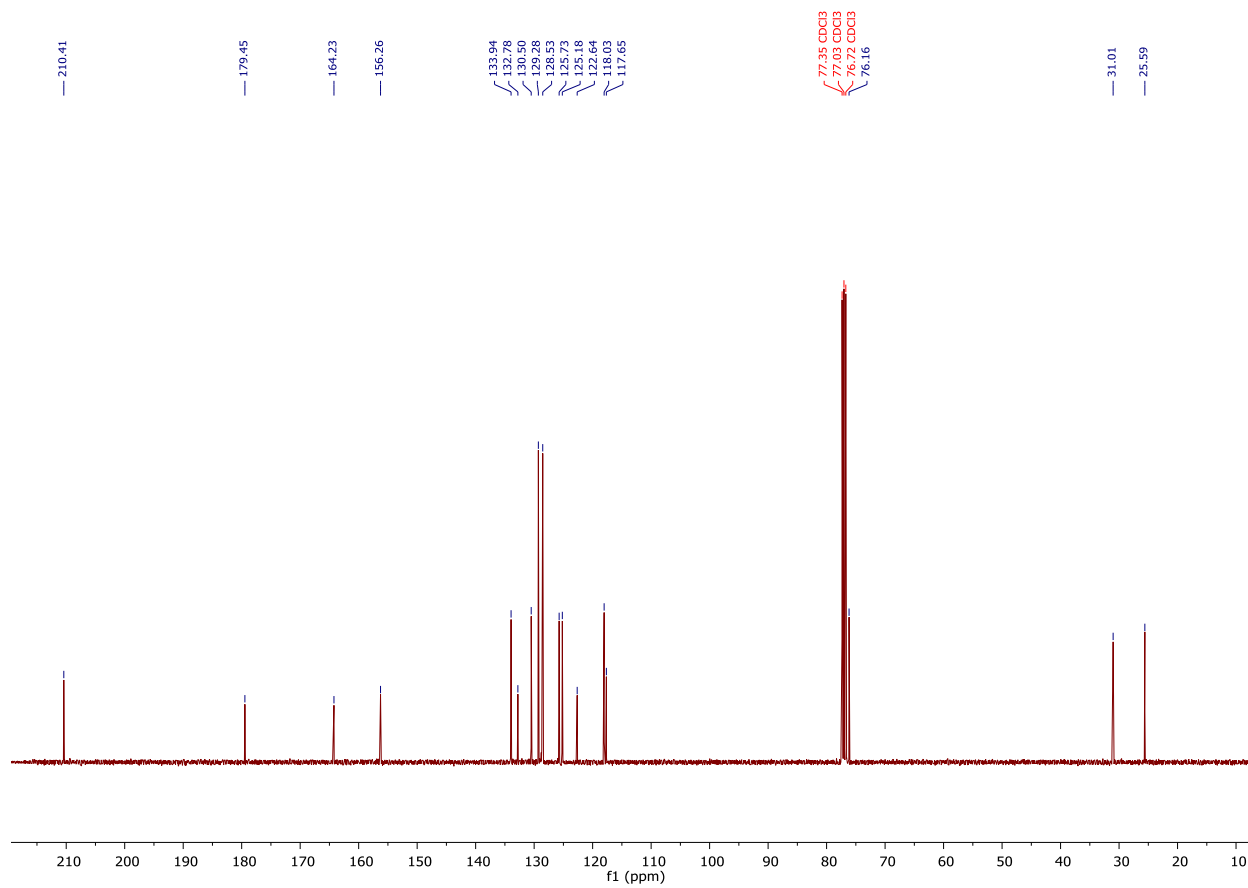


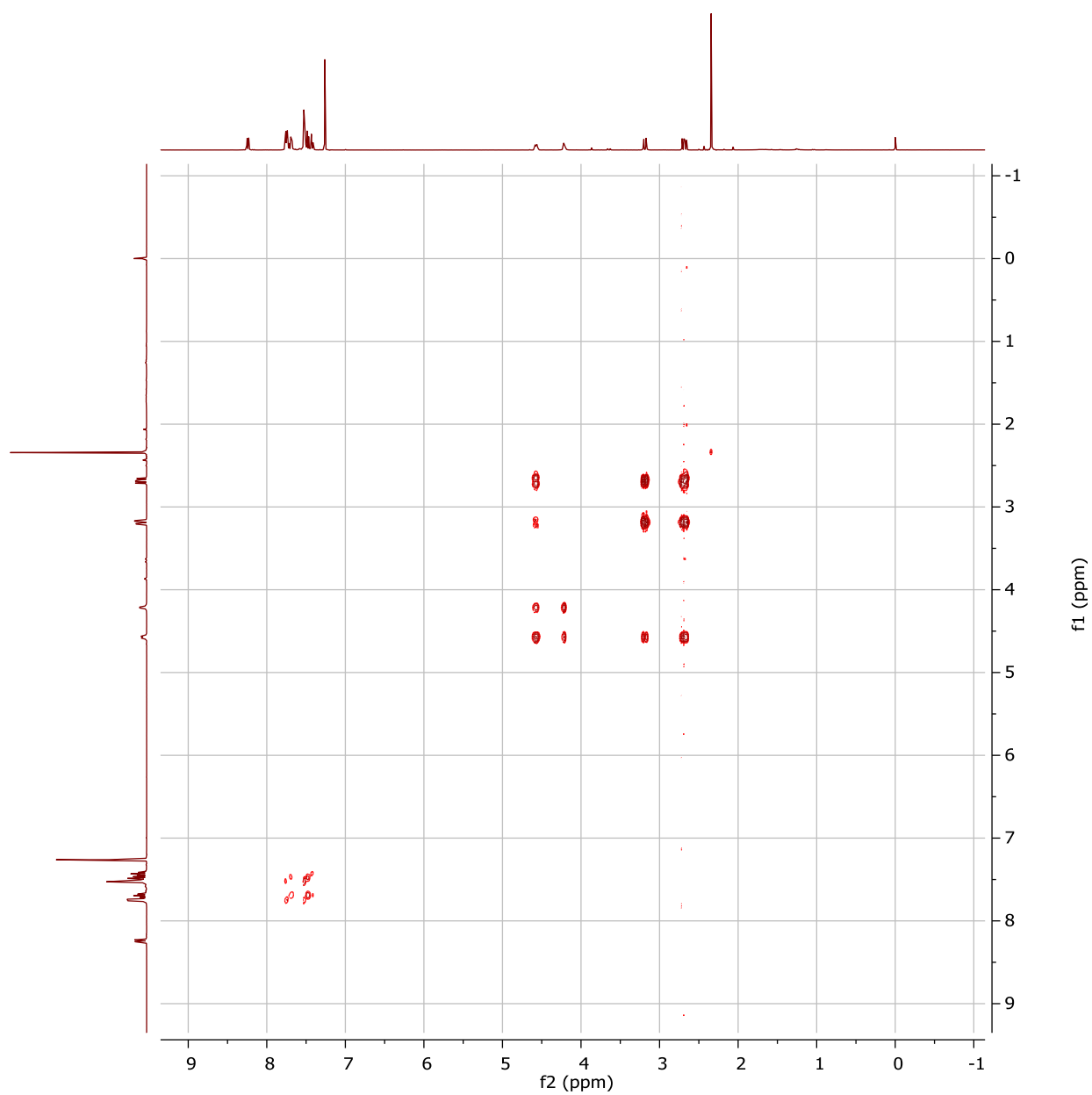


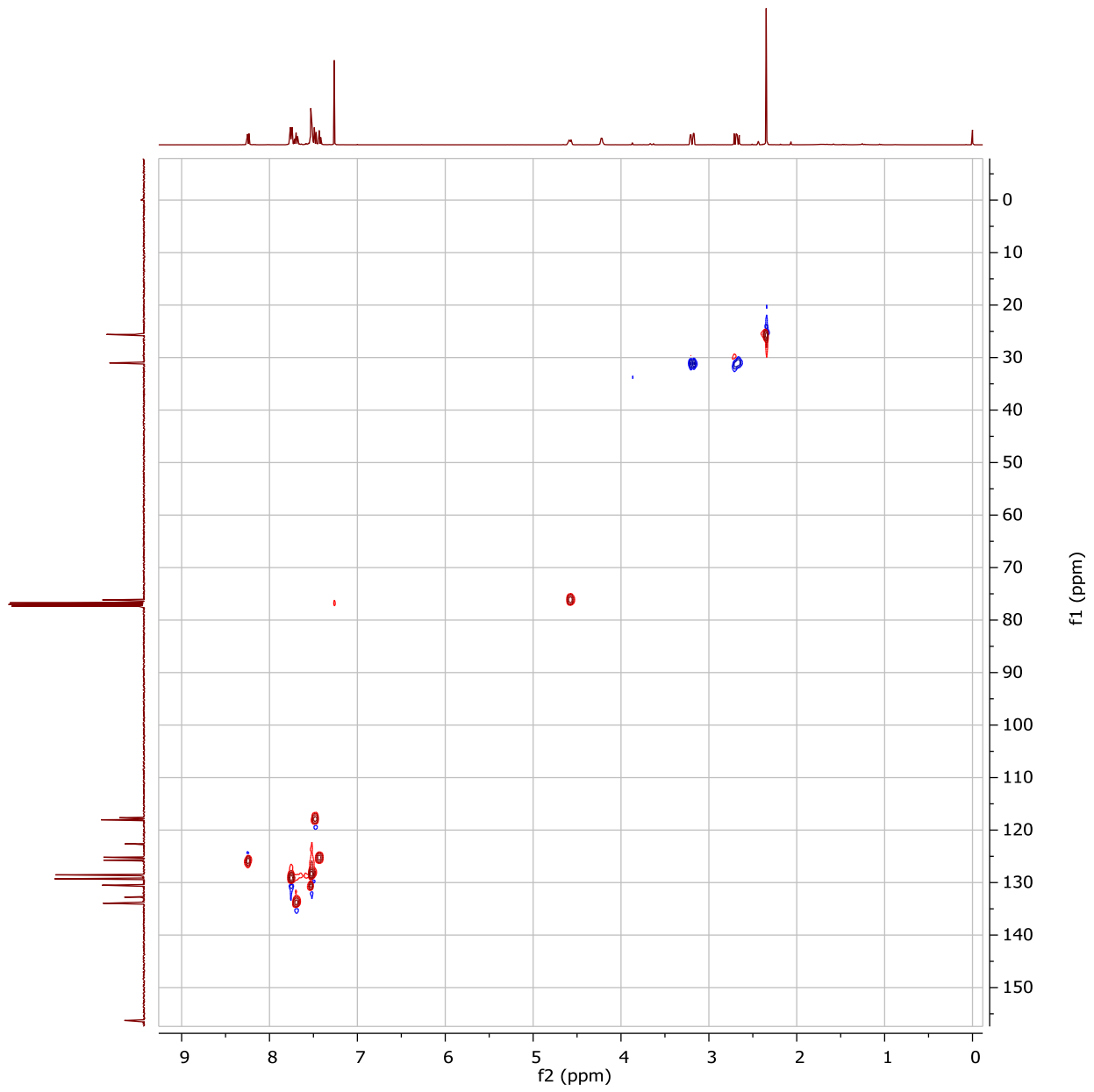


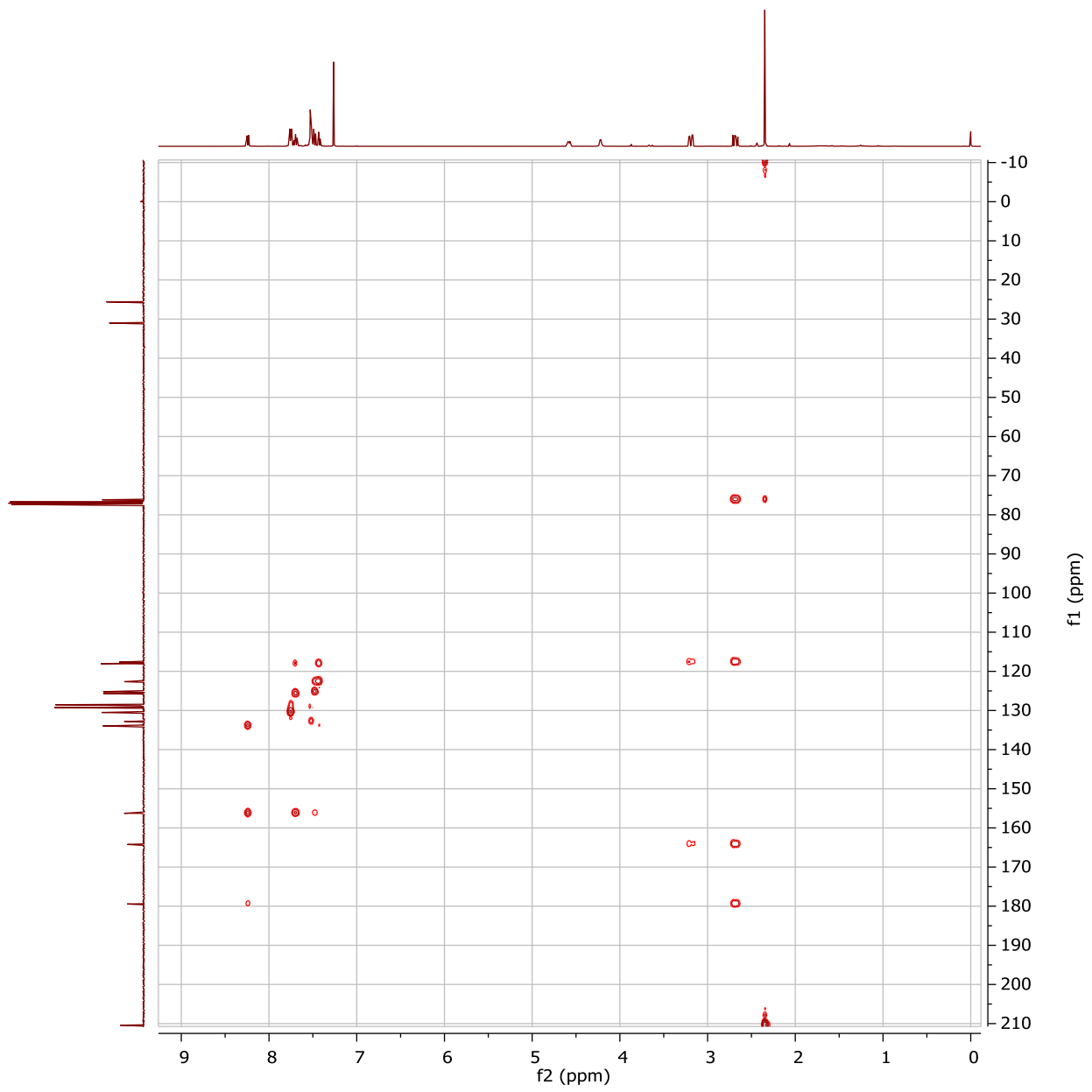
**3-(2-hydroxy-3-oxobutyl)-2-phenyl-4H-chromen-4-one (19b):**  $^1\text{H}$  NMR (400 MHz, Chloroform-*d*),  $^{13}\text{C}\{^1\text{H}\}$  NMR (101 MHz, Chloroform-*d*). COSY, HSQC, HMBC.



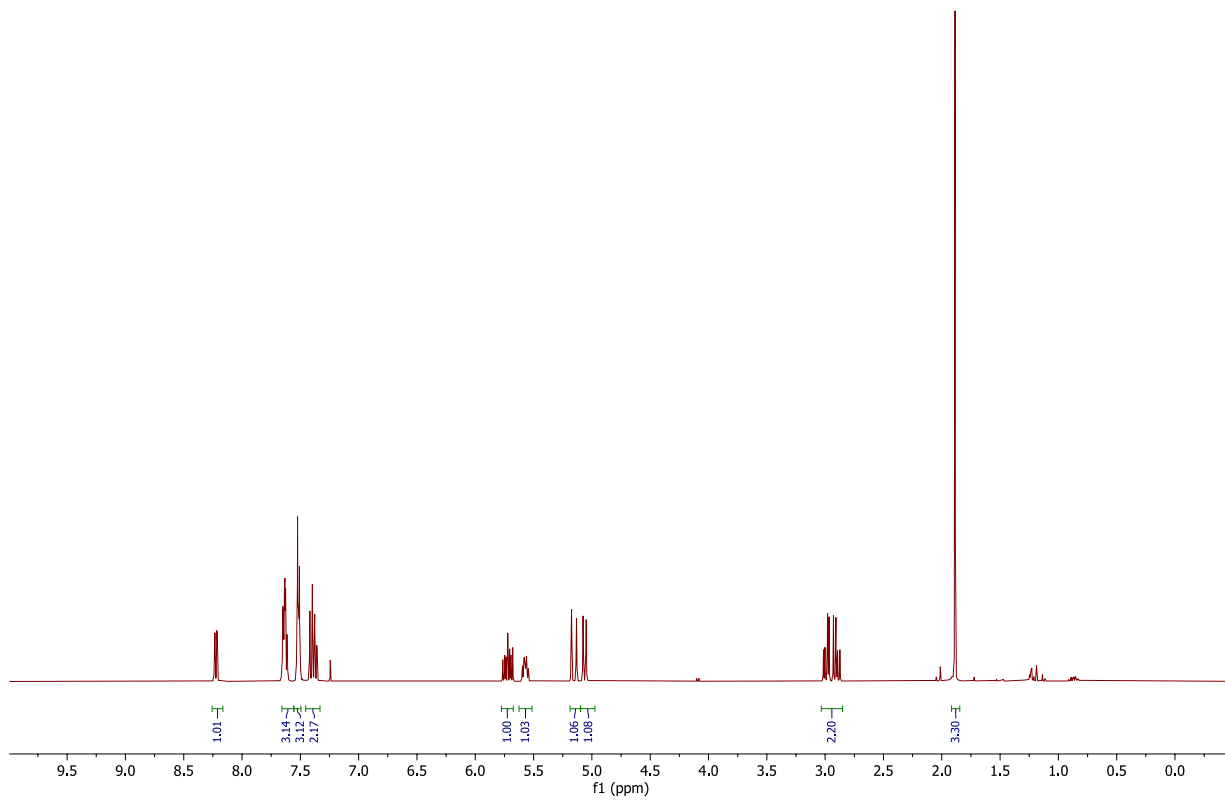
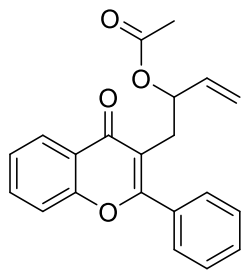


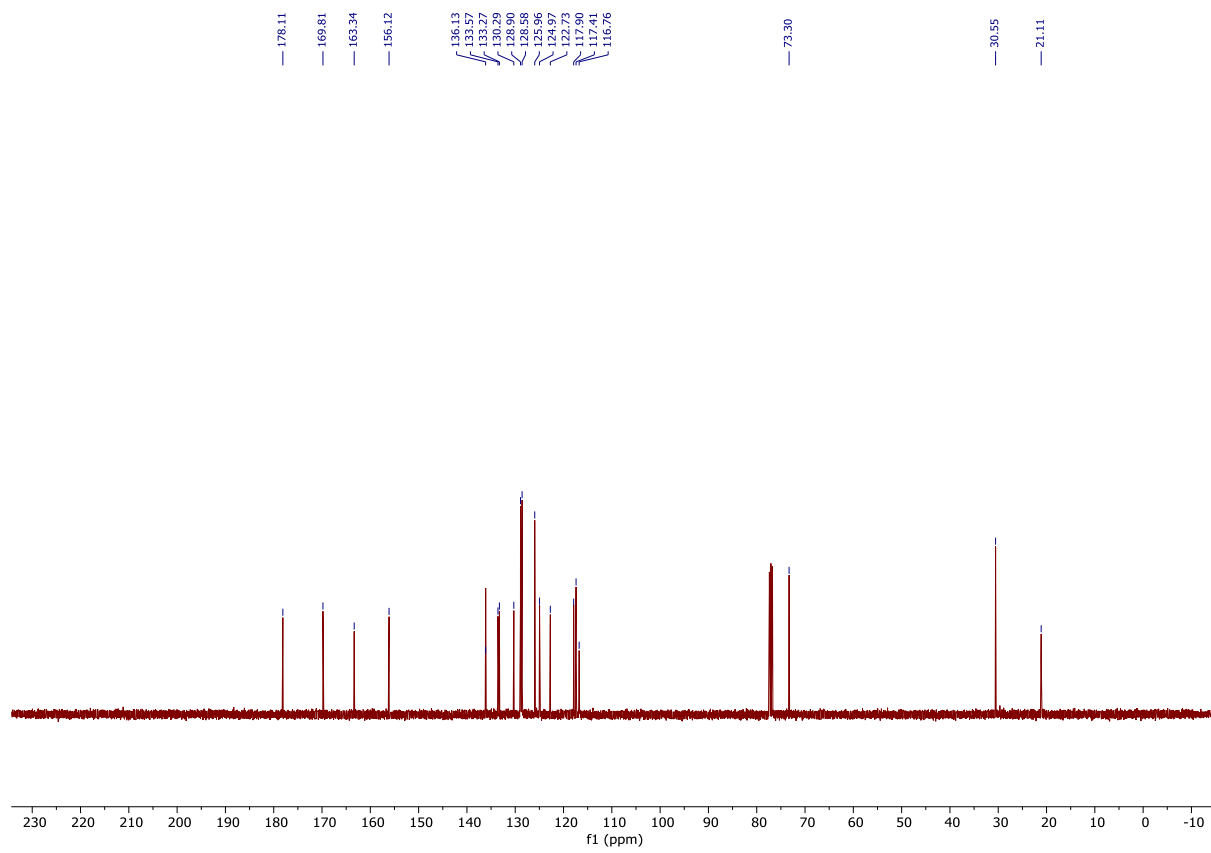




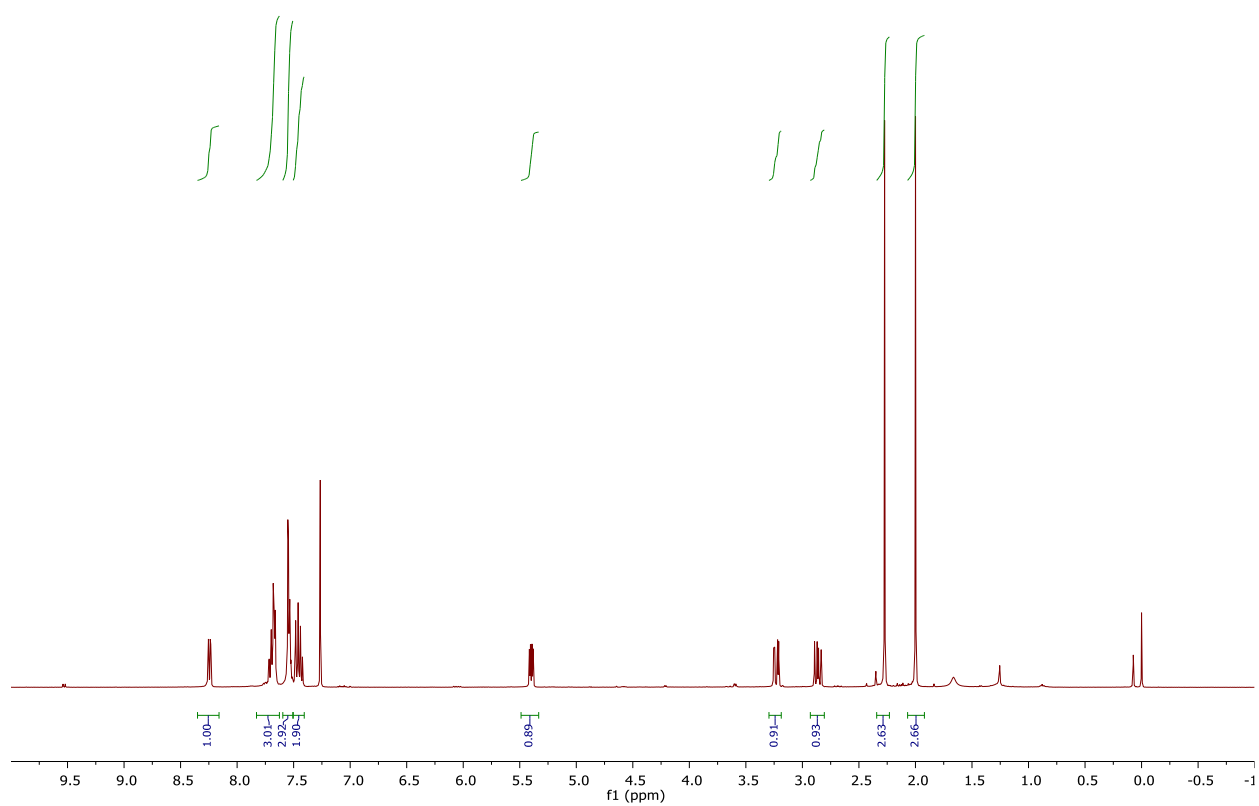
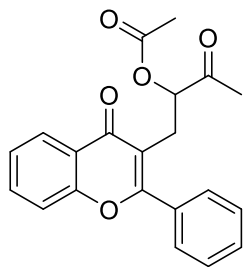


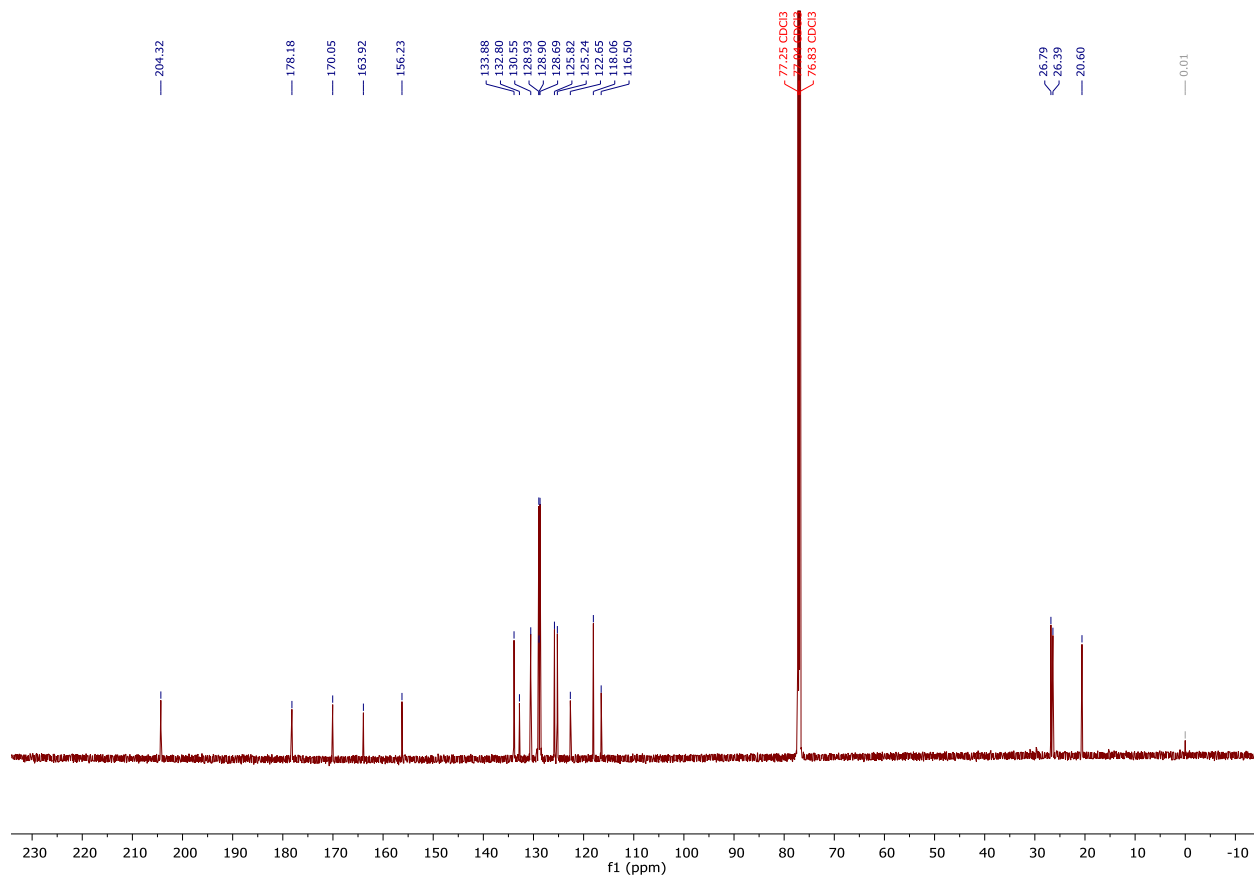
**1-(4-oxo-2-phenyl-4H-chromen-3-yl)but-3-en-2-yl acetate (20a):**  $^1\text{H}$  NMR (400 MHz, Chloroform-*d*),  $^{13}\text{C}\{^1\text{H}\}$  NMR (100 MHz, Chloroform-*d*).

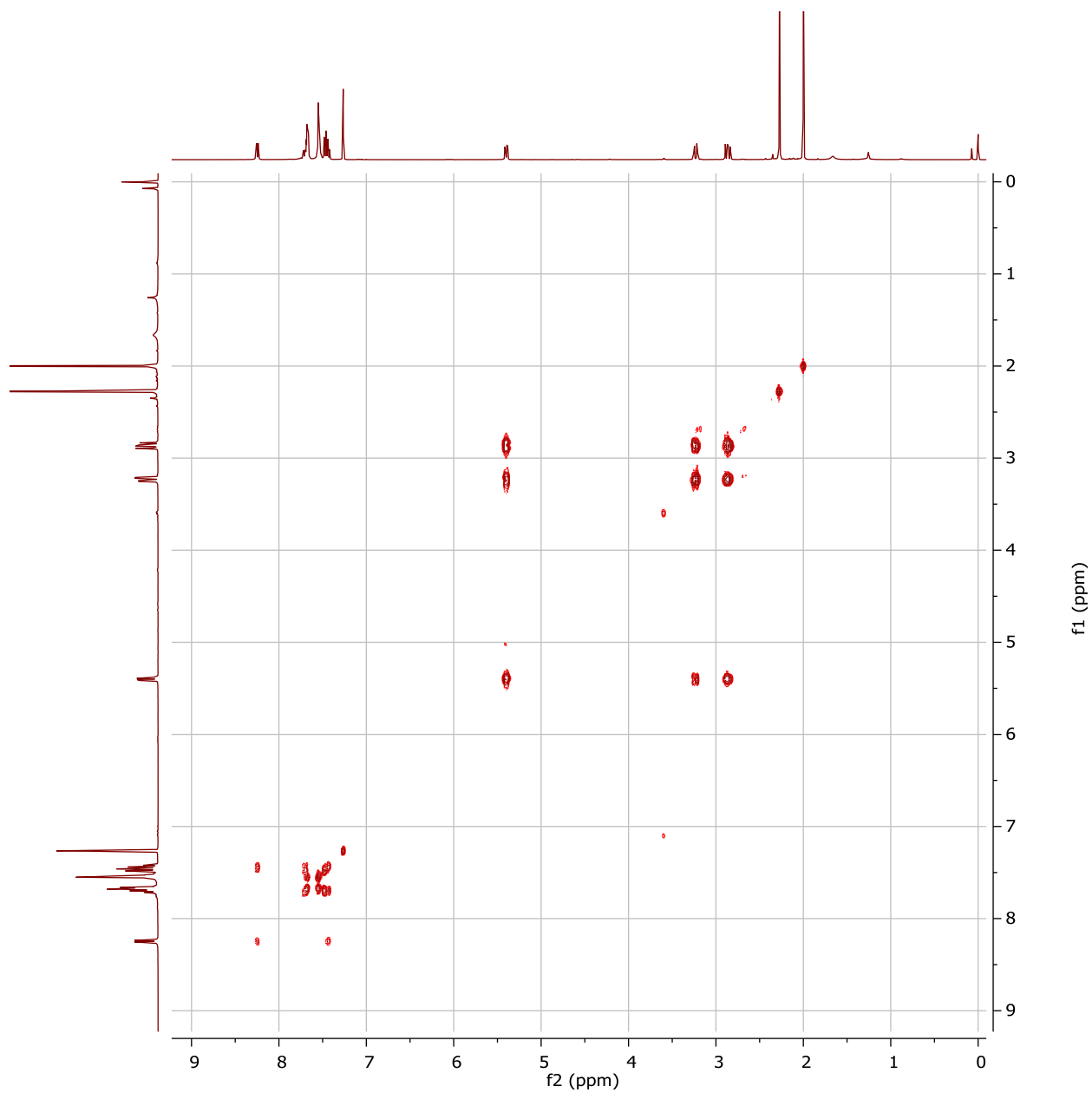


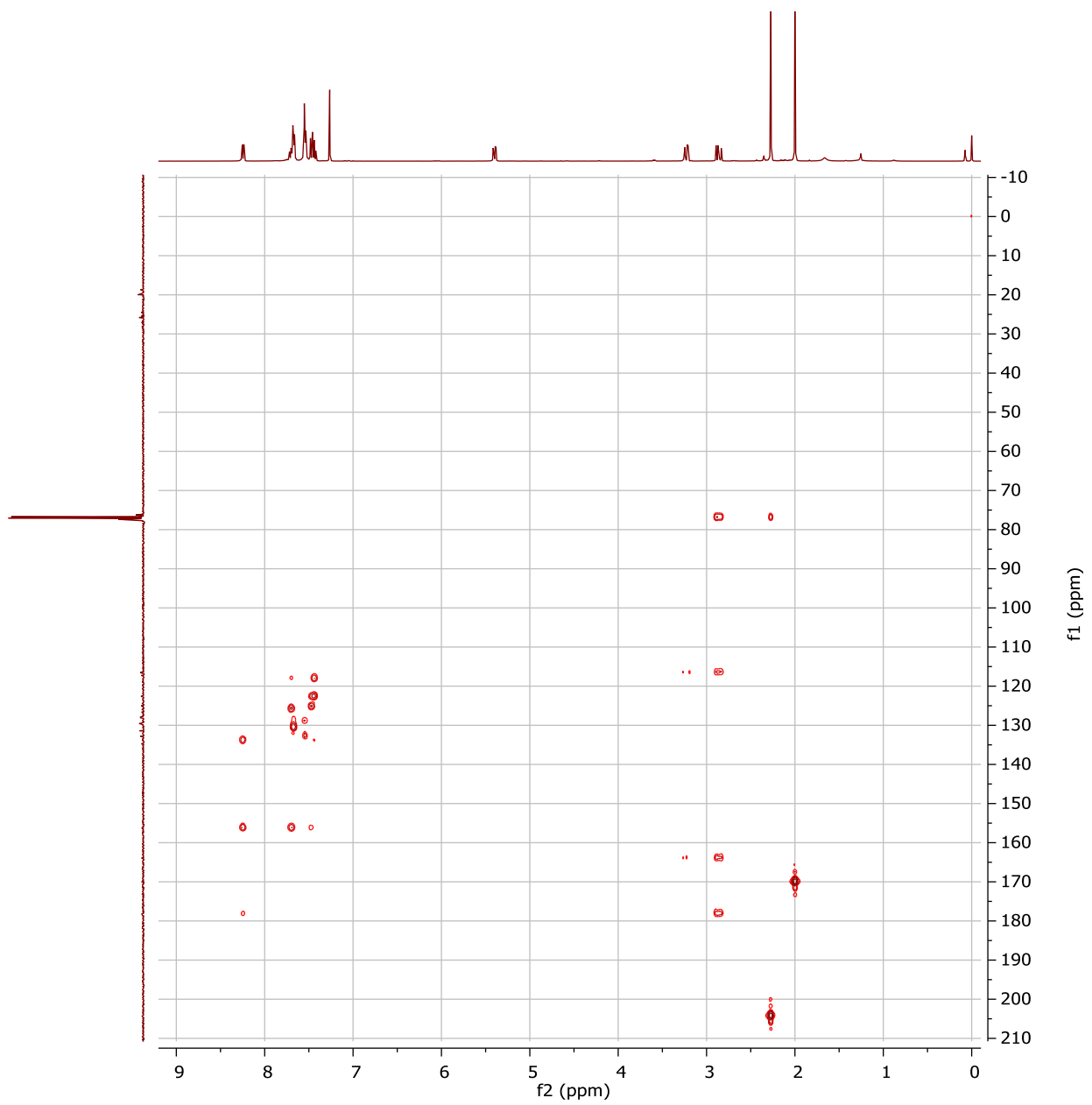


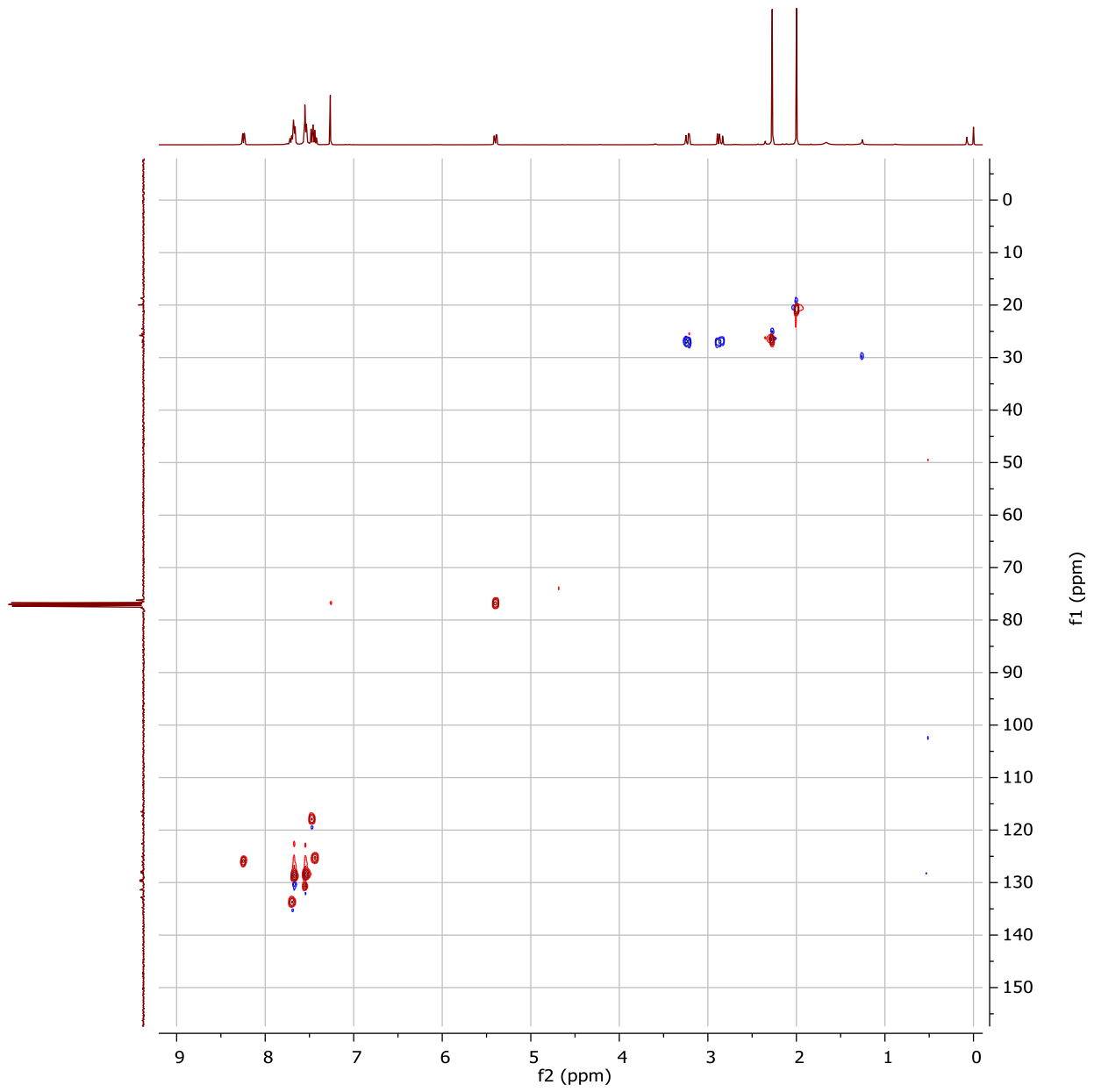
**3-oxo-1-(4-oxo-2-phenyl-4H-chromen-3-yl)butan-2-yl acetate (20b):**  $^1\text{H}$  NMR (400 MHz, Chloroform-*d*).  $^{13}\text{C}\{^1\text{H}\}$  NMR (101 MHz, Chloroform-*d*). COSY, HMBC, HSQC.



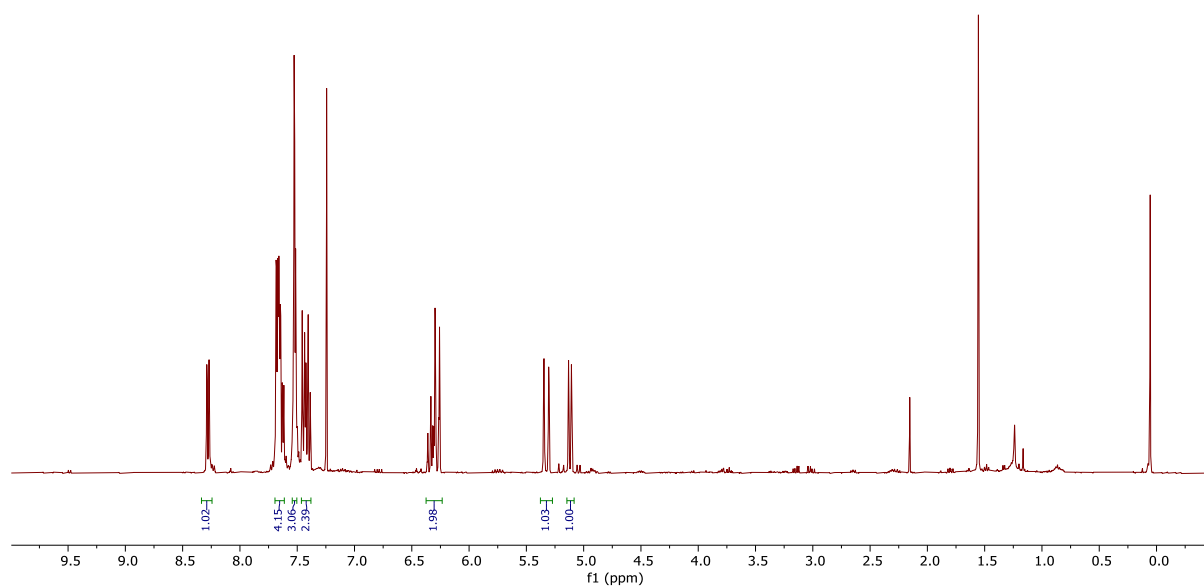
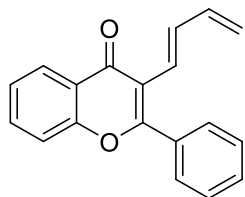


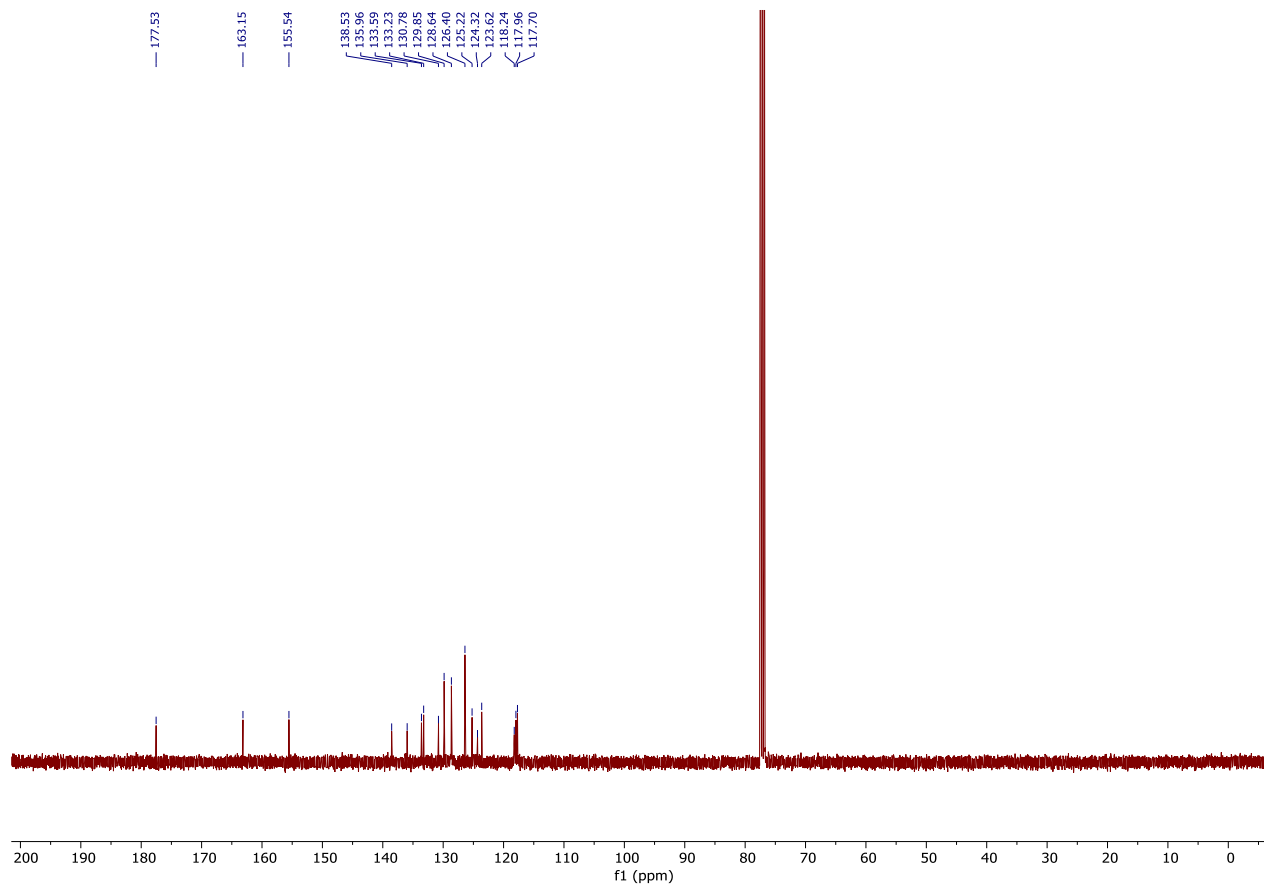




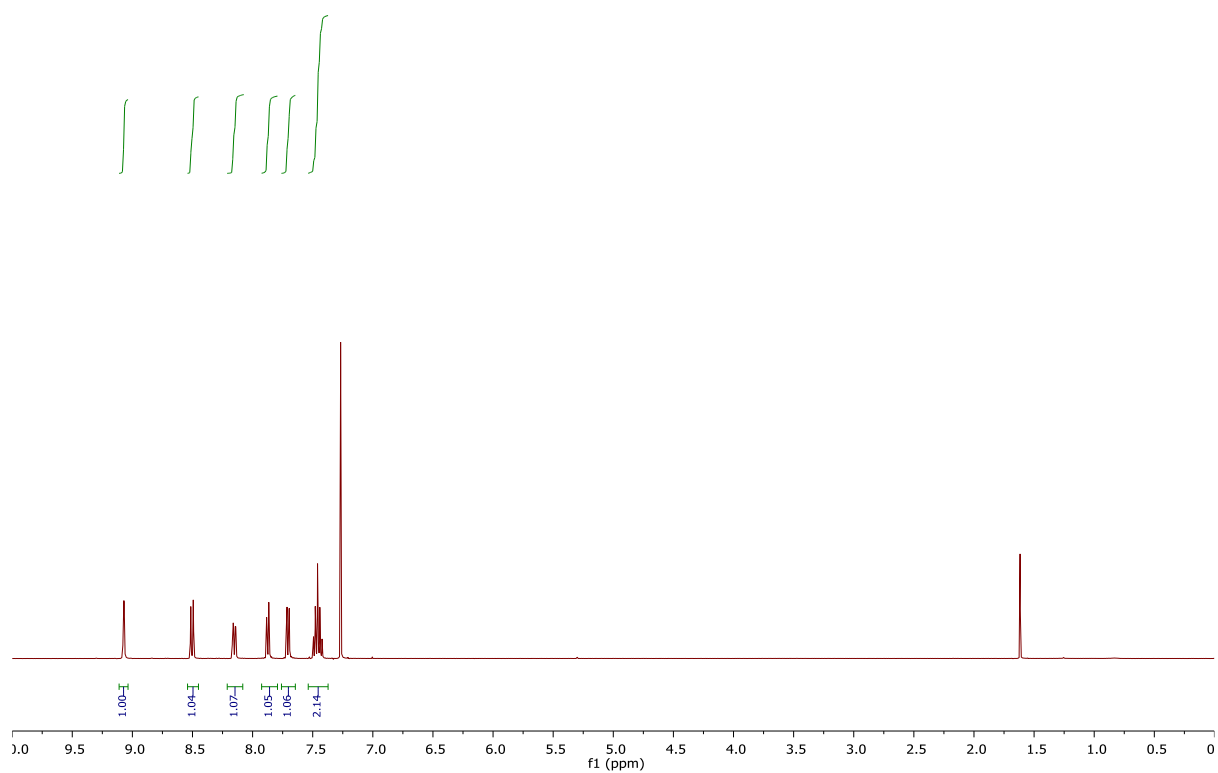
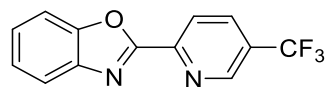


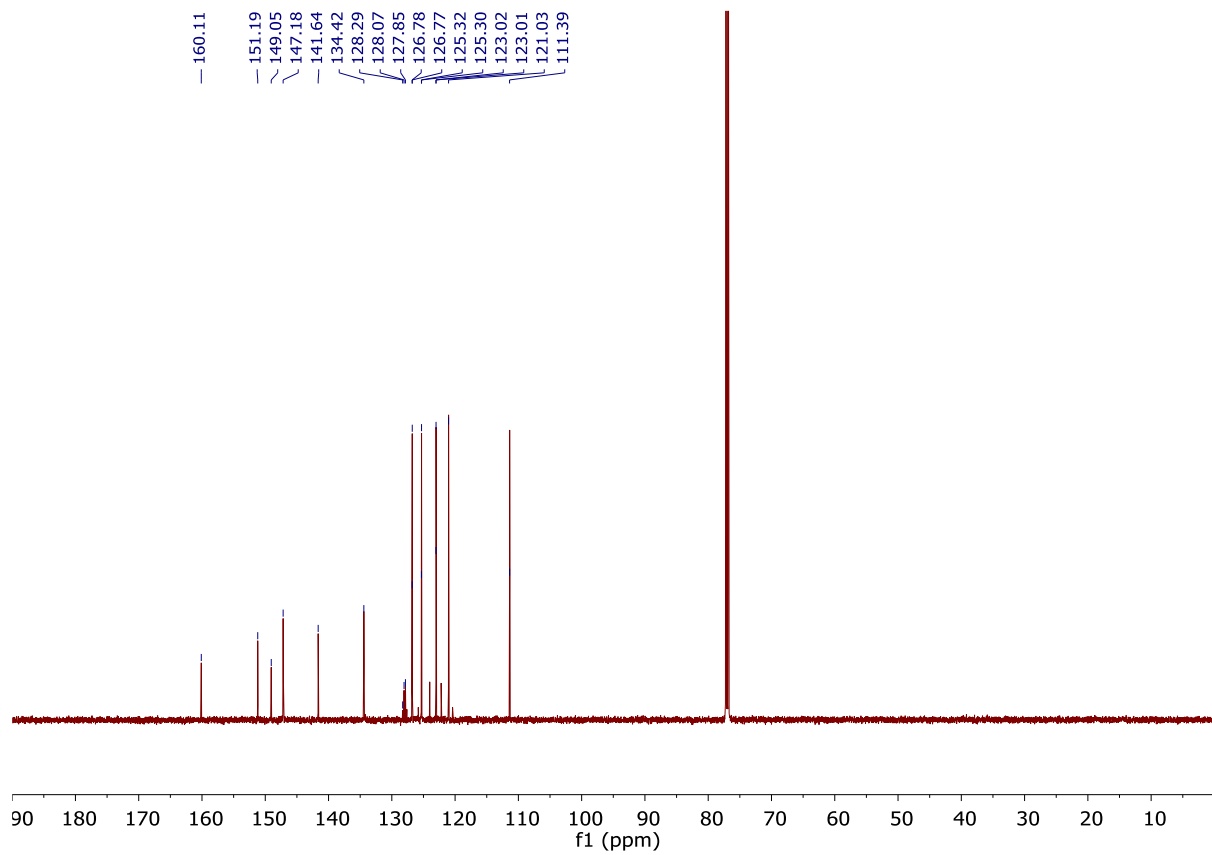
**(E)-3-(buta-1,3-dien-1-yl)-2-phenyl-4H-chromen-4-one (23a):**  $^1\text{H}$  NMR (400 MHz, Chloroform-*d*),  $^{13}\text{C}\{^1\text{H}\}$  NMR (100 MHz, Chloroform-*d*).

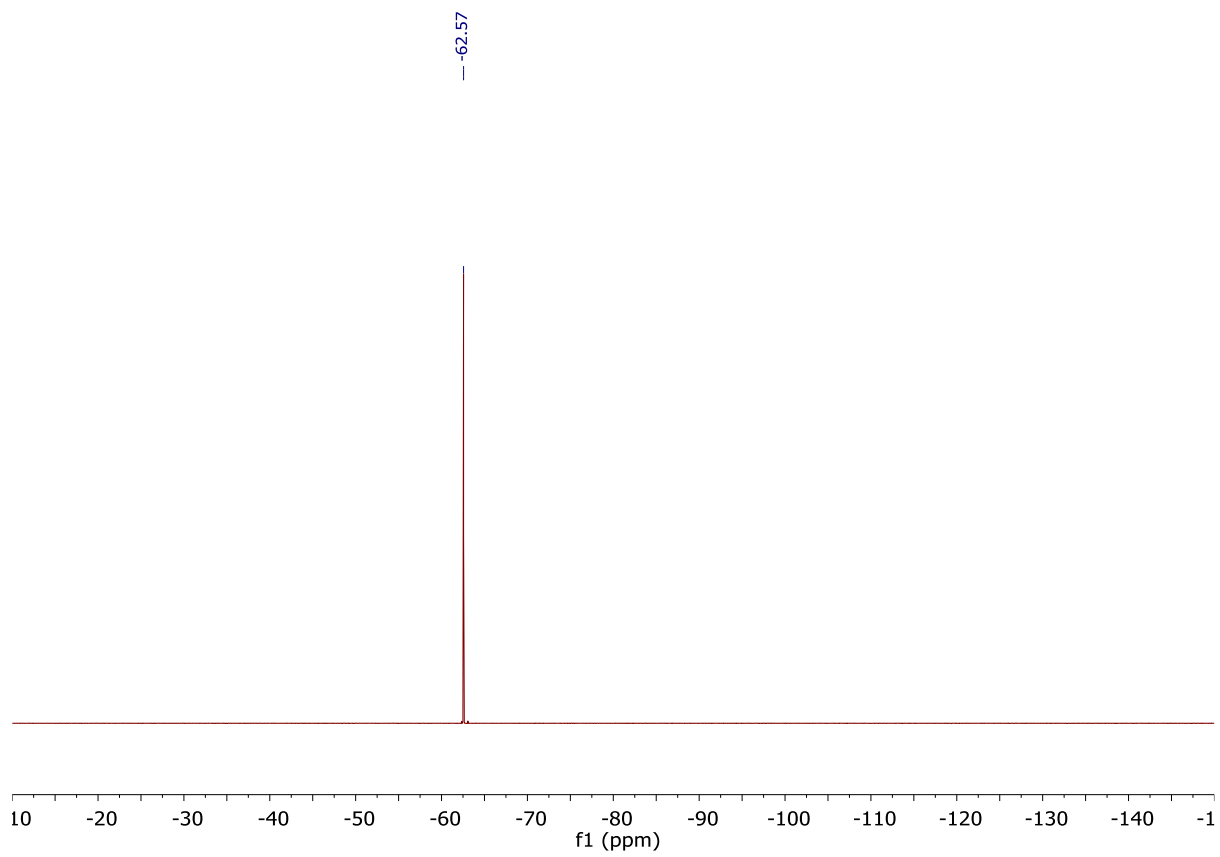




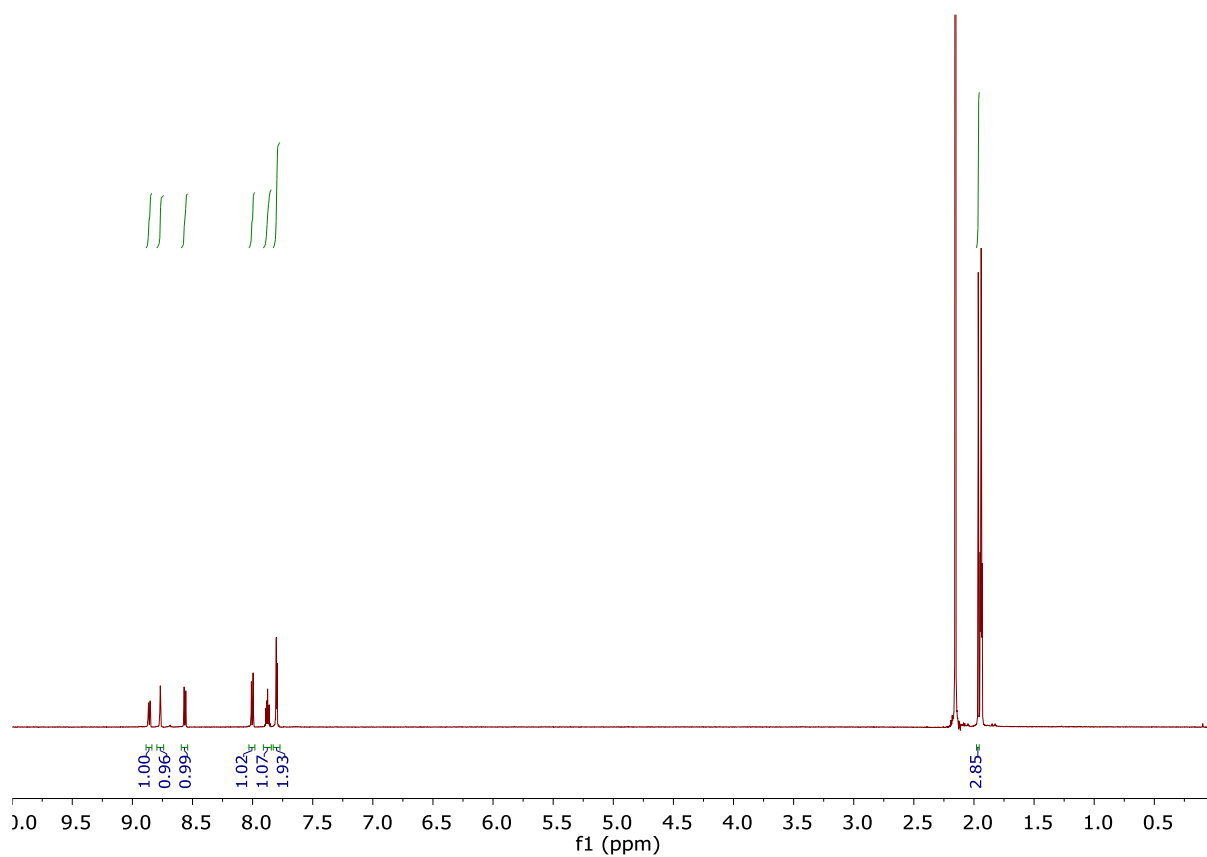
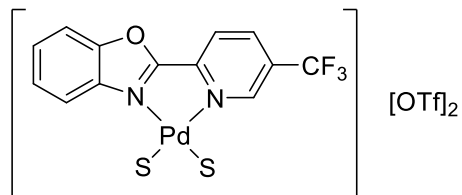
**2-(5-(trifluoromethyl)pyridin-2-yl)benzo[d]oxazole (5-CF<sub>3</sub>(PBO))**: <sup>1</sup>H NMR (400 MHz, CDCl<sub>3</sub>), <sup>13</sup>C{H} NMR (101 MHz, Chloroform-*d*) and <sup>19</sup>F{H} NMR (376 MHz, Chloroform-*d*).

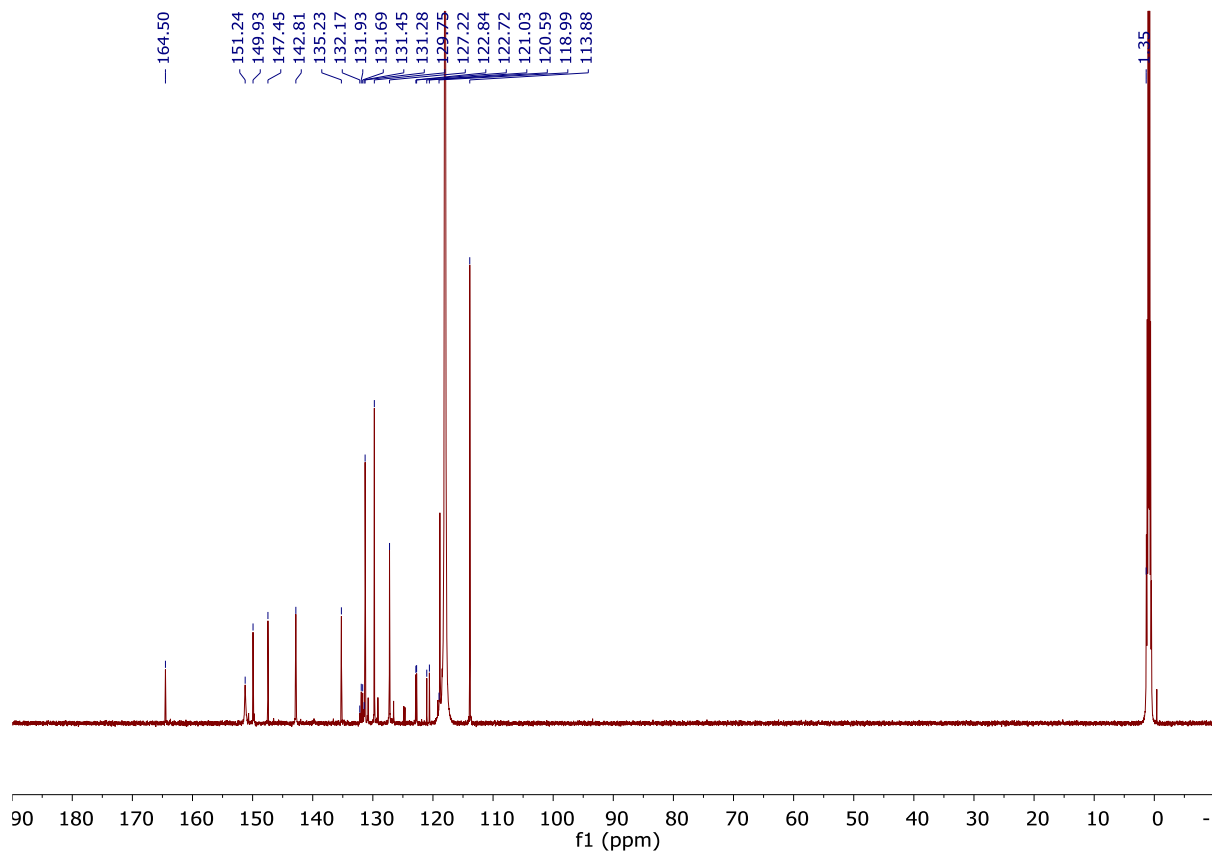


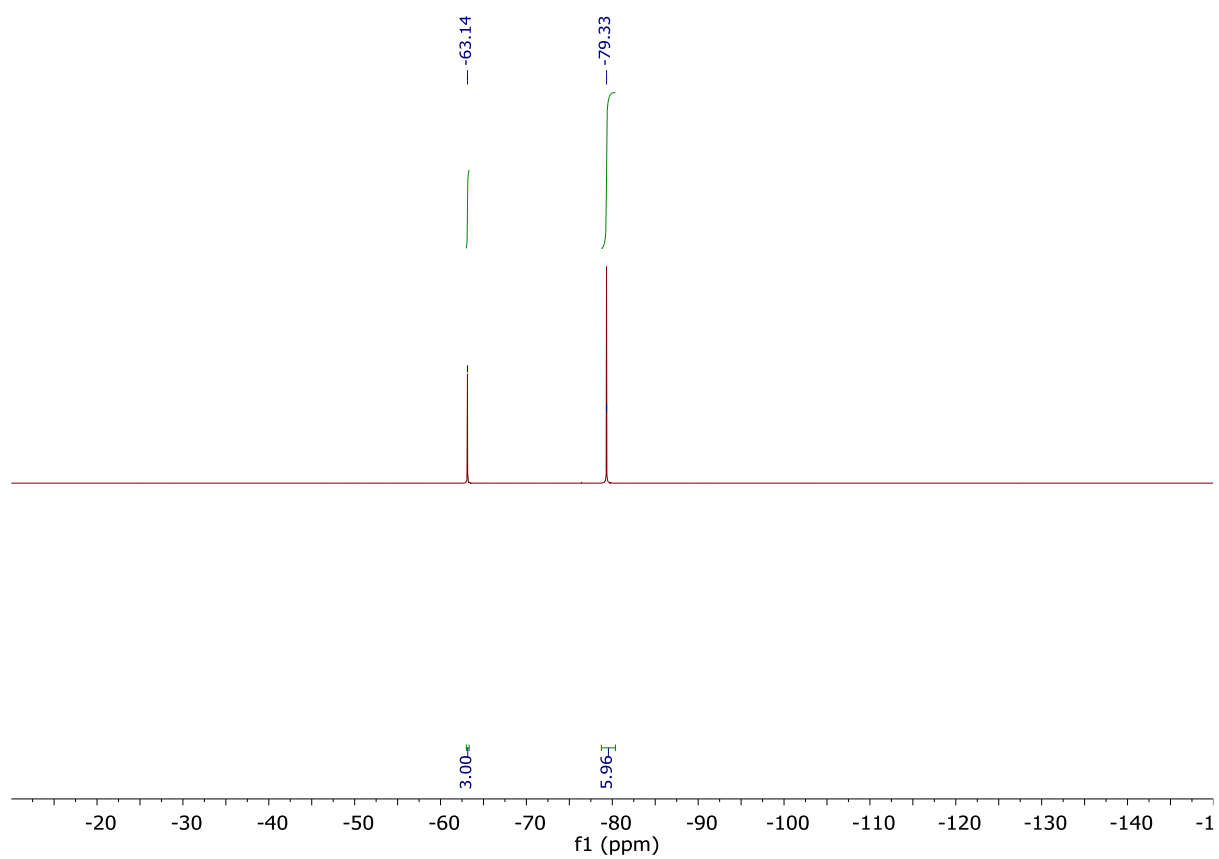




**[Pd(5-CF<sub>3</sub>-PBO)(S)<sub>2</sub>][OTf]<sub>2</sub>**: <sup>1</sup>H NMR (600 MHz, Acetonitrile-*d*<sub>3</sub>) <sup>13</sup>C{H} NMR (151 MHz, Acetonitrile-*d*<sub>3</sub>), <sup>19</sup>F{H} NMR (376 MHz, Acetonitrile-*d*<sub>3</sub>).







## 6 References

1. M. N. Blair, M. Murray-Williams, C. Maguire, C. L. Brown, Q. Cao, H. Chai, Y. Li, R. L. O'Hagan, P. Dingwall, P. Manesiotis, C. L. Lyall, J. P. Lowe, U. Hintermair, P. C. Knipe and M. J. Muldoon, *Catal. Sci. Technol.*, 2023, **13**, 6224-6232.
2. S. Tamura, Y. Shimoyama, D. Hong and Y. Kon, *Mol. Catal.*, 2020, **496**, 111178.
3. B. W. Michel, A. M. Camelio, C. N. Cornell and M. S. Sigman, *J. Am. Chem. Soc.*, 2009, **131**, 6076-6077.
4. X. Xia, X. Gao, J. Xu, C. Hu and X. Peng, *Synlett*, 2017, **28**, 607-610.
5. S. Saha, S. Yadav, N. U. D. Reshi, I. Dutta, S. Kunnikuruvaan and J. K. Bera, *ACS Catal.*, 2020, **10**, 11385-11393.
6. R. J. Smith and B. C. Hawkins, *Eur. J. Org. Chem.*, 2019, **2019**, 6847-6854.
7. R. Andrezzi, V. Caprio, S. Crescitelli and G. Russo, *J. Hazard. Mater.*, 1988, **17**, 305-313.
8. Y.-W. Wang and C.-M. Shu, *Ind. Eng. Chem. Res.*, 2010, **49**, 8959-8968.
9. Y.-W. Wang, *Ind. Eng. Chem. Res.*, 2012, **51**, 7845-7852.
10. T. Willms, H. Kryk, J. Oertel, C. Hempel, F. Knitt and U. Hampel, *Thermochim. Acta*, 2019, **672**, 25-42.
11. B. Li, S. M. Guinness, S. Hoagland, M. Fichtner, H. Kim, S. Li, R. J. Maguire, J. C. McWilliams, J. Mustakis, J. Raggon, D. Campos, C. R. Voss, E. Sohodski, B. Feyock, H. Murnen, M. Gonzalez, M. Johnson, J. Lu, X. Feng, X. Sun, S. Zheng and B. Wu, *Org. Process Res. Dev.*, 2018, **22**, 707-720.
12. M. Magosso, L. J. W. Hazen, M. van den Berg and J. van der Schaaf, *Ind. Eng. Chem. Res.*, 2021, **60**, 15540-15548.
13. R. D. Mair and A. J. Graupner, *Anal. Chem.*, 1964, **36**, 194-204.
14. F. Derridj, J. Roger, F. Geneste, S. Djebbar and H. Doucet, *J. Organomet. Chem.*, 2009, **694**, 455-465.
15. I. Triandafillidi, M. G. Kokotou and C. G. Kokotos, *Org. Lett.*, 2018, **20**, 36-39.
16. A. E. Prosenko, A. F. Markov, A. S. Khomchenko, M. A. Boiko, E. I. Terakh and N. V. Kandalintseva, *Pet. Chem.*, 2006, **46**, 442-446.
17. A. K. El-Qisairi, H. A. Qaseer and P. M. Henry, *J. Organomet. Chem.*, 2002, **656**, 168-176.
18. R. Hemelaere, F. Carreaux and B. Carboni, *Eur. J. Org. Chem.*, 2015, **2015**, 2470-2481.
19. T. Maji and J. A. Tunge, *Org. Lett.*, 2015, **17**, 4766-4769.
20. J. Rudolph, L. Chen, D. Majumdar, W. H. Bullock, M. Burns, T. Claus, F. E. Dela Cruz, M. Daly, F. J. Ehgott, J. S. Johnson, J. N. Livingston, R. W. Schoenleber, J. Shapiro, L. Yang, M. Tsutsumi and X. Ma, *J. Med. Chem.*, 2007, **50**, 984-1000.
21. X. Tan, L. Kong, H. Dai, X. Cheng, F. Liu and C. Tschierske, *Chem. Eur. J.*, 2013, **19**, 16303-16313.
22. Y. Mao, Y. Liu, Y. Hu, L. Wang, S. Zhang and W. Wang, *ACS Catal.*, 2018, **8**, 3016-3020.
23. C. Böttcher, G. Zeyat, S. A. Ahmed, E. Irran, T. Cordes, C. Elsner, W. Zinth and K. Rueck-Braun, *Beilstein J Org Chem*, 2009, **5**, 25.
24. S. Gai, N. T. Lucas and B. C. Hawkins, *Org. Lett.*, 2019, **21**, 2872-2875.
25. R. J. Smith, D. Nhu, M. R. Clark, S. Gai, N. T. Lucas and B. C. Hawkins, *J. Org. Chem.*, 2017, **82**, 5317-5327.
26. N. Ayyagari and J. D. Belani, *Synlett*, 2014, **25**, 2350-2354.
27. R. J. Smith, D. A. Mills, D. Nhu, E. W. Tan, N. T. Lucas and B. C. Hawkins, *J. Org. Chem.*, 2016, **81**, 2099-2105.
28. M. G. Kulkarni, Y. B. Shaikh, A. S. Borhade, S. W. Chavhan, A. P. Dhondge, D. D. Gaikwad, M. P. Desai, D. R. Birhade and N. R. Dhattrak, *Tetrahedron Lett.*, 2013, **54**, 2293-2295.